STATE HIGHWAY ADMINISTRATION

RESEARCH REPORT

GEOENVIRONMENTAL IMPACTS OF USING HIGH CARBON FLY ASH IN STRUCTURAL FILL APPLICATIONS

DR. AHMET AYDILEK AND DR. BORA CETIN
UNIVERSITYOF MARYLAND-COLLEGE PARK

Project number SP909B4P
FINAL REPORT

March 2013

Technical Report Documentation Page

1. Report No.	2. Government Accession No.	3. Recipient's Catalog No.
MD-13-SP909B4P		

4. Title and Subtitle	5. Report Date
Geoenvironnmental Impacts of Using High Carbon Fly Ash in Structural Fill Applications	March 2013
	6. Performing Organization Code

7. Author/s	8. Performing Organization Report No.
Ahmet Aydilek and Bora Cetin	

9. Performing Organization Name and Address	10. Work Unit No. (TRAIS)
University of Maryland Department of Civil and Environmental Engineering 1163 Martin Hall College Park, MD 20742	11. Contract or Grant No. SP909B4P

12. Sponsoring Organization Name and Address	13. Type of Report and Period Covered
Maryland State Highway Administration 707 North Calvert Street Baltimore MD 21202	Final Report
	14. Sponsoring Agency Code (7120) STMD - MDOT/SHA

15. Supplementary Notes

16. Abstract

Fly ash produced by power plants in the United States occasionally contains significant amounts of unburned carbon due to the use of the increased prevalence of low nitrogen-oxide and sulphur-oxide burners in recent years. This ash cannot be reused in concrete production due to its reactivity with air entrainment admixtures, so it is largely placed in landfills. Highway structures have high potential for large volume use of high carbon fly ashes (HCFAs). However, in such applications, even though mechanical properties of the fly ash-amended highway base layers and embankments are deemed satisfactory, a key issue that precludes such highway embankments built with fly ash is the potential for negative groundwater effects caused by metals in the fly ash. This study evaluated the leaching potential of metals from highway base layers stabilized with HCFA and highway embankment structures amended with HCFA. Three different laboratory tests were conducted: (1) batch water leach tests, (2) toxicity characteristics leaching procedure tests, (3) column leach test. Additionally, two numerical modeling analyses were conducted: (1) WiscLEACH and (2) MINTEQA2. Analyses were conducted on eight fly ashes and two locally available sandy soil materials that are mainly used in highway base layer and highway embankment structures. Laboratory test results indicated that an increase in fly ash content in the soil-fly ash mixtures yielded an increase in leached metal concentrations with the exception of zinc (Zn). The pHs had significant and different effects on the leaching of metals. The leaching of chromium (Cr), zinc, (Zn), aluminum (Al), arsenic (As) and selenium (Se) increased with increased pH levels, while leaching of barium (Ba), boron (B), cooper (Cu), iron (Fe), magnesium (Mn), silver (Sb), vanadium (V) decreased with increased pH levels.. Numerical model WiscLEACH was used to simulate the leaching behavior of leached metals from HCFA-stabilized highway base layers and HCFA-amended highway embankment structures. WiscLEACH predicted field metal concentrations were significantly lower than the metal concentrations obtained in laboratory leaching tests, and field concentrations decreased with time and distance due to dispersion in soil vadose zone. Numerical model MINTEQA2 predicted that leaching of metals were solubility controlled except As, Se and Sb. Speciation analyses indicated that leached metals were present at their less or non-toxic forms.

17. Key Words	18. Distribution Statement: No restrictions
Fly ash, structural fill, leaching, environmental suitability, metals	This document is available from the Research Division upon request.

19. Security Classification (of this report)	20. Security Classification (of this page)	21. No. Of Pages	22. Price
None	None	253	

Form DOT F 1700.7 (8-72) Reproduction of form and completed page is authorized.

EXECUTIVE SUMMARY

Fly ash produced by some of the power plants in the United States occasionally contains significant amounts of unburned carbon due to the use of the increased prevalence of low nitrogen-oxide and sulphur-oxide burners in recent years. This ash cannot be reused in concrete production due to its reactivity with air entrainment admixtures, so it is largely placed in landfills. Highway structures have high potential for large volume use of high carbon fly ashes (HCFAs). However, in such applications, even though mechanical properties of the fly ash-amended highway base layers and embankments are deemed satisfactory, a key issue that precludes such highway embankments built with fly ash is the potential for negative groundwater effects caused by the leaching of metals in the material.

This study evaluated the leaching potential of metals from HCFA used as a stabilizing agent and soil amendment in highway base layers and highway embankment structures, respectively. Three different laboratory tests were conducted: (1) batch water leach tests, (2) toxicity characteristics leaching procedure (TCLP) tests, and (3) column leach tests. Additionally, two numerical modeling analyses were conducted: (1) WiscLEACH and (2) MINTEQA2. Analyses were conducted on eight fly ashes and two locally available sandy soil materials that are mainly used in highway base layer and highway embankment structures.

Laboratory test results indicated that an increase in fly ash content in the soil-fly ash mixtures yielded an increase in leached metal concentrations with the exception of

zinc (Zn). The pHs had significant and different effects on the leaching of metals. The leaching of chromium (Cr), zinc, (Zn), aluminum (Al), arsenic (As) and selenium (Se) increased with increased pH levels, while leaching of barium (Ba), boron (B), cooper (Cu), iron (Fe), magnesium (Mn), silver (Sb), vanadium (V) decreased with increased pH levels..

Numerical model WiscLEACH was used to simulate the leaching behavior of leached metals from HCFA-stabilized highway base layers and HCFA-amended highway embankment structures. WiscLEACH predicted that field metal concentrations were significantly lower than the metal concentrations obtained in laboratory leaching tests, and field concentrations decreased with time and distance due to dispersion in soil vadose zone. Numerical model MINTEQA2 predicted that leaching of metals were solubility controlled except As, Se and Sb. Speciation analyses indicated that leached metals were present at their less or non-toxic forms.

TABLE OF CONTENTS

LIST OF TABLES

LIST OF FIGURES

1 INTRODUCTION

According to the American Coal Ash Association (ACAA), 45% of the electricity in the United States in 2009 was supplied from the power plants that burn coal. Approximately 92.8 million of tons of coal combustion byproducts (CCBs) are produced in the United States each year as a result of burning coal at the electric power plants (ACAA 2008). As of 2009, 78% of these CCBs are fly ashes, and 42.3 million tons of fly ash is landfilled. ACAA estimates that this landfilled or stockpiled amount will continue to increase every year.

Fly ash is siliceous or alumino-siliceous pozzolanic material that can form cementitious compounds in the presence of water. The physical, chemical, and mineralogical properties of the fly strongly depend on the type of the coal burning, combustion process, pollution control facilities, and handling (Bin-Shafique, et al. 2006). Based on its chemical composition, fly ashes are classified either as F or C. The C-type (self-cementitious) fly ashes are readily available, whereas F-type fly ashes are commonly reused as concrete additive or in cement production.

Fly ashes produced by several power plants in the United States in the last five years contain significant amounts of unburned carbon (i.e., high loss on ignition) due to the increasingly common use of low nitrogen oxide (NO_x) and sulphur oxide (SO_x) burners. This ash, called high-carbon fly ash (HCFA), has a carbon content of 12-25%. HCFA cannot be efficiently re-burned by using current technology and has no value as a concrete additive because the unburned carbon tends to adsorb the air entrainment

admixtures that are added to cement to prevent crack formation and propagation. These ashes are typically classified as off-spec fly ashes, which means they do not meet the physical and chemical requirements criteria outlined in ASTM C618. As a result, high percentages of HCFA are disposed of in landfills.

Fly ashes may contain high concentrations of such trace elements as arsenic, boron, chromium, copper, zinc, vanadium, and nickel. Stockpiling of fly ashes or disposing large amounts of fly ashes into landfills can cause leaching of these heavy metals to the groundwater through the soil vadose zone and may threaten aquatic life, the environment, as well as human health. There have been efforts to reuse fly ash materials in construction in order to decrease the disposal rate.

Fly ashes produced by several power plants in Maryland and elsewhere occasionally contain enough unburned carbon that they cannot be used in concrete production. Geotechnical applications such as highways base layers and highway embankments pose great potential for beneficial reuse of fly ashes due to their lightweight and satisfactory mechanical properties. In the current study, the applications for reusing fly ash in construction of highway base layers (Sections 2 and 3) and embankments (Section 4) are discussed.

Several studies have been conducted on leaching behavior of metals from coal combustion by-products and mechanisms that control the release of these metals (Bin-Shafique, et al.; Chen, et al. 2006; Deng, et al., 2008; Dutta, et al., 2009; Gosh, 2008; Goswami & Mahantam, 2007; Komonweeraket, et al., 2010; Srivastava et al. 2008; Vitkova et al. 2008; Wang, et al., 2006). However, there is little information about

leaching of these contaminants from high-carbon fly ash mixtures. The environmental risks associated with fly ash stabilization may be reduced when HCFAs are used as a stabilizing agent. On the other hand, unburned carbon or activated carbon is often used for pollution control. The high organic carbon content of HCFA may act as a sorbent to the heavy metals in the fly ash, and reduce the amount of metals released into the environment. The environmental benefits of the high carbon content may also result in a broader range of permissible reuse applications for fly ash.

The objective of this study was to evaluate the leaching potential of borrow materials mixed with HCFAs relative to those stabilized with conventional additives (low-carbon fly ashes), and to evaluate the potential groundwater and soil vadose zone effects. The experimental program consisted of the following tasks:

1) Determining the concentrations of minor, major, and trace elements and other chemical properties of interests, speciation in leachates from soil-fly ash mixtures and both fly ashes and soil alone;
2) Running small-scale water leaching tests to estimate metal leaching behavior;
3) Running long-term column leaching tests to study metal leaching behavior and the controlling mechanisms of the trace metals from the mixtures and fly ash;
4) Running TCLP tests to determine the leaching potential of these fly ashes and mixtures under acidic conditions;
5) Comparing the results of different test results in order to estimate the metal concentrations in the field;
6) Determining the groundwater impacts through computer modeling; and

7) Predicting the species of the trace metals and determining the mechanisms that control leaching of these metals species with the help of a geochemical modeling tool.

This study focused on the leaching characteristics and behavior of ten metals (aluminum, arsenic, antimony, boron, chromium, copper, iron, manganese, selenium, vanadium and zinc) from laboratory-simulated HCFA-stabilized base layer and embankment fill materials. This report contains six main sections: Sections 2 and 3 evaluate the leaching potential of fly ashes that are used as stabilizing agents in highway base layers with stabilized soils. Section 4 contains the results of leaching tests on soil-HCFA mixtures and evaluates the potential for use in embankment constructions. Section 5 is geochemical modeling analysis with a discussion the speciation of leached metals and their mechanisms controlling leaching in aqueous solutions. Section 6 provides a summary of findings and general conclusions obtained from the research study.

2 LEACHING OF TRACE METALS FROM HIGH-CARBON FLY ASH STABILIZED HIGHWAY BASE LAYERS

2.1 INTRODUCTION

Using fly ash in highway applications is gaining importance because of the potential to solve landfill problems and to provide geomechanically stable material. One of the most important problems in highway construction is building a suitable base layer that can provide adequate support for the asphalt layer. There are two conventional methods for stabilizing the base layer. One is to remove the soft soil and replace it with a material that possess higher stiffness, such as granular materials (gravel). The other is in-situ stabilization of the soil via physical and chemical techniques. However, these two conventional methods can be costly and time consuming. Alternative approaches such as fly ash amendment could be more practical and provide an economical solution to stabilize the existing soil (Cetin et al., 2010). Metal leaching from HCFA-stabilized soil layers is, however, the main concern for construction applications (Bin Shafique et al., 2002; Goswami & Mahanta 2007; Sauer et al., 2005).

Limited information exists on the reuse of high-carbon off-spec fly ash in construction of highway embankments. This is particularly important when high-carbon fly ash is non-cementitious and calcium-rich activators are required to generate pozzolanic reactions. In order to evaluate the environmental suitability of high-carbon fly ash-stabilized soils for potential highway applications, a series of short term batch water and long term column leaching experiments were conducted to evaluate the

leaching of six heavy metals (Al, Cr, Fe, Mn, Sb, V). Results were used to determine leaching patterns and relationships between concentrations from the two laboratory tests.

2.2 MATERIALS

Unpaved road material, commonly used in constructing low-volume roads (which will be referred to as soil hereafter) and three fly ashes were used in this study. The soil was used in soil–fly ash–lime kiln dust mixtures in all tests, as well as being a reference material in both column- and water-leach tests. Mixtures of fly ashes and lime kiln dust were selected based on strength and moduli determined in an earlier study (Cetin et al., 2010). Soil was collected from a highway construction site in Caroline County, Maryland, and was stored in airtight buckets to preserve its natural water content. Any debris and foreign materials in the soil were removed by hand and by sieving through a 19-mm sieve. The soil was classified as poorly graded sand with gravel (SP) according to the Unified Soil Classification System (USCS), and A-1-b according to the American Association of State Highway and Transportation Officials (AASHTO) Classification System. Soil was chosen because it satisfied the gradation and maximum dry unit weight requirements identified by the Maryland State Highway Administration (SHA). Physical properties of the soil and fly ashes are summarized in Table 2.1. The optimum moisture contents (w_{opt}) and maximum dry unit weights (γ_{dmax}) of the soil-fly ash- LKD mixtures prepared using the standard Proctor effort (ASTM D 698) ranged from of 9% to 13.4% and, from 17 kN/m^3 (108 pcf) to 19.4 kN/m^3 (123.6 pcf), respectively (Table 2.3).

Table 2.1. Index properties of the materials used in current study

Soil/ Fly ash	C_u	G_s	w_{opt} (%)	γ_{dmax} (kN/m^3/ pcf)	LL (%)	PI (%)	Gravel Content(>4.75 mm) (%)	Fines Content (<75 μm) (%)	Fineness (>45 μm) (%)	Classification	
										USCS	AASHTO
Soil	6.7	2.64	13.4	18.8 (120)	NP	NP	30	3	0	SP	A - 1 – b (0)
BS	0.43	2.17	—	—	NP	NP	—	80	60	ML	A - 2 – 4 (0)
PS	11	2.2	—	—	NP	NP	—	95	86	ML	A - 2 – 4 (0)
DP	3.6	2.37	—	—	NP	NP	—	85	77	ML	A - 2 – 4 (0)

Table 2.2. Chemical compositions and total metal contents of the materials utilized. The compositions and concentrations were determined by X-ray fluorescence spectroscopy analysis, and total elemental analysis, respectively.

Soil/ Fly ash	Chemical Composition												
	pH	LOI (%)	SiO_2 (%)	Al_2O_3 (%)	Fe_2O_3 (%)	CaO (%)	$CaCO_3$ (%)	Al (mg/L)	Cr (mg/L)	Fe (mg/L)	Mn (mg/L)	Sb (mg/L)	V (mg/L)
Soil	6.5	2.4	NA	NA	NA	NA	NA	2400	15.5	6300	26.5	0.02	16.5
BS	9.6	13.4	45.1	23.1	3.16	7.8	NA	28600	65.7	34600	115	0.01	164
PS	7.55	10.7	50.8	26.9	5.5	0.7	NA	10000	24.3	10700	38.2	0.02	53.7
DP	8.8	20.5	34.9	24.4	12.6	3.2	NA	19200	47.1	12700	38.3	0.02	82.4
LKD	12.7	NA	10	NA	NA	60	30	NA	NA	NA	NA	NA	NA

Notes:, PS: Paul Smith fly ash, DP: Dickerson Precipitator fly ash, BS: Brandon Shores fly ash, LKD: Lime kiln dust, LOI: Loss on ignition. G_s: Specific gravity, C_u: Coefficient of uniformity, w_{optm}: Optimum water content, γ_{dmax}: Maximum dry unit weight, LL: Liquid limit, PI: Plasticity index NP: Nonplastic, NA: Not available

Table 2.3. Legend and compositions of the mixtures.

Specimen name	Soil Content (%)	Fly Ash Content (%)	LKD Content (%)	Optimum Water Content, w_{opt} (%)	Maximum Dry Unit Weight, γ_{dmax} (kN/m^3/pcf)
Soil	100	0	0	13.4	18.8 (120)
10 BS + 2.5 LKD	90	10	2.5	10	19.2 (122)
10 BS + 5 LKD	90	10	5	9.5	19.2 (122)
20 BS + 5 LKD	80	20	5	13	17.4 (111)
10 PS + 2.5 LKD	90	10	2.5	9.0	18.8 (120)
10 PS + 5 LKD	90	10	5	10	18.8 (120)
20 PS + 5 LKD	80	20	5	13	17.0 (108)
10 DP + 2.5 LKD	90	10	2.5	9.0	19.1 (122)
10 DP + 5 LKD	90	10	5	10	19.4 (124)
20 DP + 5 LKD	80	20	5	12	18.0 (115)

Note: BS: Brandon Shores fly ash, PS: Paul Smith fly ash, DP: Dickerson Precipitator fly ash, LKD: Lime kiln dust.

The fly ashes used in this study were obtained from three power plants in Maryland: Brandon Shores (BS), Paul Smith (PS) and Dickerson Precipitator (DP). The locations of the fly ashes were shown in Appendix. All the fly ashes consisted primarily of silt-size particles and contained 76 to 90% fines (passing the 75-μm sieve). Specific gravity of fly ashes ranged between 2.17 and 2.37 per ASTM D 854. The physical properties and chemical compositions of ashes are summarized in Table 2.1 and Table 2.2. The fly ashes investigated in this study were classified as off-specification fly ashes (neither C- nor F-type according to ASTM C 618) because of their high loss on ignition values (LOI > 6), high (SiO_2 (%) + Al_2O_3 (%) + Fe_2O_3 (%) >70 %), and low lime (CaO) contents (0.7-7.8 %). The LOI data and pH measurements were analyzed according to EPA Method SW-846 and Method 9045 and are presented in Table 2.3. Because the three fly ashes do not have high cementing potential, lime kiln dust (LKD) was used to initiate pozzolanic reactions for stabilization of the soil. LKD (a disposed residue of lime production plants) was obtained from Carmeuse Lime and Stone Company, Pittsburgh, Pennsylvania, and contained approximately 60% CaO by weight. The specific gravity (G_s) of LKD by 2.97. Total elemental analyses of the three fly ashes and soil were conducted following the procedures outlined in EPA SW-846 Method 6800 and are summarized in Table 2.3.

2.3 METHODS

2.3.1 Batch Water Leach Tests (WLTs)

Batch water-leach tests were conducted on the soil, fly ashes, and soil mixtures using different percentages of fly ashes and LKD in accordance with ASTM D 3987. A constant liquid-to-solid (L:S) ratio of 20:1 was used for all materials. The air-dried soil was crushed and then sieved from U.S. No. 4 sieve (4.75-mm). Next, the soil was mixed homogeneously with fly ash and LKD at different percentages. Each specimen was cured for seven days in plastic bags in a moisture-controlled humidity chamber (21 ºC and 100% relative humidity). After curing, 2.4 g of soil mixture was added to a 50-mL plastic centrifuge tube followed by 48 mL leachant (the 0.1 M NaBr solution). The soil mixtures were rotated continuously at 29 revolutions per minute and at room temperature (~22 ºC) for 18 hours in order to reach equilibration. After equilibrium, the specimens were allowed to settle for five minutes before being placed in a Beckman GPR centrifuge. The mixtures were centrifuged at 3000 rpm for 20 minutes. The suspended solids were then filtered through 0.2-µm-pore-size, 25-mm diameter membrane disk filters fitted in a 25-mm Easy Pressure syringe filter holder using a 60-mL plastic syringe. The pH of filtered samples was measured and then acidified to less than a pH of 2 using high-purity nitric acid. The mixtures were then stored in 15-mL high-density polyethylene centrifuge tubes at 4 ºC. Triplicate WLTs were conducted on all fly ash-soil, fly ash, and soil mixtures.

2.3.2 Column Leach Tests

Column leach tests (CLTs) were conducted on soil-fly ashes mixtures and on soil and fly ashes alone in order to provide more realistic results about leaching behavior of heavy metals. The soils, fly ashes, and the combination thereof prepared for CLTs were the same materials used in WLTs. Air-dried soil was sieved from U.S. No.4 (4.75 mm) sieve. All specimens were compacted in polyvinyl chloride (PVC) molds of 101.6 mm (4 in) diameter and 116.4 mm (4.6 in) height by using standard Proctor compaction effort (ASTM D 698). PVC molds were preferred to minimize the outside effects on effluent metal concentrations. All soil mixtures were cured for seven days in a humidity chamber with 100% relative humidity and 21 ºC following compaction. The protocol for sample filtration and preservation followed those employed in WLTs. After curing, the CLTs were started immediately. A 0.1 M NaBr solution was used to provide influent with an ionic strength, which was sent to the specimen by a peristaltic pump at a rate of 60 mL/hr Morar (2007), Gelhar et al. (1992), and Papini et al. (1999). Sampling and pH measurements were conducted every four hours in the first seventy-two hours, after which time sampling two to fourteen times each week was sufficient. Detailed information about the testing procedures can be found in Morar (2007).

2.3.3 Chemical Analysis

The pH levels of the leachate samples collected from the CLTs and WLTs were determined following the methods outlined in ASTM D 1293. The pH levels of the fly ashes were determined by using SW-846 Method 9045. Three replicate samples were

measured for each sample and the mean values were reported. The metals selected for analysis were Ag, Al, Ba, Be, Ca, Cd, Co, Cr, Cu, Fe, Hg, Mn, Ni, Pb, Sb, Si, Sr, TI, V, and Zn based on total elemental analyses. Initial spectroscopy analyses showed that water leach test (WLT) and column leach test (CLT) effluent concentrations were below the detection limits for all metals, except Al, Cr, Fe, Mn, Sb, and V. The EPA identified that these six metals pose health concerns based on the recommendations of the U.S. Environmental Protection Agency (EPA), and thus were included in further analyses. These six metals also represent different mobilities. For instance, at the pH levels typical of soil-fly ash mixtures (pH=10-12.5) , Cr forms oxyanions that can be very mobile (Fendorf 1995, Daniels and Das 2006), whereas Al forms hydroxyl compounds and their attachment to the soil surface depends on the solubility level (Sparks 2003). On the other hand, Fe, Mn, Sb and V have cationic species at high pH levels and their solubility is relatively lower. (Jackson et al. 1999, Pavageau et al. 2004, Cornelis et al. 2006).

The concentrations of all metals were determined by inductively coupled plasma optical emission spectroscopy (ICP-OES) using a Varian Vista-MPX CCD Simultaneous ICP-OES instrument. Minimum detection limits (MDLs) for ICP-OES were determined for each metals and a set of calibration standards according to the U.S. Code of Federal Regulations Title 40. The MDLs for Al, Cr, Fe, Mn, Sb, and V were determined as 2.5 μg/L, 0.5 μg/L, 3.2 μg/L, 0.05 μg/L, 3 μg/L, and 0.1 μg/L, respectively.

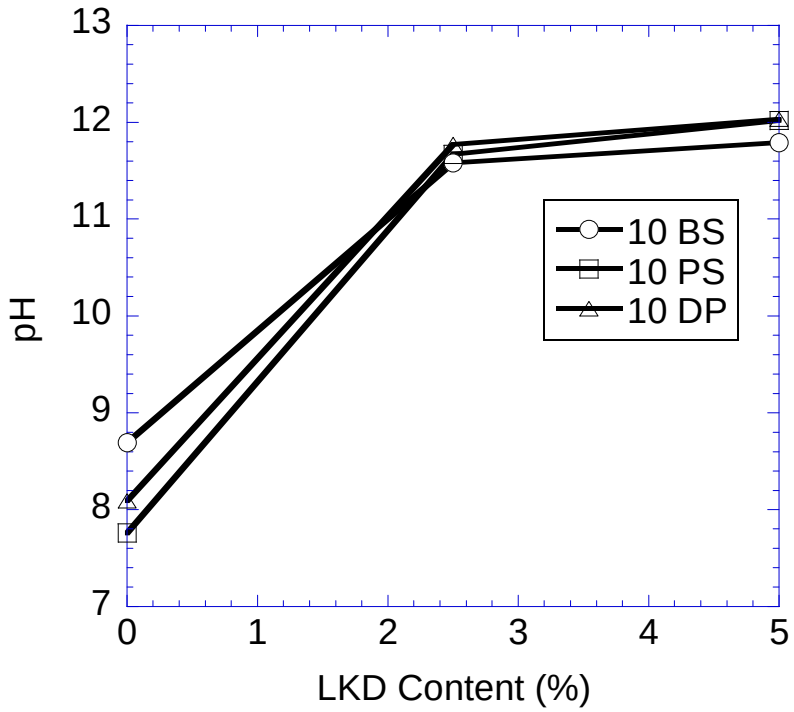

Figure 2.1. Effect of LKD content on pH of the soil mixtures. Note: 10 BS, 10 PS, 10 DP designate the specimens with 10% Brandon Shores, Paul Smith, and Dickerson Precipitator fly ash respectively. 0% LKD content corresponds to fly ash only.

2.4 RESULTS

2.4.1 Batch Water Leach Tests

Triplicate batch water leach tests (WLTs) were conducted on soil only, fly ash only, and several soil-fly ash- LKD mixtures. Table 2.4 summarizes the pH levels of the specimens tested. Figure 2.1 shows that the rate of increase in pH was began high and that an addition of LKD above 2.5% by weight did not affect pH significantly. It is speculated that an increase in LKD amount increased the release of free lime (CaO), hydrated calcium silicate (C-S-H) and portlandite Ca $(OH)_2$, which resulted in an increase in pH values. Compared to LKD, the fly ashes had a relatively smaller effect on pH of the mixture due to its lower calcium content (Table 4). All three fly ashes except the BS fly ash had calcium contents of less than 5%, compared to a calcium content of approximately 60% for LKD. LKD calcium content was the dominant factor that controlled the effluent pH levels of effluent solutions because of its high CaO content (60%) compared to high-carbon fly ashes used in this study.

Table 2.4 shows the concentrations of the six metals the EPA identified as posing health risks for several different soil mixtures as compared to the U.S. EPA maximum concentration limits for drinking waters (MCLs), EPA water quality limits (WQLs) for protection of aquatic life and human health, and Maryland aquatic toxicity limits (ATLs) for fresh water. The results show that, except for Al, higher metal concentrations were obtained for fly ashes alone than for the soil-fly ash–LKD mixtures. Of the three fly ashes tested, generally the mixture with BS fly ash yielded the highest metal concentrations followed by the mixtures prepared with DP and PS fly ashes. Trace metal

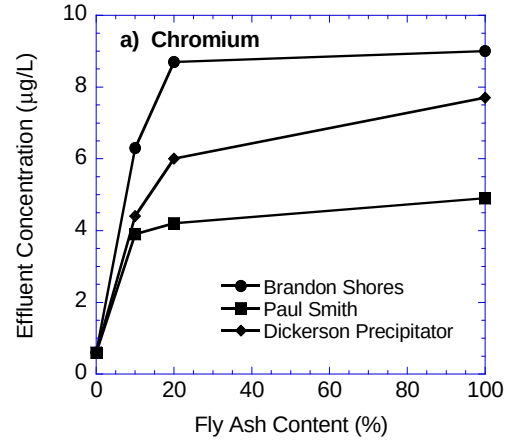
a) Chromium
Effluent Concentration (µg/L)
Fly Ash Content (%)
Brandon Shores
Paul Smith
Dickerson Precipitator
0
2
4
6
8
10
0
20
40
60
80
100

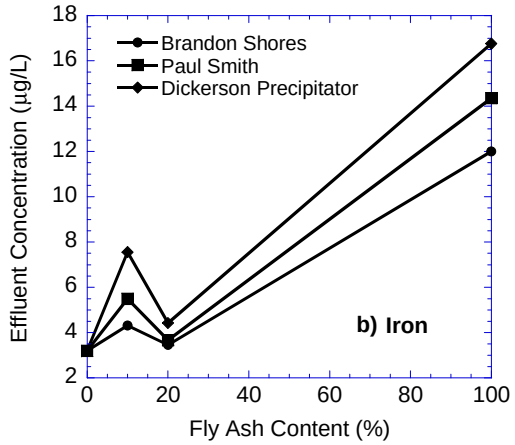
b) Iron
Effluent Concentration (µg/L)
Fly Ash Content (%)
Brandon Shores
Paul Smith
Dickerson Precipitator
2
4
6
8
10
12
14
16
18
0
20
40
60
80
100

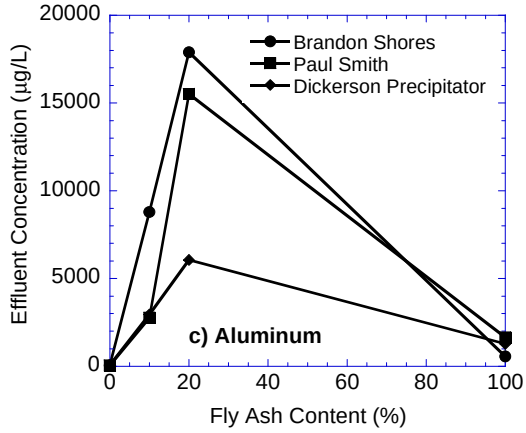
c) Aluminum
Effluent Concentration (µg/L)
Fly Ash Content (%)
Brandon Shores
Paul Smith
Dickerson Precipitator
0
5000
10000
15000
20000
0
20
40
60
80
100

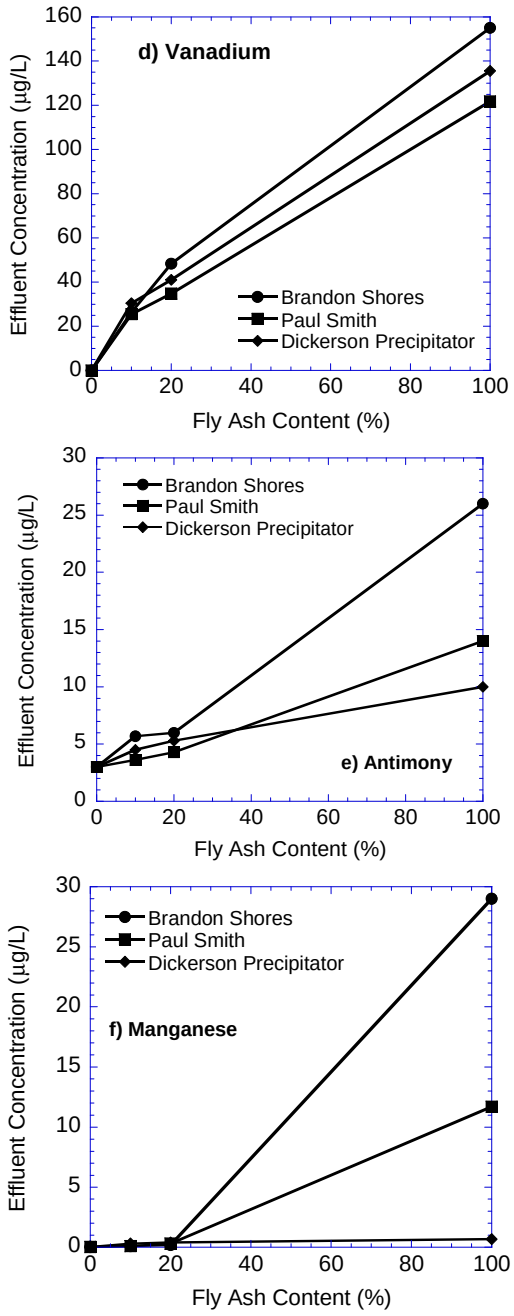

Figure 2.2. Effect of fly ash content on WLT concentrations of a) chromium, b) iron, c) aluminum, d) vanadium, e) antimony, and f) manganese. Mixtures prepared with 10% and 20% fly ash are amended with 5% LKD. 0% and 100% fly ash content corresponds to soil only and fly ash only specimens, respectively.

contents were also generally the highest in BS fly ash based on total element analysis (Table 2.3). However, regardless of the increase in metal concentrations all trace metal concentrations, except Al, were below the MCL, WQL and Maryland ATL.

The variation in concentrations of these six metals was plotted against fly ash content for mixtures prepared with 5% LKD in Figure 2.2. Al, Cr, V, Sb, and Mn showed similar trends: The concentrations generally increased with increasing fly ash content. The rate of increase of these five metals concentrations, however, was different without recognizably consistent variation; we speculate this is partially due to differences of metal contents based on total elemental analysis (Table 2.4). The effluent concentrations of all metals were higher for the fly ash alone than for the soil alone (0% fly ash). For the soil-fly ash-LKD mixtures, higher fly ash proportions generally yielded higher effluent metal concentrations. However, the increase of metal concentrations was not linearly related to fly ash content, even though the mass of metals in soil mixture increases approximately linearly with increasing fly ash content. Therefore, the use of linear dilution calculations will underestimate the resulting concentrations of metals from soil mixtures.

Fe concentrations increased with increasing the fly ash content from 0% to 10% because of the addition of the main metal source. Similar Fe increases were observed when the ash content was increased from 20% to 100% because the of the increase in metal source as well as a lack of LKD addition. However, an increase in fly ash content from 10% to 20% caused a decrease in Fe concentrations because of the high pH levels (i.e., pH >11) of the effluent solutions, which was achieved by adding LKD. Fe forms

cationic species and precipitates as different complexes (e.g., $FeCO_3$) under such alkaline conditions, so the solubility of Fe play a more dominant role than an increase in the metal source (Goswami & Mahanta, 2007; Pandian & Balasubramonian, 2000)

High concentrations of Al were observed in the effluent leachates from soil-fly ash–LKD mixtures. The solubility of Al is minimum at a pH level of about 6.5; Al's solubility increases with increasing pH thereafter (Komonweeraket et al. 2010; Lim et al., 2004). As seen in Table 2.4, the aluminum concentrations with fly ashes were at least three times lower than that of the mixtures. The addition of the LKD is most probably responsible for leaching of Al, which increases the pH levels of the effluent solutions due to the release of high amounts of CaO from LKD. Aluminum produces anionic species and cannot be absorbed by the negatively charged surface in alkaline conditions. High pH levels may have resulted in a significant change in the size of negatively charged particle surface occupied by the hydrogen ions, causing a serious space decrease for Al and other metals (Sparks 2003).

Table 2.4. Stabilized pH and peak effluent concentrations in CLTs. Concentrations exceeding MCLs in **bold**.

Specimen Name	Fly Ash Content (%)	LKD Content (%)	pH	Al (µg/L)	Sb (µg/L)	Cr (µg/L)	Fe (µg/L)	Mn (µg/L)	V (µg/L)
100 BS	100	-	8.6	**1590**	**304**	43	223	**76**	1533
10 BS + 2.5 LKD	10	2.5	12.1	**4870**	**17**	28	216	2	100
10 BS + 5 LKD	10	5	12.5	**6850**	**9**	40	197	0.5	72
20 BS + 5 LKD	20	5	12.5	**7572**	**49**	44	64	0.6	649
100 PS	100	-	7. 6	**262**	**156**	76	174	**1654**	891
10 PS + 2.5 LKD	10	2.5	12.3	**6030**	**19**	11	18	1	89
10 PS + 5 LKD	10	5	12.5	**6660**	**8**	12	15.2	0.3	53
20 PS + 5 LKD	20	5	12.5	**7230**	**24**	15	13	0.4	487
100 DP	100	-	7.9	**950**	**48**	**252**	162	**257**	1093
10 DP + 2.5 LKD	10	2.5	12.1	**5810**	**10**	16	30	0.5	170
10 DP + 5 LKD	10	5	12.4	**6250**	**7**	26	21	0.3	78
20 DP + 5 LKD	20	5	12.6	**8640**	**8.7**	31	16	1	195
Soil	-	-	6.5	122	33	0.8	91	3.5	32
U.S. EPA MCL				200	6	100	300	50	NA
U.S. EPA WQL				750	NA	570	NA	NA	NA
MD ATL				NA	NA	74 (Chronic) 570 (Acute)	NA	NA	NA

Notes: MCL= maximum contaminant levels for drinking water; MCL for Al is based on a secondary non-enforceable drinking water regulation; WQL= water quality limits for protection of aquatic life and human health in fresh water. MD ATL = Maryland State aquatic toxicity limits for fresh water.

2.4.2 Column Leach Tests

pH Measurements

Figure 2.3 shows the effluent pH levels of the soil alone, fly ash alone and soil-fly ash mixtures as a function of pore volumes of flow. All tests were continued until a minimum of 200 pore volumes of flow were obtained in order to examine the behavior and persistency of pH. In most cases, pH levels initially decreased during the first 30-100 pore volumes of flow. This decrease was followed by an essentially constant pH. Even though the pH levels of the influent solutions were kept between 6.5 and 7, the stabilized pH level of the effluent solutions were still relatively high (pH>11) due to buffering capacities of the fly ashes and LKD.

Soil had the lowest pH level, and when either fly ash or LKD were added, the pH levels increased regardless of the percentage of the additive (Figure 2.3). As with the WLT, the addition of LKD appears to have a greater effect on pH levels than the addition of fly ash due to relatively higher CaO content. Levels of pH can also be correlated with the Ca content of the ash. For instance, PS fly ash (CaO=0.7%) has lower calcium content than BS fly ash (CaO = 7.8%), which resulted in a relatively lower stabilized pH values in CLTs (Figure 2.3).

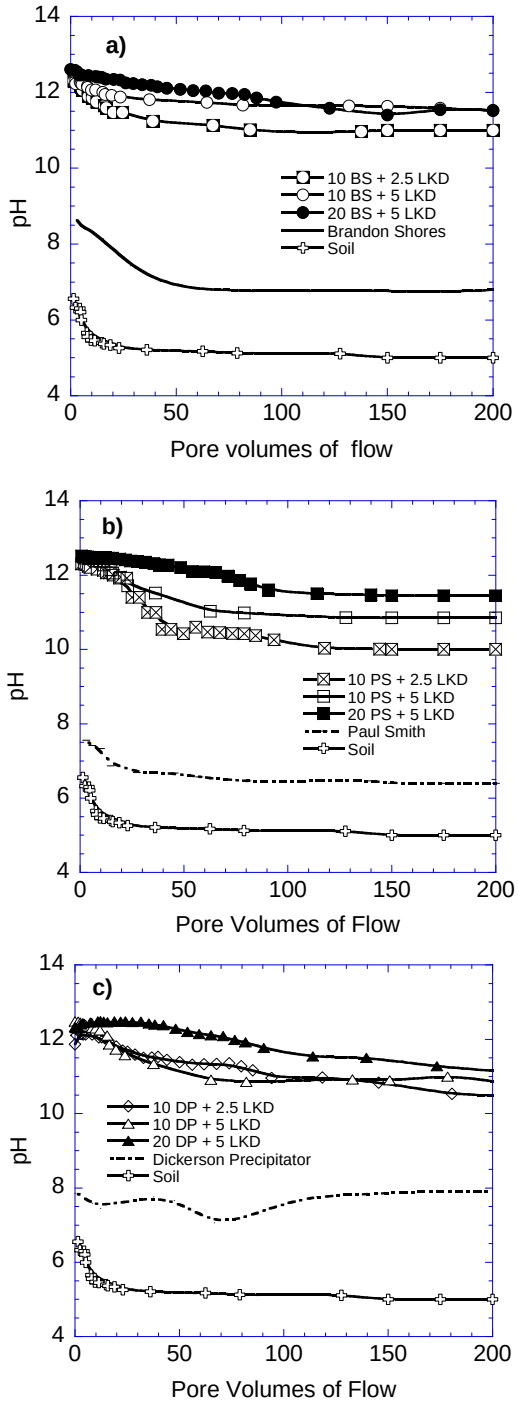

Figure 2.3 Effluent pH in CLTs conducted on mixtures prepared with a) Brandon Shores fly ash , b) Paul Smith fly ash, and c) Dickerson Precipitator fly ash.

Metal Leaching

Table 2.5 shows that the peak metal concentrations in soil-fly ash mixtures, were below the groundwater quality limits. The only exception was Al. It should be noted that Al is on the EPA`s list of secondary drinking water regulations, and there are no limits for Al specified in the Maryland groundwater protection guidelines.

Figure 4 shows a series of CLT elution curves. All elution curves are not presented herein for brevity, but similar trends were obtained in the omitted curves. The elution curves in Figure 2.4, with few exceptions, suggest a high initial leaching of the metals followed by a sharp decrease to near constant concentrations after approximately 10-100 pore volumes of flow. This type of leaching behavior is called first flush pattern and is the result of the release of the metals from the water soluble fraction and the sites with low adsorption energies (Bin-Shafique et al., 2006; Morar 2008). The initially high effluent pH values of the mixtures (pH~12) provide a possible explanation for the first flush pattern leaching of Al and Cr. In this pH range, Al and Cr are likely to be available in their anionic species in the environment, and the dominant Al species are $Al(OH)_4^-$ and $Al(OH)_5^{-2}$, and the Cr species are CrO_7^{-2} and CrO_4^{-2} (Quina et al., 2009). Cr (VI) is a toxic Cr species, and an acute irritant for living cells, and can be carcinogenic to humans (Whalley et al. 1999). Of the six metals the EPA identified as posing a risk to human health, Cr and Al are the only ones that increased with increasing pH. While anionic species of Fe, Sb, Mn and V may exist in the environment, the pH range observed in the current study is most conducive to the existence of their cationic species (Goswami & Mahanta 2007; Jegadeesan et al., 2008; Komonweeraket et al., 2010).

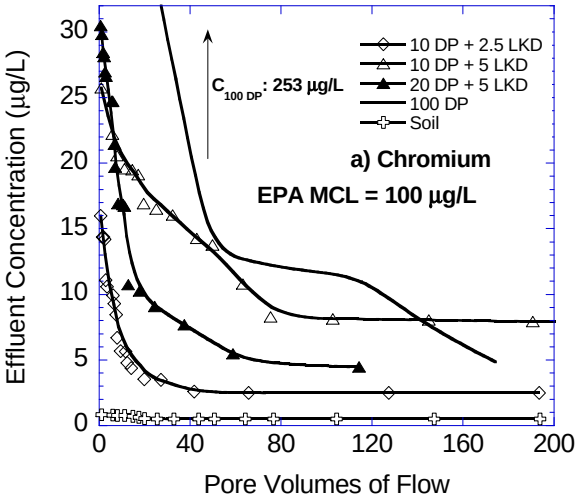
Effluent Concentration (µg/L)
Pore Volumes of Flow
10 DP + 2.5 LKD
10 DP + 5 LKD
20 DP + 5 LKD
100 DP
Soil
C100 DP: 253 µg/L
a) Chromium
EPA MCL = 100 µg/L

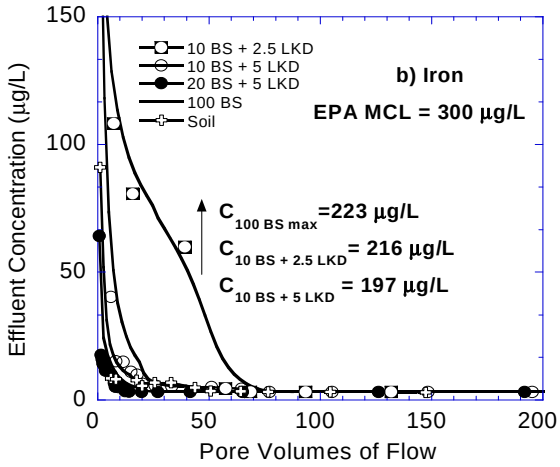
Effluent Concentration (µg/L)
Pore Volumes of Flow
10 BS + 2.5 LKD
10 BS + 5 LKD
20 BS + 5 LKD
100 BS
Soil
b) Iron
EPA MCL = 300 µg/L
C100 BS max=223 µg/L
C10 BS + 2.5 LKD= 216 µg/L
C10 BS + 5 LKD = 197 µg/L

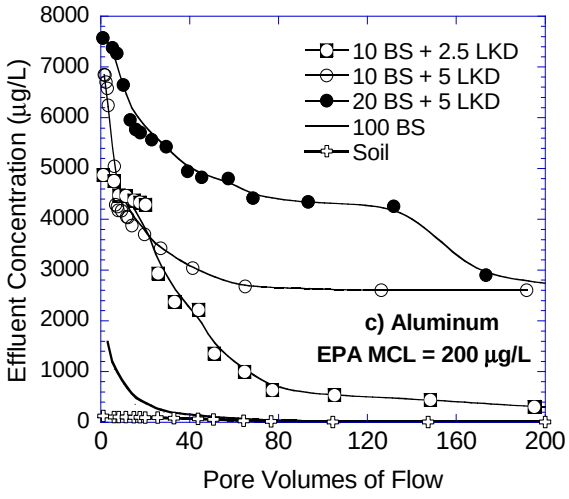
Effluent Concentration (µg/L)
Pore Volumes of Flow
10 BS + 2.5 LKD
10 BS + 5 LKD
20 BS + 5 LKD
100 BS
Soil
c) Aluminum
EPA MCL = 200 µg/L

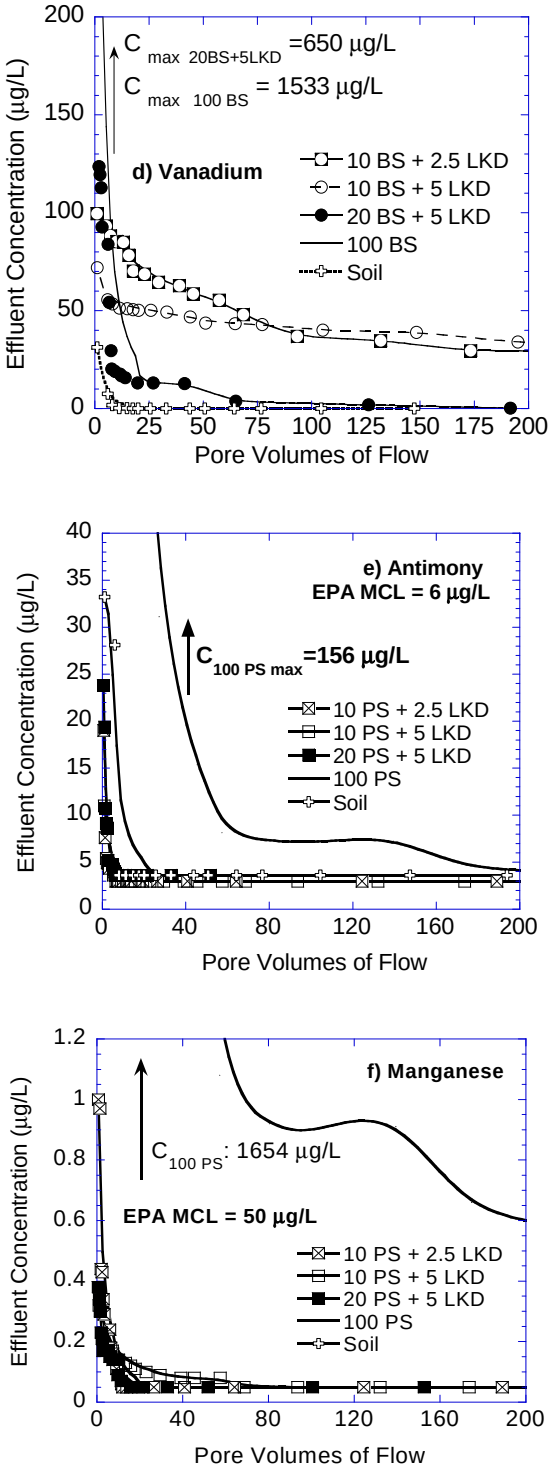

Figure 2.4 CLT elution curves for a) chromium, b) iron, c) aluminum, d) vanadium, e) antimony, and f) manganese.

When pH levels are basic, the availability of deprotonated (negatively charged) surfaces of the soil fly ash particles increases (Stumm & Morgan, 1996). This decreased availability may have led to an increase in adsorption of cationic species and caused a decrease in the concentrations of Cr, Fe, V, Sb, and Mn in the solution. Since the initial pH of the effluent was high, it probably enhanced the solubility of anionic species of Cr and Al because of unavailability of positively charged surface species for complexation. However, pH levels decreased from 12 to 10.5 after nearly 50-100 pore volumes of flow and caused a decrease in the solubility of anionic species of Al and Cr in the effluent solution.

The leaching of aluminum from the soil-fly ash mixtures is controlled by the solubility of aluminum hydroxides (Komonweeraket et al., 2010). The leaching behavior of Al shows an amphoteric pattern which represents higher leaching concentrations at extreme pH levels and lesser leaching concentration at neutral pH (Kenkel 2003 Langmuir 1997,). Tables 2.4 and 2.5 show that Al concentrations increased with an increase in LKD and fly ash contents, confirming an amphoteric pattern. Aluminum is very insoluble at neutral pH (Sparks, 2003); its solubility is controlled by dissolution-precipitation oxide and hydroxide minerals (Komonweeraket et al., 2010). This is in good agreement with other studies which showed that Al leaching is the lowest at neutral pH and highest under very alkaline conditions (Komonweeraket et al., 2010; Lim et al., 2004; Stumm & Morgan 1996).

Chemical compositions of the fly ashes based on total element analysis are also important to defining the metal leaching behavior. The Al content, for example, is high in

all three fly ashes (Table 2.3) resulting in significantly high Al concentrations in the effluent leachate. Similar to other metals studied, Al also showed the first flush leaching behavior mainly due to basic conditions at the initial pore volumes which probably enhanced the Al solubilization. Edil et al., (1992) and Chichester and Landsberg (1996) reported similar first-flush patterns for metals with high concentrations: A sharp decrease at early pore volumes of flow followed by flattening of the elution curves during column testing of soil-fly ash mixtures. Ogunro and Inyang (2003) also observed wash-out and detachment of Al and Cu by percolating solution during the initial stages of a column test. They attributed this phenomenon to an increase in the chemical potential which initiated the leaching of metals from the solid matrix into the surrounding solution. This increased chemical potential continued to occur until the concentration difference between the leachant and the solid material was reduced and a steady-state condition was reached.

Figure 2.4 shows that an increase in the initial Cr concentrations occurs with increasing fly ash content. This increase is probably due to the large amounts of Cr concentrations in the fly ash itself. At initial pore volumes of flow, relatively high levels of Cr were observed in mixtures that included 20% fly ash. However, after nearly 20 pore volumes of flow, the concentrations for all mixtures were comparable. Solubility of Cr is highly dependent on pH of the aqueous solution. Cr mobility is very low at a neutral pH, but the metal is very mobile at very acidic and basic conditions. As seen in Table 2.5, an increase in LKD caused an increase in pH and peak Cr concentrations in the effluent leachate. At high pH levels, Cr generally produces anionic species that cannot be retained

on the negatively charged fly ash surfaces. No testing was conducted to identify the oxidation state of Cr speciation in the leachate, Cornelis et al., (2008), however, claimed that Cr generally forms as Cr^{6+} in alkaline conditions and that insoluble Ca-Cr^{3+} minerals cause low concentrations of Cr^{3+} species such as $Cr(OH)^{-}_{4}$ at high pH levels. Speciation analyses conducted on sand-BS fly ash mixtures at pH=11 by Becker et al. (2011) support this claim. Cr^{3+} could be found only in the soil mixtures having high reduction potential, which may cause an increase in the concentrations of Cr^{3+} species in the aqueous solutions (Cornelis et al., 2008; Samaras et al., 2008). Ca–Cr^{3+} compounds may also exist in the effluent solutions with high pH levels, such as $Ca_2Cr_2O_5$ (Jing et al., 2006). At basic conditions, the solubility of $CaCrO_4$ is very high compared to other Cr containing compounds (Allison et al., 1991). On the other hand, most of the oxyanionic species tend to produce surface adsorption complexation with Fe oxides (Goswami & Mahanta, 2007). Dzombak and Morel (1990) showed that Cr^{3+} and Cr^{6+} can be released from Fe oxides at pH >12.5 and pH >7, respectively. Pourbaix diagrams for the Cr-O-H system indicate that Cr measured in WLT and CLT leachates is likely to exist as CrO_4^{-2} or $HCrO_4^{-}$ for the pH conditions present in the current study (pH= 10 to 12.5) (Brookins, 1988). Thus, it should be kept in mind that most of the Cr concentrations determined in the leachate are likely to be Cr^{6+} which is a concern to environmental safety (Whalley et al. 1999).

Table 2.5 shows that the leaching of Sb decreases with increasing pH, and increases with increasing fly ash amount most probably due to an increase in main metal source in the mixture. Leaching Sb significantly relates to the redox potential and pH

conditions of the aqueous solution. Cornelis et al. (2008) suggest that Sb^{5+} is more commonly found in alkaline waste leachates (where pH>10). However, Leuz et al. (2006b) suggest that the Sb^{3+} is oxidized faster and more completely than Sb^{5+} at high pH levels because of its lower solubility. Jackson et al. (1999) and Komonweeraket et al. (2010) found that Sb leachest most around neutral pH levels and decreases at extreme pH conditions; these results agree with the findings of this study.

There is growing interest in studying leaching behavior of V from fly ashes over the past years. Similar to antimony, V is also very redox- and pH-sensitive (Cornelis et al., 2008; Komonweeraket et al., 2010). Some oxidation states of V can form oxyanions at very alkaline conditions, which result in desorption of V from the soil surfaces. This desorption results from the negatively charged surfaces on the soil surface. Table 5 shows retention of total V is higher than the release of its oxyanionic species, which may be a cause in decrease in V concentrations with increasing LKD content (from 2.5% to 5% by weight). Since the oxidation states of both influent and effluent solutions were not constant, the oxidation states of V may fluctuate and may not transform into the oxyanionic vanadium species $V(OH)^{+}_{2}$, $VO(OH)^{+}_{2}$, VO^{-3}_{4}.

Concentrations of Fe and Mn in aqueous solutions decreased or remained nearly the same with increasing pH levels (Table 2.5). Both Mn oxides and Fe oxides are very important for the surface complexation of other oxyanions in the aqueous solutions (van der Hoek et al.,1996; Kumpiene et al., 2007; Piantone et al., 2004,). Most of the oxyanions can complex during the co-precipitation of iron metals in the vadose zone (Dixit & Hering 2003; Dutta et al. 2009; Jegadeesan et al. 2008; Peacock & Sherman

2004). Precipitation of Fe^{3+} starts as $Fe_x(OH)_y$ at pH > 6 (Cornelis et al., 2008; Dutta et al., 2009; Espana et al., 2005;) and metal adsorption of iron oxides increases with pH, causing a decrease in the effluent metal concentrations (Cornell & Schwertmann, 2003). The current study showed that both Mn and Fe concentrations decrease with pH, a result consistent with prior studies (Cornelis et al., 2008; Dutta et al., 2009; Komonweeraket et al., 2010).

2.5 COMPARISON OF WLTS AND CLTS

Comparisons were made between the WLT and CLT results. The peak effluent concentrations in the CLTs (C_i) are consistently higher than the WLT concentrations (C_w), as shown in Figure 2.5. Differences in Liquid:Solid ratio between the two leaching tests (a ratio of 20:1 in WLTs versus 0.1:1 in CLTs at the initial pore volume flows) could be responsible for the metal concentration differences measured in these two leaching tests. Figure 5 shows that C_i for Al is 2 times higher than C_w. Similarly, C_i for Cr, Fe, V, Sb and Mn are up to 20, 100, 10, 10, and 500 times higher than C_w, respectively. The lack of a linear relationship between C_W and C_i for most metals could be attributed to the variation in effluent pH levels. Bin Shafique et al. (2006) made similar observations during comparison of WLTs and CLTs.

The scale factors mentioned above should be used with caution as the testing conditions between the CLT and WLT were different. First, the liquid:solid ratio remains constant in WLTs but varies in CLTs (Ogunro & Inyang, 2003). Second, duration of tests must be considered. CLT is a dynamic test during which data fluctuate for an extended period of

time, while WLTs are finalized in 24 hours. The peak concentrations in CLTs typically occur in the transient stage, and may be different than the ones observed in WLTs.

Third, the water flows smoothly through the CLT set-up while the WLT samples are agitated aggressively. The agitation of WLT samples likely increases surface contact between the leaching solution and the solid particulates. This may result in both a higher leaching rate of the metals and a shorter period of time to the equilibrium state between the liquid and solid phases. The pH conditions may be influenced by this agitation and the dissolution of the mineral components of the metals that were tested. Because the speciation of Al, Cr, V, and Sb are highly dependent on redox conditions, the different environments for the two tests are likely to contribute to the difference in the test results.

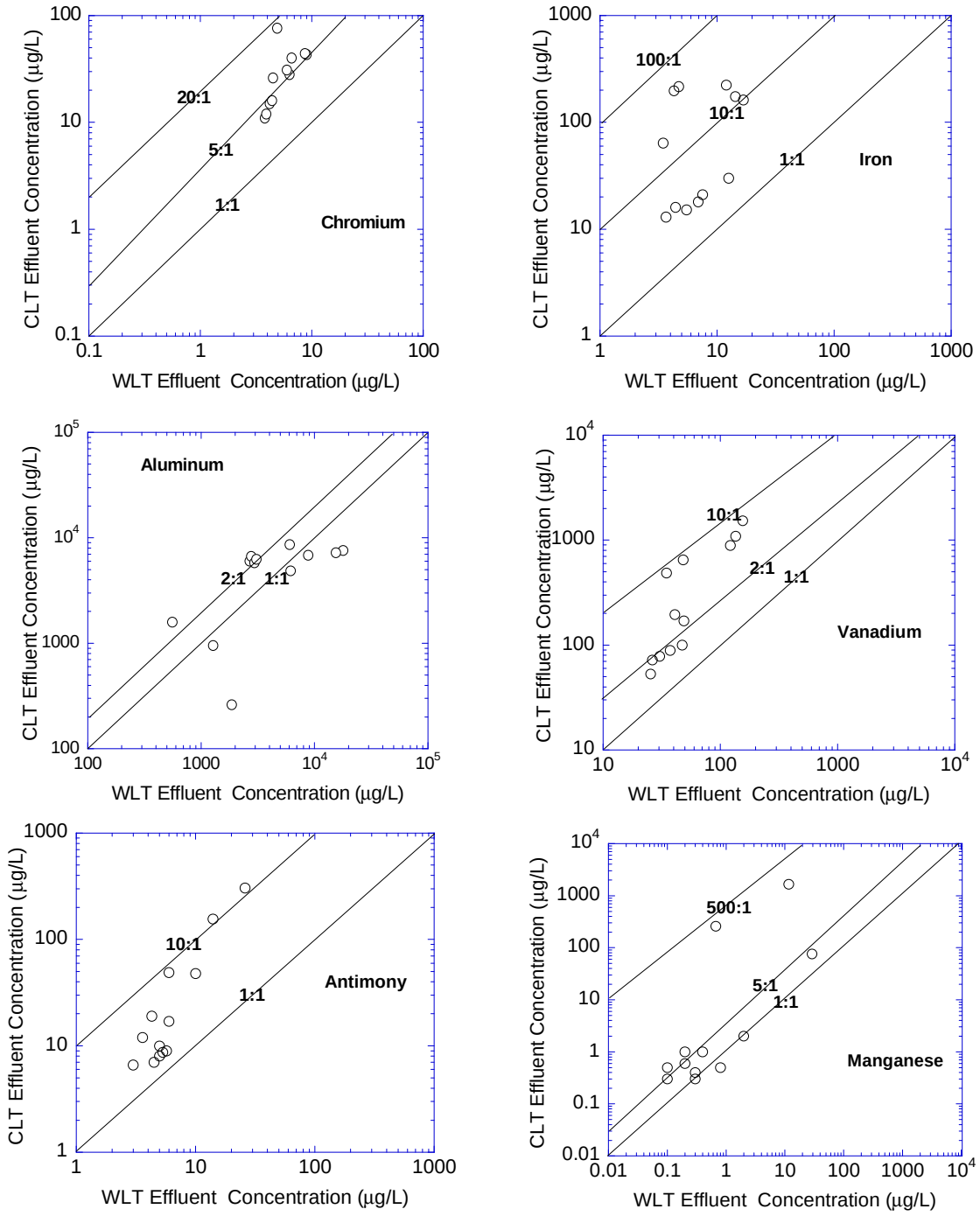

Figure 2.5 Comparison of peak effluent concentrations of six metals from the CLTs and the WLTs

2.6 CONCLUSIONS

A laboratory study was conducted to investigate the environmental feasibility of reusing chemically stabilized road surface material in construction of highway bases. Non-cementitious off-spec high-carbon fly ash was activated with lime kiln dust and used to stabilize an unpaved road material. The effects of both fly ash and lime kiln dust addition on environmental suitability of highway base layers were studied through laboratory leaching tests. The observations from the current study are as follows:

1. The concentrations of Cr, Sb, V, Mn, and Fe were below the EPA MCLs, WQLs and Maryland ATLs. Al was only the exception. It should be noted that Al is on the EPA list of secondary drinking water regulations, and there are no limits for Al specified in Maryland groundwater protection guidelines.
2. The initial pH values from CLTs were relatively higher than those measured in WLTs most likely due to a difference between the liquid-to-solid-ratio in two tests (a ratio of 20:1 in WLTs versus 0.1:1 in the initial PVFs in CLTs).
3. The metal concentrations increased with increasing fly ash content in WLTs, which may be a result of the increased total metal amount in the soil compound. The addition of fly ash caused an increase in pH values and in concentrations of Sb, V, Cr, Al and Mn.
4. The addition of lime kiln dust (LKD) had different effects on the leaching of the six metals analyzed. LKD addition caused a decrease in CLT concentrations of Fe, Sb, V, and Mn due to an increase on the negative surface charge of the solid

surface. Al and Cr concentrations, however, increased with LKD addition due to an increase in the solubility of their anionic species.

5. The release of all metals from the soil mixtures in CLTs exhibited a first-flush pattern followed by a decrease in concentrations. Most of the metals leached out at the initial stages, and steady-state conditions were reached within 10-120 pore volumes of flow. The higher initial pH values of the effluent solutions may have contributed to an increase in the solubility of anionic species, especially for Al and Cr.

An attempt was made to correlate CLT and WLT concentrations. The concentrations of Al, V, Fe, Sb, Cr, and Mn can be conservatively estimated from WLTs by multiplying the concentrations with 2, 10, 100, 10, 10, and 500, respectively. However, caution should be exercised in using these correlation factors as the testing conditions are different for these two systems, due to different liquid-to-solid ratios, test durations, and agitation motion in the batch procedure as compared to the relatively smooth fluid movement inside the column set-up.

3 EXPERIMENTAL AND NUMERICAL ANALYSIS OF METALS LEACHING FROM FLY-ASH AMENDED HIGHWAY BASES

3.1 INTRODUCTION

As mentioned in Chapter 2, use of conventional methods in highway constructions cause significant economic loss. Alternative uses of high-carbon fly ash (HCFA) amendment could provide a practical and economical solution for stabilization of the soil. However, the environmental suitability of these fly ashes must be evaluated due to the reasons explained previously.

The objective of this portion of the study was to evaluate the leaching potential of HCFA-stabilized highway base layers and to assess their potential impact on groundwater. Laboratory batch water leach and column leach tests, and computer modeling were used to make these assessments. Soils and HCFAs used in this part of the study but this part was focused on the leaching of four trace metals: barium (Ba), boron (B), copper (Cu) and zinc (Zn).

3.2 MATERIALS

The materials used in this part of the study were same as those described in Chapter 2. Some of the physical and chemical properties are repeated in Table 3.1.

Table 3.1 Physical and chemical properties of the materials used in current study. Chemical compositions and metal concentrations are based on X-ray fluorescence spectroscopy and total elemental analysis, respectively.

Property			Soil	Brandon Shores (BS) fly ash	Paul Smith (PS) fly ash	Dickerson Precipitator (DP) fly ash
Index Properties		G_s	2.64	2.17	2.2	2.37
		w_{opt} (%)	13.4	26	22	36
		$\gamma_{d\ max}$ (kN/m^3/pcf)	18.8 (120)	11.9 (76)	10 (64)	9.9 (63)
		PI (%)	NP	NP	NP	NP
Chemical Properties	Chemical Composition (%)	LOI	NA	13.4	10.7	20.5
		SiO_2	NA	45.1	50.8	35
		Al_2O_3	NA	23.1	26.9	24.4
		Fe_eO_3	NA	3.16	5.5	12.6
		CaO	NA	7.8	0.7	3.2
	Total Metal Concentration (mg/L)	Barium	4.62	13.7	30	19.7
		Boron	2.86	17.3	45.3	24.5
		Copper	1.28	74.7	25.3	58.7
		Zinc	82.3	58.2	28.5	45.6
		pH	6.5	9.6	7.6	8.8

Note: LOI: Loss on ignition. G_s: Specific gravity, w_{optm}: Optimum water content, γ_{dmax}: Maximum dry unit weight, NP: Nonplastic, NA: Not available.

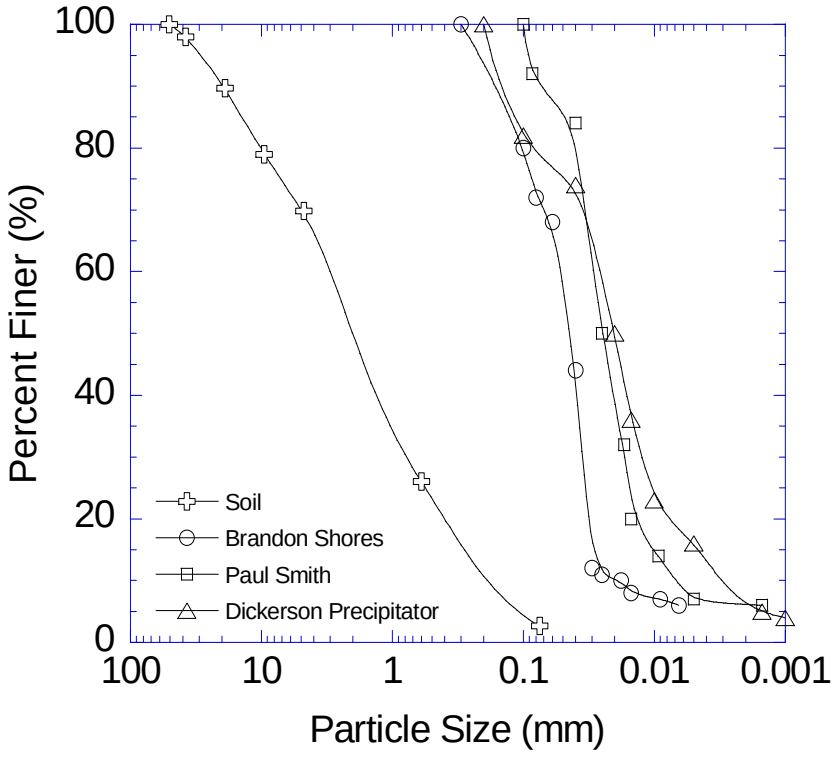

Figure 3.1 Particle size distributions of soil and fly ashes.

3.3 METHODS

3.3.1 Chemical Analysis

The procedures listed in Chapter 2 were also used to conduct water leach tests and column leach tests in this chapter. The metals selected for analysis, however, differ (this chapter focuses on Ba, B, Cu, and Zn). These metals were selected because of their potential risk to the environment and animal/human health, and because of their range of mobilities in groundwater (Bankowski et al., 2004; Chavez et al. 2010; Goswami & Mahanta 2007; Jankowski et al. 2006; Kim et al., 2006; Praharaj et al., 2002; Quina et al., 2010). For example, acute excessive exposure to B may cause rapid respiration, eye inflammation, swelling of the paws, and may even affect male reproductive organs of animals (Ischii et al., 1993; Wegman et al., 1994; US-EPA, 2008). In human adults, B can cause nausea, vomiting, skin redness, difficulty swallowing, and diarrhea. Long-term Ba exposure may cause hypertension in humans (Perry et al. 1989; Wones et al., 1990). Exposure to K with Ba may cause detrimental cardiac and skeletal effects in human body (US EPA 1990). Furthermore, Cu and Zn are both very soluble and non-biodeagrable. Furthermore, Cu and Zn can accumulate in animals, plants, and humans during an extended exposure (Elsayed-Ali et al. 2011; Svilovic et al. 2009).

The total elemental analyses method covers the digestion and analysis of fly ash samples for major and minor element contents by using an ICP-OES (Thermo Jarrell Ash IRIS Advantage Inductively Coupled Plasma Optical Emission Spectrometer). The digestion process began by weighing the sample in a 50-mL glass digestion tube. 5 mL of concentrated HNO_3 (trace element grade) was added to each tube and the tubes were

then loosely capped and placed on a digestion block heated to 120^0 C. The fly ash and soil samples were digested for 15-16 hours at 120^0 C and removed from the block. After cooling, 1mL of H_2O_2 was added to each tube and the tubes were put back on the block for 30 min. The last step was repeated twice and as the samples were removed from the block and allowed to cool down during each cycle. The sample volume was brought to 50 mL, mixed and allowed to sit for 3 hours before analysis on the ICP-OES was performed.

The concentrations of all metals were determined by inductively coupled plasma optical emission spectroscopy (ICP-OES) using a Varian Vista-MPX CCD Simultaneous ICP-OES instrument. All sampling equipment that came into contact with leachate samples was cleaned with acid, dried, and stored in clean, sealed bags. Blanks were run after each 10-20 analyses and calibration was verified after each 10 analyses. A reagent blank was tested after each 20 samples and a spiked sample was analyzed after each 10 samples. Minimum detection limits (MDLs) for ICP-OES were determined for each metal and each set of calibration standards according to the U.S. Code of Federal Regulations Title 40. The MDLs for Ba, B, Cu, and Zn were determined to be 2 µg/L, 4 µg/L, 0.7 µg/L, and 1 µg/L, respectively.

3.3.2 Chemical Transport Modeling

The transportation of metals in a highway environment was simulated using WiscLEACH, a reliable algorithm for simulating water and solute movement in two-dimensional variably saturated media (Li et al., 2007). Three analytical solutions to the advection-dispersion-reaction equation are combined in WiscLEACH to develop a

method for assessing effects to groundwater caused by trace elements leaching from fly ashes used in highway layers. The analytical method in WiscLEACH has been verified with the predictions made with HYDRUS-2D, a well-known software package for simulating flow and transport in variably saturated media (Li et al., 2007).

WiscLEACH simulated the locations of maximum soil vadose zones and groundwater concentrations (e.g., at the centerline of the pavement structure, at the vicinity of point of compliance) and contours of trace metals were developed at different years as a function of depth to groundwater, thickness of the base layer, percent fly ash by weight, hydraulic conductivity of the base layer, hydraulic conductivity of the aquifer material and initial concentration of the metal in the fly ash (Figure 3.2). Model inputs included annual Maryland precipitation rates obtained from National Weather Service records. Additionally, points of compliance and physical properties of pavement layers were selected according to the SHA roadway design manual (2004). Finally, transport parameters and hydraulic conductivities were determined in the current laboratory study.

WiscLEACH assumes all materials in the profile are homogeneous and isotropic. Precipitation falling on the pavement's surface, shoulders, and surrounding ground infiltrates into the ground or is shed as runoff (Li et al., 2007). As water flows through the profile, trace elements leach from the fly ash and migrate toward subgrade soils until they reach the ground water table. Flow in the fly ash and subgrade is assumed to occur only in the vertical direction. Steady 1D unit gradient flow is assumed in the pavement layers and the vadose zone, with the net infiltration rate controlled by the least conductive layer in the profile and the annual precipitation rate. Surface runoff and evaporation from the

pavement surface, the shoulders, and the surrounding ground were not considered. Infiltration of runoff along the edges of the pavement structure is ignored.

Transport in the vadose zone beneath the fly ash layer was assumed to follow the advection-dispersion-reaction equation (ADRE) for 1D steady state vertical flow with 2D dispersion and linear, instantaneous, and reversible sorption. Trace elements that reach the groundwater table are transported horizontally and vertically through the groundwater flow, although the flow of ground water is assumed to occur predominantly in the horizontal direction. Steady saturated groundwater flow is assumed, and transport in groundwater is assumed to follow the ADRE with instantaneous, reversible, and linear sorption. Chemical and biological reactions that may consume or transform trace elements are assumed to be absent. In addition, flow in the fly ash and subgrade is assumed to occur only in the vertical direction. Steady 1D unit gradient flow is assumed in the pavement layers and the vadose zone, with the net infiltration rate controlled by the least conductive layer in the profile and the annual precipitation rate. Transverse flow on top of the subgrade toward the edge of the road structure is ignored.

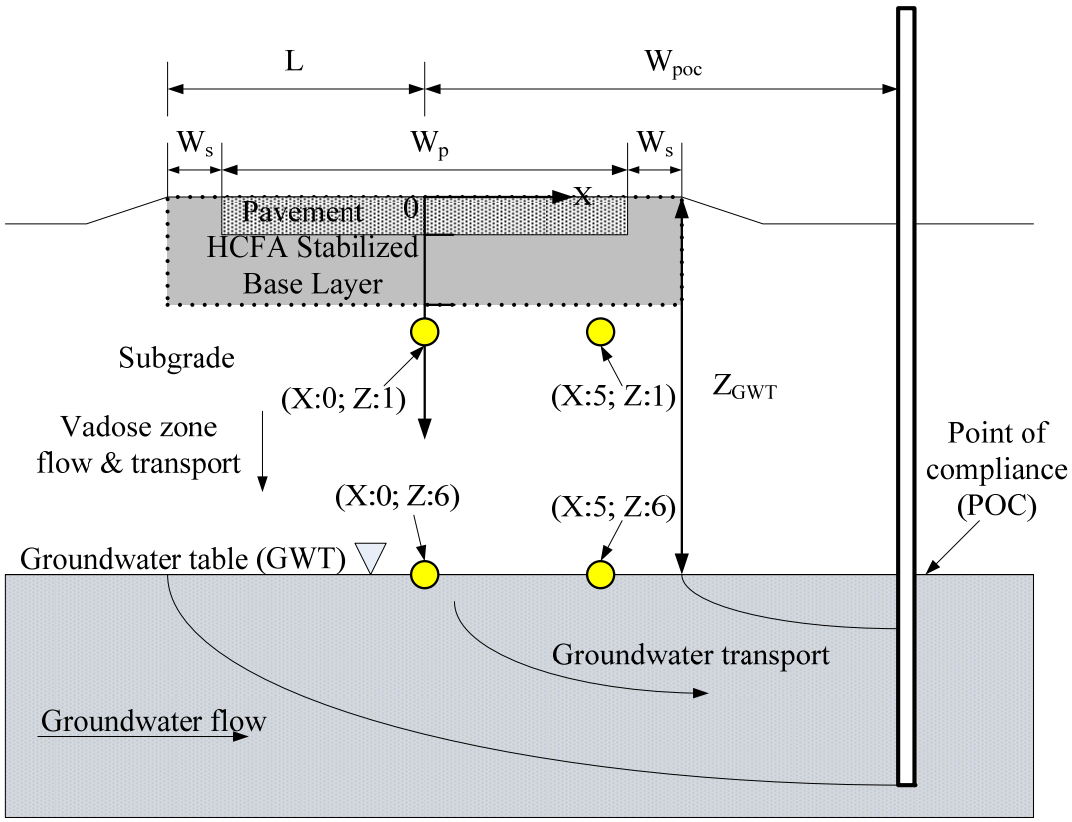

Figure 3.2 Conceptual model in WiscLeach for predicting impacts to the vadose zone and groundwater from HCFA stabilized highway base layer,

3.3.3 Model Formulation in Vadose Zone

WiscLEACH considers only steady 1D unit gradient flow in pavement layers and the soil vadose zone. The rate of flow, q_v, is determined by the comparison of the least conductive layer in the profile and the annual precipitation rate. The program uses the lowest of these values as the rate of flow. It is assumed that possible horizontal movement of the flow is ignored, whereas the rate of vertical flow may change with depth. The net infiltration rate, however, is assumed to equal q_v. No water loss is assumed -- the water is assumed to infiltrate the soil vadose zone toward groundwater without any loss on the pavement and ground surface. Surface runoff and evaporation from the pavement surface are ignored (Li et al., 2007). In the current study, the leaching pattern is first-flush leaching from the HCFA-stabilized base layer. In WiscLEACH a first-flush leaching from the HCFA base layer is assumed to follow the ADRE with linear, instantaneous, and reversible sorption (Li et al., 2007).

In WiscLEACH, transport in the vadose zone beneath the HCFA layer is assumed to follow the ADRE for 1D steady state vertical flow with 2D dispersion and linear, instantaneous and reversible sorption (Li et al., 2007).

$$\boldsymbol{R\frac{\partial c}{\partial t} = D_x\frac{\partial^2 c}{\partial x^2} + D_z\frac{\partial^2 c}{\partial z^2} - \vartheta_z\frac{\partial c}{\partial z}} \qquad (1)$$

where C is metal concentration, T is time, x is horizontal distance from the centerline of the pavement, z is depth below ground surface, v_z is seepage velocity in vertical direction,

D_x is dispersion coefficient in x direction, D_z is dispersion coefficient in z direction and R is retardation factor.

The analytical solution to Equation 1 is obtained by applying the following initial and boundary conditions (Li et al., 2007):

$$\boldsymbol{C(x,z,t=0)} = \begin{cases} \boldsymbol{C_0} & \boldsymbol{at\ z_t < z < z_B \quad and -L < x < L} \\ \boldsymbol{0} & \boldsymbol{otherwise} \end{cases} \tag{2a}$$

$$\boldsymbol{\vartheta_z C - D_z \frac{dC}{\partial z}\Big|_{z=0} = 0} \tag{2b}$$

$$\boldsymbol{\frac{\partial c}{\partial x}(\pm\infty, z, t) = 0} \tag{2c}$$

$$\boldsymbol{\frac{\partial c}{\partial z} = (x, \infty, t) = 0} \tag{2d}$$

where C_o is initial metal concentration, Z_T is depth of the top of the fly ash stabilized layer, Z_B is depth of the bottom of the fly ash stabilized base layer, L is sum of the shoulder and half of the pavement width.

Equations 2a and 2b indicate the HFCA-stabilized base layer is the only source of trace elements and that no trace elements leached from the pavements or ground surface above the base layer. Equations 2c and 2d imply that the effect of dispersion and diffusion in the soil vadose zone is insignificant with a distance from the pavement surface and the centerline of the pavement structure. The analytical solution to Equations 1 and 2 is (Li et al., 2007):

$$C(x,z,t) = \frac{C_0}{4}\left\{ e^{\left(\frac{\vartheta_z z}{D_z}\right)} \left[\left(\frac{1+\vartheta_z z}{D_z}\left(z + z_T + \frac{\vartheta_z t}{R}\right)\right) x erfc\left(\frac{R(z+z_T)+\vartheta_z t}{\sqrt{4RD_z t}}\right)\right] - exp\left(\frac{\vartheta_z z}{D_z}\right) x\left[\left(1 + \frac{\vartheta_z}{D_z}\left(z + z_B + \frac{\vartheta_z t}{R}\right)\right) erfc\left(\frac{R(z+z_B)+\vartheta_z t}{\sqrt{4RD_z t}}\right)\right] + erfc\left(\frac{R(z-z_B)-\vartheta_z t}{\sqrt{4RD_z t}}\right) - erfc\left(\frac{R(z-z_T)-v_z t}{\sqrt{4RD_z t}}\right) + \sqrt{\frac{4v_z^2 t}{\pi RD_z}} \exp\left(\frac{v_z z}{D_z}\right)\left[exp\left(-\frac{[R(z-z_B)+v_z t]^2}{4RD_z t}\right) - exp\left(-\frac{[R(z+z_T)+\vartheta_z t]^2}{4RD_z t}\right)\right]\right\} x \left[erfc\left(\frac{x-L}{\sqrt{\frac{4D_x t}{R}}}\right) - erfc\left(\frac{x+L}{\sqrt{\frac{4D_x t}{R}}}\right)\right]$$

(3)

Equation 3 is applied from the surface of the pavement to the groundwater table (Fig. 3.2).

3.3.4 Model Formulation in Groundwater

Transportation of trace metal elements into the groundwater is horizontal and vertical, although the direction of horizontal flow movement is dominant in the groundwater (Li et al., 2007). The groundwater flow is assumed to be saturated, and the transport of the trace elements is assumed to follow the ADRE with instantaneous, reversible, and linear sorption as assumed in transportation in soil vadose zone (Li et al. 2007).

$$R_w \frac{\partial C}{\partial t} = D_{xw} \frac{\partial^2 C}{\partial x^2} - \vartheta_h \frac{\partial C}{\partial x} + D_{zw} \frac{\partial^2 C}{\partial z^2} - \vartheta_z \frac{\partial C}{\partial z} \quad (4)$$

Where C is metal concentration, T is time, v_h is groundwater seepage velocity in the horizontal direction, D_{xy} is hydrodynamic dispersion coefficient in horizontal direction,

D_{zw} is hydrodynamic dispersion coefficient in vertical direction, R_w is retardation factor in groundwater.

In Equation 4, cross-dispersion terms are ignored because of the dominant horizontal flow of groundwater in a uniform and isotropic medium (Li et al., 2007). An analytical solution to Equation 4 for the following initial and boundary conditions:

$$\boldsymbol{C(x,z,t=0)=0} \quad (5a)$$

$$\left(\vartheta_z C - D_{zw}\frac{\partial C}{\partial z}\right)\Big|_{z=z_{GWT}} = f(x) = \begin{cases} \vartheta_z g(x, z_{GWT}, t), & x_1 < x < x_2 \\ 0, & otherwise \end{cases} \quad (5b)$$

$$\frac{\partial C}{\partial x}(\pm\infty, z, t) = 0 \quad (5c)$$

$$\frac{\partial C}{\partial z}(x, \infty, t) = 0 \quad (5d)$$

where z_{gwt} is depth of groundwater table, g(t) is metal concentration at the groundwater table and x_1, x_2 arelateral extents over g(t) applies.

It is assumed that, at the beginning, groundwater is not contaminated by trace or other elements that can affect the sorption of trace elements (suggested by Equation 5a). Equation 5b indicates that the amount of trace elements in the vadose zone of the soil directly above the groundwater table is equal to the amount in the groundwater. Equations 5c and 5d indicate that the effect of diffusion and dispersion in groundwater can be ignored at locations far from the centerline of the pavement-groundwater table. The solution to Equations 4 and 5 for a condition if Z is larger than Z_{GWT} is (Li et al. 2007):

$$C(x,z,t) = \int_0^t \frac{\vartheta_z g(t-\tau)}{2R_w}\left[erfc\left(\frac{R_w(x-x_2)-\vartheta_{/\!/}\tau}{\sqrt{4R_w D_{xw}\tau}}\right) - erfc\left(\frac{R_w(x-x_1)-\vartheta_{/\!/}\tau}{\sqrt{4R_w D_{xw}\tau}}\right)\right] x$$
$$\left[\sqrt{\frac{R_w}{\pi D_{zw}\tau}}\, exp\left(-\frac{(R_w(z-z_{GWT})-\vartheta_z\tau)^2}{4R_w D_{zw}\tau}\right) - \frac{\vartheta_z}{2D_{zw}}\, exp\left(\frac{v_z(z-z_{GWT})}{D_{zw}}\right)\right.$$
$$\left. xerfc\left(\frac{R_w(z-z_{GWT})+\vartheta_z\tau}{\sqrt{4R_w D_{zw}\tau}}\right)\right] \qquad (6)$$

Equation 6 estimates the metal concentrations that leached from a line source at the groundwater table between X_1 and X_2.

3.4 RESULTS OF WATER LEACH TESTS

WLT concentrations of four metals (Ba, B, Cu, and Zn) for all mixtures are shown in Table 2. All concentrations are below the EPA maximum concentration limits for drinking water (MCLs). The results show that fly ashes alone yielded higher metal concentrations (with the exception of Zn) than soil-fly ash–LKD mixtures. Based on total element analysis (TEA), the BS fly ash had the highest concentrations of Cu and Zn, and Ps fly ash had the highest concentrations of Ba and B (Table 3.1). However, no consistent relationship exists between TEA-based and WLT-based metal concentrations manifested. This lack of consistent relationships indicates that leaching of metals is dependent on the metals' concentrations in the main source and other factors, such as pH levels and electrical conductivity.

The variation in concentrations of these four metals was plotted against fly ash content for mixtures prepared with 5% LKD in Figure 3.3. The data for soil only (0% fly ash content0 as well as fly ash only (0% soil content) were added for comparison

purposes. Ba, B, and Cu showed similar trends. The concentrations of these three metals generally increased with an increase in fly ash content. Figure 3.3 indicates that the rate of increase in Ba, B, and Cu concentrations in the effluent solutions was generally higher when the fly ash content was increased from 0% to 10% than when fly ash content was increased from 10% to 20%. For the soil-fly ash-LKD mixtures, higher ash content generally yielded higher effluent concentrations of Ba, B, and Cu because the fly ash used in the analyses contained high amounts of these metals (Table 3.1). However, the linear dilution calculations cannot be used because the rate of increase in metal concentrations in the mixtures was not consistent with the increase in fly ash content.

Figure 3.3 shows that as fly ash content increases, Zn concentration decrease because soil contains higher amounts of Zn than the three fly ashes (based on total elemental analyses). On the other hand, an increase in LKD content from 2.5% to 5% increased the Zn concentrations in the aqueous solution even under moderate increases in pH leels (Table 3.3 and Figure 3.4). Goh and Tay (1993) and Ghosh and Subbaroa (1998) also showed that Zn concentrations increased when pH was increased from 9 to 12.

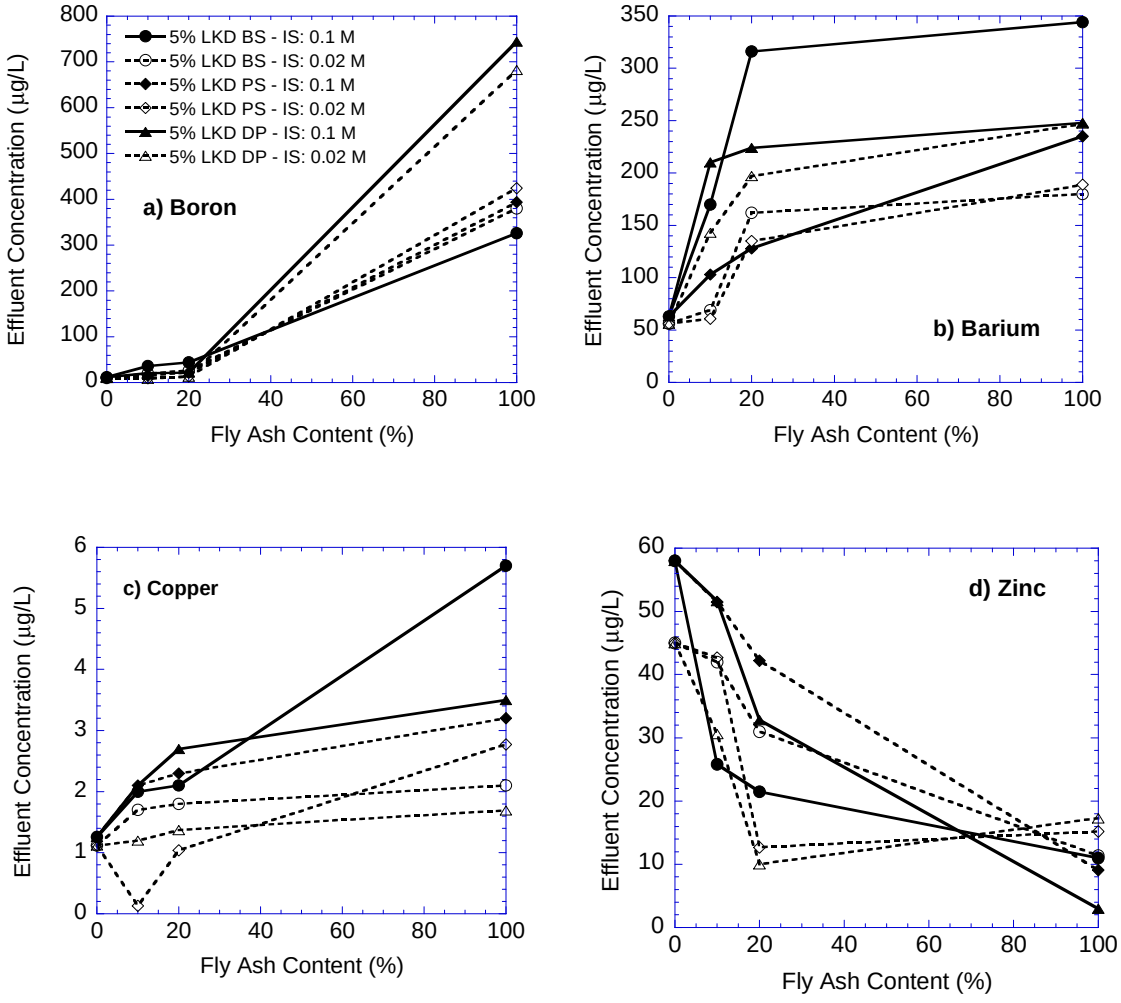

Figure 3.3 Effect of fly ash content on effluent concentrations of a) boron, b) barium, c) copper, and d) zinc in WLTs. 0% and 100% fly ash content corresponds to soil only and fly ash only specimens, respectively.

It is widely known that Ba, B, and Cu follow a cationic pattern where the concentrations of these metals decrease dramatically with increasing pH (Komonweeraket et al. 2010). Since an increase in LKD caused an increase in pH of the solution, decreased levels of Ba, B, and Cu concentrations was expected and found, as seen in Figure 3.4. Similar observations were made by Karuppiah and Gupta (1997), Jankowski et al., (2006), and Liu et al., (2008). Conversely, Zn tends to follow an amphoteric pattern, which indicates that the metals leach the most at extreme pH levels and leach the least at neutral pH (Komonweeraket et al. 2010; Lim et al., 2004 ; Ricou et al., 1999). Jegadeesan et al., (2008) showed that a Zn's decreased leaching at lower pH levels is due to its surface complexation with Fe-Al-oxide or silicate material or the formation of insoluble hydroxides. Furthermore, beyond neutral pH levels, Zn begins to precipitate as $Zn(OH)_2$. It dissolves completely under very alkaline conditions as $Zn(OH)_3^-$ (Cotton & Wilkinson, 1999). The cationic pattern for Ba, B, and Cu and the amphoteric pattern for Zn can be clearly observed when the WLT concentrations are plotted against pH (Figure 3.5).

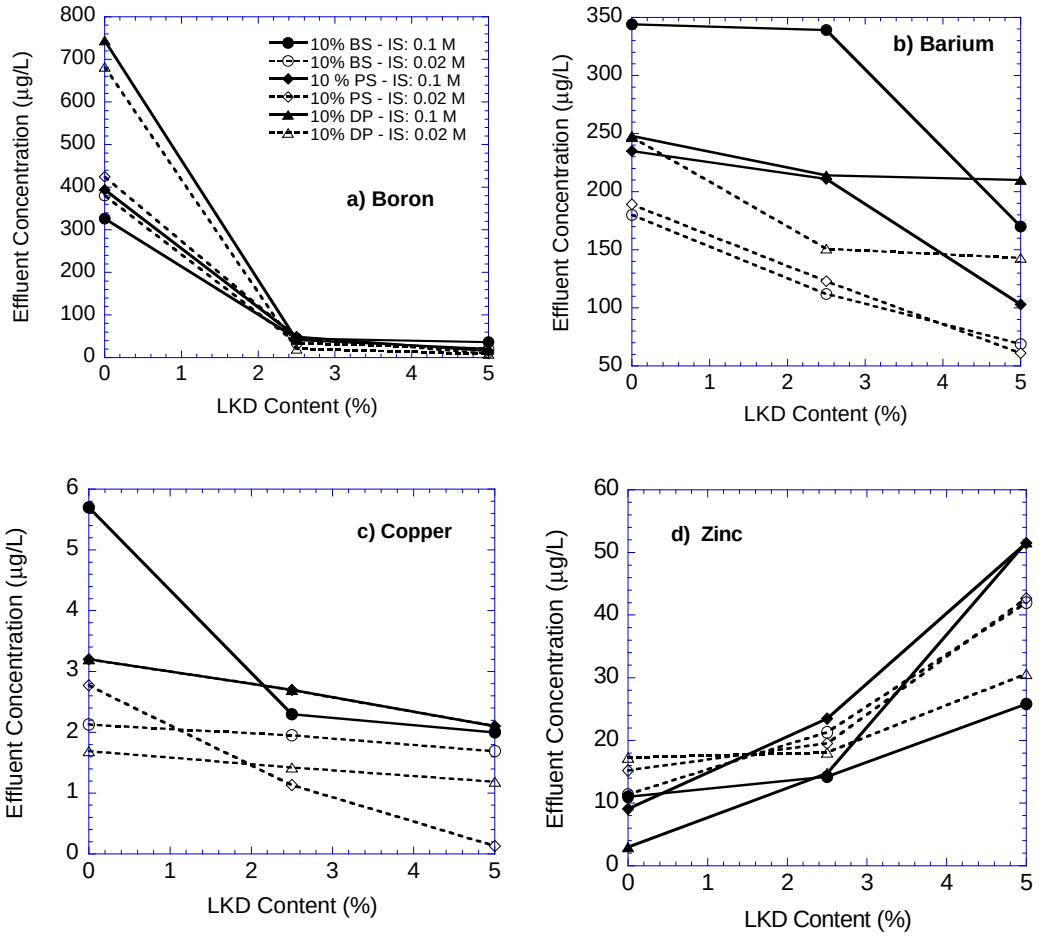

Figure 3.4 Effect of lime kiln dust content on effluent concentrations of a) boron, b) barium, c) copper, and d) zinc in WLTs. 0% lime kiln dust content corresponds to fly ash only.

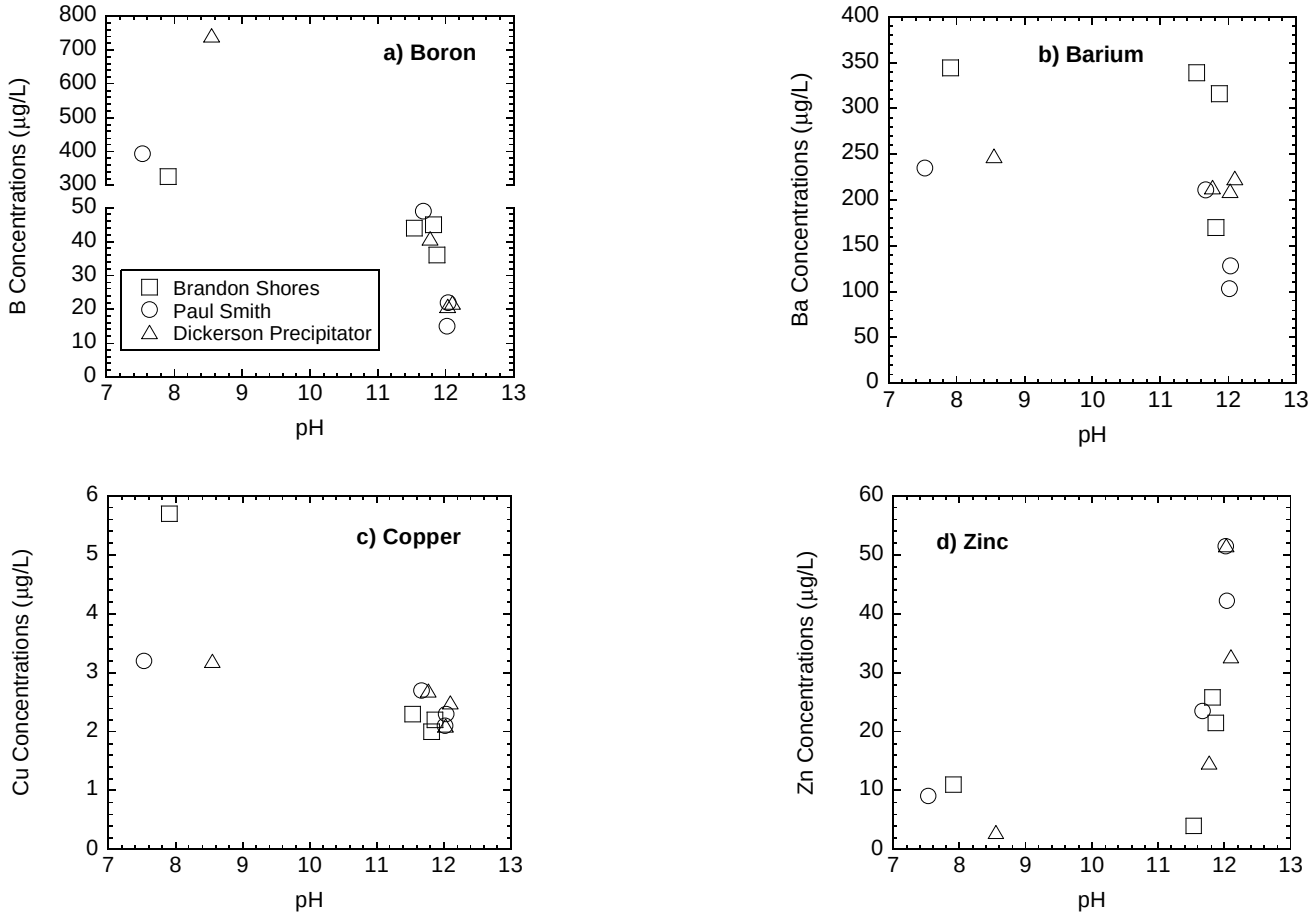

Figure 3.5 Effect of pH on effluent concentrations of a) boron, b) barium, c) copper, and d) zinc in WLTs.

Table 3.2 Aqueous concentrations of metals from WLTs.

Specimen Name	Fly Ash Content (%)	LKD Content (%)	$pH^{IS=0.1}$	$pH^{IS=0.02}$	Barium (µg/L)		Boron (µg/L)		Copper (µg/L)		Zinc (µg/L)	
					$C_{aq}^{IS=0.1}$	$C_{aq}^{IS=0.02}$	$C_{aq}^{IS=0.1}$	$C_{aq}^{IS=0.02}$	$C_{aq}^{IS=0.1}$	$C_{aq}^{IS=0.02}$	C_{aq}^{NaBr}	C_{aq}^{DI}
100 BS	100	-	7.9	8.1	344	180	326	380	5.7	2.1	11	11
10 BS + 2.5 LKD	10	2.5	11.5	11.6	339	112	44	34	2.3	1.9	14	21
10 BS + 5 LKD	10	5	11.8	11.8	170	69	45	26	2.0	1.7	26	42
20 BS + 5 LKD	20	5	11.8	11.9	316	162	36	20	2.2	1..8	22	31
100 PS	100	-	7.5	7.8	235	189	394	424	3.2	2.8	9.1	15
10 PS + 2.5 LKD	10	2.5	11.7	11.7	211	123	49	46	2.7	1.1	24	20
10 PS + 5 LKD	10	5	12	11.9	103	61	15	9.4	2.1	0.13	52	43
20 PS + 5 LKD	20	5	12	12.1	128	135	22	14	2.3	1.1	42	13
100 DP	100	-	8.6	8.7	248	247	744	682	3.2	1.7	3	17
10 DP + 2.5 LKD	10	2.5	11.8	11.9	214	151	41	21	2.7	1.4	15	18
10 DP + 5 LKD	10	5	12	12	210	143	21	8	2.1	1.2	52	31
20 DP + 5 LKD	20	5	12.1	12	224	197	22	13	2.5	1.4	33	10
Soil	100	-	4.8	5.1	63	56	12	10	1.3	1.1	58	45
U.S. EPA MCL (µg / L)					2000		NA		1300		5000	

Notes: MCL: maximum contaminant levels for drinking water; NA: Not available.

Table 3.3 Peak effluent concentrations of Ba, B, Cu, and Zn for column leach tests and pH at peak concentrations. Concentrations exceeding MCLs in **bold**.

Specimen Name	Fly Ash Content (%)	LKD Content (%)	pH	Barium (µg/L)	Boron (µg/L)	Copper (µg/L)	Zinc (µg/L)
100 BS	100	-	8.6	1507	15000	26	128
10 BS + 2.5 LKD	10	2.5	12.1	1030	590	25	92
10 BS + 5 LKD	10	5	12.5	590	225	15	113
20 BS + 5 LKD	20	5	12.5	**2220**	2227	57	51
100 PS	100	-	7.6	1460	26400	43	129
10 PS + 2.5 LKD	10	2.5	12.3	677	539	15	141
10 PS + 5 LKD	10	5	12.5	334	314	9	151
20 PS + 5 LKD	20	5	12.5	1263	599	40	88
100 DP	100	-	7.9	**3193**	11900	181	78
10 DP + 2.5 LKD	10	2.5	12.1	1444	568	18	64
10 DP + 5 LKD	10	5	12.4	377	174	17	94
20 DP + 5 LKD	20	5	12.6	**2038**	291	24	60
Soil	100	-	6.5	209	112	49	258
U.S. EPA MCL (µg / L)				2000	NA	1300	5000

Notes: MCL:maximum contaminant levels for drinking water; NA: Not available.

The data in Table 3.2 suggest that the pH levels of WLT effluents are not affected by the change in ionic strength of the influent solutions. Metal leaching, however, was generally enhanced by an increase in ionic strength of influent solution. An increase in Na^+ concentrations in the soil matrix by adjusting ionic strength from 0.02 M to 0.1 M may have decreased the surface negativity of the fly ash and soil particles, which released the Ba^{2+}, B^+, Cu^{2+} and Zn^{2+} ions from the solid surface into the aqueous solution by electrostatic effects (Sparks 2003). Praharaj et al., (2002) claimed that the surface area of the fly ash particles decrease and coarseness of the particles increase upon leaching. These changes may have contributed to a decrease on the active surface sites and caused the loosely attached soluble species to be released into the aqueous solution.

3.5 RESULTS OF COLUMN LEACH TESTS

CLTs were conducted on soil alone, fly ash alone and soil-fly ash-LKD mixtures to evaluate the leaching of metals under flow-through conditions. All CLTs continued until the pH levels of the effluent solutions stabilized and a minimum of 200 pore volumes of flow was observed. Levels of pH of influent solutions was kept between 6.5 and 7 to simulate typical field conditions in Maryland. Levels of pH of effluent solutions were relatively high (pH=11-12) compared to that of influent solution because of the release of CaO from LKD (Wehrer & Totsche, 2008). Table 3.3 shows that an increase in fly ash content did not influence effluent pH levels. The effect of LKD addition on effluent pH levels was more pronounced because of the higher CaO content of LKD compared to fly ashes (60% versus 0.7-7.8%). Small amounts of LKD addition (2.5% by weight)

increased the pH of soil by ~5.6 pH units and further addition of LKD had a moderate effect on pH increase.

The peak CLT concentrations of four metals for all specimens are shown in Table 3.3. Most concentrations are below the EPA maximum concentration limits. The exception was the Ba concentrations for 100% Dickerson Precipitator fly ash and two mixtures. Maryland aquatic chronic toxicity limit for copper in fresh water was exceeded for all specimens, whereas 38% of the specimens exhibited Zn concentrations above the Maryland ATLs.

Figure 3.6 shows a series of CLT elution curves. The elution curves for all mixtures are not presented herein for brevity. All specimens exhibited a first-flush leaching pattern, consistent with the past studies (Chichester & Landsberger, 1996; Sauer et al., 2005). The first-flush pattern generally occurs for metals with cationic species. An LKD addition may have caused significant release of CaO into the aqueous solution, which may have contributed to the existence of such a leaching pattern. At initial CLT leach stages, most metals were probably washed out and released from the surface of the fly ash and soil particles into the aqueous solution until the concentration difference between the metal source and aqueous solution was reduced (Ogunro & Inyang, 2003). A first-flush pattern is expected for B since the metal is usually attached onto the fly ash and soil particles and because it remains present in the water–soluble fraction (which increases its leaching rate significantly) (Jankowski et al., 2006).

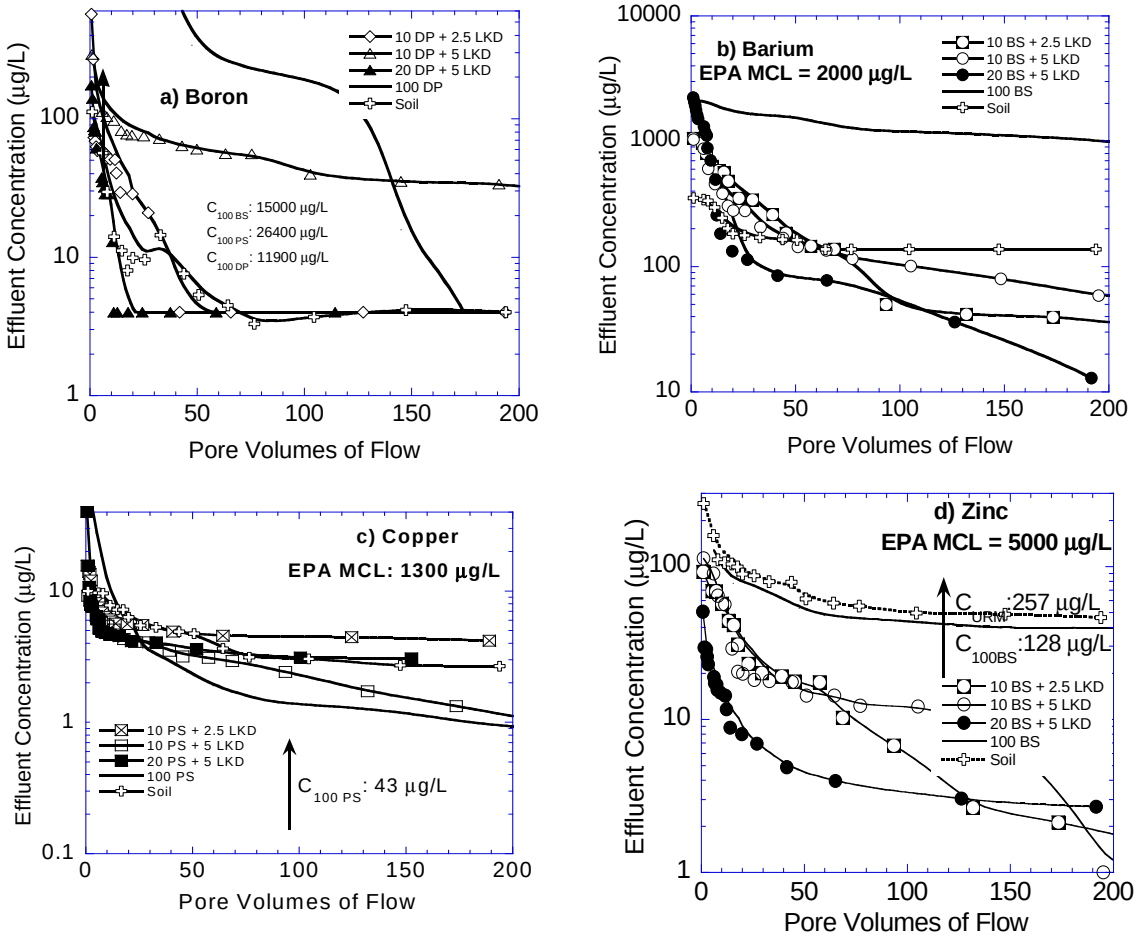

Figure 3.6 CLT elution curves for a) boron, b) barium, c) copper, and d) zinc.

The solubilities of all four metals are highly dependent on effluent pH levels. Table 3.3 shows that pH levels of the mixtures was high (pH> 11.5), which indicates a basic effluent solution. It is recognized in previous studies that the solubility of Cu decreases significantly with increasing pH (Goswami & Mahanta, 2007; Liu et al., 2008; Ricou et al., 1999; Yan et al., 2001). It is assumed that Cu is either included in low-solubility minerals or fixed in precipitates in alkaline conditions (Wehrer & Totsche, 2008), which is consistent with the findings obtained in this study. As seen in Table 3.3, an increase in LKD amount from 2.5% to 5% by weight increased the effluent pH level. This increase in the effluent pH level may have resulted in reduced Cu concentrations in the aqueous solution because of the adsorption of Cu metals onto the fly ash surface (Sparks 2003). Jegadeesan et al., (2008) showed that leaching of cationic metals such as Cu can be very low under alkaline conditions (pH > 10). Material amendments into soils that include Fe oxides and alkaline materials can also reduce the mobility and availability of metals in soil by adsorption, complexation, precipitation or combination (Brown at al. 2005, Kumpiene et al. 2007). The relatively high amounts of Fe_2O_3 (3.16-12.6% by weight, see Table 3.1) may have enhanced the sorption of Cu, thereby causing a reduction in metal concentrations in the current study

The highest Zn concentrations were observed in the soil-only mixtures; Zn concentrations decreased with increasing fly ash content (Figure 3.6). Table 1 indicates that the Zn content of soil is higher than the Zn contents of fly ashes used in this study. The effect of the difference in Zn content is that a higher amount of Zn may release into the aqueous solutions with an increase in soil content in the mixtures. Komonweeraket

et al.,(2010) showed that Zn leaching follows an amphoteric pattern; however, no relationship was observed when peak CLT zinc concentrations were plotted against effluent pH (data not shown). Even though an amphoteric pattern was evident for Zn in WLTs (Figure 3.5), the dynamic flow conditions in CLTs may have inhibited the formation of such a pattern.

B generally tended to show an amphoteric leaching pattern. Recent studies indicated that B is in anionic form in alkaline solutions (Jankowski et al., 2006; Querol et al., 2001). B (III) atoms generally do not exist in their cationic forms, instead tending to present as boric acid, $B(OH)_3$. Moreover, in basic conditions (pH>7) boric acid is hydrolyzed and converted into borate ions (Baes & Mesmer, 1976). In the current study, the concentrations of B in the effluent solutions from only-fly ash specimens were significantly higher than the concentrations of B from soil-fly ash-LKD specimens even though the pH level of each specimen was approximately 12. These results indicated that the amount of main metal source was more dominant than the influence of the pH on the leaching behavior of B. Elseewi et al. (1980) showed that leaching of B is usually higher at low pH levels and decreases with an increase in pH. An increase in LKD amount from 2.5% to 5%, however, increased the pH of the specimens a non-significant 3 to 5 %. Therefore, this minimal change in pH may not be an accurate representation of the effect of pH on leaching behavior of B at these alkaline conditions. In addition, at basic conditions, it is expected to see the precipitation of B with $CaCO_3$ (Hollis et al., 1988), which may have also caused a decrease in the B concentrations in the aqueous solutions.

Table 3.3 shows that the Ba concentrations in the effluent increased with fly ash content most probably because of an increase in the amount of the main metal source in the mixtures. Ba concentrations decreased, however, with increasing effluent pH. Bankowski et al. (2004) found that formation of precipitates and complexation of Ba with silicates may have caused a decrease in Ba concentrations in the aqueous solutions as Ba^{2+} ions tend to attach to the surface of fly ash and soil, and exist as $Ba(OH)^{+}$ at extreme pH conditions.

3.6 TOTAL LEACHED AMOUNT OF METALS FROM WLTS AND CLTS

The high-carbon fly ashes used in this study contain relatively high amounts of toxic metals. High concentrations of toxic metals, however, do not necessarily mean that the material will release great amounts of toxic metals into the environment (Apul et al., 2007). Leached amounts of Ba, B, Cu, and Zn and total metal concentrations in WLTs and CLTs are shown in Figures 3.7 and 3.8, respectively. An increase in total metal contents for all specimens generally yielded an increase in metal concentrations in the leachates of WLTs and CLTs. This indicates that the amount of total metal source used in the specimens had direct affect on the leaching amount of metals to the aqueous solutions.

The leached amounts of Ba, B, Cu, and Zn from the WLT specimens were up to 98%, 65%, 2.3%, and 1.2% respectively. These maximums indicate that the initial metal content used in the mixtures had significant effects on the leaching of Ba and B metals.

Leaching of Cu and Zn, on the other hand, is solubility-controlled, which indicates that their leaching amount is highly dependent on the pH of the effluent solutions (Quina et al., 2009). Therefore, it is expected that the pH of the effluent solutions has a greater effect on the leached amount of Cu and Zn metals than the total Cu and Zn amount in the mixtures.

Figure 3.8 indicates that the leached amounts of Ba, B, Cu, and Zn in CLTs were reached maximums of 3.5%, 8.7%, 0.4%, and 0.05%, respectively (Figure 3.8). Even though CLT peak effluent concentrations were much higher than the WLT concentrations for all four metals, the mass of leached metals in WLTs were higher than those in CLTs. A lower liquid-to-solid ratio (L:S) is probably responsible for the metal concentrations in the CLTs than the WLTs. On the other hand, the agitation motion in the WLTs as compared to the smooth fluid movement inside the column set-up may have increased the surface contact between the influent solution and the solid particles (Morar, 2007), and resulted in higher leached metal amounts into the effluent solutions in WLTs.

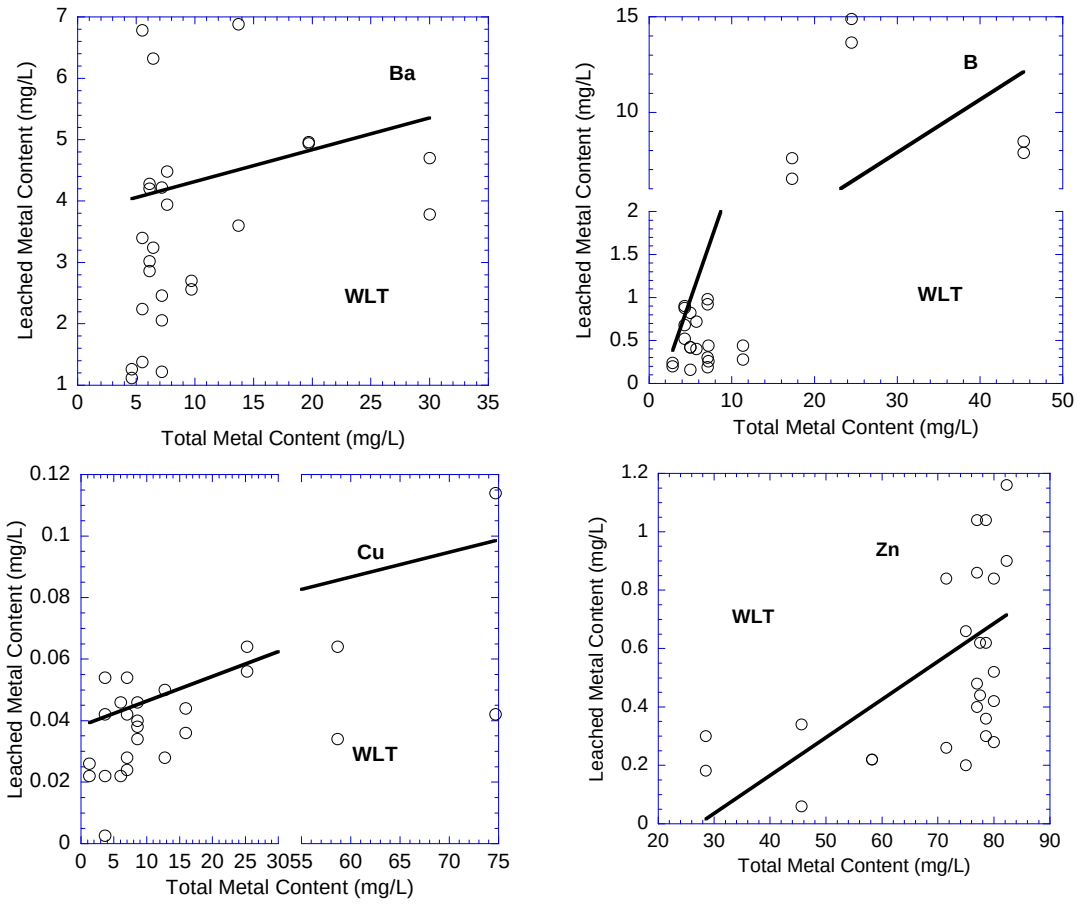

Figure 3.7 Relationship between leaching amounts and concentration of metals in fly ashes (WLTs). Note: WLT=Water Leach Test.

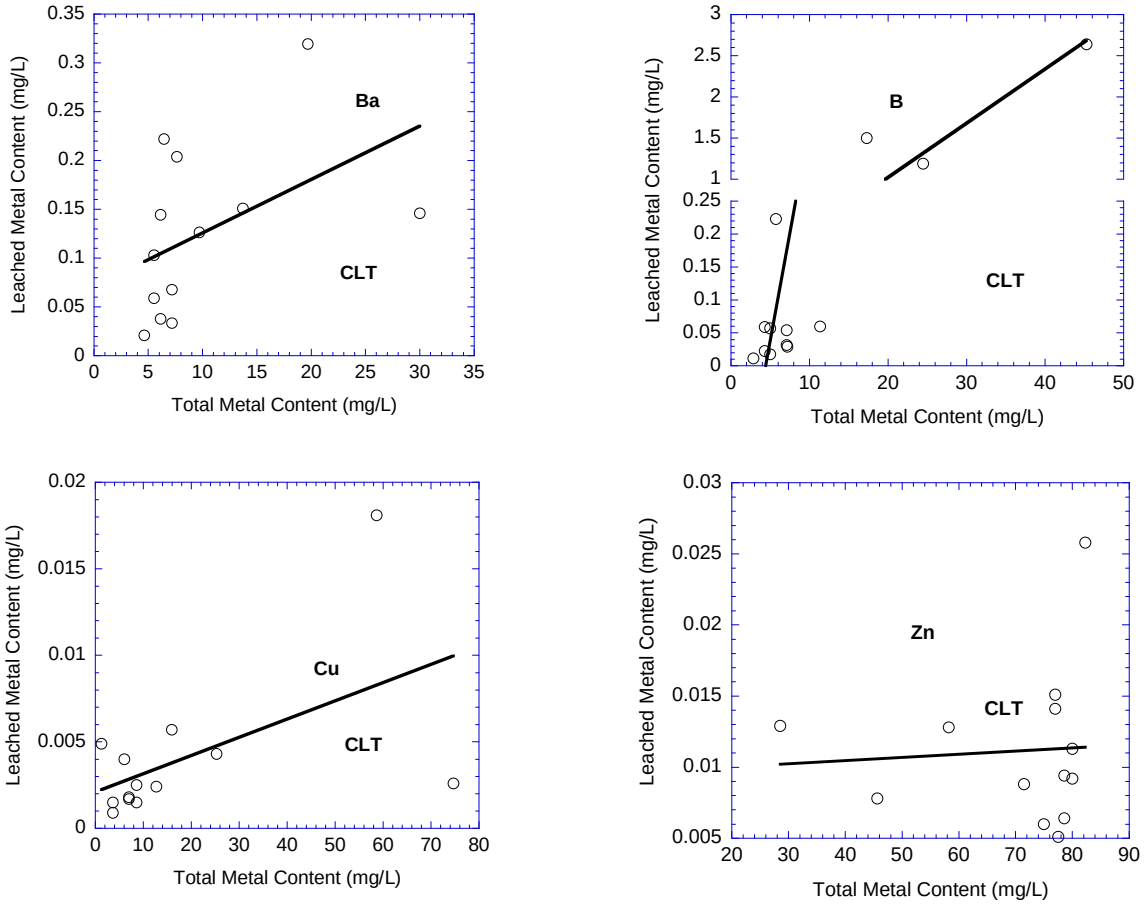

Figure 3.8 Relationship between leaching amounts and concentration of metals in fly ashes (CLTs). Note: CLT=Column Leach Test

3.7 NUMERICAL MODELING

WiscLEACH was used to predict metal concentrations at different depths and years under field conditions. Inputs included transport parameters and hydraulic conductivities determined by the current study and are provided in Tables 3.4 and 3.5. The pavement width (W_p) and shoulder width (W_s) were assumed to be 10.4m (34ft) and 1.5m (4.9 ft), respectively. The point of compliance (W_{poc}) was assumed to be 20 m (66 ft) from the center of the roadway, with a depth to the groundwater table (Z_{GWT}) of 6 m (## ft). Over a maximum simulation time (T_{max}) of 100 years, an annual precipitation rate of 1 m/year (3.28 ft/year) was assumed. Br tracer tests were conducted to determine the transport parameters. Effective porosities and dispersion coefficients were determined by fitting the Ogata-Banks (1961) equation to the effluent Br concentrations in the tracer tests. By using the dispersion coefficients obtained from tracer tests, the longitudinal dispersivities of each specimen was determined. The transverse dispersivity was assumed to be equal to 10% of the longitudinal dispersivity (Apul et al., 2007). The retardation factors for each metal were obtained by fitting van Genuchten (1981) analytical leaching model to the metal concentrations in the effluent of the column leaching tests.

Figures 3.9 and 3.10 show the contour plots for the predicted concentrations of Zn and Cu, respectively. Contour plots for all metals and mixtures not shown may be found in Appendix B. The contour plots provide the predictions of the metal concentrations after 1, 2, 4, and 8 years of construction. As expected, metal concentrations decreased significantly with time and distance from the HCFA-stabilized layer surface. This effect is most probably due to the dispersion of the metals in the soil vadose zone. The

concentrations of Cu and Zn metals after even 1 year is much lower than peak Cu and Zn concentrations obtained from CLTs, which suggests that CLTs measure concentration conservatively, The metal concentrations mostly were adsorbed in the soil vadose zone before reaching groundwater. High retardation factors of subgrade would be increasing the rate of adsorption of metals before reaching to the groundwater.

WiscLEACH simulations were also conducted to study the locations of maximum groundwater concentrations (e.g. at the centerline of the pavement structure, in the vicinity of the point of compliance) as a function of depth to groundwater. Figure 3.11 shows the variations of the B and Zn concentrations at different depths and horizontal distances for a base layer comprised of 85% soil, 10% DP fly ash and 5% LKD. The same tests were run for all other mixtures. Results similar to those for B and Zn were obtained but have been omitted for brevity. Figure 3.11 shows a decrease in B and Zn concentrations as depth increases and as distance from the center alignment of the fly ash-stabilized layer increases in the vadose zone and groundwater, most probably due to dispersion and adsorption of metals in the vadose zone.

Figure 3.12 shows that as fly ash content increased (10% to 20% by weight), WiscLEACH-based concentrations of B, Ba, and Cu increased and Zn concentrations decreased, This finding is consistent with the observations made in laboratory WLTs and CLTs. WiscLEACH-based maximum field concentrations are lower than those measured in the laboratory column leach tests. Furthermore, all metal concentrations estimated by WiscLEACH are below the EPA MCLs indicating that the use of these mixtures has minimal threat to the environment.

In WiscLEACH, the geometric variables (pavement width, depth to groundwater, shoulder width, and thickness of stabilized base layer) and hydraulic variables (porosity and hydraulic conductivity of the fly ash-stabilized base layer) could have significant effects on the leaching of metal concentrations in the groundwater. In order to study these effects, a series of sensitivity analyses were conducted at a point of compliance (POC) of 20 m from the center of the roadway in the current study. This POC was chosen as the target location because Li et al. (2007) argued that the concentrations of metals at POC are less sensitive to the pavement width and shoulder width. In addition, the pavement and shoulder width are less important because the source is distributed over a broad area for all pavement and shoulder widths used in the simulations.

An example set of analyses for Zn concentrations from a specimen prepared with 75% soil, 20% DP fly ash, and 5% LKD is shown in Figure 3.13. These preliminary analyses show that depth to groundwater, thickness of the fly ash-stabilized base layer, and annual precipitation rate are critical parameters that affect the metal concentrations in the WiscLEACH simulations. Depth to groundwater is important because it may affect the amount of dispersion and dilution that occurs between the fly ash-stabilized base layer and the POC (Li et al., 2007). Figure 3.13a shows that an increase in depth to the groundwater table decreased Zn concentrations at the POC due to the dispersion. On the other hand, thicker fly ash-stabilized base layer yielded higher Zn concentrations at the POC because of an increase in the total Zn mass in the base layer structure (Figure 3.13b).

Table 3.4 Hydraulic conductivities and transport parameters for all materials

Specimen	Layer Thickness (m), (ft)	Hydraulic Conductivity, K_s,(m/s)	Effective Porosity, n_e	Hydraulic Gradient	Longitudinal dispersivity, α_L (m)	Transverse dispersivity, α_T (m)
10 BS + 5 LKD	0.407 (1.34	1.34×10^{-7}	0.23	1.0	0.04	0.004
20 BS + 5 LKD	0.356 (1.17)	1.04×10^{-7}	0.31	1.0	0.07	0.007
10 PS + 5 LKD	0.375 (1.20)	2.22×10^{-7}	0.26	1.0	0.06	0.006
20 PS + 5 LKD	0.396 (1.30)	2.5×10^{-7}	0.33	1.0	0.03	0.003
10 DP + 5 LKD	0.375 (2.60)	2.86×10^{-7}	0.24	1.0	0.01	0.001
20 DP + 5 LKD	0.396 (0.41)	1.87×10^{-7}	0.29	1.0	0.02	0.002
Soil	0.791	8.2×10^{-5}	0.32	1.0	0.085	0.0085
Pavement	0.125	5.8×10^{-7}	0.35	1.0	0.1	0.01
Subgrade	NA	3.2×10^{-8}	0.35	1.0	0.1	0.01
Aquifer	NA	1.2×10^{-4}	0.30	1.0	0.1	0.01

Notes: The properties for the mixtures were determined from the laboratory tests in the current study. The properties for pavement, subgrade and aquifer are adopted from Li et al. (2006), NA: Not available.

Table 3.5 Retardation factors of the soil mixtures for different metals

Specimen	Retardation Factor, R_d			
	Barium	Boron	Copper	Zinc
10 BS + 5 LKD	3.1	5	5.8	3.4
20 BS + 5 LKD	4	2.6	1.2	2.8
10 PS + 5 LKD	3.2	3.6	3.5	2.8
20 PS + 5 LKD	4.1	1.8	1.2	1.8
10 DP + 5 LKD	2.4	1.4	1.7	2.3
20 DP + 5 LKD	1.6	1.8	1.2	1.8
Soil	1.93	2.2	2.22	2.04
Pavement	1	1	1	1
Subgrade	3.5	3.5	3.5	3.5
Aquifer	2	2	2	2

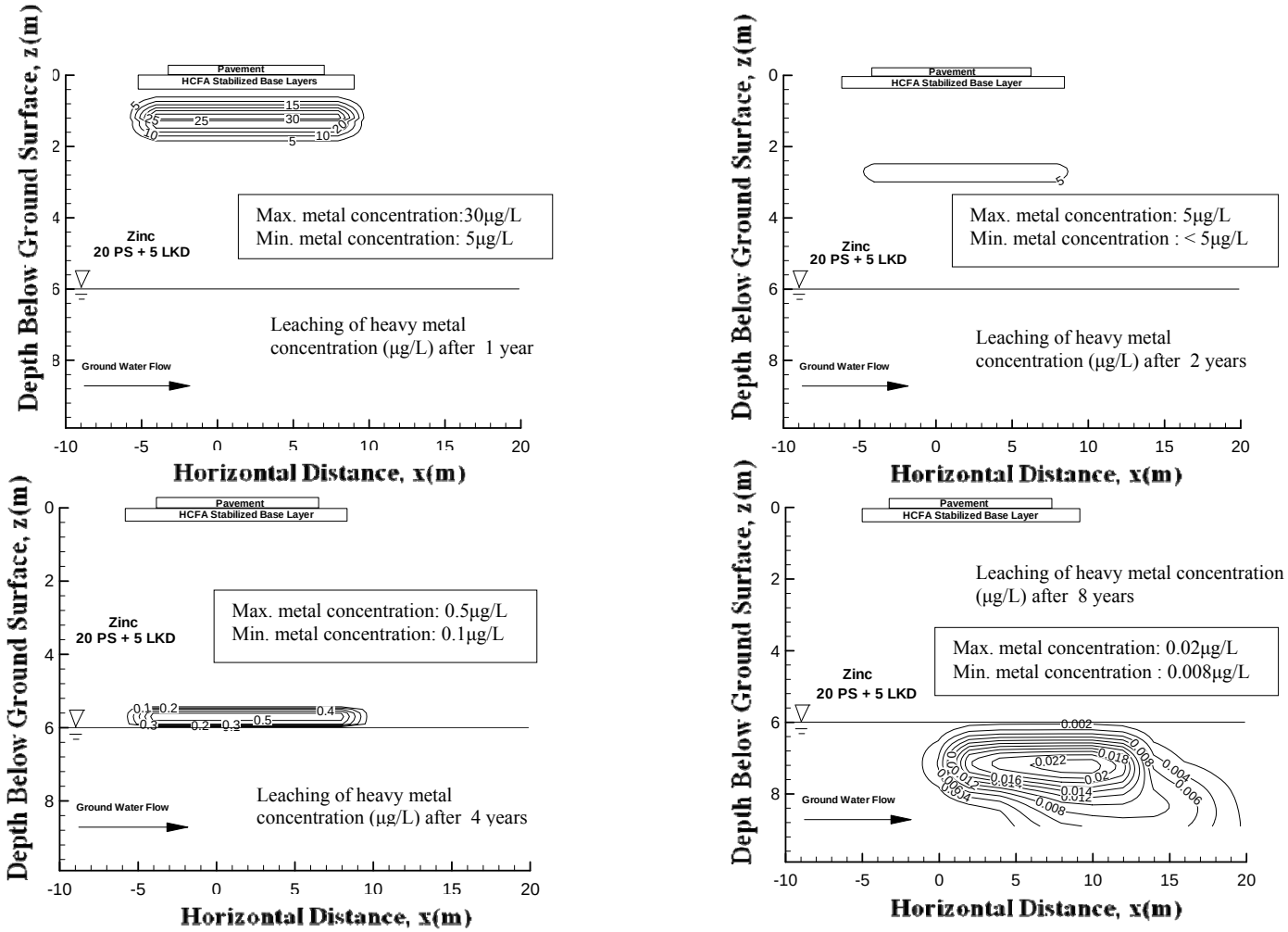

Figure 3.9 Predicted Zn concentrations in vadose zone and ground water. Note: 20 PS + 5LKD designate the specimens with 20% Paul Smith fly ash and 5% lime kiln dust by weight.

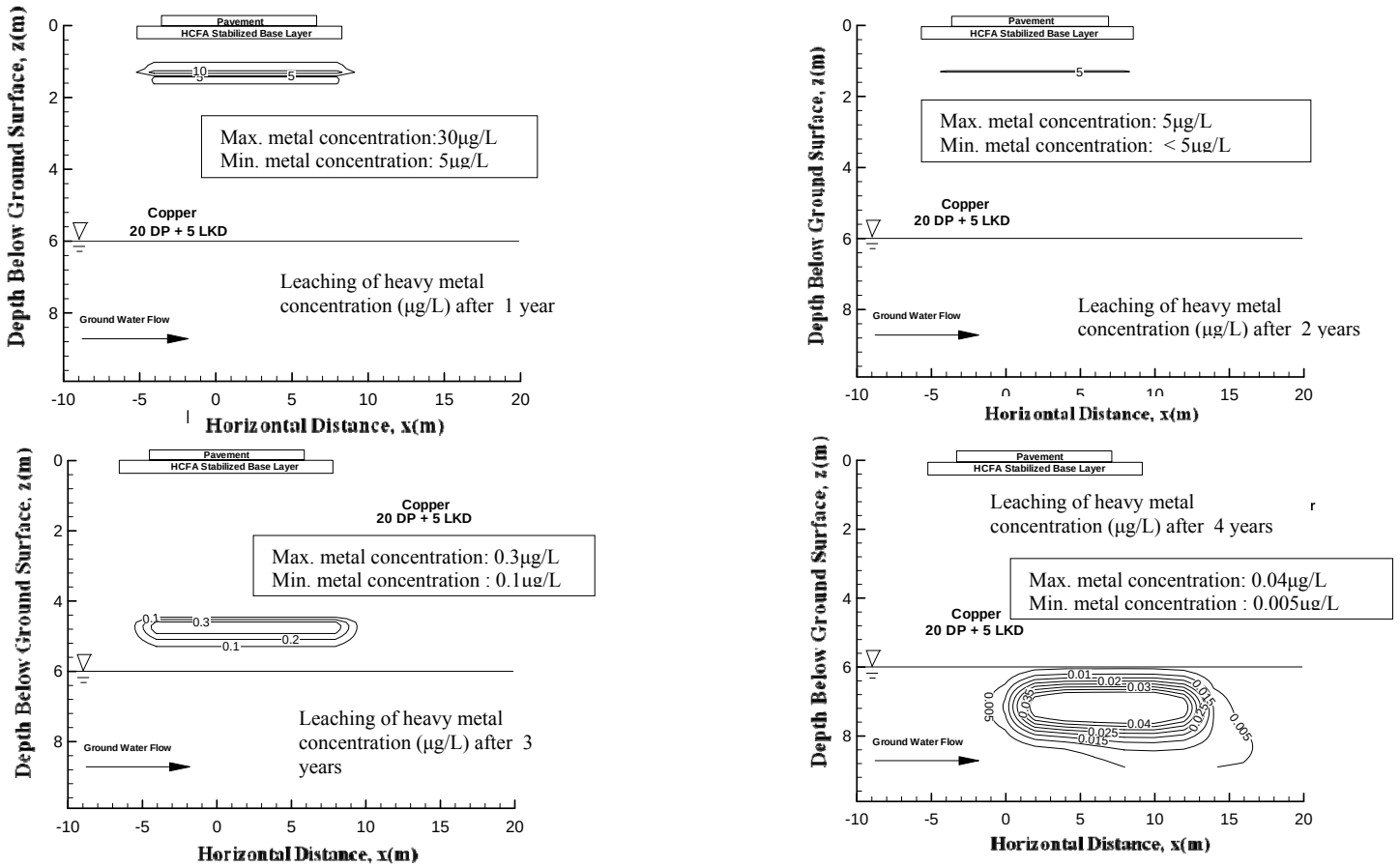

Figure 3.10 Predicted Cu concentrations in vadose zone and ground water Note: Note: 20 DP + 5LKD designate the specimens with 20% Dickerson Precipitator fly ash and 5% lime kiln dust by weight.

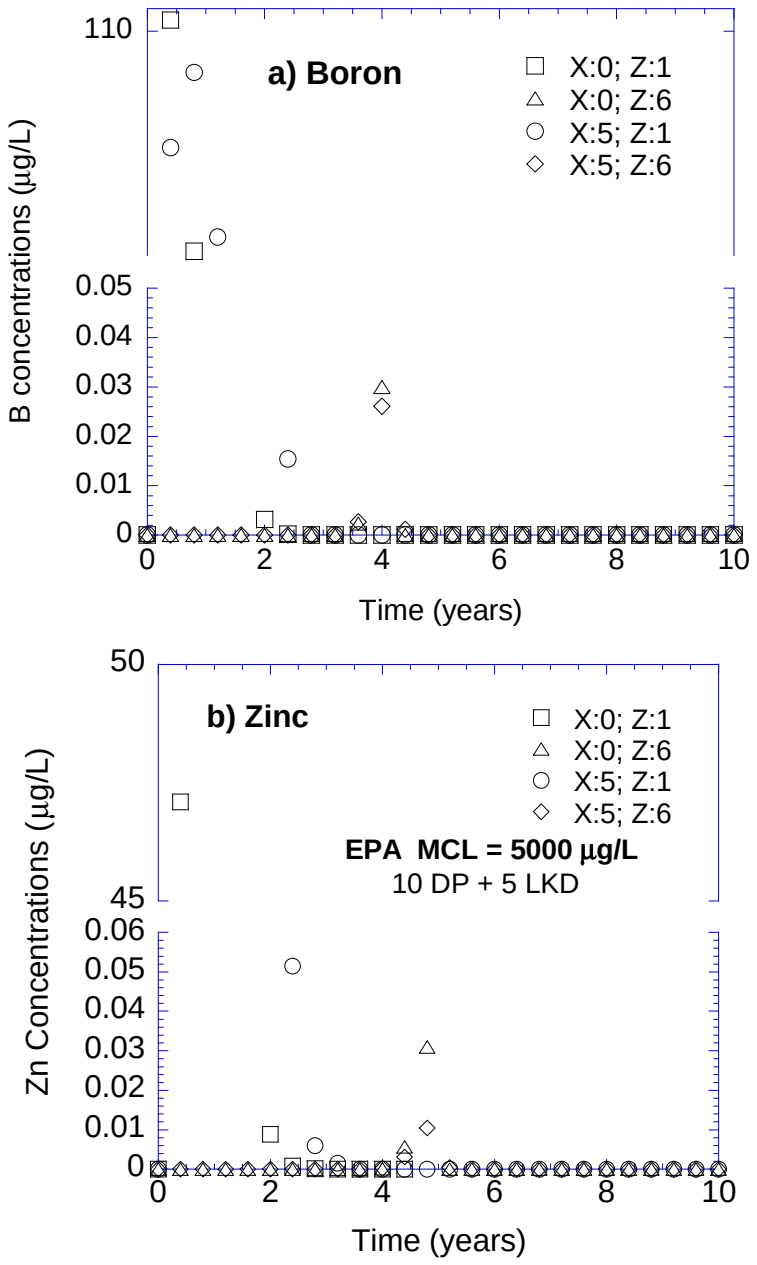

Figure 3.11 WiscLEACH-based concentrations of a) boron and b) zinc at different locations beneath the pavement. X and Z are the horizontal and vertical distances measured from the center alignment of fly ash stabilized layer.

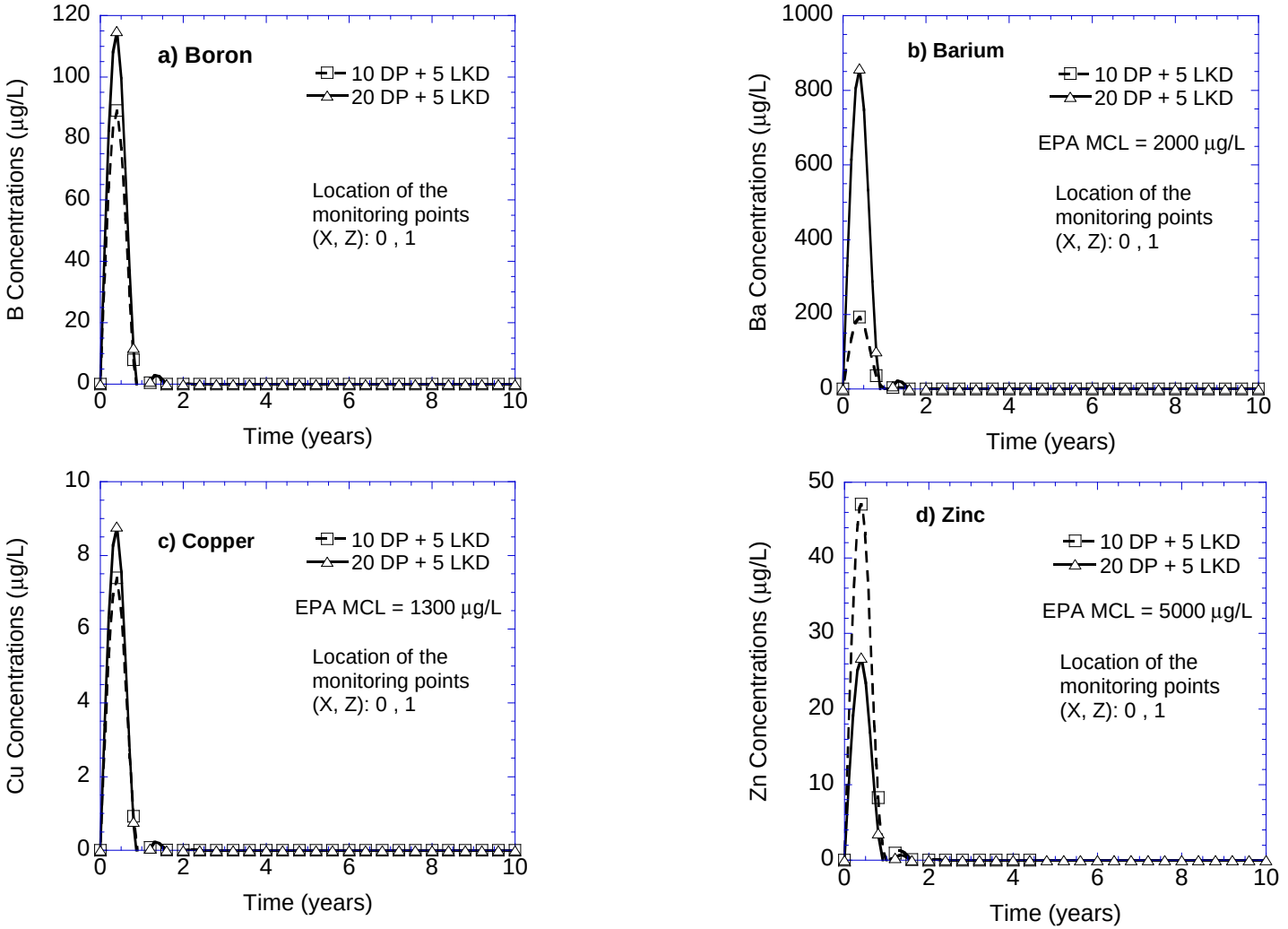

Figure 3.12 Effect of fly ash content on WiscLEACH-based concentrations of a) and b) boron, and c) and d) zinc. X and Z are the horizontal and vertical distances measured from the center alignment of fly ash stabilized layer.

In these WiscLEACH simulations, the least conductive layer in the highway profile controls the seepage velocity. The same is true for the precipitation rate. If the precipitation rate is less than the hydraulic conductivity of the least conductive layer in the highway profile, the seepage velocity is controlled by the precipitation rate (Li et al., 2007). Because Maryland's precipitation rate is significantly lower than the hydraulic conductivities of the soil profiles used in this study, the amount of metal concentrations at the POC will depend on annual precipitation. Figure 3.13c confirms that an increase in precipitation rate resulted in increasing the Zn concentrations at the POC due to higher dilution rate in the groundwater.

3.8 CONCLUSIONS

A study was conducted to investigate how Ba, B, Cu, and Zn leach from high-carbon fly ash-stabilized highway base layers through laboratory tests and numerical modeling. The following conclusions are warranted:

1) Concentrations of all four metals (Ba, B, Cu, and Zn) were below the regulatory limits determined by EPA MCLs (Maximum Contaminant Limits) in 98% of the tests. Ba concentrations were 2% to 60% over the MCLs in three CLTs. Field predicted concentrations of all these metals were also significantly below the EPA MCLs.
2) An increase in LKD content caused an increase in pH levels of the effluent solutions. Ba, B, and Cu concentrations decreased with LKD addition, indicating a cationic leaching pattern that is characterized by greater leaching at acidic pH levels. The Zn concentrations in the effluent showed an amphoteric pattern that is

characterized by greater leaching at extreme acidic and basic pH conditions.

3) Ba, B, and Cu concentrations increased with fly ash content even though the pH levels of the leachates was basic. This demonstrates that an increase in the amount of total metal source in the mixtures contributes more to the increase in leaching of these three metals than the increase of pH due to addition of fly ash. Zn concentrations, however, decreased as fly ash content increased since the soil had more Zn than the fly ashes.

4) Although an increase in ionic strength (IS: 0.02 M to IS: 0.1 M) did not change the effluent pH consistently, it did generally increase metal leaching. An increase in the cation amount in aqueous solutions may have decreased the surface negativity of the fly ash and soil particles, and thus increased the leaching of Ba^{2+}, B^{+}, Cu^{2+} and Zn^{2+} from the solid surface into the aqueous solution by electrostatic effects.

5) CLT elution curves exhibited a first-flush leaching pattern for all mixtures tested. Initial leaching rates were the highest, and then stabilized after 70-75 pore volumes of flow with few exceptions.

6) WiscLEACH numerical simulations suggest that the metal concentrations decreased over time and distance and that all the metals were sufficiently dispersed in the vadose zone WiscLEACH results also indicated that the metal concentrations of metals were much lower than the metal concentrations obtained from the column leach tests, which suggests that results of laboratory tests are likely to provide a conservative estimate of metal leaching in the field.

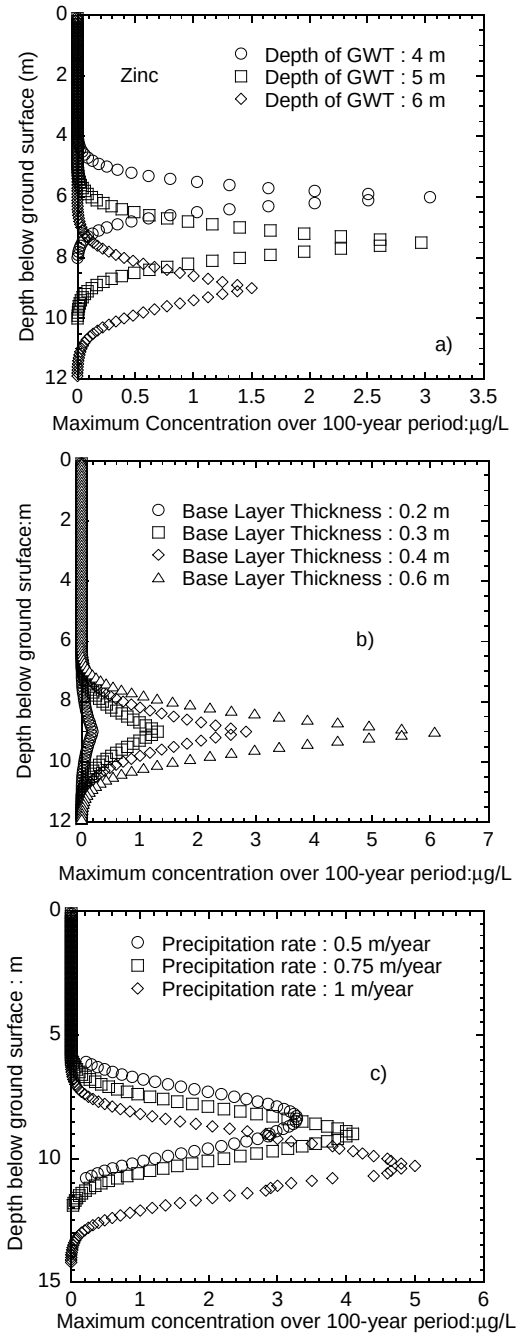

Figure 3.13 Maximum concentrations at POC over a 100 year-period: a) effect of groundwater depth, b) effect of base layer thickness, c) effect of precipitation rate. POC is 20 m down gradient from pavement centerline. Groundwater table (GWT) is fixed at 6 m below ground surface for b) and c).

7) The leaching of heavy metals from fly ash-stabilized base layers into groundwater did not exceed the EPA MCLimits, EPA WQLimits and Maryland ATLimits according to the WiscLEACH results due to the adsorption and dispersion of heavy metals in the soil vadose zone.

8) WiscLEACH results indicated the leaching of metal concentrations into groundwater would change with site conditions. An increase in depth to groundwater table decreases the heavy metal concentrations that reached the groundwater. Higher infiltration rates and a thicker HCFA-stabilized base layers yielded an increase in heavy metal leaching concentrations.

9) The flow in the fly ash and subgrade in WiscLEACH is assumed to occur only vertically. Steady 1D unit gradient flow is assumed in the pavement layers and the vadose zone, with the net infiltration rate controlled by the least conductive layer in the profile and the annual precipitation rate. This also ignores the transverse flow on the top of the base layers toward the edge of the highway structures in case of subgrade has the least hydraulic conductivity.

4 LEACHING OF TRACE METALS FROM HCFA-AMENDED STRUCTURAL FILLS

4.1 INTRODUCTION

The Kingston Fossil Plant dike built with 100% fly ash failed in 2008. This failure released approximately 5.4 million cubic yards of impounded fly ash onto surrounding Tennessee land and into the adjacent Emory River. This event directly affected most citizens living close by and indirectly affected all coal burning utilities and other large coal users. As a result of this event, the EPA directed plant operators and power companies to conduct on-site assessments to determine the structural integrity and vulnerabilities of all ash management facilities to order repairs where needed. In both 1993 and 2000, the EPA determined that waste from the combustion of coal and other fossil fuels should be regulated as nonhazardous. However, many organizations, including the U.S. Congress, are urging the EPA to propose new rules regulating coal combustion waste under the Resource Conservation and Recovery Act (RCRA).

The Kingston release also resulted in new attention on all aspects of Coal Combustion Byproducts (CCP) management. Even though it was quickly recognized that the dike material was pure fly ash, additional research was undertaken to ensure the environmental suitability of future soil-fly ash embankments. Moreover, high-carbon fly ashes may have different behavior than conventional F- or C-type fly ashes, so such behavior needs to be studied. In order to study the water quality impacts of fly ash amendment into embankments in Maryland, this study was initiated. The objectives of this chapter of the current study are to determine the leaching patterns of the heavy

metals as well as the effects of fly ash content and type on the leaching behavior of the trace metals from the embankments constructed with HCFA.

4.2 MATERIALS

Sandy soil (borrow material) was used to prepare the soil-fly ash mixtures. Soil was collected from Centerville, Maryland, and was sieved through No. 4 sieve (4. 75 mm) upon transporting to the laboratory. The soil was classified as poorly graded sand with silt (SP-SM) according to the Unified Soil Classification System, and A-3 (fine sand) according to the American AASHTO Classification System. The soil showed no plasticity based on consistency limit tests per ASTM D4318-10. The physical properties of the soil along with the fly ashes are summarized in Table 4.1.

The fly ashes used in this study were collected from the Brandon Shores (BS), Paul Smith Precipitator (PSP), Dickerson Precipitator (DP), Morgan Town (MT) and Columbia (Co) power plants. Even though some of these fly ashes share the same name as those used in the chapters 2 and 3 of this report, their chemical and physical properties were different. All fly ashes, except that from Columbia, were classified as off-spec fly ashes according to ASTM 618C. The Columbia ash, a C-type fly ash, was collected from a power plant in Wisconsin. Its inclusion in the testing was warranted because of its high CaO content and low loss on ignition value. All of the fly ashes consisted primarily of silt-size particles and contained 80 to 90% fines (passing the 75-mm sieve). Specific gravity of fly ashes ranged from 2.1 to 2.5 (ASTM D 854), and the pH levels ranged from 4.5 to 9.5 (EPA Method SW- 846 Method 945). The physical properties and chemical compositions of the materials are summarized in Tables 4.1 and 4.2. Total elemental

analyses of the five fly ashes and sandy soil were conducted following the procedures outlined in EPA SW-846 Method 6800 and are summarized in Table 4.3.

Fly ash addition to the soil was 10%, 20%, and 40% by weight. The lower percentages are within the typical range used in soil stabilization; the highest was chosen in order to study the effects of ash content on the leaching behavior. All column leach test specimens were compacted at their 2% dry of optimum moisture contents (OMCs) in an acrylic tube with a 101.6 mm (4 in) inside diameter and that ws 305 mm (12 in) height. By compacting to the dry of OMC, higher hydraulic conductivities could be achieved that allow enough sample to be collected in a reasonable amount of time. Standard Proctor effort (ASTM D 698) was used during compaction consisting of 8 layers with 29 blows per layer to achieve a target dry unit weight of 19.2 kN/m^3 (122 pcf), which is a minimum value for highway embankments specified by the Maryland SHA. The mixtures prepared with Maryland fly ashes were used directly after compaction. However, because fo their high calcium content, Columbia fly ash mixtures were cured for 7 days at 95% relative humidity and 23 Cº. Table 4.4 provides the list of soil mixtures that are used in the current study along with their maximum dry unit weights and optimum moisture contents.

Table 4.1 Physical properties of the soil and fly ashes

Sample	G_s	w_{opt} (%)	γ_d (kN/m^3)	LL (%)	PI (%)	Fines Content (<75 μm) (%)	Fineness (>45 μm) (%)
Soil	2.6	11	19.2 (122)	NP	NP	2	-
BS	2.28	16	11.87 (76)	NP	NP	84	13
PSP	2.17	22	9.96 (64)	NP	NP	87	20
DP	2.43	36	9.93 (63)	NP	NP	82	15
MT	2.4	25	13.8 (88)	NP	NP	80	16
Co	2.7	21	15.6 (100)	NP	NP	90	14.4

BS: Brandon Shores, PSP: Paul Smith Precipitator fly ash, DP: Dickerson Precipitator fly ash, BS: Morgantown fly ash, Co: Columbia fly ash, G_s: Specific gravity, w_{optm}: optimum water content, γ_{dmax}: maximum dry unit weight, LL: liquid Limit, PL: plastic limit, NP: Nonplastic.

Table 4.2 Chemical compositions of the fly ashes tested. Concentrations of major minerals were determined by X-ray fluorescence spectroscopy analysis. All concentrations are in percentage by weight.

	Chemical Composition								
Fly ash	pH	LOI (%)	SiO_2 (%)	Al_2O_3 (%)	Fe_2O_3 (%)	CaO (%)	MgO (%)	$SiO_2 + Al_2O_3 + Fe_2O_3$, min (%)	Moisture Content, (max)(%)
BS	6.1	6.2	45	27	3.2	1.1	0.6	75	0.007
PSP	6.6	6.8	53	21	6.7	0.4	1.2	81	0.004
DP	8.1	16	40	32	14.7	0.6	1.5	87	0.006
MT	9.5	8.1	49	26	13.7	2.5	1.9	88	0.011
Co	12.4	0.4	31	18	6.1	19.4	3.7	56	0.004
Class C (ASTM C618)	NA	6	40	17	6	24	5	70	3
Class F (ASTM C618)	NA	6	55	26	7	9	2	50	3

BS: Brandon Shores PSP: Paul Smith Precipitator fly ash, DP: Dickerson Precipitator fly ash, BS: Morgan Town fly ash, Co: Columbia fly ash, LOI: Loss on ignition. FW: Future Work, NA : Not applicable.

Table 4.3.Total metal content of the fly ashes and sandy soil material from the total elemental analysis results.

Sample	Al (mg/L)	As(mg/L)	B (mg/L)	Cr (mg/L)	Mn (mg/L)	Se (mg/L)
Soil	28760	<3	3	16	38	<3
BS	21333	24.16	21	50	34	39
PSP	11770	52.08	30	30	216	21
DP	17638	41.63	79	42	62	9
MT	29123	39.68	241	68	208	46
Co	91848	15.01	600	65	92	24

Table 4.4 Legend and compositions of the mixtures.

Legend of Mixtures	Fly Ash Content (%)	Optimum Water Content (%)	Maximum Dry Unit Weight (kN/m^3/pcf)
100 Soil	0	11	19.2 (122)
S – 10 BS	10	9	19.3 (123)
S – 20 BS	20	11	18.8 (120)
S – 40 BS	40	13	16.7 (106)
100 BS	100	26	11.9 (76)
S – 10 PSP	10	11	19.1 (122)
S – 20 PSP	20	13	18.7 (119)
S – 40 PSP	40	17	16 (102)
100 PSP	100	22	10 (64)
S – 10 MT	10	10	19.2 (122)
S – 20 MT	20	11	19 (121)
S – 40 MT	40	12	18 (115)
100 MT	100	25	13.2 (84)
S – 10 DP	10	14	16.8 (107)
S – 20 DP	20	15	15.6 (99)
S – 40 DP	40	18	13.2 (84)
100 DP	100	36	10 (64)
S – 10 Co	10	11	119 (76)
S – 20 Co	20	13	18..9 (120)
S – 40 Co	40	16	16.4 (104)
100 Co	100	21	15.6 (99)

Note: BS: Brandon Shores fly ash, PSP: Paul Smith Precipitator fly ash, DP: Dickerson Precipitator fly ash, MT: Morgan Town fly ash, Co: Columbia fly ash. The numbers that follow the fly ashes indicate the percentages by weight of admixtures added to the soil.

4.3 METHODS

The procedures listed in sections 2 and 3 were also followed for the WLTs and CLTs. In addition, a series of toxicity leaching characteristic procedure (TCLP) tests were also conducted on the soil-alone, fly ash-alone and soil-fly ash mixtures.

The soils, fly ashes their mixtures prepared for TCLP tests were the same materials prepared for WLTs. The TCLP test is designed to determine the mobility of organic and inorganic compounds present in liquid, solid, and multiphase wastes. EPA Method 1311 was followed during TCLP tests. The soil mixtures were sieved through U.S. No. 3/8 inches sieve. A liquid-to-solid ratio of 20:1 was used for all test specimens. An acetic acid solution (pH = 5) was used as an extraction fluid. The extraction fluid was added only once, at the start of the extraction. Levels of pH and electrical conductivity measurements were recorded immediately after the sample collection. The protocol for sample preparation and preservation followed those employed in WLTs except the filtration procedure. The samples were vacuum filtered through TCLP glass fiber filters. Then filtered leachates were acidified to pH<2 with 2% HNO_3 acid solution and preserved in 4 C^o for chemical analysis.

4.4 RESULTS

4.4.1 Water Leach Tests

Duplicate-batch WLTs were conducted on fly ash alone, soil alone and soil – fly ash mixtures. The pH values for each specimen were measured and are summarized in Table 4.5. The pH values of mixtures, in descending order, are Columbia (Co), Morgantown (MT), Dickerson Precipitator (DP), Paul Smith Precipitator (PSP) and

Brandon Shores (BS) fly ashes. The pH levels of the effluent solutions was between 5.5 and 12.2 (Table 4.5). The specimens prepared with Co and MT fly ashes had the highest pH levels; specimens prepared with the PSP and BS fly ashes had the lowest pH levels. Table 4.2 shows the chemical compositions of the fly ashes obtained from X-ray diffraction analysis. There is a strong relationship between the pH of the leachate and the CaO and MgO contents of the materials used in the soil mixtures because of the basic nature of these minerals (Gitari et al., 2009; Jankowski et al., 2006; Mudd et al., 2004; Quina et al., 2009). Johnson et al. (1999) said that release of Ca from CaO minerals yields $Ca(OH)_2$ in aqueous solutions. $Ca(OH)_2$ is an oxide mineral that significantly contributes to alkalinity. Therefore, it was an expected behavior for the specimens prepared with Co and MT fly ashes to produce higher pH values than the specimens prepared with BS and PSP fly ashes.

Figure 4.1a shows the effect of fly ash addition into the sandy borrow material. As expected, an increase in fly ash contents in the soil-fly ash mixtures significantly increased the pH levels of the effluent solutions. Generally, pH levels increased the most when fly ash content was increased from 0% to 10% by weight in the soil-fly ash mixtures. The rate of increase was lowest in pH values when increments in fly ash contents were varied between 40% and 100% by weight. An increase in BS, PSP, and DP fly ash contents did not affect the rate of increase of pH levels in the effluent solutions as it did in Co and MT fly ashes because of the relatively lower CaO and MgO contents of BS, PSP and DP fly ashes.

Table 4.5 Stabilized pH and effluent concentrations in WLTs. Concentrations exceeding EPA MCL are in **bold**.

Specimen Name	Fly Ash Content (%)	pH	Al (mg/L)	As (µg/L)	B (µg/L)	Cr (µg/L)	Mn (µg/L)	Se (µg/L)
S – 10 BS	10	6.3	0.08	<0.01	<0.02	<0.001	0.028	<0.03
S – 20 BS	20	6.4	0.001	<0.01	0.18	<0.001	0.034	<0.03
S – 40 BS	40	6.81	0.05	0.01	0.12	<0.001	**0.075**	<0.03
100 BS	100	5.5	**0.15**	<0.01	0.34	<0.001	0.031	<0.03
S – 10 PSP	10	6	**0.22**	<0.01	NA	<0.001	0.017	<0.03
S – 20 PSP	20	6.4	<0.05	<0.01	0.16	<0.001	0.027	<0.03
S – 40 PSP	40	7.02	<0.05	**0.21**	0.34	0.01	**0.12**	**0.09**
100 PSP	100	7.7	**0.68**	**0.23**	0.58	0.007	0.018	**0.13**
S – 10 MT	10	7.2	0.2	<0.01	0.75	0.011	<0.001	<0.03
S – 20 MT	20	8.7	**0.35**	<0.01	1.36	0.021	<0.001	**0.076**
S – 40 MT	40	9.64	**2.4**	**0.06**	2.23	0.06	<0.001	**0.12**
100 MT	100	9.8	**6.7**	**0.08**	6.56	**0.13**	<0.001	**0.28**
S – 10 DP	10	7.05	<0.05	<0.01	0.2	0.002	**0.07**	<0.03
S – 20 DP	20	7.11	<0.05	<0.01	0.33	0.008	0.03	0.04
S – 40 DP	40	7.78	<0.05	**0.04**	0.74	0.01	0.01	**0.12**
100 DP	100	7.96	0.07	**0.05**	1.45	0.015	0.03	**0.17**
S – 10 Co	10	11.88	**45**	<0.01	0.65	0.04	<0.001	<0.03
S – 20 Co	20	11.95	**48**	<0.01	0.22	0.06	<0.001	<0.03
S – 40 Co	40	12.07	**57**	<0.01	0.16	0.06	<0.001	<0.03
100 Co	100	12.15	**55**	<0.01	<0.02	0.04	<0.001	<0.03
Soil	-	6.74	<0.05	<0.01	<0.02	<0.001	<0.001	<0.03
MDL (mg/L)			0.05	0.01	0.02	0.001	0.001	0.03
U.S. EPA MCL (mg / L)			0.2	0.01	NA	0.1	0.05	0.05
U.S. EPA WQL (mg / L)			0.75	0.34	NA	0.57	NA	0.005
MD ATL (µg / L)			NA	NA	13000	0.57	NA	NA

Note: MDL: Minimum Detection Limits, MCL= maximum contaminant levels for drinking water; MCL for Al is based on a secondary non-enforceable drinking water regulation; WQL= water quality limits for protection of aquatic life and human health in fresh water. ATL = aquatic toxicity limits for fresh water. The numbers that follow the fly ashes indicate the percentages by weight of admixtures added to the soil.

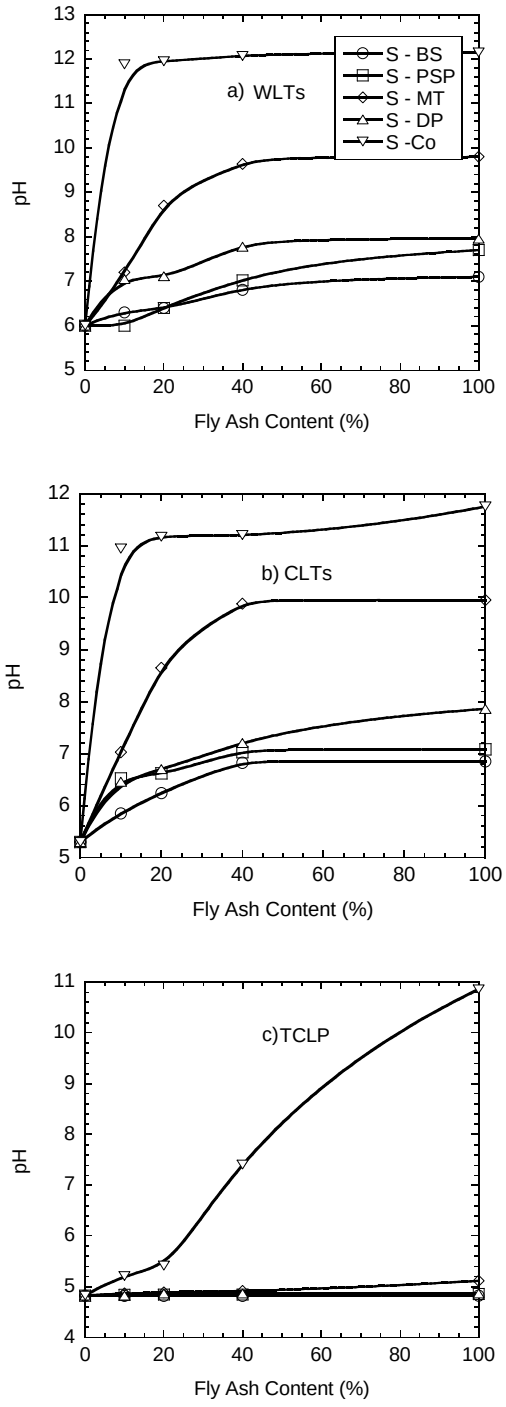

Figure 4.1 Effect of fly ash content on pH of the soil mixtures a) Water leach tests, b) Column leach tests, c) TCLP tests. (Note: BS: Brandon Shores Fly Ash, PSP: Paul Smith Precipitator Fly ash, MT: Morgantown Fly ash, DP: Dickerson Precipitator Fly Ash, Co: Columbia Fly Ash)

Table 4.5 shows that, with few exceptions, the concentrations of six metals (Al, As, B, Cr, Mn and Se) that leached from the soil-fly ash mixtures prepared with 10% and 20% fly ash contents by weights are below the U.S EPA maximum concentration limits for drinking water (MCLs), EPA water quality limits (WQLs) for the protection of aquatic life and human health, and Maryland aquatic toxicity limits (ATLs) for fresh water. As and Se concentrations are below the detection limits in most soil mixtures; the exceptions are those specimens prepared with 40% and 100% PSP, MT, and DP fly ashes by weight. This indicates that as the total metals in source material increases in the soil-fly ash mixtures, the leaching potential of these heavy metals also increases. This relationship poses a threat to the environment. This trend suggests that extra care should be taken in the design of soil-fly ash mixtures to ensure that concentrations of leached metals do not exceed the environmental regulation limits. The specimen prepared with 100% MT fly ashes was the only specimen that leached Cr concentration above the EPA regulatory limits.

Figure 4.2 shows the effects of fly ash content on leaching concentrations of the above-listed six metals. An increase in fly ash contents in the soil-fly ash mixtures increased concentrations of As, B, and Se regardless of fly ash type. No consistent increase was observed for the leaching of Al and Mn with addition of fly ash in the soil-fly ash mixtures. The pH levels of effluent solutions were between 6.5 and 7.5, especially in specimens prepared with BS, PSP, and DP fly ashes. The mobility of Al and Mn metals at this pH range is minimal, so very low concentrations of these metals in these conditions are expected.

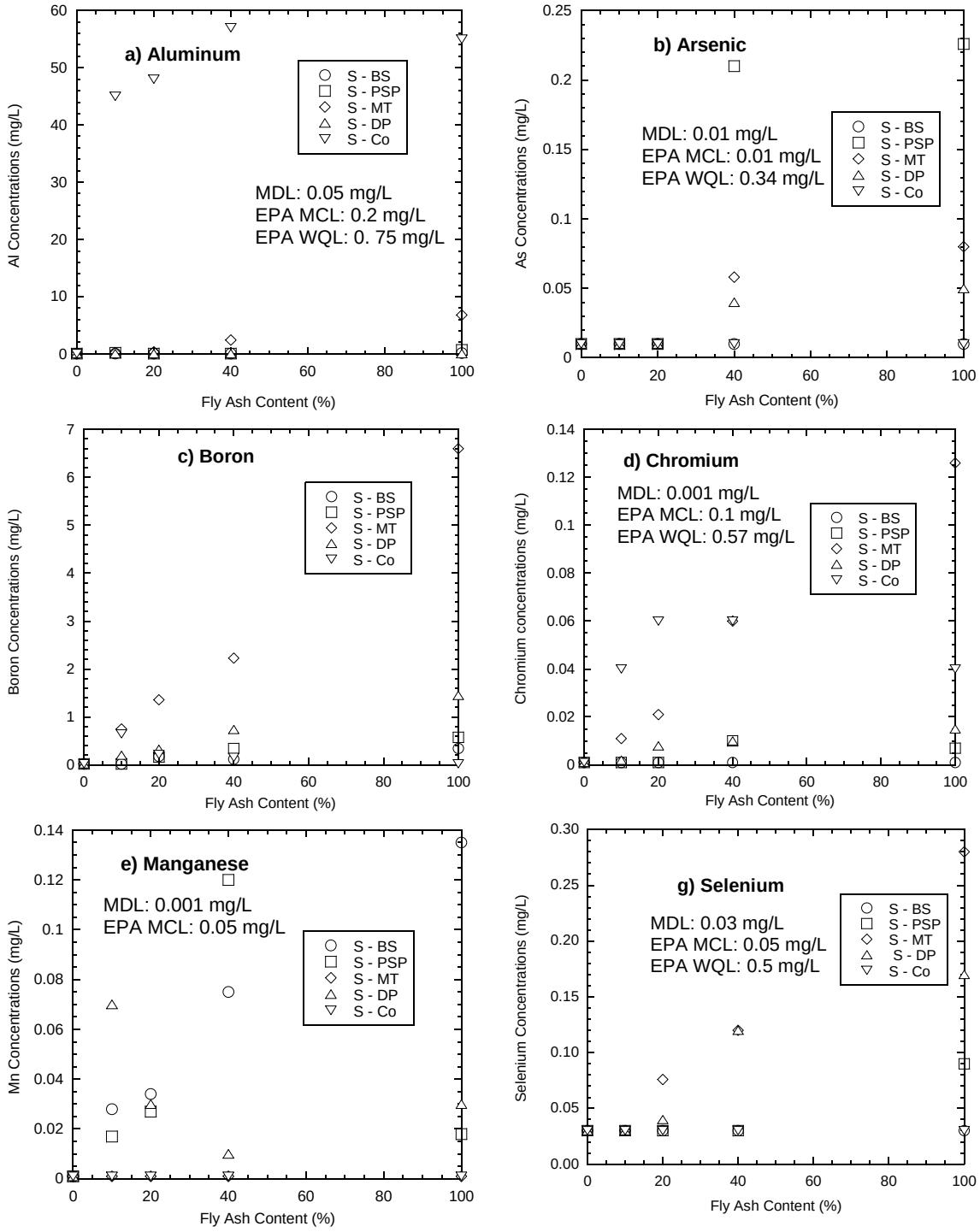

Figure 4.2 Concentrations of six metals in the effluent from WLTs(Note: BS: Brandon Shores, PSP: Paul Smith Precipitator, MT: Morgan Town)

It seems that the effect of pH levels of the aqueous solutions were more dominant than the increase of fly ash content on leaching of Al and Mn for specimens prepared with BS, PSP, and DP fly ashes.

Leached Al concentrations from the soil-fly ash mixtures prepared with Co fly ash were the highest, most probably due to the higher total Al content in this fly ash (Table 4.3). In addition, Al tends to show an amphoteric leaching pattern (Cetin et al., 2012; Komonweeraket et al. 2010), which means that release of Al increases at extreme pH levels. The pH levels values of the Co soil mixtures were between 11.9 and 12.15. In these alkaline conditions, the surface charge of the soil and fly ash particles are negative and anionic forms of Al tend to be released significantly into the aqueous solutions, which also probably raise Al concentrations (Gitari et al., 2009). These findings are consistent with what Johnson et al., (1999) found.

Even though an increase in fly ash content increased the As and Se concentrations in the effluent solutions, the concentrations of these metals were mostly below the detection limits. Thus, it was not possible to define the leaching pattern of these two toxic metals. Table 4.5 shows that a change in pH from neutral to alkaline pH levels also increased the concentrations of As and Se metals, consistent with a behavior observed from previous studies (Jankowski et al. 2006, Komonweeraket et al. 2010). At these pH levels, As and SE start forming the anions $HAsO_4^{2-}$ and $HSeO_3^-$ and are released from the fly ashes (Izquierdo et al., 2011).

Cr concentrations leached from specimens prepared with BS and PSP fly ashes were below the detection limits with few exceptions. Specimens prepared with MT fly

ashes released the highest Cr concentrations into the aqueous solutions. Table 4.3 shows that MT fly ashes contain the highest amount of total Cr, which resulted in higher Cr release than the other fly ashes. Moreover, Cr leaching depends greatly on the pH of the effluent solutions (Cetin et al., 2012; Jegadeesan et al., 2008,; Komonweeraket et al., 2010). The pH levels of specimens prepared with MT fly ashes varied between 7.2 and 9.8. At these pH levels, the insoluble form of Cr (Cr(III)) starts oxidization into soluble Cr(VI) and creates the CrO_4^{2-} anionic form (Engelsen et al. 2010; Geelhoed et al., 2002; Gitari et al., 2009). Therefore, an increase in pH would increase the oxidation rate of insoluble Cr(III) to highly soluble Cr(VI), which would in turn increase concentrations of released Cr into the aqueous solutions.

B concentrations increased with the addition of fly ash except specimens prepared with Co fly ashes. B leaching is sensitive to pH levels of aqueous solutions. Furthermore, B tends to show cationic leaching pattern, which indicates that its solubility is very high at low pH levels and that we should expect a decrease as pH levels increase (Elseewi et al., 1980; Gitari et al., 2009). As shown in Table 4.5 the pH levels of the specimens prepared with Co fly ash were very high. These high levels could result in a decrease in B concentrations as the Co content increases in soil-fly ash mixtures. In addition, at high pH levels adsorption of cationic species are very likely. The increase in pH levels with addition of Co fly ash may have caused an increase in the adsorption of B by soil and fly ash surfaces and caused a decrease in B concentrations in the aqueous solutions (Mudd et al., 2004). Furthemore, B may co-precipitate with $CaCO_3$ minerals, so is expected to observe large amount of these minerals in the effluent solutions of the

soil-fly ash mixtures prepared with Co fly ash due to its high CaO content (Hollis et al., 1988).

In the soil-fly ash mixtures, the Mn concentrations increased as fly ash increased (except those prepared with MT and DP fly ashes) (Table 4.5). Mn increases are not linear with fly ash content, even though the mass of metals in soil mixtures increases approximately linearly with fly ash content. Therefore, the use of linear dilution calculations will underestimate the resulting concentrations of Mn from soil-fly ash mixtures. Mn concentrations below the detection limits for the specimens prepared with Co fly ashes. Mn metals tends to show cationic leaching pattern, so it is difficult to determine Mn concentrations at very basic conditions such as provided by soil-fly ash mixtures prepared with Co fly ash (pH11-12.5) (Engelsen et al., 2009; Gitari et al., 2009,).

Mn concentrations decreased with increasing fly ash content in soils amended with MT and DP fly ashes. The leaching pattern of Mn is generally controlled by the pH levels of effluent solutions (Goswami & Mahanta 2007). Since the pH levels of effluent solutions vary between 7.2 and 10 for the soil-MT fly ash mixtures and the soil-DP fly ash mixtures, precipitation of Mn with Al oxides and Fe oxides occur and generate a decrease in Mn concentrations in the aqueous solutions even though the main source of metals was increased. (Jegadeesan et al., 2008; McBride 1994).

4.4.2 Column Leach Tests

Figure 4.3 shows that effluent pH levels vary as a function of pore volumes of flow (PVFs). All CLTs continued until a minimum of 50 pore volumes of flow was obtained in order to examine the behavior and persistency of the pH levels of soil mixtures. The pH levels of the effluent solutions fluctuated for all specimens until 20 PVFs of flow is reached, and then the pH levels remained constant. Similar to the observations made in batch water leach tests (WLTs), there is a strong correlation between the CaO and MgO contents of the fly ashes and pH of the leachate solutions. The pH levels of the CLT specimens prepared with MT and Co fly ashes has the highest pH values; pH levels of effluents leached from the specimens prepared with BS and Paul Smith Precipitator PSP had the lowest (Table 4.6). Pure sandy soil had the lowest pH values. An increase in fly ash caused an increase in the effluent pH levels of all specimens in WLTs.

Table 4.6 provides the peak metal concentrations and the stabilized pH values of the aqueous solutions. The maximum leaching concentrations of few of the metals exceeded the EPA MCLs, EPA WQLs and Maryland ATLs. However, CLTs provide relatively high metal concentrations and are typically unrepresentative of field conditions (Bin-Shafique et al., 2006; Li et al., 2007). Thus, computer models such as WiscLEACH, become useful in predicting concentration profiles in the field.

Figure 4.4 shows that, with the exception of Mn, the concentrations of Al, As, Cr, B, and Se tended to increase with as fly ash content increased in fly ash content. The soil-fly ash mixtures prepared with PSP fly ash were the only ones for which an increase in

fly ash content increased the Mn concentrations in the effluent solutions. Mn is very mobile in acidic pH levels and an increase in pH decreases the mobility (solubility) of Mn in the aqueous solutions because Mn starts precipitating as $Mn(OH)_2(s)$ (Dutta et al., 2009). Furthermore, Mn usually exists in its cationic form Mn^{2+} in the aqueous solutions, and with an increase in pH the surface of the soil and fly ash particles are being deproponated.

The cationic species, such as Mn^{2+}, attach to negatively charge surfaces, which yields a reduction in the leached Mn concentrations (Gitari et al., 2009; Su et al., 2011). Mn tended to decrease with pH. In addition, Mn metals precipitate by complexing with cationic metals that exist in the aqueous solutions (such as As and Ca) (Komonweeraket et al., 2010). Table 4.6 and Figure 4.2b show that the leaching trend of the Mn is strongly controlled by the pH levels of the effluent solutions – except for the specimens prepared with PSP fly ash. An increase in fly ash content resulted in an increase of the Mn concentrations in the leachates for the soil-PSP fly ash mixtures. Table 4.3 indicates that total Mn content of PSP fly ash is approximately 1.2 to 8 times higher than the total Mn contents of other fly ashes. Therefore, main metal sources were expected to be the dominant factor controlling leaching of Mn from the soil-PSP fly ash mixtures.

Table 4.6 Stabilized pH and peak effluent concentrations in CLTs. Concentrations exceeding EPA MCL are in **bold**.

Specimen Name	Fly Ash Content (%)	pH	Al (mg/L)	As (mg/L)	B (mg/L)	Cr (mg/L)	Mn (mg/L)	Se (mg/L)
S – 10 BS	10	5.75	0.13	<0.01	1.46	<0.001	**0.90**	<0.03
S – 20 BS	20	6.25	0.14	**0.04**	1.63	<0.001	**0.82**	<0.03
S – 40 BS	40	6.7	0.16	**0.09**	8.68	0.03	**0.82**	<0.03
100 BS	100	7.3	0.16	**0.73**	19.11	0.05	**3.1**	0.04
S – 10 PSP	10	6.3	0.062	<0.01	1.05	<0.001	**0.25**	0.031
S – 20 PSP	20	6.6	0.1	**0.09**	2.78	0.003	**0.33**	**0.09**
S – 40 PSP	40	7	**0.34**	**1.58**	30.54	0.06	**1.68**	**1.74**
100 PSP	100	7.1	**0.38**	**2.06**	56	**0.44**	**3.88**	**2.08**
S – 10 MT	10	7.2	0.11	<0.01	13.8	**0.32**	0.023	**0.063**
S – 20 MT	20	8.3	**0.3**	**0.075**	26.4	**1.59**	0.006	**0.202**
S – 40 MT	40	9.8	**2.7**	**0.34**	115	**3.23**	0.005	**1.79**
100 MT	100	10	**12.6**	**0.36**	166	**3.48**	0.01	**5.84**
S – 10 DP	10	6.6	0.07	<0.01	11.6	0.002	**1.28**	**0.11**
S – 20 DP	20	6.72	0.17	**0.34**	23.8	0.003	**0.6**	**0.37**
S – 40 DP	40	7.2	**0.32**	**0.5**	42.12	0.01	**0.39**	**1.12**
100 DP	100	7.9	**2.41**	**0.75**	43.2	0.03	0.048	**1.68**
S – 10 Co	10	11.88	**98.3**	**0.03**	1.44	**0.17**	0.003	0.05
S – 20 Co	20	11.95	**187**	**0.07**	1.52	**0.36**	**0.58**	0.08
S – 40 Co	40	12.07	**95**	**0.08**	7.86	**0.12**	<0.001	0.36
100 Co	100	12.15	**206**	**0.05**	23.6	**1.13**	0.0025	0.94
Sandy Soil	-	5.2	<0.05	<0.01	0.7	<0.001	**0.64**	<0.03
MDL (mg/L)			0.05	0.01	0.02	0.001	0.001	0.03
U.S. EPA MCL (mg / L)			0.2	0.01	NA	0.1	0.05	0.05
U.S. EPA WQL (mg / L)			0.75	0.34	NA	0.57	NA	0.005
MD ATL (µg / L)			NA	NA	13000	NA	NA	NA

Note: MDL: Minimum Detection Limits, MCL= maximum contaminant levels for drinking water; MCL for Al is based on a secondary non-enforceable drinking water regulation; WQL= water quality limits for protection of aquatic life and human health in fresh water. ATL = aquatic toxicity limits for fresh water. The numbers that follow the fly ashes indicate the percentages by weight of admixtures added to the soil.

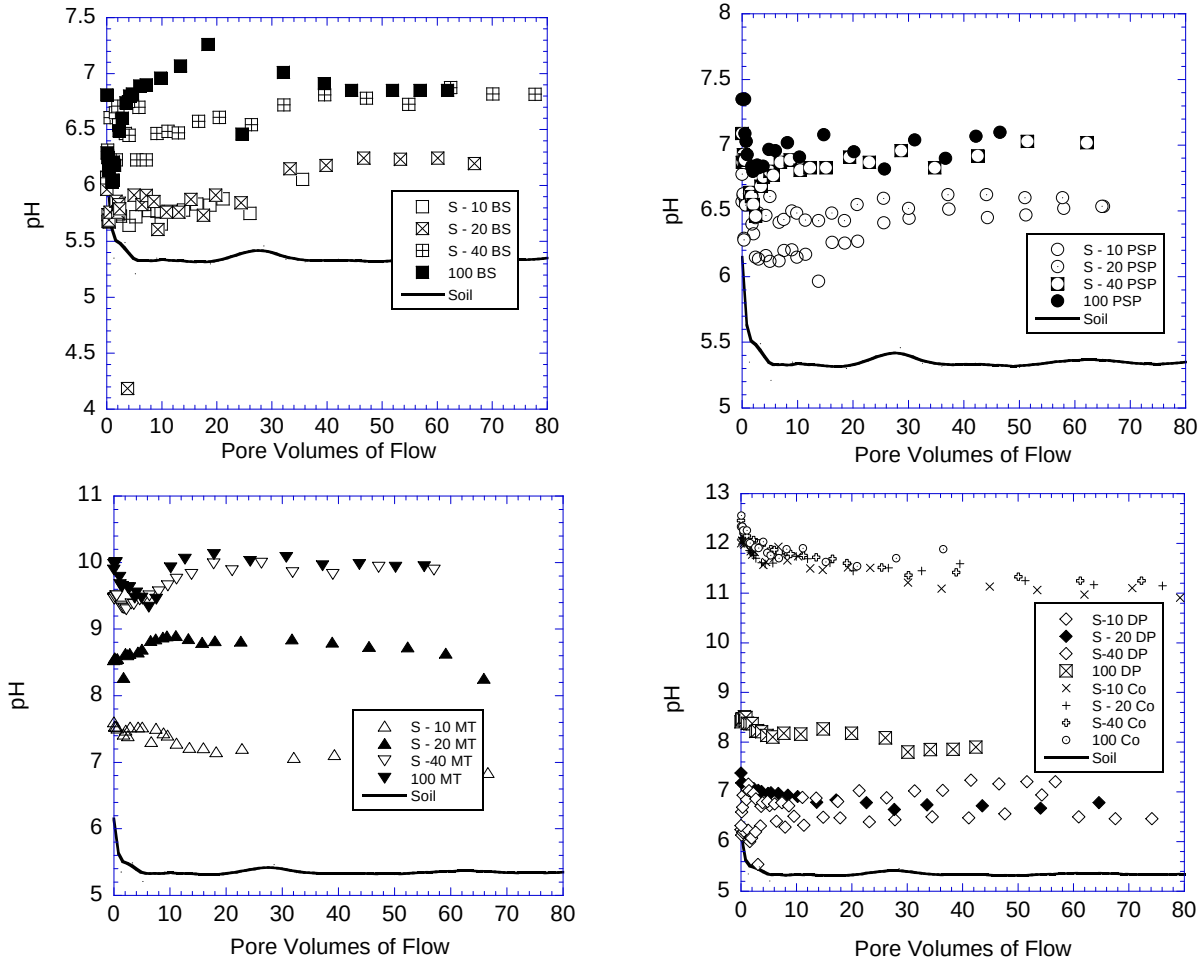

Figure 4.3 pH of the effluents from CLT on soil, fly ash and their mixtures.

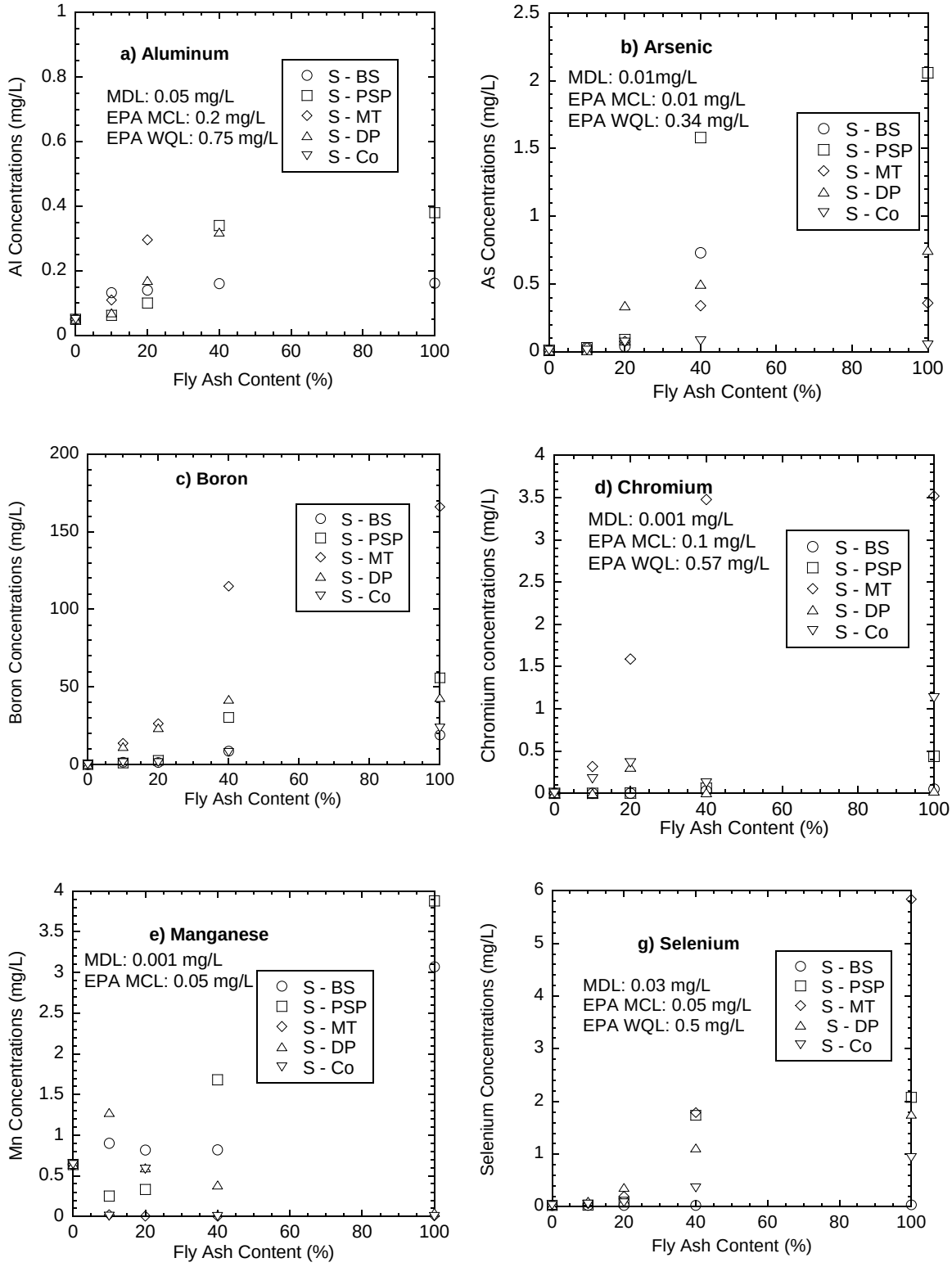

Figure 4.4 Concentrations of six metals in the effluent from CLTs (Note: BS: Brandon Shores, PSP: Paul Smith Precipitator, MT: Morgan Town)

As, Cr, Al and Se metals generally show an amphoteric leaching pattern (Cetin et al., 2012; Komonweeraket, 2010). Increased fly ash causes both an increase in the amount of main metal source and an increase in the pH of the effluent solution due to the dissolution of CaO and MgO minerals (Izquierdo et al., 2011). The observed pH range in the effluent of the column leach tests ranged from 5.75 to 12.5, so Al solubility is likely to be available in both its cationic and anionic species. Solubility of Al is generally controlled by the dissolution of precipitation of the Al carrier mineral and Al-(hydr)oxides solid phases existing in the aqueous solutions (Murarka et al. ,1991). At pH ranges of 5.75 to 9, the free Al^{3+} precipitates as $Al(OH)_3$ (gibbsite) and $Al(OH)_3$ (amorphous) which reduces the concentrations of Al^{3+} in the leachate (Astrup et al., 2006). Therefore, an increase in pH levels to between 5.75 and 9 should cause a decrease in Al concentrations. However, in this study, an increase in fly ash content increased the Al concentrations in the leachates regardless of the fly ash type. This behavior probably occurred because of the high total Al content in all fly ashes used (Table 4.3). On the other hand, an increase in Co fly ash (pH > 10) yielded Al concentrations more than 200 times higher than those leached from specimens prepared with other fly ashes. Table 4.3 indicates that total Al content of Co fly ash is 3-8 times higher than the other fly ashes. The pH levels of the effluent solutions of the soil-Co fly ash mixtures were the main reason for the release of significantly high Al concentrations because at pH >10, the anionic Al species start dissolving from the fly ash particles and particle surfaces and complex with other metals or become freely available in the aqueous solutions (Sparks 2003).

Figure 4.4d indicates that increases in fly ash content yielded increases Cr concentrations in aqueous solutions. Specimens prepared with 10% by weight BS and PSP fly ashes and specimens prepared with 20% by weight BS fly ash did not release Cr at concentrations greater than the detection limit (MDL for Cr=0.001mg/L). The pH level of the effluent solutions was the main reason for this low Cr release: At pH levels of 5.75 to 6.3, Cr is usually present at its insoluble form and, therefore, does not leach significantly (Engelsen et al., 2010). Levels of pH are greater than, 6.5-7 will increase the oxidation of these Cr(III) to Cr(VI) and also will release the anionic forms of Cr metals such as $HCrO_4^-$ and CrO_7^{-2}, CrO_4^{-2} (Goswami & Mahanta 2007; Komonweeraket et al., 2010). This trend was observed especially with the specimens prepared with MT and Co fly ashes. The concentrations of Cr leached from these specimens were at least 7 times higher than those leached from soil-fly ash mixtures prepared with BS, PSP and DP fly ashes, probably because of the high pH levels of these specimens (Table 4.6). The relatively higher Cr concentrations observed in MT fly ash mixtures (compared to Co fly ash mixtures) was attributed to total Cr content of MT fly ash (Table 4.3). Cr concentrations of all soil-MT fly ash mixtures exceeded the EPA limits, Cr (VI) is a toxic Cr species and an acute irritant for living cells and can be carcinogenic to humans via inhalation (Whalley et al., 1999). Therefore, extra care should be taken when designing embankments that contain MT fly ash.

Se concentrations leached from soil-fly ash mixtures prepared with BS fly ash were below the detection limits in all cases except for the specimens prepared with 100% BS. For the remaining mixtures, an increase in fly ash content yielded an increase in the

Se concentrations in the effluent solutions (Figure 4.4g). Soil-BS fly ash mixtures were expected to have very low Se concentrations because of it relatively low pH values (pH=5.75 to 7.3). Se tends to show amphoteric leaching patterns and its leaching is minimum at neutral pH values (Komonweeraket et al., 2010; Su et al., 2011). At alkaline pH levels, Se is remained in its anionic forms (e.g., SeO_4^{2-} and SeO_3^{2-}) (Izquierdo et al., 2011; Morar et al., 2012). Leaching of Se oxyanions is affected by the fly ash surface and soil surface site concentrations, pH levels, and other anions and cations (Su et al., 2011). Increases of aqueous solutions' pH levels cause cationic species to be adsorbed by the surfaces of soil and fly ash particles, which creates competitions between cationic and anionic species of the metals. Decreases in the available space on the surface sites of the soil fly ash particles causes dissolution of anionic Se species and increases the Se concentrations in the leachates (Wang et al., 2008). Therefore, the specimens prepared with MT fly ash yielded the highest Se concentrations because the pH levels of these soil mixtures were between 7.2 and 10. Specimens prepared with Co fly ash leached lower Se concentrations than the ones prepared with MT fly ashes even though the pH levels of specimens prepared with Co fly ash were higher than those prepared with MT fly ashes. This trend is attributed to the relatively higher total Se content of the MT fly ashes (Table 4.3).

Figure 4.4b shows that an increase in fly ash content in the soil-fly ash mixtures increases the As concentrations in the effluent solutions regardless of fly ash type. Solubility of As is highly pH dependent (Komonweeraket et al., 2010; Pandey et al., 2011; Vitkova et al., 2009). Leaching of As also tends to show an amphoteric leaching

pattern and has a high affinity to exist in its anionic forms such as $HAsO_4^{2-}$, $HAsO_3^-$ (Ettler et al., 2009; Narukawa et al., 2005). In neutral pH conditions (pH=6 to 7.5), As exhibits minimal leaching because of the maximum adsorption of As metals onto soil and fly ash surfaces. However, the soil-fly ash mixtures prepared with PSP fly ash had the highest As concentrations in the leachates, even though the effluent pH levels of these soil-PSP mixtures was neutral.

Specimens prepared with MT and Co fly ashes leached lower As concentrations than the specimens prepared with PSP fly ash, even though the effluent pH levels of the specimens prepared with MT and Co fly ashes were approximately 10 and 12, respectively. PSP fly ash had the highest total As content of all the fly ashes used in the current study. Gitari et al., (2009) also said availability of As depends on the quantity of As in the fly ashes.

Sorptions of As onto metal oxide minerals very probably occur at neutral pH levels (, Kim et al., 2009; Pandey et al., 2011; Sadiq et al., 2002). Fe-(hydro)oxides are one of the most dominant oxide minerals that have significant effects on the leaching of As (Apul et al., 2005) because they have a strong affinity for As species. Adsorption reaction between As and Fe-oxides becomes very rapidly and the reaction continues at a slower rate after the initial reaction (Sadiq et al., 2002). Fe contents of the fly ashes and leached Fe concentrations in aqueous solutions are critical in the leaching behavior of As (Kim et al., 2009). Relatively lower Fe_2O_3 contents of the PSP fly ash could be another reason they showed highest As concentrations in the leachates (Table 4.2). Since PSP fly ash had the lowest Fe_2O_3, it was expected to observe lower leached Fe concentrations

from the soil-PSP fly ash mixtures compared to MT-based mixtures. However, in this study Fe concentrations were not measured, therefore; it was not possible to make a certain conclusions about the effects of Fe-As association on the leaching behavior of As.

B concentrations generally increased with increasing fly ash content. B has cationic species that are adsorbed by the soil and fly ash particles in the aqueous solution or precipitated with Al-oxides and iron oxides at pH > 6.5 (Pagenkof & Connolly, 1982). Therefore, the B concentrations are expected to decrease with an increase in pH of the effluent solution. However, an opposite trend occurred for the specimens in the current study (Figure 4.4c and Table 4.6). Large amounts of boron in the fly ash could account for the observed pattern. Table 4.3 indicates that total B content of Co fly ash is 600 mg/kg, which is the highest among all the fly ashes used in the current study. However, specimens prepared with MT fly ashes yielded the highest B concentrations in the leachates. Precipitation of B metals with ettringite minerals at very alkaline conditions by substitution with other cations on the soil and fly ash surfaces may have yielded relatively lower B concentrations in the aqueous solutions of the soil-fly ash mixtures prepared with Co fly ash (Gitari et al., 2009).

Figures 4.5 through 4.10 show a series of CLT elution curves for the specimens tested in the current study. The curves for all metals, except As, suggest an initial leaching of metals followed by a sharp decrease to near constant concentrations after 5-15 pore volumes of flow. This is called first-flush of leaching and occurs due to the release of metals from the water soluble fraction as well as from the sites with low adsorption energies. The CLT results suggest that, in field applications, aqueous samples

should be collected (especially during the construction phase) because metal concentrations in leachates that come out of the mixtures are expected to be higher at the initial stages. However, the leaching curves for As showed a lagged flush response. The leaching of As increases through 10-20 pore volumes of flow and then decreases dramatically. The As concentrations that leached out from the specimens prepared with 10% and 20% by weight fly ashes were generally below the detection limit (0.01 mg/L) and did not exhibit any clear leaching trend. The specimens prepared with 40% and 100% fly ashes showed a lagged-response leaching pattern. As concentrations first decreased significantly in the first 3-4 pore volumes of flow, then increased through 35 – 40 pore volumes of flow. The increase was followed by a dramatic decrease. In general, the immobility of the metals causes a lagged response leaching pattern in the aqueous solution (Sauer et al., 2005). As is very mobile at extreme pH conditions (Dutta et al., 2009; Komonweeraket et al., 2010). The pH levels of the effluent solutions of all specimens in the current study are either lower than 10 or higher than 6, which could be a reason for observing a lagged response leaching pattern for As.

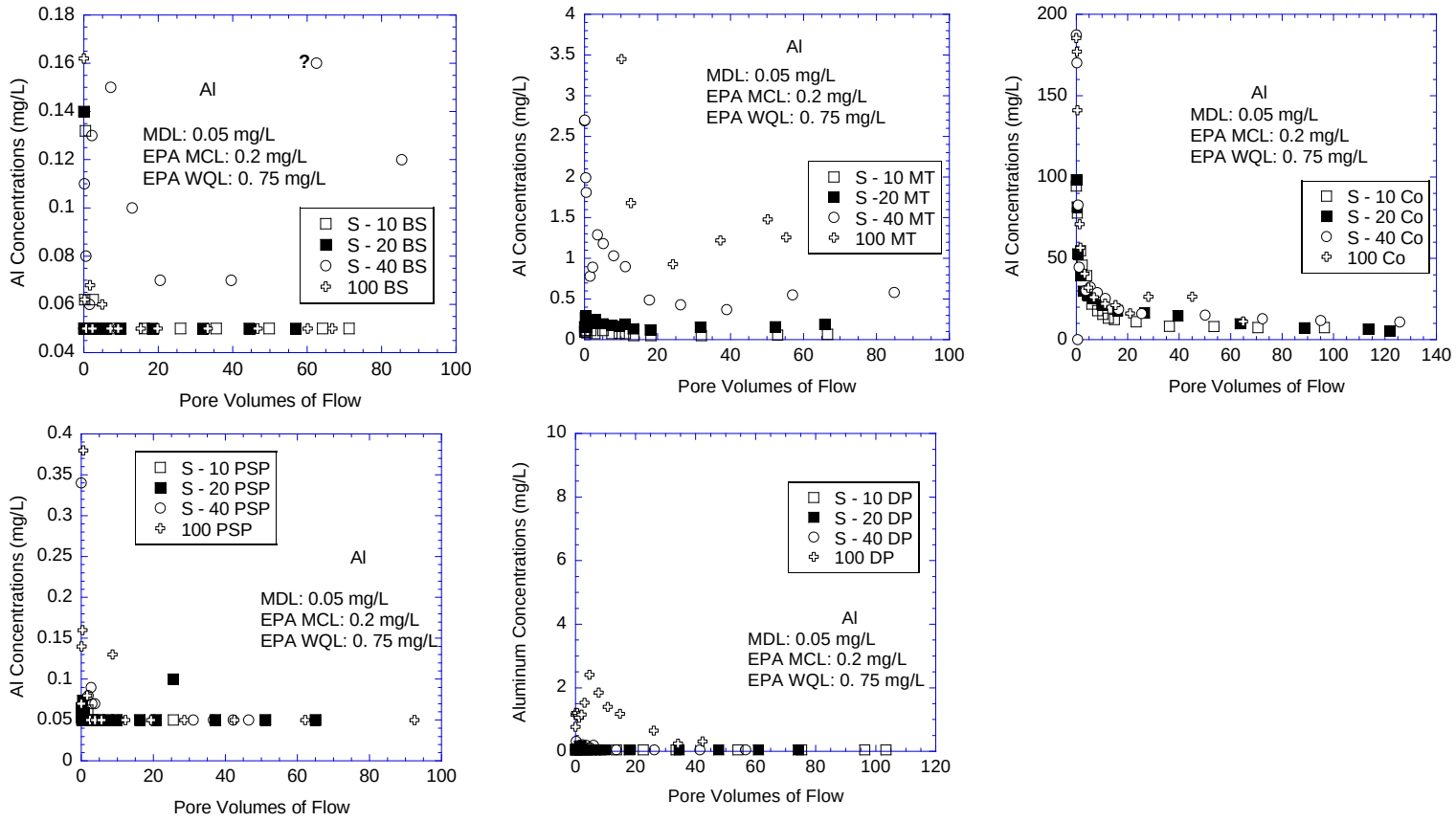

Figure 4.5 Elution curves for Aluminum Metal.

Note: MDL: Minimum Detection Limits, MCL= maximum contaminant levels for drinking water; MCL for Al is based on a secondary non-enforceable drinking water regulation; WQL= water quality limits for protection of aquatic life and human health in fresh water. The numbers that follow the fly ashes indicate the percentages by weight of admixtures added to the soil.

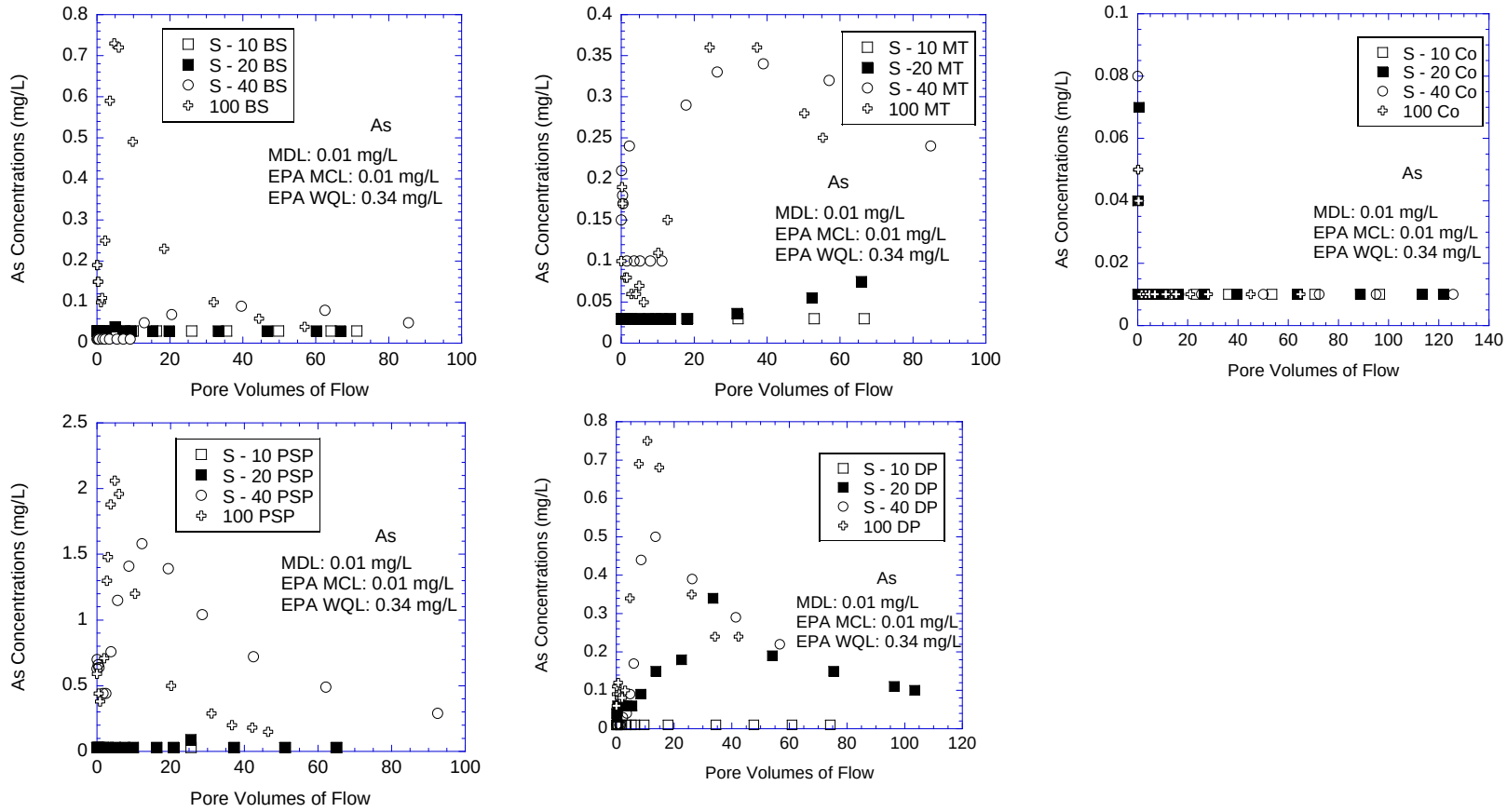

Figure 4.6 Elution curves for Arsenic Metal

Note: MDL: Minimum Detection Limits, MCL= maximum contaminant levels for drinking water; WQL= water quality limits for protection of aquatic life and human health in fresh water. The numbers that follow the fly ashes indicate the percentages by weight of admixtures added to the soil.

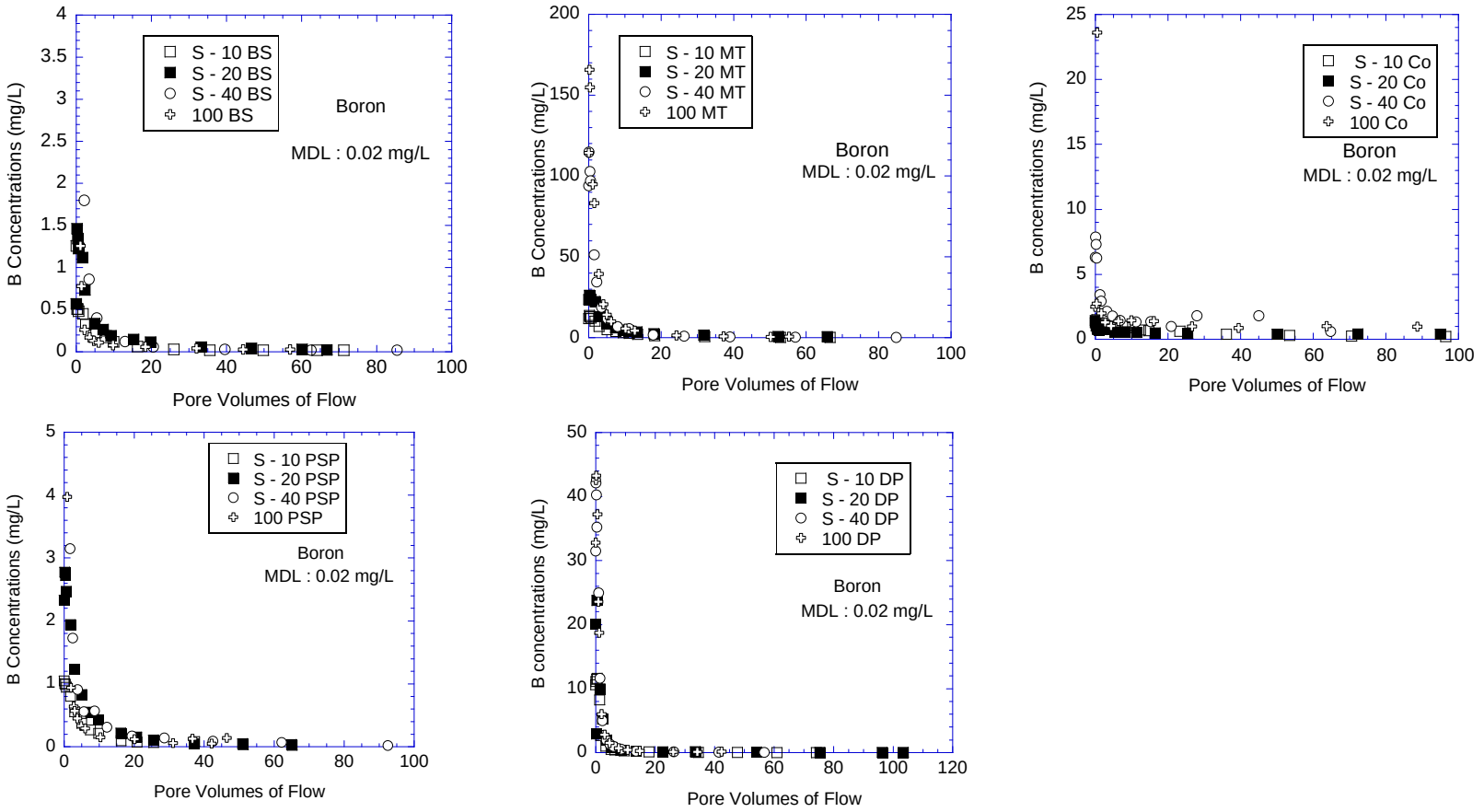

Figure 4.7 Elution Curves for Boron metal

Note: MDL: Minimum Detection Limits. The numbers that follow the fly ashes indicate the percentages by weight of admixtures added to the soil.

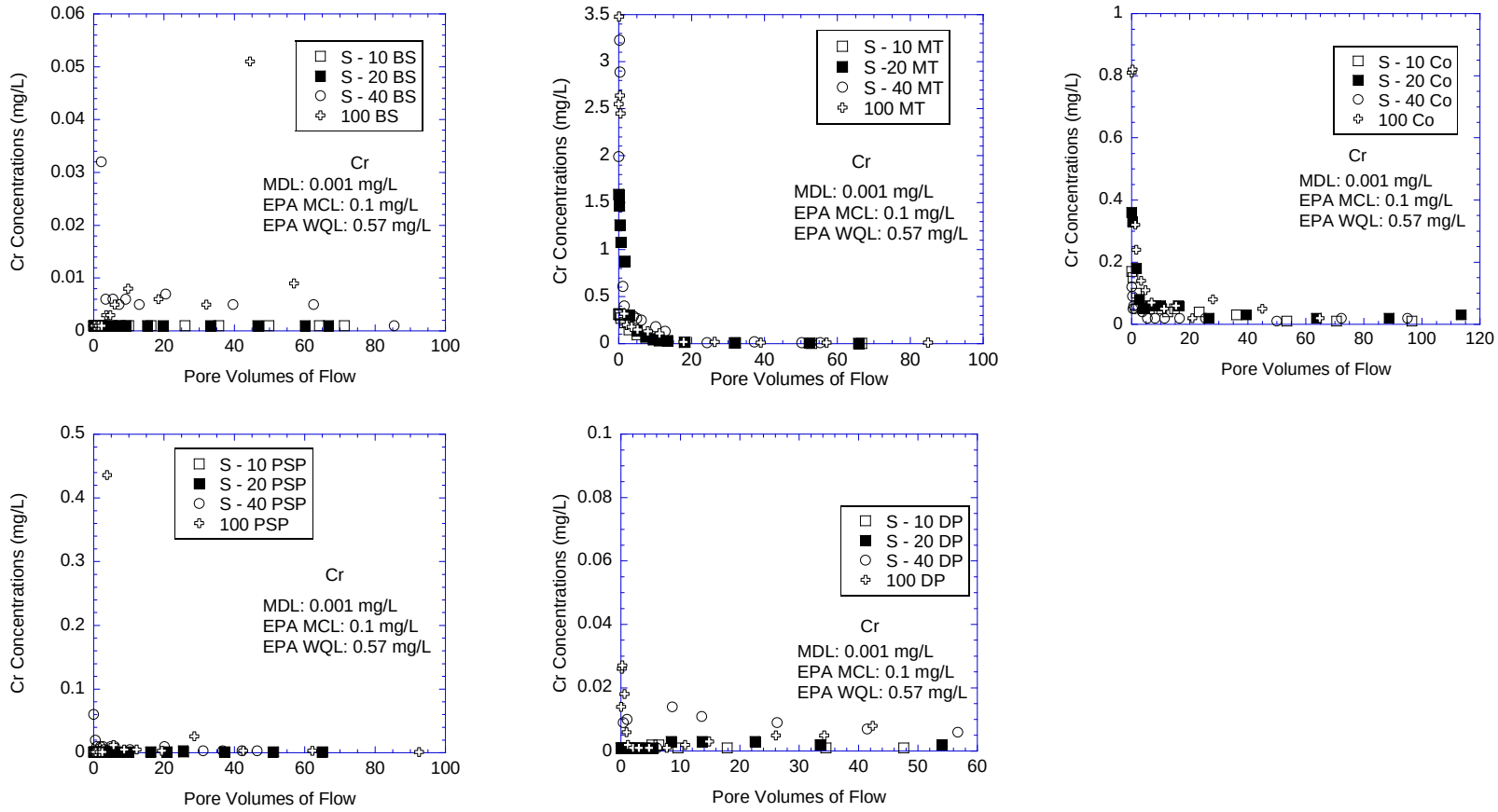

Figure 4.8 Elution curves for chromium metal

Note: MDL: Minimum Detection Limits, MCL= maximum contaminant levels for drinking water; WQL= water quality limits for protection of aquatic life and human health in fresh water. The numbers that follow the fly ashes indicate the percentages by weight of admixtures added to the soil.

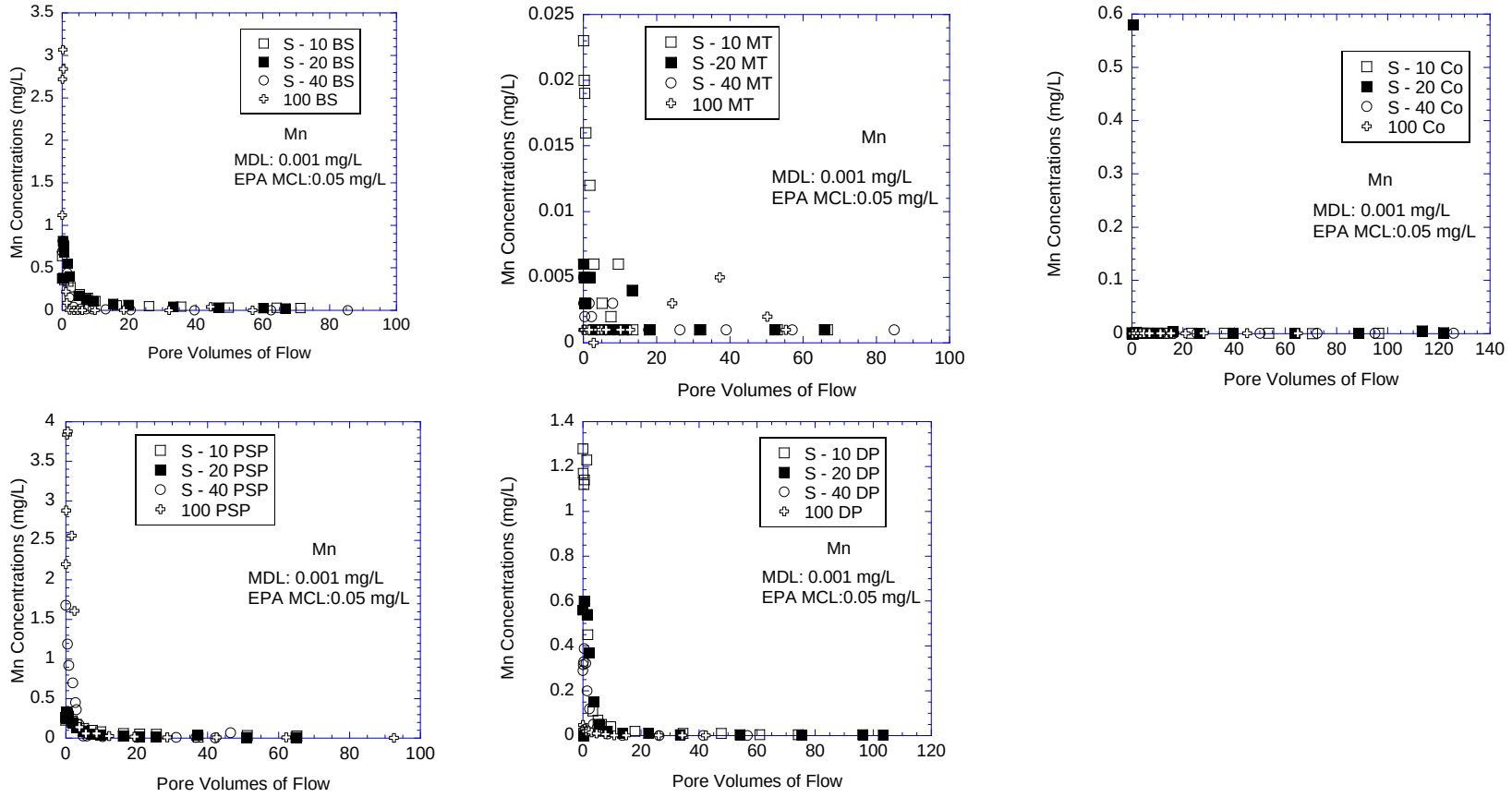

Figure 4.9 Elution curve for Manganese metal.

Note: MDL: Minimum Detection Limits, MCL= maximum contaminant levels for drinking water. The numbers that follow the fly ashes indicate the percentages by weight of admixtures added to the soil.

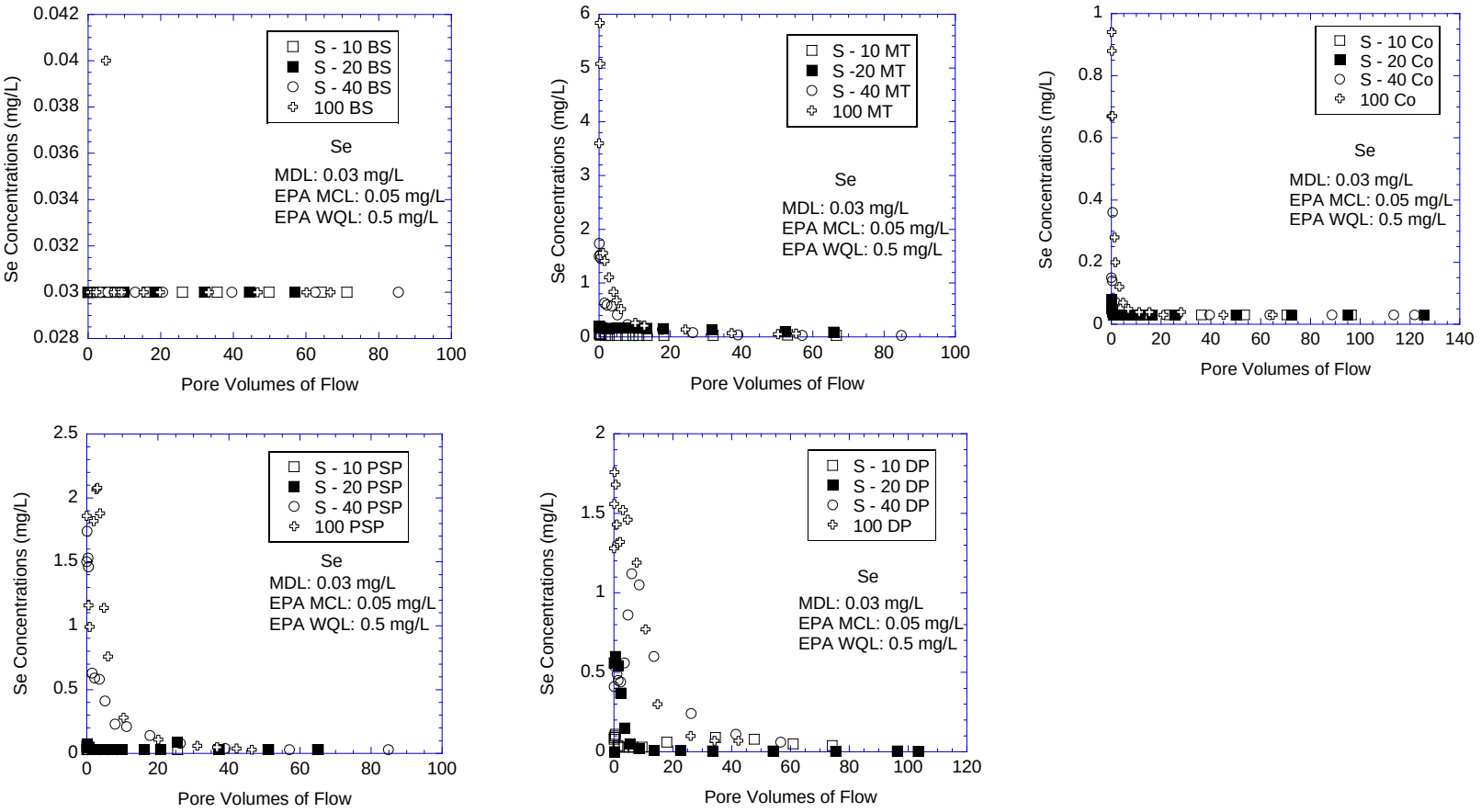

Figure 4.10 Elution curves for selenium metal.

Note: MDL: Minimum Detection Limits, MCL= maximum contaminant levels for drinking water; WQL= water quality limits for protection of aquatic life and human health in fresh water. The numbers that follow the fly ashes indicate the percentages by weight of admixtures added to the soil.

4.4.3 Results Toxicity Characteristic Leaching Procedure Tests

Toxicity characteristic leaching procedure tests (TCLPs) were conducted to determine the leaching of heavy metals under acidic conditions. Duplicate TCLPs were conducted on soil alone, fly ash alone and soil-fly ash mixtures. As expected, the effluent pH values of the specimens stabilized at pH levels of 4.8 to 5; the sole exception to this trend were the specimens prepared with 100% MT by weight and the soil-fly ash mixtures prepared with Co fly ashes. The high CaO contents of MT and Co fly ashes most probably buffered he pH levels of the effluent solutions of these specimens (Table 4.2). Therefore, the acetic acid buffer used in TCLPs was not able to keep the pH values of these specimens between 4.8 and 5.

The pH levels of the TCLP effluents specimens varied between 4.8 and 5 (Figure 4.1.c). An increase in fly ash content did not affect the pH level of the soil-fly ash mixtures for any but the specimens prepared with Co fly ash. CaO content of the Co fly ash was 19.4% (Table 4.2) and the release of Ca in high concentrations dominated the pH of the TCLP leachate, consistent with observations made by Mudd et al., (2004).

In general, leached concentrations of six metals (Al, As, B, Cr, Mn, Se) from the soil-fly ash mixtures in the TCLP tests were higher than those from WLTs and were lower than the maximum peak concentrations of metals leached from CLTs. TCLP test results indicated that at pH levels less than 5, the leached metal concentrations exceeded the environmental health regulation limits (Table 4.7). This was an expected behavior because the leaching of heavy metals is extreme at low (acidic) pH levels (Van der Hoek et al., 1994). At acidic pH levels, the surfaces of the soil and fly ash particles are

positively charged and cause them to leach significant amounts of cationic metal species into the aqueous solutions (Stumm & Morgan, 1995). For example, Al metals start precipitating in their oxide forms such as $Al(OH)_3$(am), $Al(OH)_3$(gibbsite) at pH > 5.5. At pH < 5.5, Al is dissolved from these Al-oxides and is available in its free form of Al^{3+} (Sparks, 2003). Similarly, As metals exist in their reduced form as As(III), the most toxic As species, at pH <5 (Pandey et al., 2011). Se behaves similar to As, and anionic species of Se are likely to be adsorbed by soil and fly ash particles at acidic conditions at pH<5, which yields the release of cationic species of these metals into the aqueous solutions (Su et al., 2011). Under natural conditions, Al-oxides and Fe-oxides may provide adequate surface sites for As and Se metals to be sorbed. However, at acidic pH levels, these As and Se attached metal oxides dissolve and increase the concentrations of As and Se metals (Apul et al., 2010). This may also have contributed to higher As and Se concentrations observed in the TCLP tests as compared to the WLTs.

The data in Figure 4.11 suggest that, with few exceptions, an increase in fly ash content generally resulted in an increase of metal concentrations. In TCLP tests, leaching amount of metals is expected to be dependent on the total metal content in the fly ash since the pH levels of the effluent solutions were kept nearly constant. Differences in Mn concentrations measured from TCLP tests and WLTs prove that the leaching of Mn was a cationic leaching pattern indicating that leaching of Mn was higher at low pH levels. Mn complexes with free OH^- in the aqueous solution at neutral pH levels to alkaline pH levels and precipitates as Mn-(hydro)oxides.

Table 4.7. Effluent metal concentrations in TCLP tests. Concentrations exceeding EPA MCL are in **bold**.

Specimen Name	Fly Ash Content (%)	pH	Al (mg/L)	As (µg/L)	B (µg/L)	Cr (µg/L)	Mn (µg/L)	Se (µg/L)
S – 10 BS	10	4.82	<0.05	<0.01	0.08	0.01	0.04	<0.03
S – 20 BS	20	4.82	<0.05	<0.01	0.1	0.01	**0.11**	<0.03
S – 40 BS	40	4.82	0.055	<0.01	0.14	0.01	**0.14**	<0.03
100 BS	100	4.83	0.06	**0.045**	0.39	0.02	**0.21**	<0.03
S – 10 PSP	10	4.84	<0.05	<0.01	0.11	<0.001	**0.18**	<0.03
S – 20 PSP	20	4.85	0.085	<0.01	0.15	<0.001	**0.18**	<0.03
S – 40 PSP	40	4.85	**0.27**	**0.15**	0.35	0.004	**0.3**	**0.075**
100 PSP	100	4.86	**0.58**	**0.47**	1.03	0.0045	**0.48**	**0.35**
S – 10 MT	10	4.87	0.185	<0.01	0.91	0.02	**0.15**	<0.03
S – 20 MT	20	4.89	**0.32**	<0.01	1.37	0.03	**0.16**	<0.03
S – 40 MT	40	4.92	**2.37**	<0.01	2.44	0.085	**0.29**	<0.03
100 MT	100	5.12	**5.43**	**0.03**	7.3	**0.11**	**0.43**	**0.085**
S – 10 DP	10	4.83	**4.83**	**0.61**	0.01	**0.25**	0.01	**0.23**
S – 20 DP	20	4.87	**4.87**	**1.25**	0.15	**0.38**	0.02	**0.24**
S – 40 DP	40	4.92	**4.87**	**2.07**	0.46	**0.53**	0.03	**0.24**
100 DP	100	4.87	**4.87**	**8.7**	0.5	**1.65**	**0.06**	**0.28**
S – 10 Co	10	5.21	**3.95**	<0.01	1.12	0.02	**0.21**	<0.03
S – 20 Co	20	5.42	**1**	**0.025**	1.73	0.035	**0.18**	0.045
S – 40 Co	40	7.41	0.05	**0.045**	3.1	0.07	**0.11**	**0.14**
100 Co	100	10.86	14.445	**0.06**	4.32	0.23	0.04	**0.35**
Sandy Soil	-	6.74	<0.05	<0.01	<0.02	<0.001	<0.001	<0.03
MDL (mg/L)			0.05	0.01	0.02	0.001	0.001	0.03
U.S. EPA MCL (mg / L)			0.2	0.01	NA	0.1	0.05	0.05
U.S. EPA WQL (mg / L)			0.75	0.34	NA	0.57	NA	0.005
MD ATL (µg / L)			NA	NA	13000	0.57	NA	NA

Note: MDL: Minimum Detection Limits, MCL= maximum contaminant levels for drinking water; MCL for Al is based on a secondary non-enforceable drinking water regulation; WQL= water quality limits for protection of aquatic life and human health in fresh water. ATL = aquatic toxicity limits for fresh water. The numbers that follow the fly ashes indicate the percentages by weight of admixtures added to the soil.

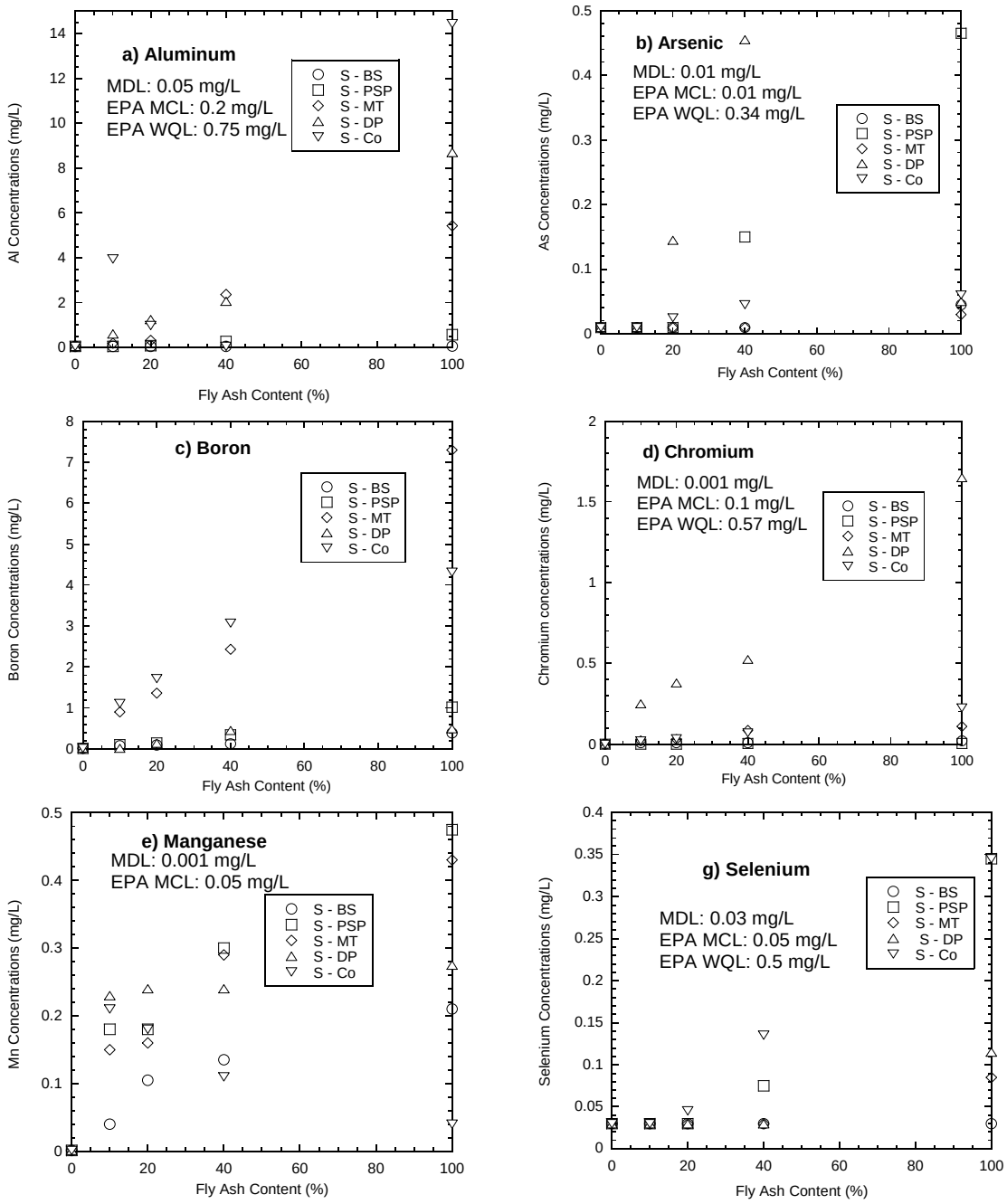

Figure 4.11 Concentrations of six metals in the effluent from TCLPs (Note: BS: Brandon Shores, PSP: Paul Smith Precipitator, MT: Morgantown); MCL= maximum contaminant levels for drinking water; MCL for Al is based on a secondary non-enforceable drinking water regulation; WQL= water quality limits for protection of aquatic life and human health in fresh water.)

These solid Mn-(hydro)oxides minerals dissolve with an increase in pH because of the hydrolysis reactions and leaving Mn^{2+} free in the effluent solutions (Gitari et al., 2009).

As mentioned in previous sections, Cr tends to follow an amphoteric leaching pattern similar to As, Se, and Al (Cetin et al., 2012). At neutral pH levels, Cr leaching is minimal, but when pH < 7, Cr leaching increases significantly (Karamalidis & Voudrias, 2008). Therefore, higher Cr concentrations were expected to leach from the soil-fly ash mixtures in TCLP tests than in WLTs. Cr exists mostly in its oxidized form Cr (III) at low pH levels (pH<6) due to reduction of Cr(VI) to Cr(III) (Geelhoed et al., 2002, Samaras et al., 2008). Even though specimens released more Cr into the aqueous solutions at acidic conditions, it is not a critical concern because Cr(III) is non-toxic and provides necessary nutrition metal for plants and animals (Quina et al., 2009). Cr(VI) is the anionic form of Cr. It is likely that these Cr(VI) forms are being adsorbed onto the soil and fly ash surfaces as aqueous solutions become more acidic. Solubility of Cr(III) is generally controlled by $Cr(OH)_3$ minerals; a decrease in pH will hydrolyze these minerals and release the Cr(III) metals into the effluent solutions (Engelsen et al., 2010). Dissolution of $Cr(OH)_3$ minerals may have caused the leaching of higher Cr concentrations in TCLP tests than WLTs.

B concentrations in the aqueous solutions increased with fly ash content (Figure 4.11c). This trend was consistent with results obtained from both WLTs and CLTs. B leaching increased as pH levels decreased. B typically remained at its maximum in acidic conditions (Querol et al., 1995). However, the B concentrations leached from soil-Co fly ash mixtures were the highest, even though the pH levels of the effluent solutions of the

soil-Co fly ash mixtures were significantly higher than the pH levels of the effluent solutions of other soil-fly ash mixtures (Table 4.7). These results could be explained by comparing the total B contents of the fly ash materials as determined by total elemental analysis. Table 4.3 indicates that Co fly ash contains 2.5 to 28 times higher total B content than the other fly ashes used in this study. A similar trend also was observed for the MT fly ash-alone specimen. Higher B concentrations were leached from the MT fly ash-alone specimen, even though its pH levels were relatively higher than the pH of the other soil-fly ash mixtures.

The Al and Mn leaching in specimens prepared with Co fly ash depended on the total metal content of the Co fly ash and the pH levels of the effluent solutions. TCLP test results indicated that the pH values of the soil-Co fly ash mixtures increase significantly as fly ash increases and were higher than buffered pH values that were between 4.8-and 5. On the other hand, the effluent pH values of other soil-fly ash mixtures in TCLP tests were at this range. An increase in Co fly ash content resulted in decreased Mn concentrations. Mn leaching is extreme at acidic pH levels, so an increase in pH would decrease the leaching capability of Mn significantly (Cetin et al., 2012; Goswami & Mahanta 2007). Therefore, the concentrations of Mn for the specimens prepared with the Co fly ash were much lower than those prepared with other fly ashes. Different leaching trends were observed for the leaching of Al from the soil-Co fly ash mixtures. The pH levels of the S-10 Co, S-20 Co, S-40 Co, and 100 Co specimens were 5.21, 5.42, 7.41, and 10.86, respectively, and the Al concentrations of these specimens with the same order were 4 mg/L, 1mg/L, 0.05 mg/L, and 14.5 mg/L, respectively. Al shows an amphoteric

leaching pattern and is very mobile at acidic pH levels and basic pH levels; its leaching is minimal at neutral pH levels (Cetin et al., 2012; Komonweeraket et al., 2010,). The results of Al leaching confirmed that Al leaching is highly dependent on the pH of the effluent solutions and that Al leaching shows amphoteric leaching pattern. An increase in Co fly ash content from 10% to 40% did not increase the Al concentrations; rather, Al concentrations decreased because of the precipitation of Al into Al-(hydr)oxide minerals (Mudd et al., 2004). On the other hand, Co fly ash alone samples leached the highest Al concentrations in all the soil-fly ash mixtures, which was due to extreme basic conditions (pH=12.2) and total Al content of the Co fly ash (Table 4.3).

4.4.4 Comparison of the Leaching Test Results

The TCLP, CLT, and WLTs were compared and appear in Figure 4.12. The peak CLT concentrations are consistently greater than the WLT concentrations. Differences in L:S ratio between the two leaching tests (a ratio of 20:1 in WLTs versus 0.1:1 in CLTs in the initial PVFs) could be responsible for the significant metal concentration differences measured in these two leaching tests. Su et al., (2011) claimed that a decrease in L:S ratio increased the concentrations of leached metals. Figure 4.12 shows that the maximum concentrations of the Al, As, B, Cr, Mn, and Se from CLTs is up to 16, 100, 100, 100, 100 and 50 times higher than the metal concentrations obtained from WLTs, respectively. In addition, the peak CLTs are consistently greater than the TCLP test concentrations. Figure 4.13 shows that the maximum concentrations of the As, Al, B, Cr, Mn and Se from CLTs is up to 10, 100, 100, 100, 10, and 10 times higher respectively than the metal

concentrations obtained from TCLPs. Figure 4.14 shows that the concentrations of the As, B, Cr, Mn, and Se from TCLPs is up to 20, 20, 10, 50, and 10 times higher respectively than the metal concentrations obtained from WLTs. No relationship TCLP and WLT test results for Al concentrations is evident because the Al concentrations in the leachates collected in WLTs were below the detection limits which yielded constant Al concentrations values for many specimens. The pH levels of effluent solutions obtained from TCLP tests were more acidic than those from WLTs. This could be the reason for obtaining higher leached metal concentrations in TCLP tests from the soil-fly ash mixtures since the leaching of metals are the highest at acidic conditions (Komonweeraket et al., 2012).

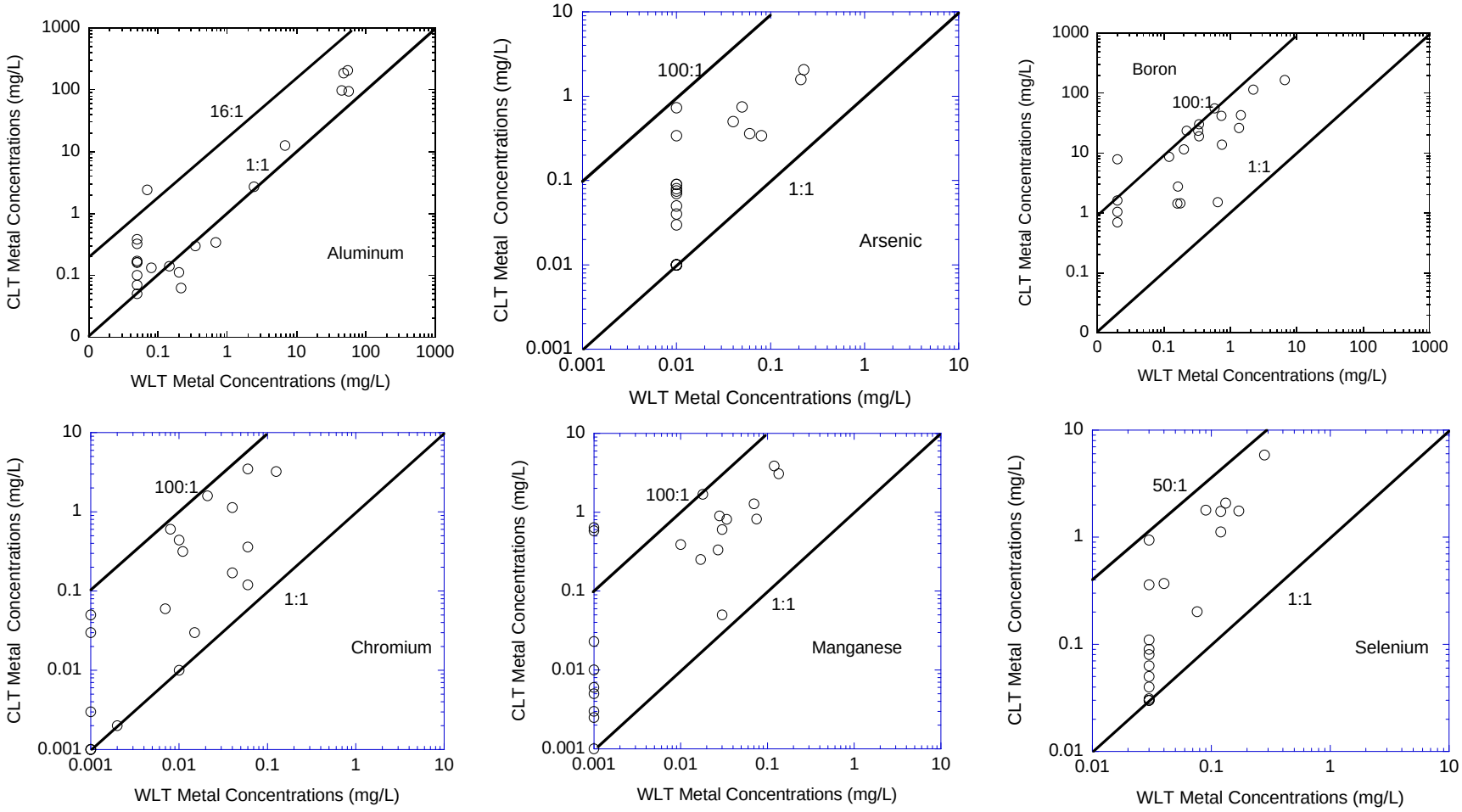

Figure 4.12. Comparison of peak effluent concentrations of six metals from the CLTs and the WLTs

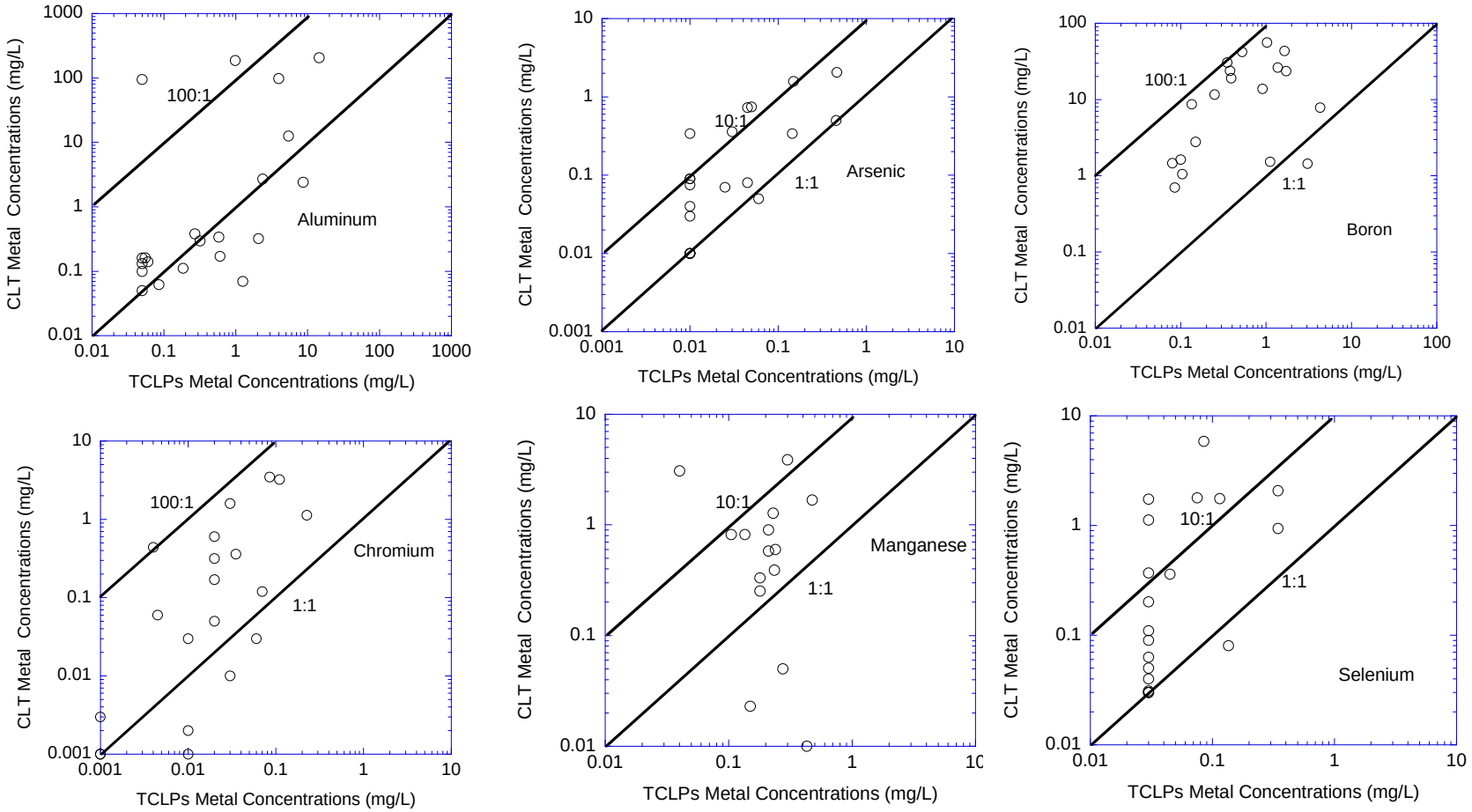

Figure 4.13. Comparison of peak effluent concentrations of six metals from the CLTs and the TCLPs

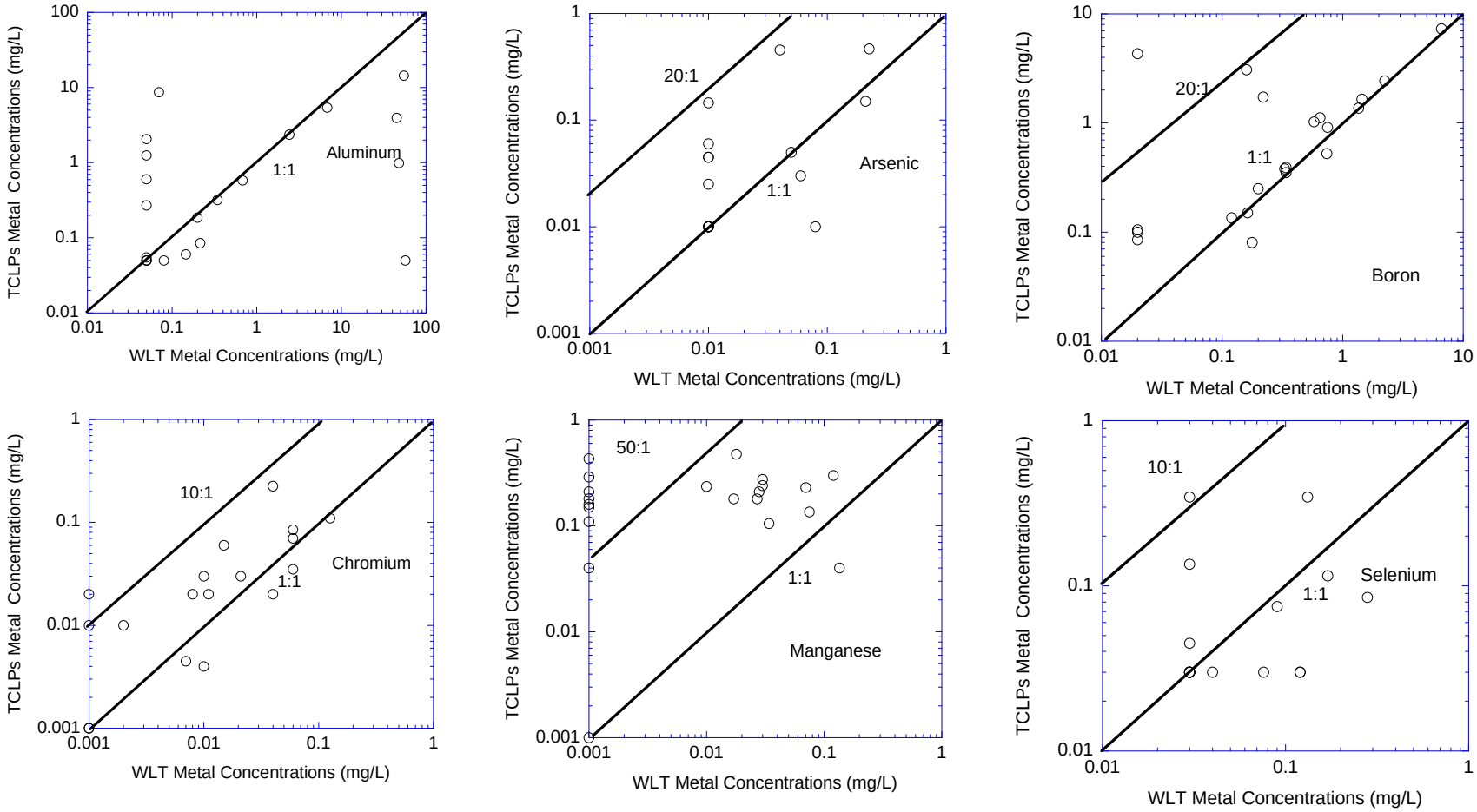

Figure 4.14. Comparison of peak effluent concentrations of six metals from the WLTs and the TCLPs

4.5 CHEMICAL TRANSPORT MODELING

4.5.1 Numerical Model

A schematic diagram of WiscLEACH for embankment structures is shown in Figure 4.15. WiscLEACH simulations were conducted to study the locations of maximum soil vadose zone and groundwater concentrations (e.g., at the centerline of the embankment structure, at the vicinity of point of compliance). Contours of trace metals are predicted at different years as a function of depth to groundwater, thickness of the embankment layer, percent fly ash by weight, hydraulic conductivity of the least conductive layer in the vadose zone, hydraulic conductivity of the aquifer material and the initial concentration in the fly ash. Model formulation of embankment version of WiscLEACH was defined in section 3, so, for brevity's sake, will not be repeated again here.

4.5.2 WiscLEACH Results

WiscLEACH predicted the metal concentrations in contour graphs at different years in order to determine the location of maximum concentrations of the trace metals in the soil vadose zone and groundwater after a period of 50 years. The data in Tables 4.8 and 4.9 were used for all soil-fly ash mixtures in order to keep things consistent. The hydraulic conductivities and transport parameters of the pavement layers and soil mixtures are summarized in Table 4.9. The transport parameters were determined from the laboratory tracer tests, and the pavement and subgrade properties were taken from Li et al., (2007). The retardation factors along with chromium concentrations for four

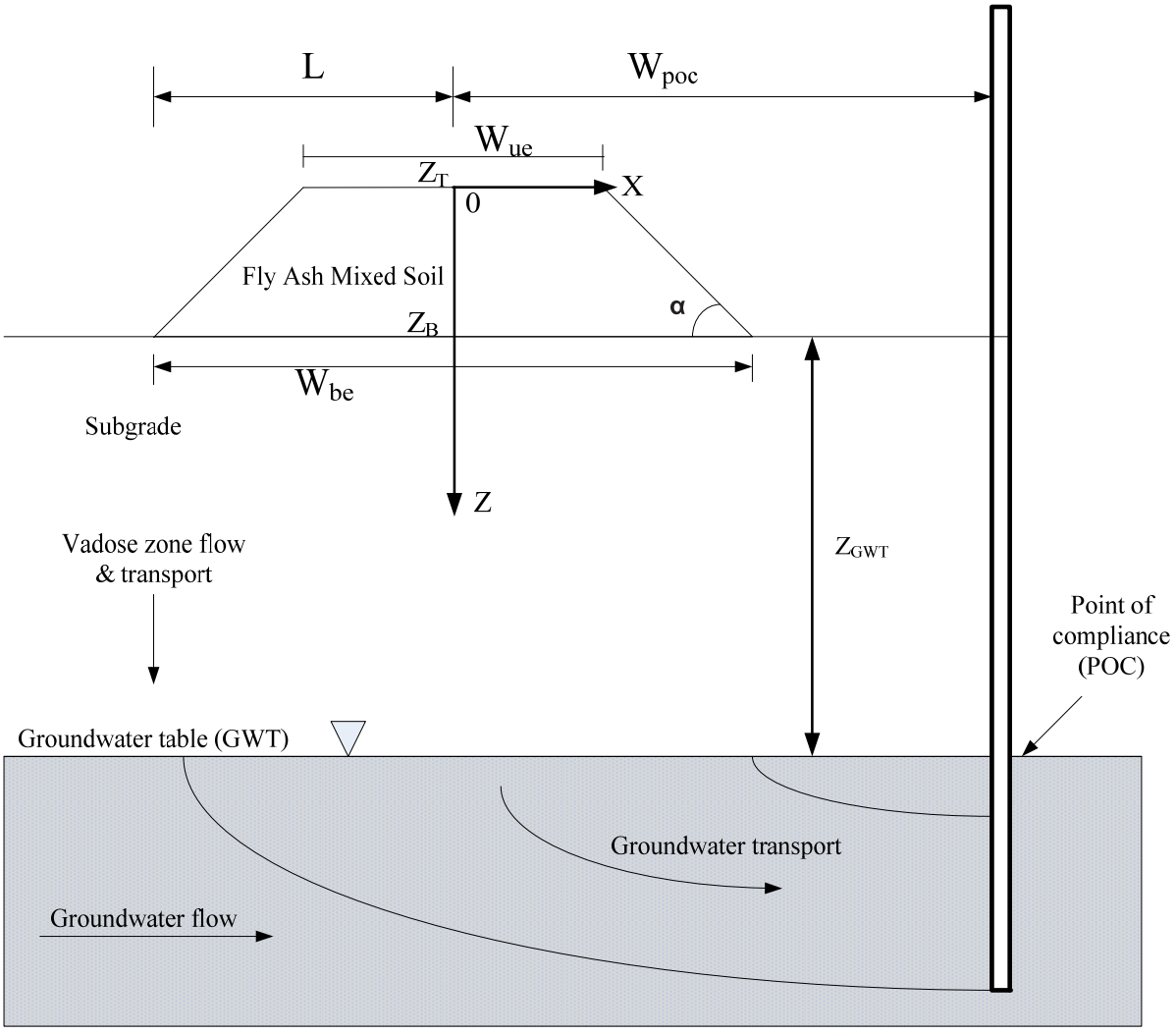

Figure 4.15. Conceptual model for embankment structure

Table 4.8 Input site parameters for embankment and soil structures.

	Wpoc m(ft)	Wp m(ft)	Ws, m(ft)	ZGWT ,m (ft)	Prcpt m/yr (ft/yr)	Tmax (yrs)	T m(ft)	Side Slope (H:V)
Constant values for all specimens	30 (98)	6 (20)	2 (6.6)	5 (16)	1.00 (3.3)	50	5 (16.4)	2:1

Notes: All measurements are in meter, W_{poc}: Point of compliance, W_p: Pavement width, W_s: Shoulder width, Z_{GWT}: Depth to groundwater table, Prcpt; Annual precipitation rate in m/year, T_{max}: 50 years, Thickness of embankment structure,

Table 4.9 Hydraulic and transport parameters or pavement, embankment, soil aquifer structures to be used as an input in WiscLeach

Specimen	Hydraulic Conductivity, K_s,,m/yr (ft/yr)	n_e	Hydraulic Gradient	α_L (m)	α_T (m)	R_d for Cr
S – 20 PSP	8.67 (28.4)	0.302	0.001	0.193	0.0193	27
S – 40 PSP	6 (20)	0.395	0.001	0.485	0.0485	8
S – 20 DP	25.23 (83)	0.42	0.001	0.401	0.0401	1.1
S – 40 DP	20.08 (66)	0.489	0.001	0.671	0.0671	15
Pavement	18.29 (60)	0.35	0.001	0.1	0.01	1
Subgrade	1.01 (3.3)	0.35	0.001	0.1	0.01	3.5
Aquifer	3784 (12,412)	0.30	0.001	0.1	0.01	1

Notes;α_L : Longitudinal dispersivity, α_T : Transverse dispersivity, hydraulic gradients is assumed as 0.001 to simulate the natural conditions, n_e : effective porosity, Cr: Chromium.

different soil mixtures, S – 20 DP, S – 40 DP, S – 20 PSP, S – 40 PSP (Note: 20 DP, 40 DP, 20 PSP, 40 PSP designate the specimens with 20% and 40% Dickerson Precipitator, 20% and 40% Paul Smith Precipitator fly ash respectively) are shown in Table 4.9. The annual precipitation rate selected in this study was 1 m/year, the average annual rainfall in the Maryland, according to the U.S. Geological Survey.

Figures 4.16 through 4.19 show the contour plots of the predicted concentrations of Cr in the soil vadose zone and groundwater. The contour plots provide predictions of the metal concentrations after 5, 10, 20, and 50 years of construction. WiscLEACH simulations indicate that Cr concentrations for all specimens were below the EPA MCL of 100 μg/L, except the S – 40 PSP. The results indicated that the maximum Cr concentrations were reached in approximately 10 to 20 years and that they were below the EPA MCL at the groundwater table (Figures 4.16- 4.19).

As shown in figures 4.16 through 4.19 the Cr metal concentrations decreased with distance from the ground surface of HCFA-amended embankments and the surface of groundwater. This was probably because of the dispersion of the metals in the soil vadose zone. High annual precipitation rate may also have factored into the increase in the leaching rate of the metals from HCFA amended embankment and absorbing the metals before reaching to the groundwater.

The WiscLEACH computer model was also redesigned to simulate metal leaching from embankment structures built in multiple fly ash-alone and soil-alone layers. A multiple-layer version of WiscLEACH was used to predict the concentrations of four metals of concern (As, Cr, Mn, and Se) at different years and determine the maximum

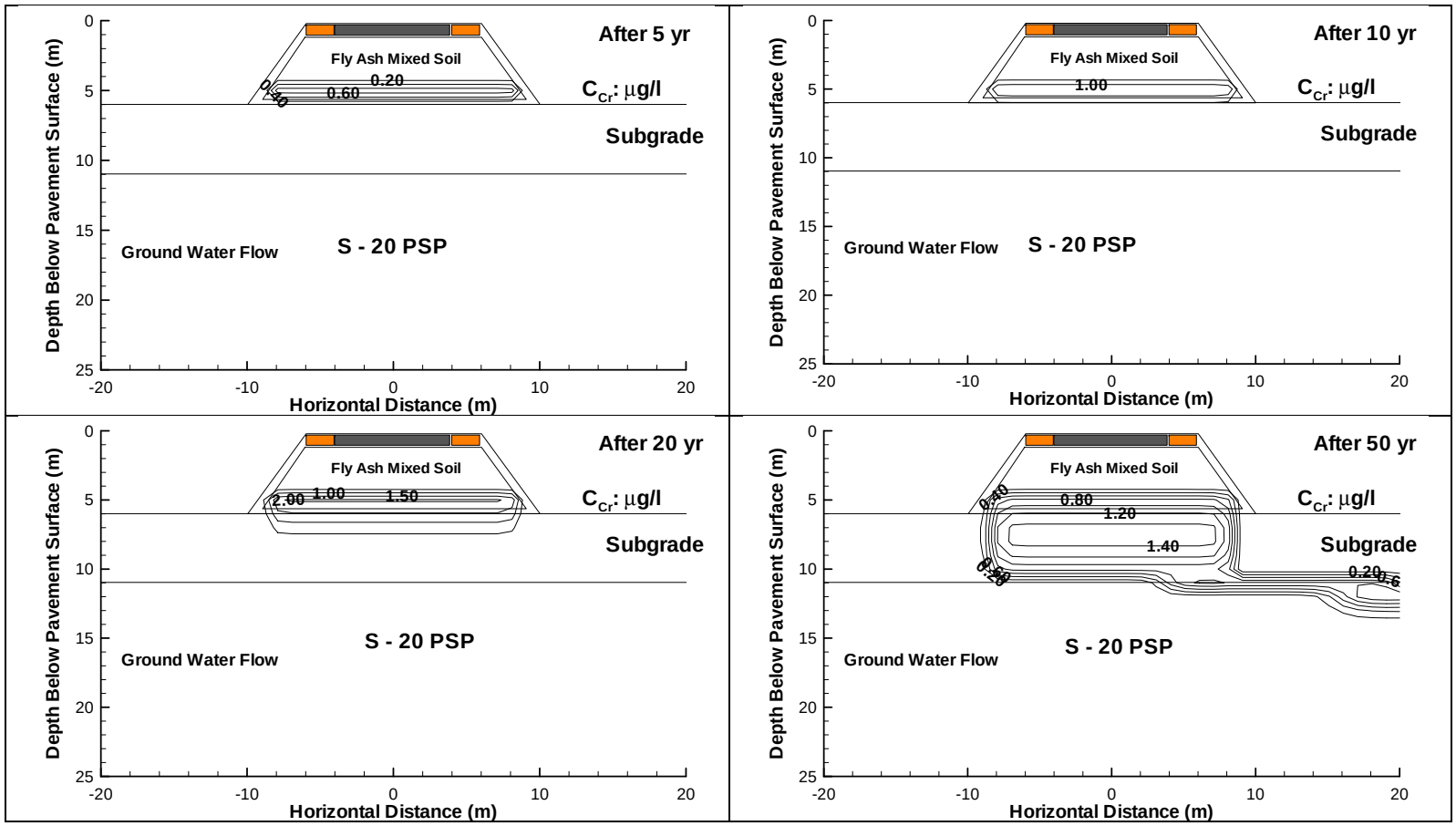

Figure 4.16.Predicted Cr concentrations in vadose zone and ground water (Note: 20 PSP designate the specimens with 20 % Paul Smith Precipitator fly ash.)

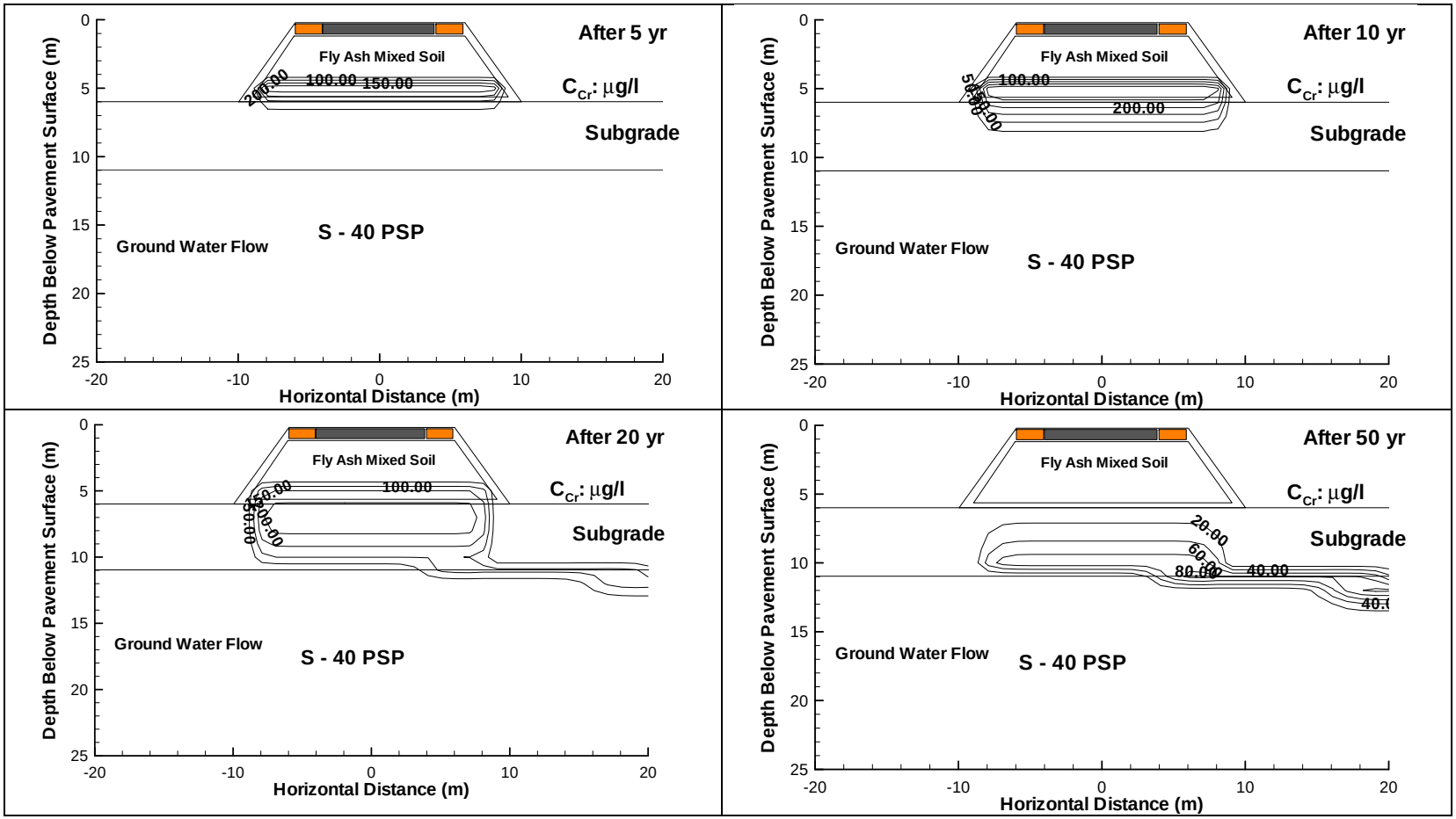

Figure 4.17.Predicted Cr concentrations in vadose zone and ground water (Note: 40 PSP designate the specimens with 40 % Paul Smith Precipitator fly ash.)

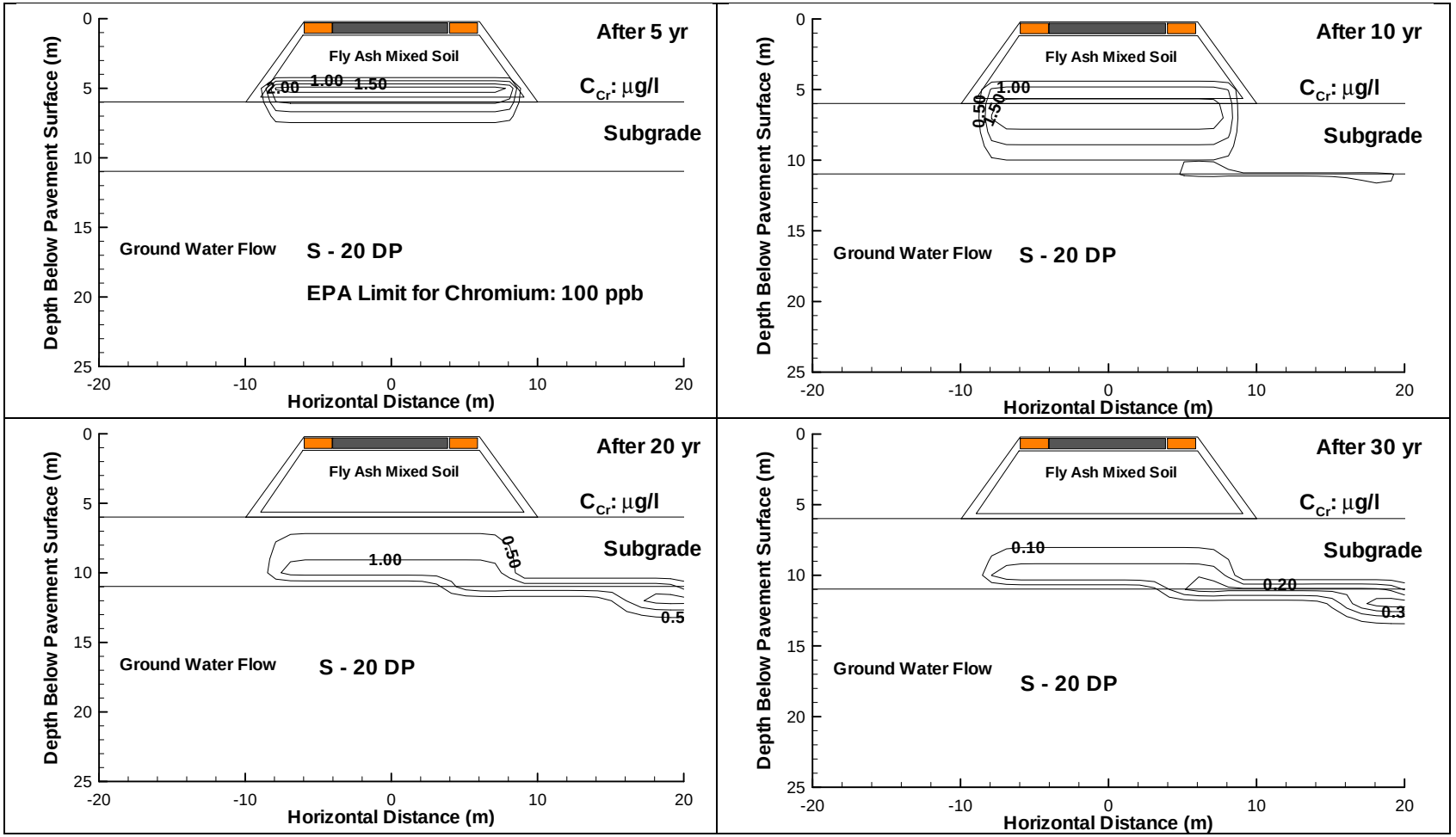

Figure 4.18 Predicted Cr concentrations in vadose zone and ground water (Note: 20 DP designate the specimens with 20 % Dickerson Precipitator fly ash.)

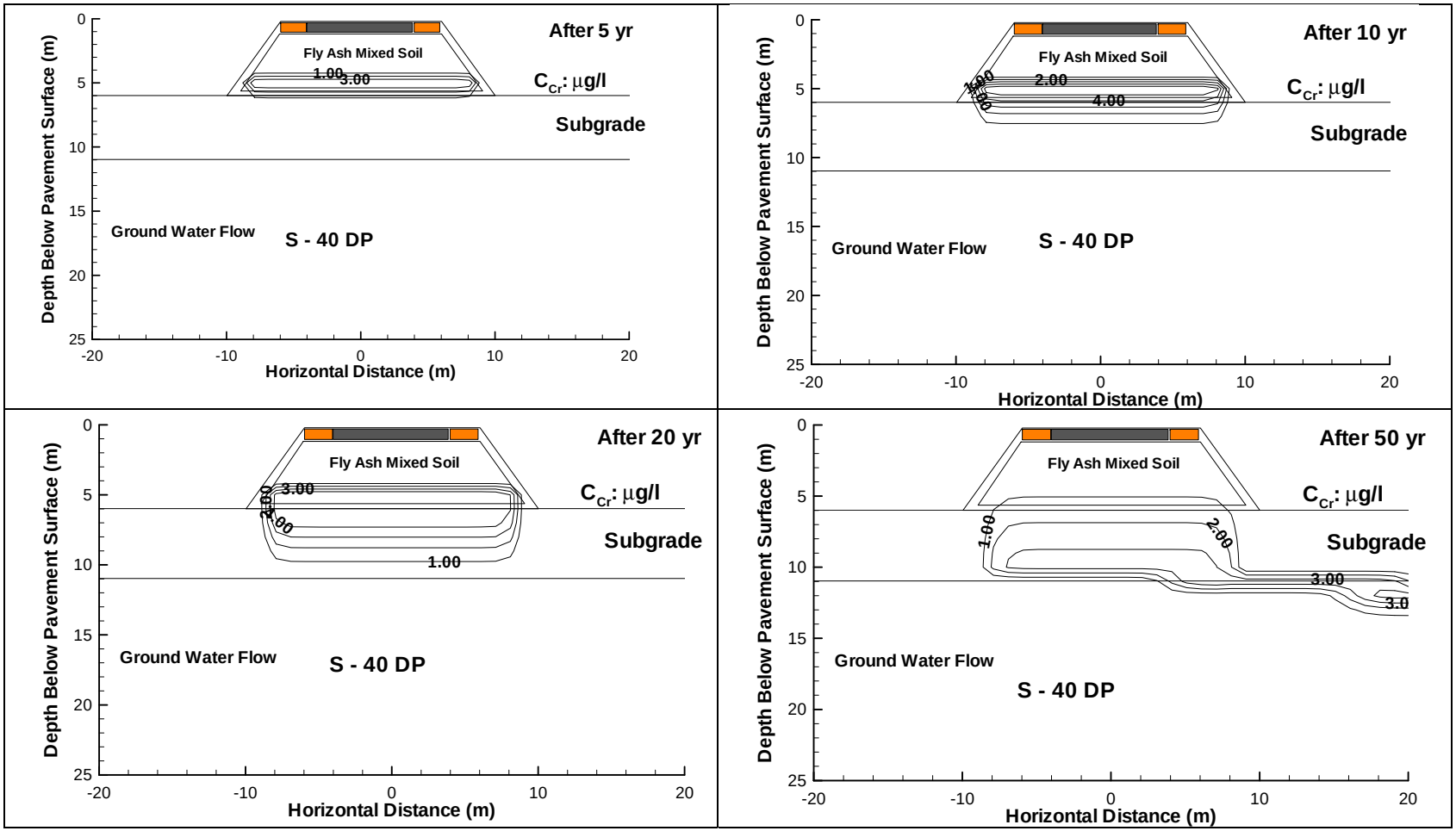

Figure 4.19 Predicted Cr concentrations in vadose zone and ground water (Note: 40 DP designate the specimens with 40 % Dickerson Precipitator fly ash.)

concentrations of the trace metals in the groundwater after a period of 100 years at the point of compliance (POC). The input data used in the analyses of the WiscLEACH is summarized in Table 4.10.

Figure 4.20 shows the schematic diagram of the multiple layer embankment construction. It contains a series of three soil layers and three fly ash layers placed on top of each other. Each layer is 1 m (~3-ft) thick. The hydraulic conductivities, transport parameters of the pavement layers, both fly ashes, and the retardation factors for each of the 4 analyzed trace metals are summarized in Table 4.9 .

Figures 4.21 to 4.28 show the contour plots of the predicted concentrations of As, Cr, Mn, and Se in the soil vadose zone in the groundwater. The contour plots provide the predictions of the metal concentrations after 1, 10, 20, and 40 years of construction. WiscLEACH simulations indicated that As, Mn, Se concentrations will exceed the EPA Maximum Concentration Limits for drinking waters (MCLs). However, as mentioned in the previous section, the soils prepared with 20% fly ashes by weight yielded lower metal concentrations that were far below the EPA MCL. This indicates that extra care should be taken when using fly ash in geotechnical applications. Using pure fly ash as an embankment fill may cause serious environmental problems. WiscLEACH simulations showed that the maximum concentrations of all 4 metals are reached in approximately 10 to 20 years. After the maximum concentrations are reached, metal concentrations in the vadose zone start to decrease with time. Furthermore, Figures 4.23 and 4.27 indicate that the Cr concentrations are far below the MCL when it reaches to the groundwater.

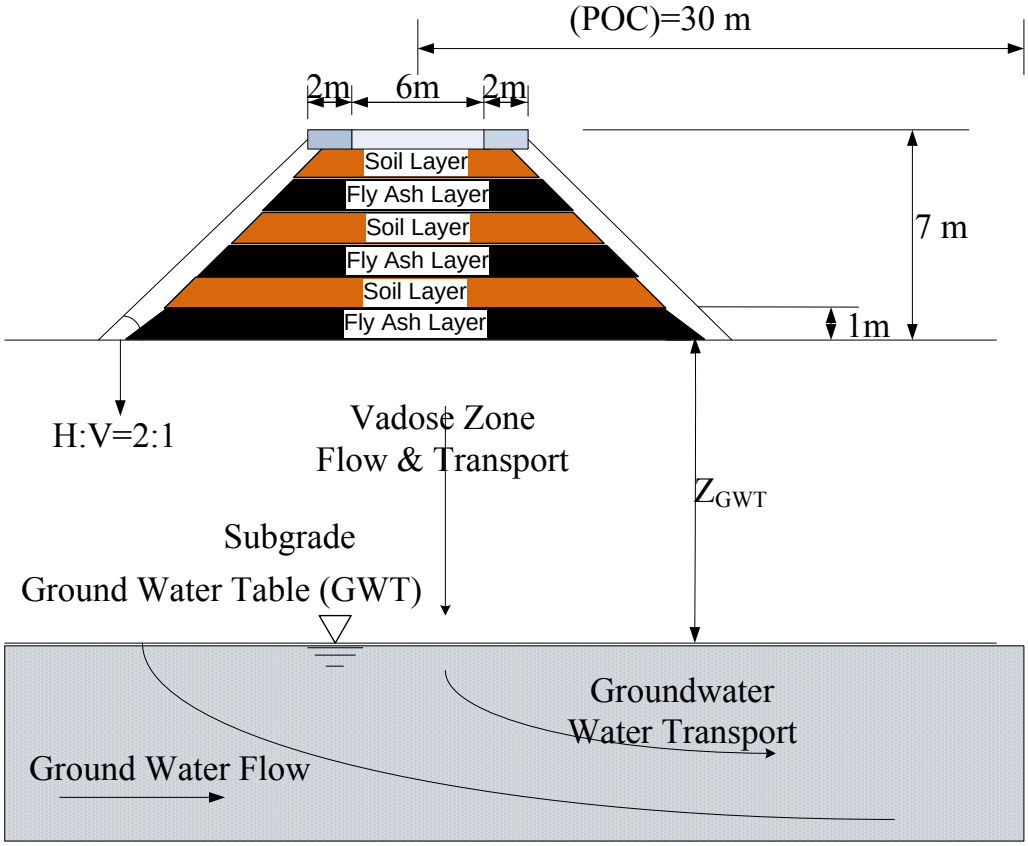

Figure 4.20.Conceptual model of WiscLEACH for multiple layer fly ashes. Note: POC = Point of compliance

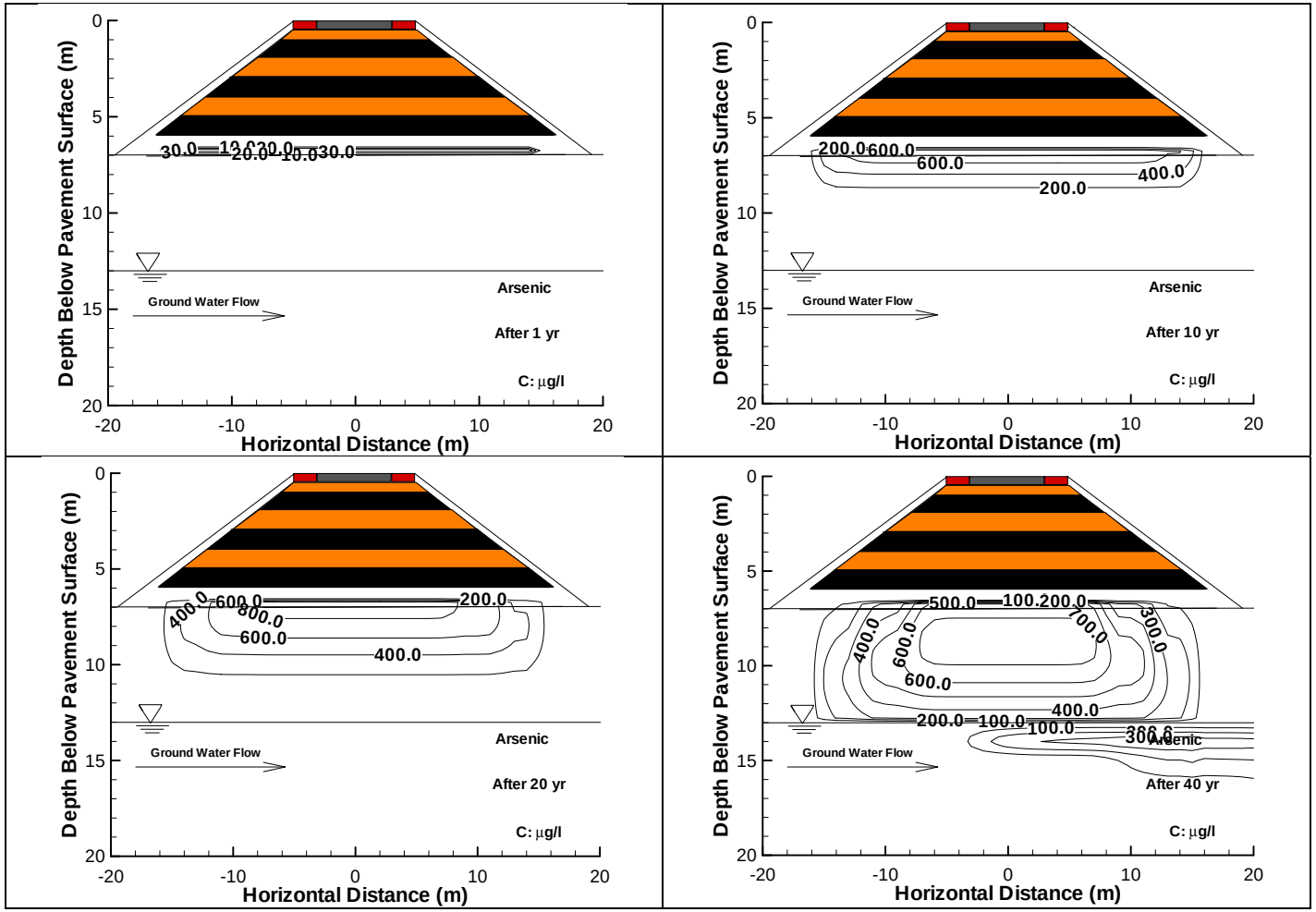

Figure 4.21.Predictions of As concentrations in soil and groundwater for 100 PSP fly ash. PSP: Paul Smith Precipitator fly ash.

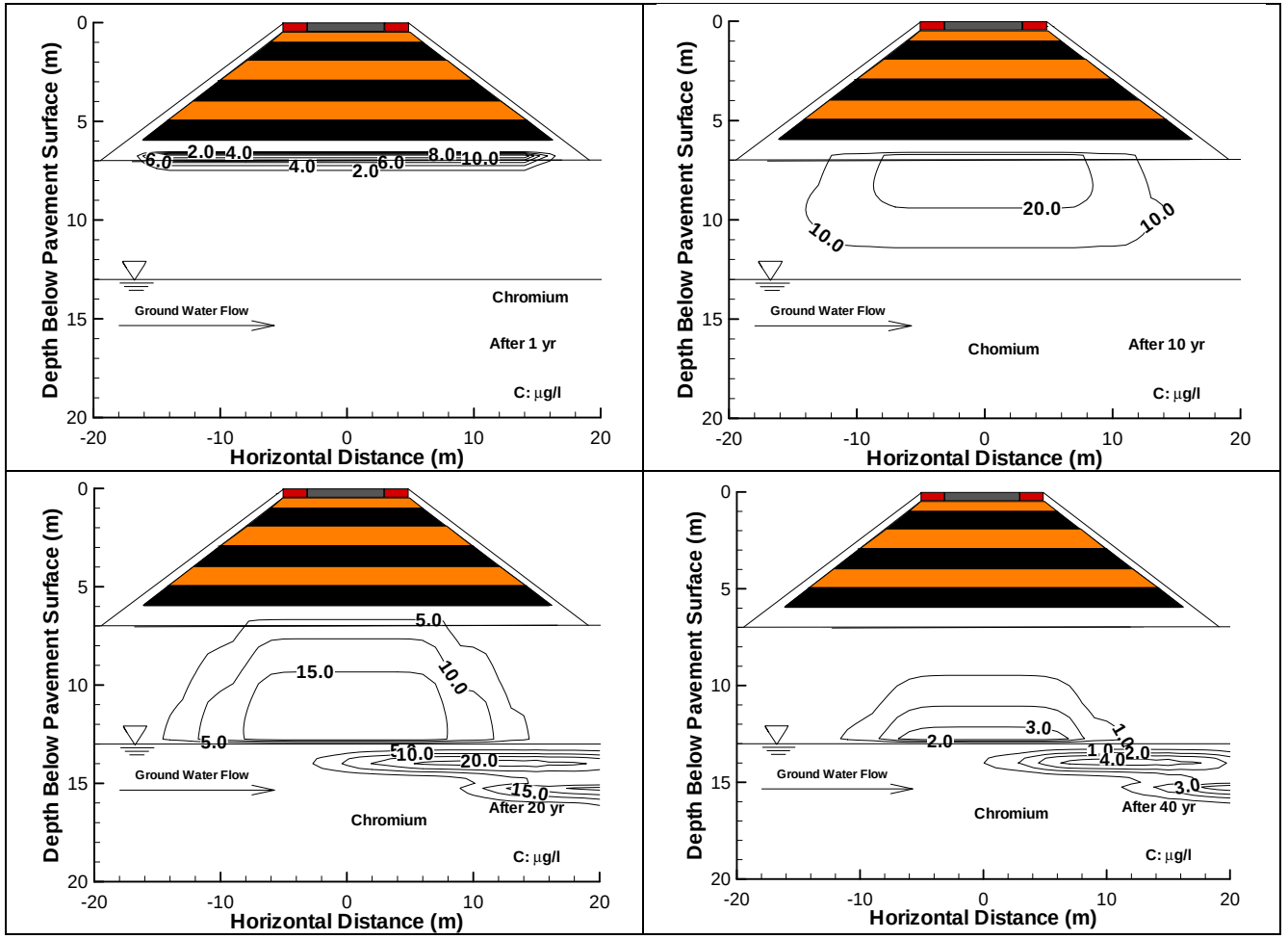

Figure 4.22 Predictions of Cr concentrations in soil and groundwater for 100 PSP fly ash. PSP: Paul Smith Precipitator fly ash.

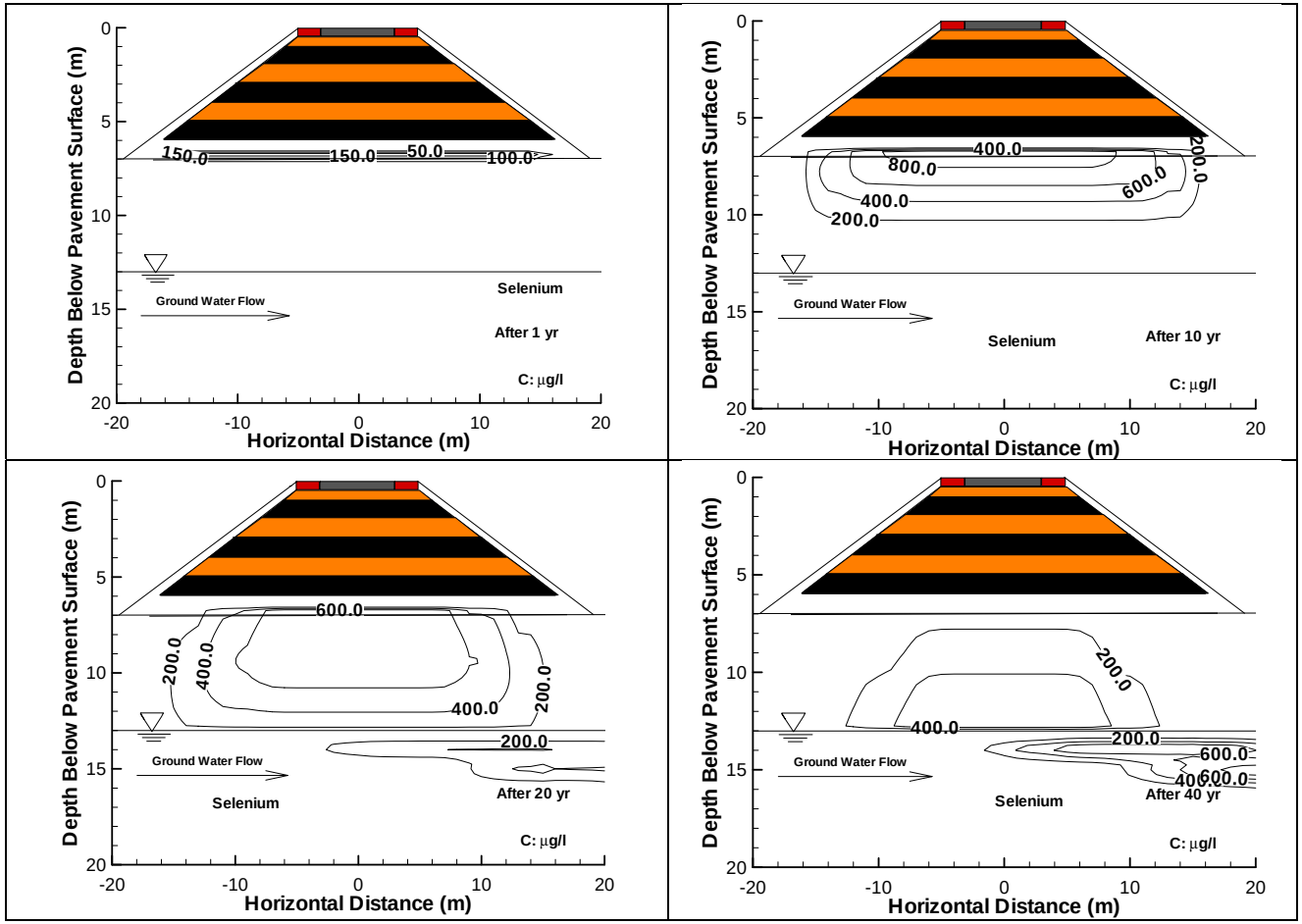

Figure 4.23 Predictions of Se concentrations in soil and groundwater for 100 PSP fly ash. PSP: Paul Smith Precipitator fly ash.

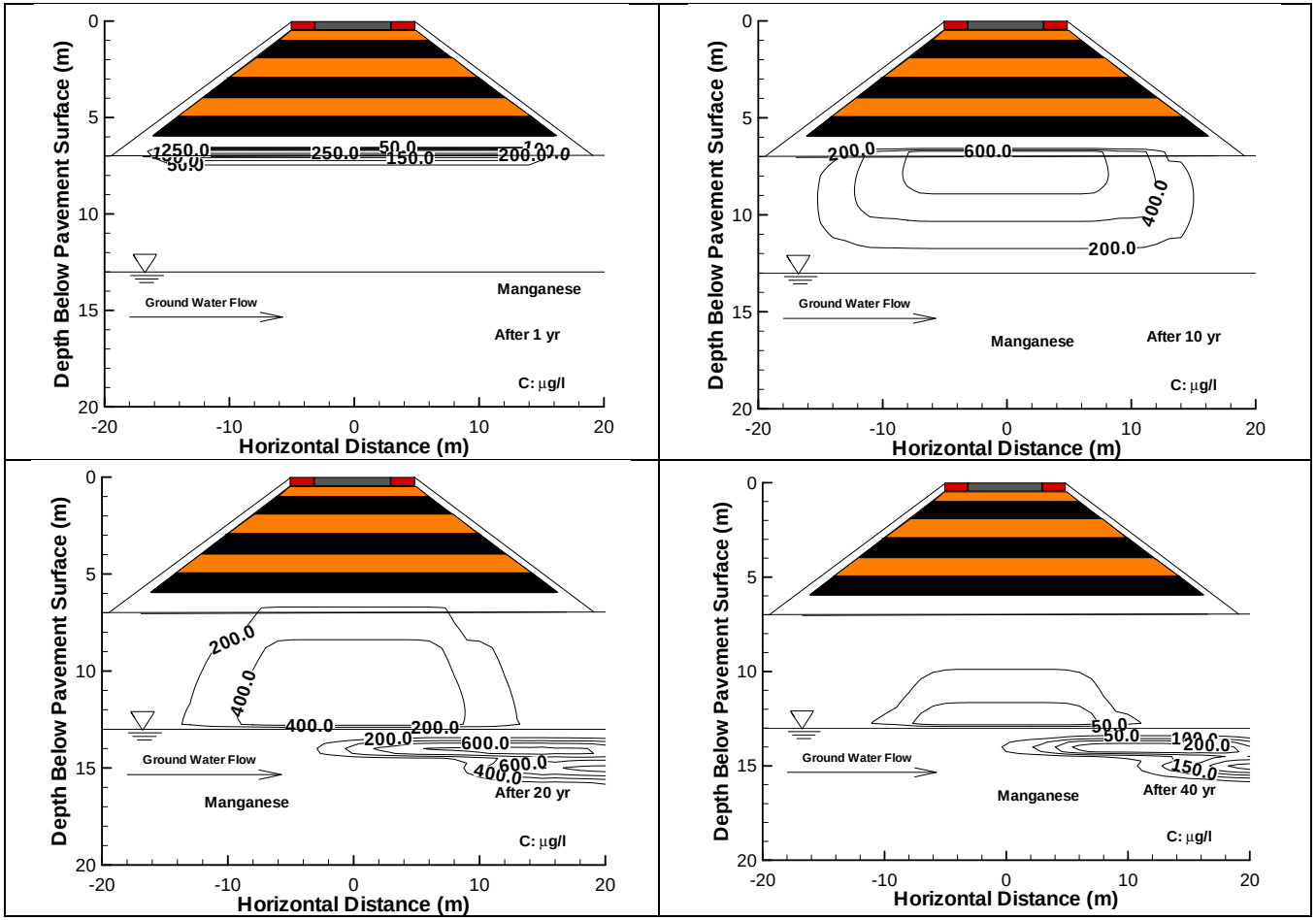

Figure 4.24 Predictions of Mn concentrations in soil and groundwater for 100 PSP fly ash. PSP: Paul Smith Precipitator fly ash

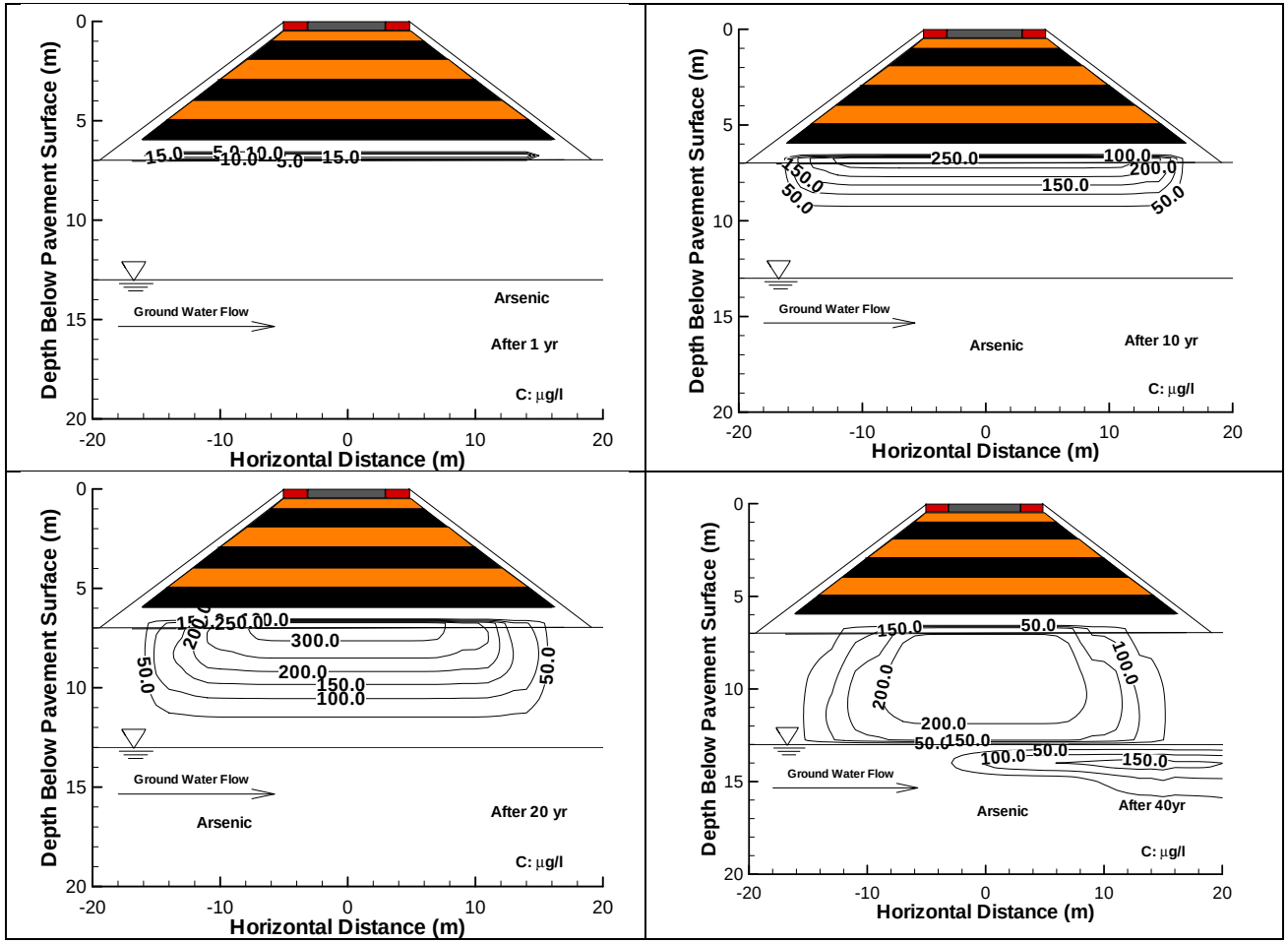

Figure 4.25 Predictions of As concentrations in soil and groundwater for 100 DP fly ash. DP: Dickerson Precipitator fly ash.

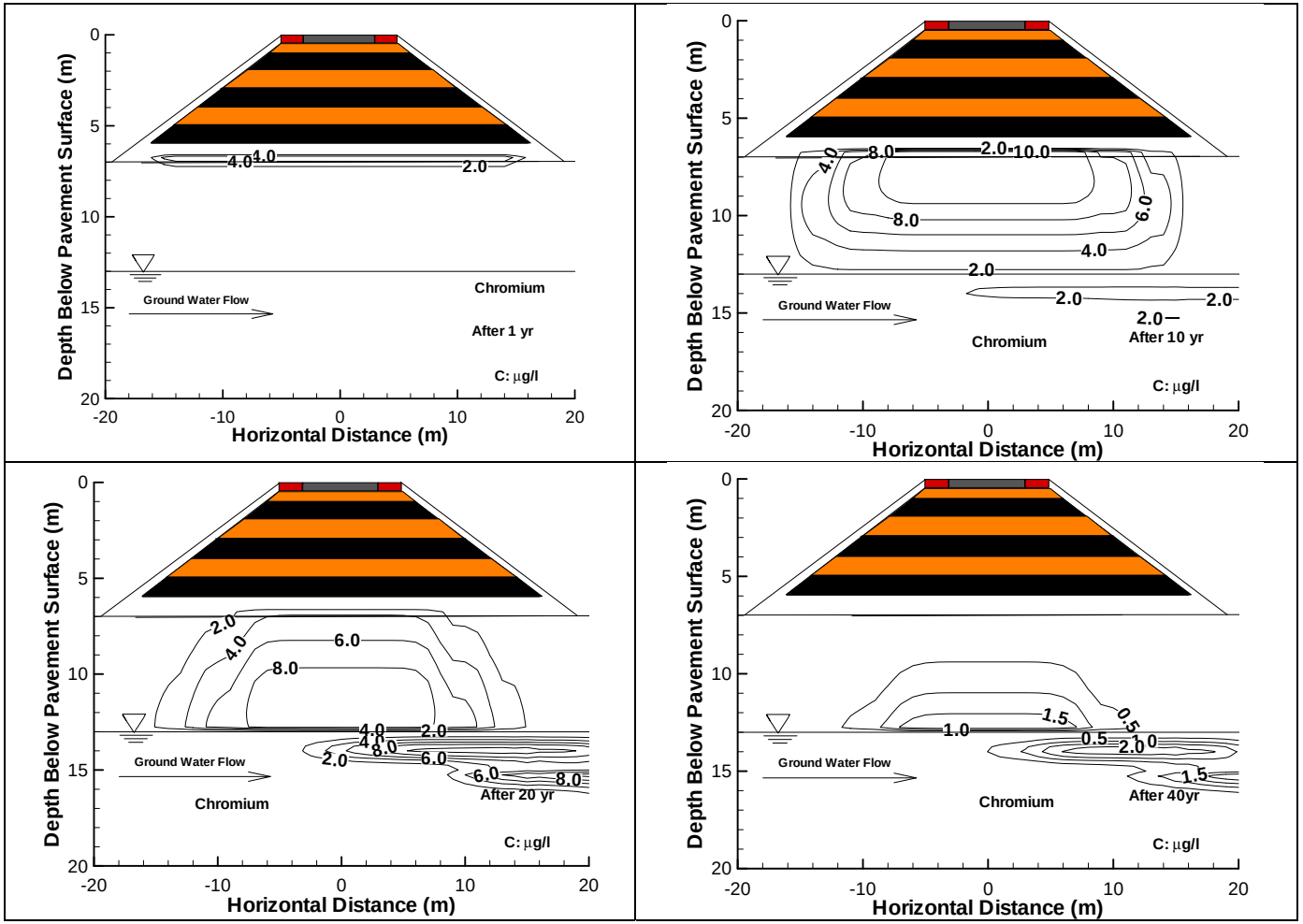

Figure 4.26.Predictions of Cr concentrations in soil and groundwater for 100 DP fly ash. DP: Dickerson Precipitator fly ash

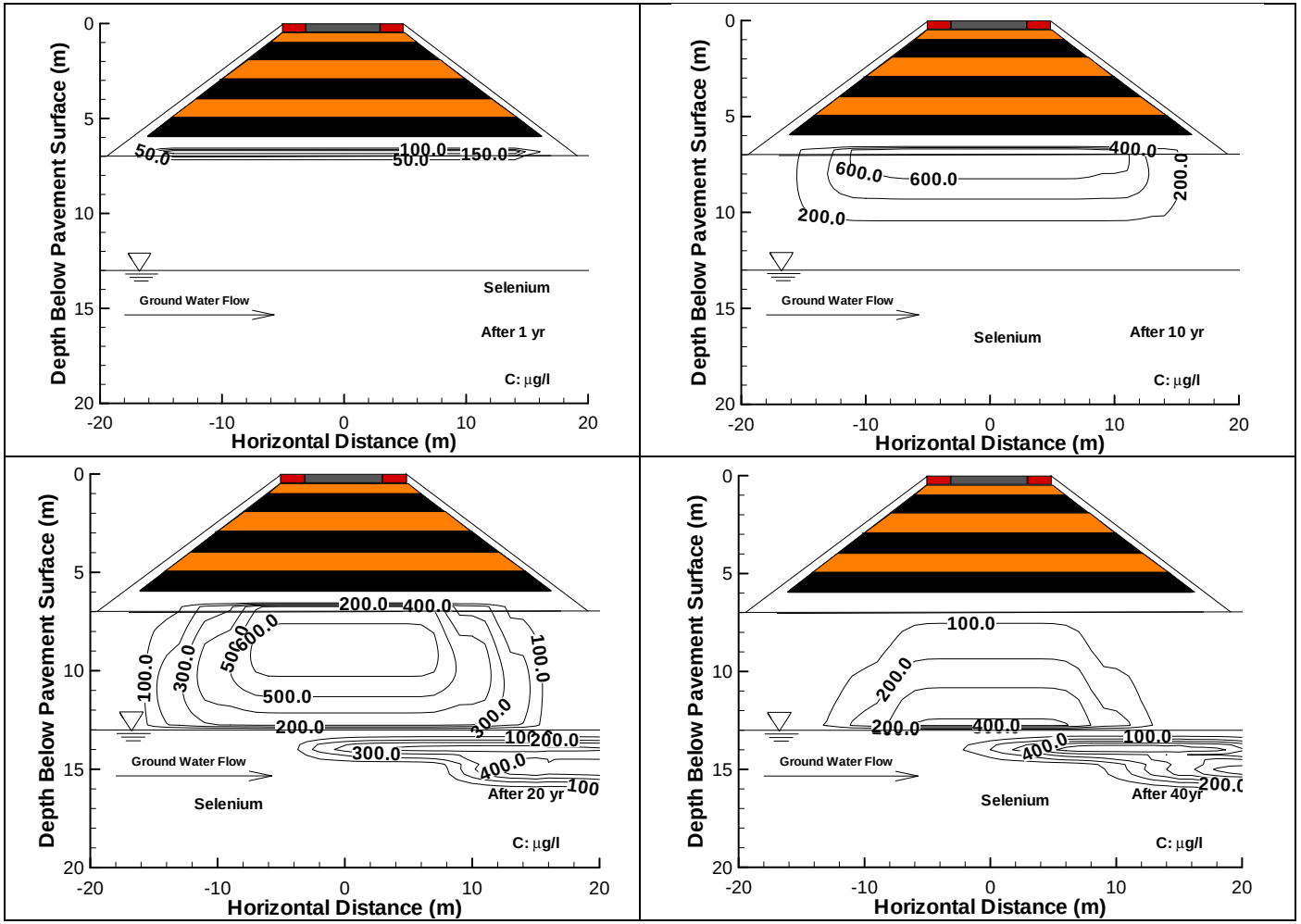

Figure 4.27Predictions of Se concentrations in soil and groundwater for 100 DP fly ash. DP: Dickerson Precipitator fly ash

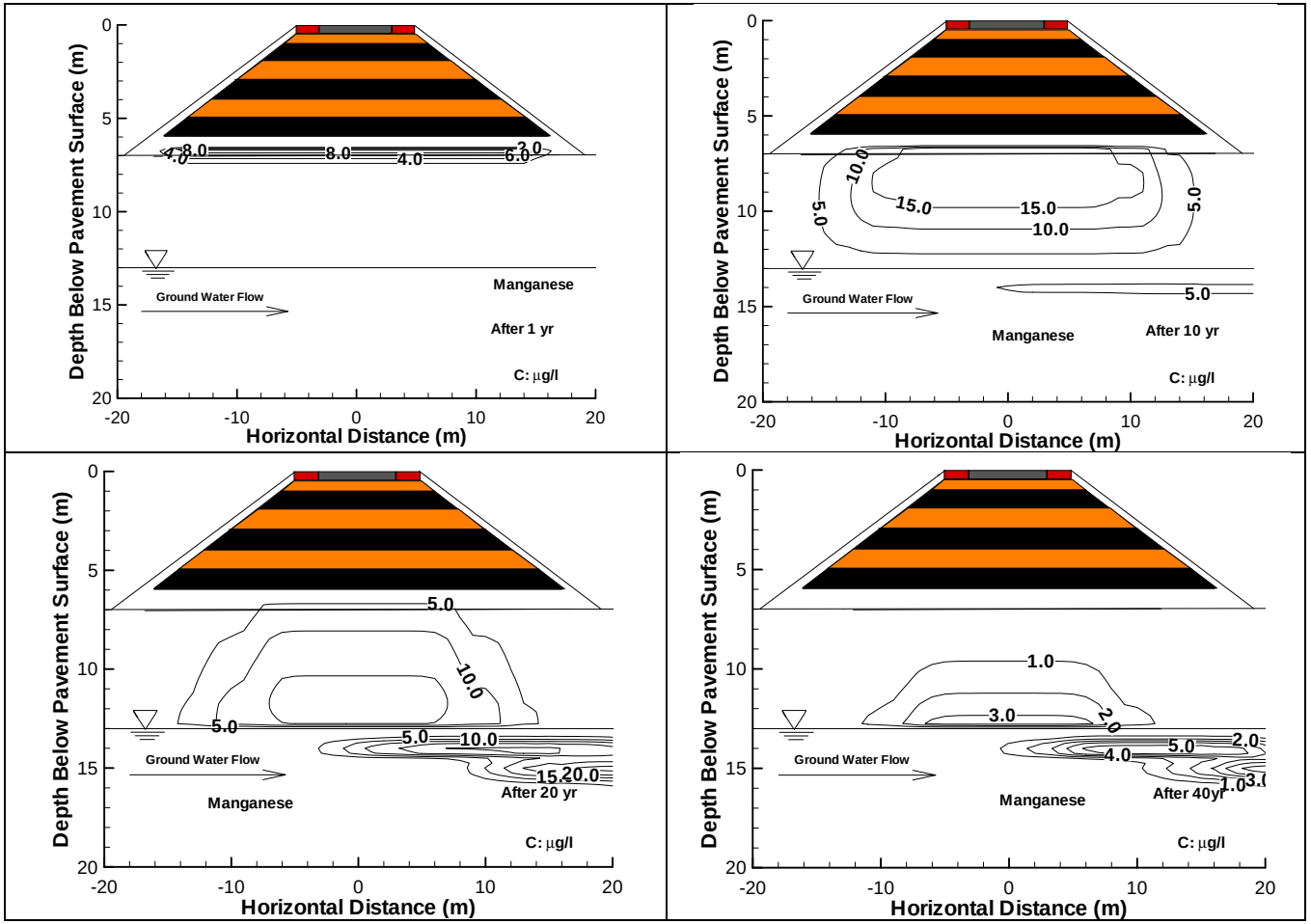

Figure 4.28 Predictions of Mn concentrations in soil and groundwater for 100 DP fly ash. DP: Dickerson Precipitator fly ash

Table 4.11 summarizes the maximum concentrations of the four metals at 1, 10, 20 and 40 years for multiple layer embankments built with 100% PSP and 100% DP fly ashes. Table 4.11 indicates that for the embankments with PSP and DP fly ashes, As does not reach the groundwater table before 40 years. However, at 40 years, As concentrations were approximately 400 μg/L, which exceed the EPA MCL (10μg/L). High retardation factors of these two fly ashes for As metals could be the reason for delaying the leaching of As metals to ground water as fast as the leaching of other metals (Table 4.10). Cr, Mn, and Se metals reach the groundwater table after 20 years. Relatively low retardation factors of the fly ashes for these three metals may have caused these heavy metals to the groundwater earlier than the As. Table 4.11 shows that, in both cases, the leached concentrations of Cr metal were far below the EPA MCL.

The embankment designed with 100% PSP fly ash yielded Mn and Se leaching in concentrations that exceeded the EPA MCL significantly. Furthermore, after 20 years, the Se concentrations from the embankment constructed with 100% DP fly ash were above the EPA MCL, but Mn concentrations still remained below the EPA MCLs. These results indicate that extra care should be taken, especially for As and Se leaching from the multiple layer embankments.

Maximum concentrations of these four trace metals at the point of compliance (POC) with groundwater depths during a 100-year period were also simulated. From an environmental perspective, the metal concentrations in groundwater at the POC are much more important than the metal concentrations in groundwater located directly under the

embankment construction. A POC of 30 m was selected in the current study. Figures 4.29 and Figure 4.30 show the concentrations of leached metals at the POC for the fly ash layered embankments designed with two different covers. Two different cover materials were used to encapsulate the multiple soil-fly ash layers in the embankment: Physical and chemical properties of these two different types of cover materials are summarized in Table 4.10.

Figures 4.29 and 4.30 show the variation of metal concentrations at the POC during a 100-year period. The results indicate that using the clayey material to encapsulate fly ashes in embankments significantly decreased the leached metal concentrations in the groundwater at the POC. Low hydraulic conductivity ($k \sim 1 \times 10^{-7}$ cm/sec), and relatively higher retardation factor (R_d) of the clayey soil most likely accounted for these results. Relatively lower k values prevented the leaching of metals from embankment to the soil vadose zone for short period of time and high R_d values yielded adsorption of metals by the clay particles. Clay particles have a much higher surface area than sandy soil grains, which increase the adsorption potential of the trace metals by this type of soils (Sparks, 2003).

Table 4.10. Input parameters for specific soil-fly ash mixtures analyzed in WiscLEACH.

	Pavement	Subgrade	Sand Borrow Material for embankment cover	Clay Material for embankment cover	100 DP				100 PSP			
					As	Cr	Mn	Se	As	Cr	Mn	Se
R_d	-	3.5	1	7.2	15	1.15	1.24	5	18	1.1	1.61	6.35
Metal Conc. (μg/L)	-	-	-	-	2060	60	1680	2080	750	30	50	1760
k (m/year)	18.25	3	4	0.0315	1.57				1.58			
n_e	0.33	0.3	0.33	0.25	0.59				0.61			
α_L (m)	-	-	-	-	0.74				0.6			
α_T (m)	-	-	-	-	0.074				0.06			

Note: α_L (m)= Longitudinal dispersivity, α_T (m)= Transverse dispersivity

Table 4.11 Predicted maximum metal concentrations in groundwater at 1, 10, 20, and 40 years for specimens prepared with 100% PSP and DP fly ashes. Concentrations exceeding MCLs in **bold**.

Time (years)	Metal Concentrations leached from PSP fly ash (μg/L)				Metal Concentrations leached from DP fly ash (μg/L)			
	As	Cr	Mn	Se	As	Cr	Mn	Se
10	-	20	-	-	-	-	-	-
20	-	4	**600**	**200**	-	8	20	**400**
40	**300**	-	**200**	**600**	**150**	2	5	**400**
EPA MCL (μg/L)	10	100	50	30	10	100	50	30

Notes; MCL = Maximum contaminant levels for drinking water; PSP=Paul Smith precipitator fly ash, DP=Dickerson precipitator fly ash.

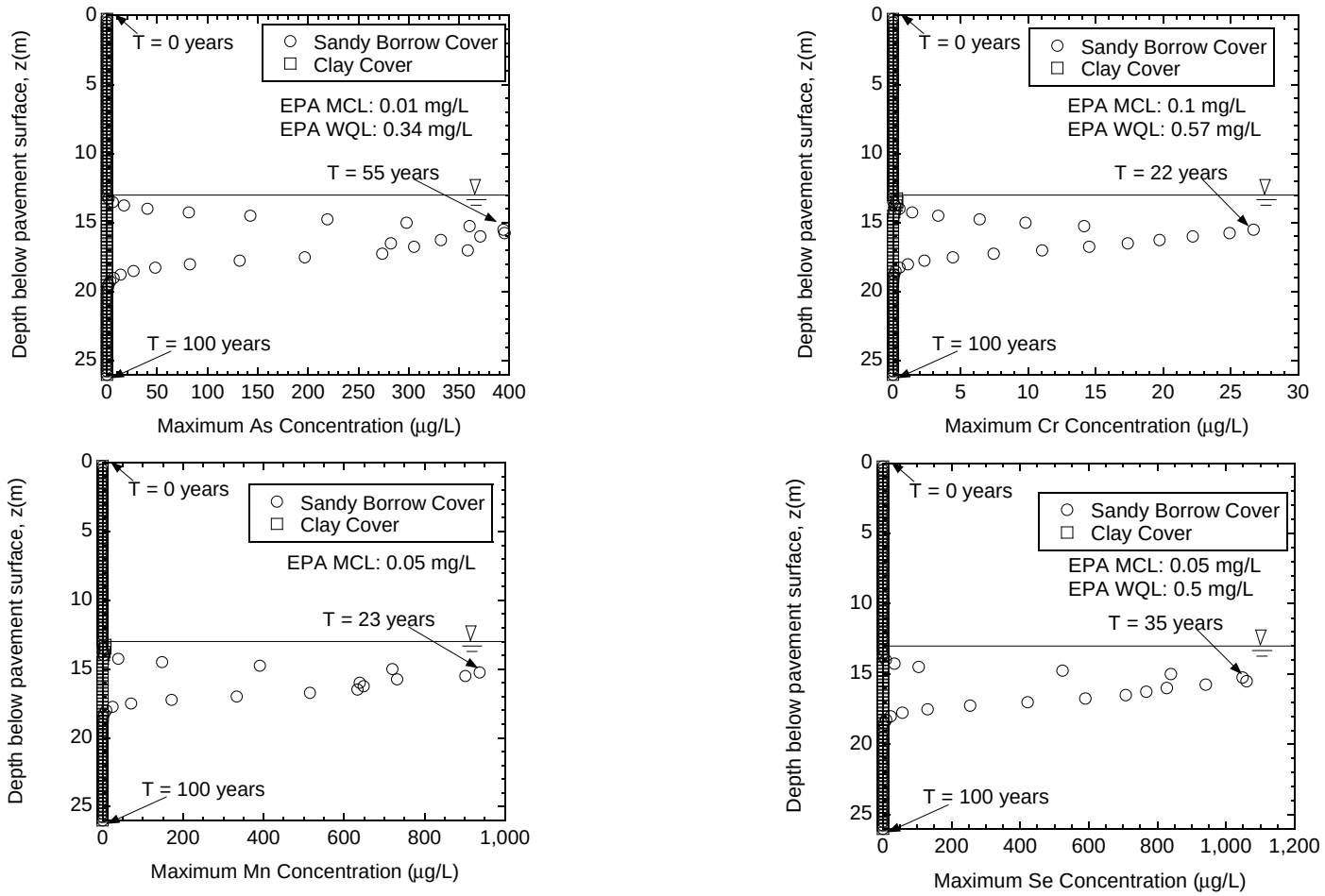

Figure 4.29 Maximum metal concentrations within 100 years at point of compliance for specimens prepared with 100% PSP. Note: PSP= Paul Smith Precipitator fly ash. MCL= maximum contaminant levels for drinking water; WQL= water quality limits for protection of aquatic life and human health in fresh water.

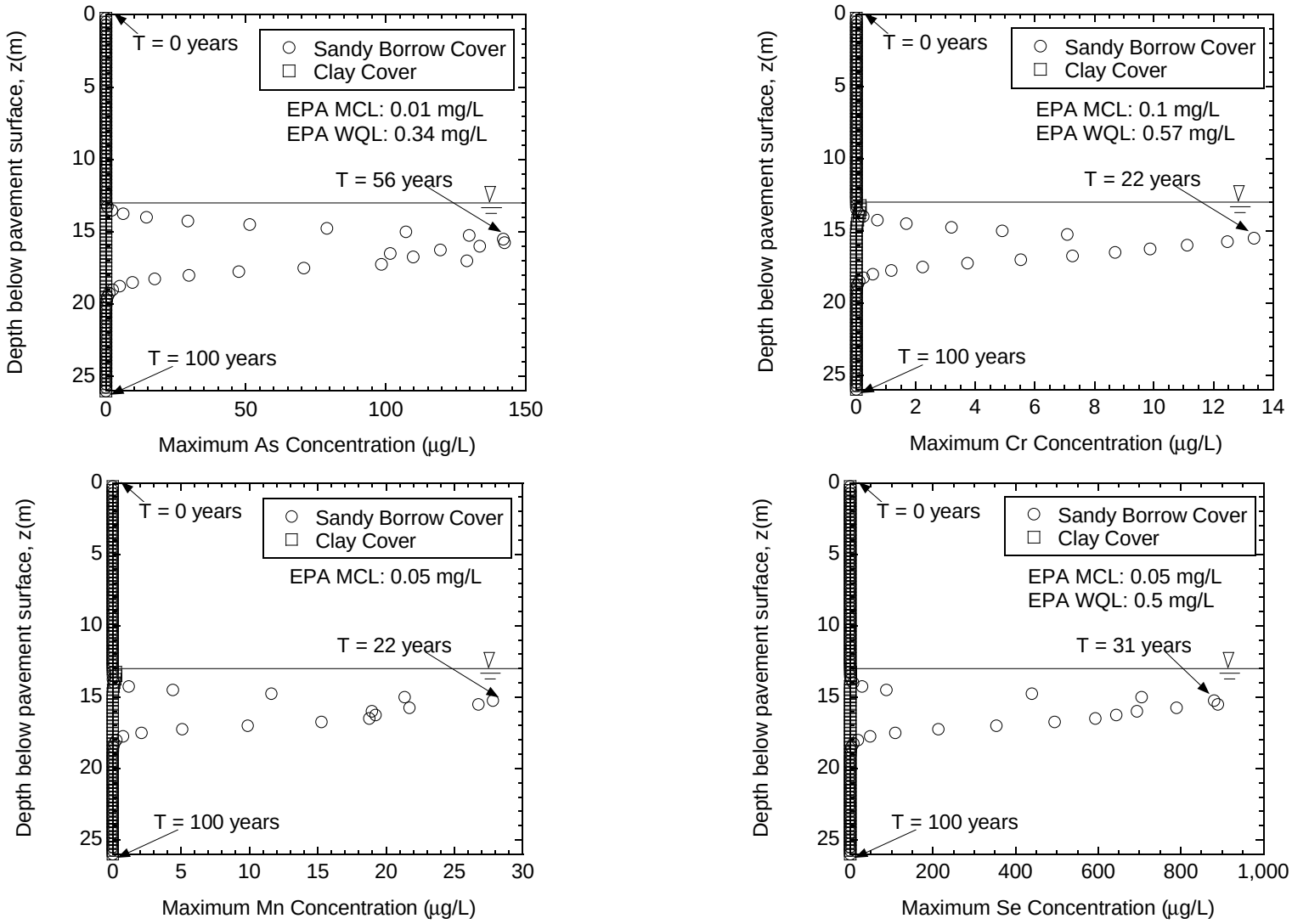

Figure 4.30 Maximum metal concentrations within 100 years at point of compliance. for specimens prepared with 100% DP. Note: DP=Dickerson Precipitator fly ash. MCL= maximum contaminant levels for drinking waterWQL= water quality limits for protection of aquatic life and human health in fresh water.

4.6 CONCLUSIONS

The primary objective of this study was to investigate the leaching behavior of the heavy metals from fly ash-amended soils used in embankment constructions. The effect of adding fly ashes and the feasibility of its use in geotechnical applications are studied. To achieve these objectives, a series of batch water leach test (WLTs) and column leach test (CLTs) were conducted to evaluate the leaching pattern of the metals from fly ash mixed soils. The conclusions from the current study are summarized as follows:

1) An increase in fly ash content increased the pH values of the soil – fly ash mixtures significantly due to the release of CaO, and MgO minerals. An increase in fly ash content from 0 to 40% is by weight had greater influence on increased pH levels than an increase in fly ash content from 40 to 100%.
2) Arsenic, aluminum, chromium, boron, and selenium concentrations increased with increasing fly ash content. The solubility of Mn, on the other hand, is highly dependent on the effluent pH level; at pH > 6, Mn metals precipitate with Al – oxides and Fe – oxides.
3) The CLT elution curves for all but As exhibit a first-flush leaching pattern that occurs as the result of metals releasing from the water soluble fraction and from sites with low adsorption energies. The concentrations of Al, B, Cr, Mn, and Se begin to stabilize after 10- 15 pore volumes of flow. Only the leaching curves for As metals showed a lagged flush response. The leaching of As metals continued to increase until 10 – 20 pore volumes of flow was reached, after which the

concentrations started to decrease dramatically.

4) The concentrations of the six metals are influenced by the pH level of the effluent solution significantly, which suggests that the leaching pattern is highly dependent on the pH level of the aqueous solutions.
5) The concentrations of the Al, As, Se, and Cr metals exceeded the EPA MCLs at and beyond 20% for MT and Co fly ashes. The reason for this is the high pH of the MT and Co fly ashes themselves. Addition of these fly ashes increase the pH of effluent solutions and the metal concentrations because these metals generally exhibit an amphoteric leaching pattern.
6) The WiscLEACH results indicated that the maximum Cr concentrations are reached in approximately 10 to 20 years. Cr concentrations in the vadose zone decrease significantly with time, and are far below the EPA MCL at the groundwater table. Therefore, according to the WiscLEACH results, using fly ash as a soil amendment in embankment construction is safe when used at rate of 10 – 20% by weight.
7) Based on WiscLEACH simulations, metal concentrations decrease with distance from the embankment and groundwater surface, most probably due to the dispersion of the metals in the soil vadose zone. High annual precipitation rate may also have caused an increase in the leaching of the metals from the HCFA amended embankment.
8) Simulations using the multiple layer version of WiscLEACH indicated that As, Cr, Se metals concentrations exceeded the EPA MCL. However, as mentioned in

the single version of WiscLEACH results, the soils prepared with 20% fly ash by weight yielded lower metal concentrations that were far below the EPA MCLs. This indicates that extra care should be taken when using fly ash in this geotechnical application.

9) All metal concentrations reached the groundwater between 10 and 20 years except As metals. As metals reached the ground water after 40 years. High retardation factors of both fly ashes for As metal could cause the delay in leaching of As metals through the embankment and soil vadose zone.
10) Using clayey material instead of the more common sandy borrow material as an encapsulation layer around the embankment reduced the leached metal concentrations to 25 times to 1000 times lower in the groundwater at the point of compliance significantly due to very high retardation factor of clay material as compared to sandy borrow material.

5 GEOCHEMICAL MODELING

5.1 INTRODUCTION

Metals can exist in different species in aqueous solutions, so they can have different oxidation states (e.g., Cr(VI), Cr(III)). Leaching of metals and metal transportation processes are highly dependent on the oxidation states of the metals (Dijkstra et al.,2004), and such states may affect the toxicity of metals (Shah et al 2007). For instance, Cr (III) is critical to the normal functions of various living organisms, but Cr (VI) is very toxic and can threaten the human health (Geelhoed et al., 2002). Similarly, As(III) is most toxic arsenic species whereas As(V) is not known as a toxic metal (Pandey et al., 2011). The most common selenium species are Se(IV) and Se(VI) are both very toxic (Narukawa et al., 2005).

Previous studies showed that the two main equilibrium mechanisms that control the metal leaching from coal combustion byproducts are solubility (dissolution-precipitation) and sorption (Komonweeraket et al., 2010; Mudd et al., 2004; Wang et al., 2004). Dissolution-precipitation reactions control the leaching of metals, so geochemical equilibria models based on thermodynamic data have been shown to predict aqueous concentrations (assuming equilibrium between the leachate and the solubility-controlling solids). A more complex model that incorporates sorption of kinetic algorithms is required to predict solute concentrations if sorption reactions or dissolution kinetics control the leaching of metals(Fruchter et al., (1990).

The objective of this part of the research was to determine the predominant oxidation states of metals released from fly ash-alone, a soil-fly ash mixture, and soil-fly ash-LKD mixtures. Further, the research team wanted to examine whether the leaching of these metals from fly ash-amended soils are controlled by solubility (dissolution-precipitation) or sorption. MINTEQA2, a numerical model developed by the EPA simulates equilibria and speciation of inorganic solutes in aqueous solutions. This program was used to determine the predominant oxidation states and leachate controlling mechanisms of these leached constituents. Total peak metal concentrations from column leach tests, leachate pH, electrical conductivity (EC) and leachate Eh, were input into the MINTEQA2 geochemical modeling program. This study was conducted on the mixture of the two types of soils and eight different fly ashes and LKDs. It should be noted that no laboratory metal speciation tests were conducted to determine the dominant metal species.

In this part of the study, the results obtained from part 2, part 3 and part 4 were input into MINTEQA2. These data are summarized in Appendix C and it includes effluent pH, EC, Eh and aqueous metal concentrations corresponding to soil alone, fly ash alone, soil-fly ash mixtures, and soil-fly ash-LKD mixtures.

5.2 GEOCHEMICAL ANALYSIS

MINTEQA2 simulations were run in two phases. In the first phase, speciation analyses were conducted on all CLT leachates in order to identify the predominant oxidation states of the leached metals that are redox sensitive. The second phase

calculated aqueous concentrations of all metals species in the effluent solutions and saturation indices of the leachates with respect to solids or minerals.

5.2.1 Speciation Analysis

Aqueous concentrations of metals, EC, pH and Eh data from previously conducted column leach tests were used to determine speciation analyses Speciation analyses determine the dominant oxidation state of the leached metals. Explanations of this process follow. zEh and redox couple are specified as equilibrium constraints in MINTEQA2 in order to calculate the amount of the metals in each of the two oxidation states corresponding to the specified equilibrium Eh (Allison et al., 1991). Thus, the metal species with the highest concentrations were assumed to be the dominant oxidation state of leached metals. Speciation analyses were conducted only on redox-sensitive metals: As, Cr, Cu, Fe, Mn, Sb, V, and Se. List of all species determined by MINTEQA2 of the redox-sensitive metals are summarized in Appendix C. The analyses indicated that the predominant oxidation states of As was As(V), Cu was Cu(II), Fe was Fe(III), Mn was Mn(II), Sb was Sb(V), Se was Se(IV), and , V was (IV) for all specimens. However, the predominant oxidation states of Cr varied depending on the type of mixtures. Based on the predictions from MINTEQA2, Cr(III) is the predominant oxidations states for the fly ash alone and soil-fly ash mixtures. Conversely, Cr(VI) was the predominant oxidation state for the specimens activated with lime kiln dust (LKD). Under alkaline conditions As exists in its anionic and oxidized forms, such as AsO_4^{3-} and $HAsO_4^{2-}$ (Ettler et al., 2010), and leaching of As increases with an increase in pH under alkaline conditions (Su et al., 2011). Speciation analyses indicated that As(V) is the

most dominant oxidation state of the leached As metals in soil-fly ash mixtures; this state is the less toxic As species (As(III) is the most toxic of the species (Shah et al., 2007)). This finding is consistent with previous studies that focused on speciation of As metals from similar waste materials (Ettler et al., 2010; Pandey et al., 2011,). Small amounts of As(III) may have leached from the fly ash-amended soils; however, the oxidation of As(III) occurs quickly in alkaline and aerobic conditions (Su et al., 2011; Turner 1981). The effluent solutions were collected in a beaker exposed to atmosphere in the current study, so it was speculated that these As(III) species were oxidized to As(V) and that all leached As metals were present in their oxidized forms as AsO_4^{3-}.

Cr leaching depends highly on the pH of aqueous solutions (Karamalidis & Voudrias, 2009). Therefore, different oxidation states of Cr were observed for the specimens prepared with different materials. For instance, Cr(III) was the dominant oxidation state of Cr leached from specimens prepared with a mixture of soil and fly ash. The pH of the soil-fly ash mixtures was between 6 and 10, which explains why Cr(III) was the dominant Cr species in the aqueous solutions. At neutral and low pH, Cr(VI) reduces to Cr(III) and results in elevated concentrations of Cr(III) in the aqueous solutions (Geelhoed et al., 2002). In contrast, Cr leached from soil-fly ash-LKD mixtures were in oxidized forms (Cr(VI)) as CrO_4^2 because of high pH levels (pH > 10), which is consistent with Karamalidis and Voudrias (2008), Engelsen et al., (2010), and Izquierdo et al., (2011). Cr(III) was used as the dominant oxidation state for soil-fly ash mixtures while, Cr(VI) was used as dominant oxidation states for soil-fly ash-LKD mixtures in the geochemical modeling study.

To verify the dominant oxidation states of leached Cr metals produced by MINTEQA2 in soil-fly ash mixtures and soil-fly ash-LKD mixtures, a Cr oxidation quick test was conducted (Barret & James, 1979). This test was performed on the specimens that released Cr in concentrations exceeding the EPA Cr MCL (100 μg/L). The dominant oxidations states were determined by observing the color change in the effluent solutions with addition of s-diphenyl carbazide reagent into the leachate. If the color of the effluent solutions turns pink (magenta) after addition of s-diphenyl carbazide, then the Cr(VI) species is present in the leachates. As shown in Table 5.1, MINTEQA2 predicted the dominant Cr species that contradicted the speciation laboratory test. MINTEQA2 analyses predicted Cr(III) would be the dominant oxidation states of Cr for the specimens prepared with 40%, 100% Morgantown fly ashes and all specimens prepared with Columbia fly ashes. The laboratory speciation analysis showed these soil-fly ash mixtures leached Cr(VI) in addition to the Cr(III) species. This was an expected behavior since the pH of the specimens prepared with 40%-100% MT and Co fly ashes had very high pH levels. In basic conditions, Cr typically oxidized to its Cr(VI) form. These results indicated that conducting laboratory speciation tests besides MINTEQA2 analysis is critical in determination of the dominant oxidation states of the leached metals.

The dominant species of the metals were estimated with MINTEQA2 using the measured Eh, EC, pH and total leached metal concentrations. MINTEQA2 predicted the leached Se would exist in its reduced form, Se(IV). This prediction is consistent with the literature (Narukawa et al., 2005; Su et al., 2011). In the current study, Se(IV) was used as the dominant oxidation states of Se in the effluent solutions but it should be kept in

mind that there may still be some oxidized forms of Se(VI) and this form may reduce to Se(IV) over time.

5.2.2 Analysis of Controlling Mechanisms

The main objective of this part of the study was to determine if the leaching of metal concentrations are controlled by solubility reactions. To achieve this goal, laboratory data obtained from CLTs were input into MINTEQA2. Leaching behaviors of metals that could not be defined by solubility reactions were then considered to be sorption controlled without conducting any further modeling. Simulating the sorption reactions in aqueous solutions is out of the scope of the current study, but should be considered in future research.

MINTEQA2 analyzed the aqueous phase equilibrium composition and saturation indexes (SI) of all effluent solutions, with respect to solids or minerals, by allowing aqueous complexation reactions and oversaturated solids to precipitate at given laboratory test conditions. Electrical conductivity (EC), pH, redox potential (Eh), and aqueous metal concentrations of each metal leached from the different specimens were used as an input in the geochemical analyses. An assumption was that total leached metal concentrations were leached in their dominant oxidations states as determined above. These metals include: Al^{3+}, As(V) as AsO_4^{3-} , Cu^{2+}, B(III) as $B(OH)_4^-$, Ba^{2+}, Ca^{2+}, Cl^-, Cr(III) as $Cr(OH)_2^+$, Cr(VI) as CrO_4^{2-}, Fe^{3+},Na^+ Mg^{2+} Mn^{2+}, Sb(V) as $Sb(OH)_6^-$, Se(IV) as $HSeO_3^-$, V(IV) as VO^{2+}, and Zn^{2+}. The aqueous phase concentration analyses and the SI calculation were performed assuming equilibrium between the effluent solution and

potential solubility-controlling minerals in the solid in an open system (25ºC under the influence of atmospheric CO_2.)

The leachates of the specimens in the column leaching tests were collected in beakers exposed to atmosphere. Therefore, those aqueous solutions were assumed to be in equilibrium with the partial pressure of atmospheric CO_2 at 3.16×10^{-4} atm. (Langmuir, 1997).

MINTEQA2 provides the activities of metals in the leachates rather than their concentrations. To calculate the single ion activities for each of the leached metal species, the Davies equation was used. In this process, MINTEQA2 required the ionic strength of the each difference effluent solutions. This was computed using the EC values of the leachates, multiplied by a factor of 0.013, a constant empirically derived from a large number of river water samples that determined the ionic strength of aqueous solutions (Griffin & Jurinak, 1973).

Next, MINTEQA2 computed the saturation indexes of the metal species with respect to minerals and solid phases in the MINTEQA2 database by calculating single ion activities. Saturation index is the parameter used in the determination of whether or not the metal leaching is solubility controlled with respect to a mineral or solid phase (Johnson et al., 1999). High negative or positive SI values are indications that leached metals are undersaturated and oversaturated, respectively, which suggests that leaching of particular metals could be controlled by other minerals or solid phases, or its leaching could be sorption controlled. If metal leaching is solubility controlled, the computed metal activities should be close to the solubility line that represents the

dissolution/precipitation reactions of the minerals at equilibrium (Komonweeraket et al., 2010). If the activities of these metals are far from these solubility lines, it is typically claimed that the leaching of these metals are not solubility controlled.

Log-activity diagrams were developed by plotting the MINTEQQA2-based log activities of each metal against the corresponding CLT- based pH values. These diagrams were used to determine whether the leached metals are controlled by minerals or solid phases that were included in the MINTEQA2 database.

5.2.3 Speciation of Al

The solubility of Al is mainly controlled by the dissolution or precipitation of the Al hydroxides including $Al(OH)_3$ amorphous, $Al(OH)_3$ gibbsite, Al_2O_3 (s), diaspore-α-AlO(OH), and boehmite-α-AlO(OH) (Astrup et al., 2006; Gitari et al., 2009). Figure 5.1 indicates that the Al^{3+} metals are controlled by $Al(OH)_3$ gibbsite, a crystalline form of the $Al(OH)_3$ mineral in a pH range of 6 to 12.4, which is consistent with the findings of Murarka et al., (1992), Astrup et al., 2006, and Komonweeraket et al., (2010) during the testing of coal by-products and municipal waste combustion.

Johnson et al., (1999) and Gitari et al., (2009) said that solubility of Al^{3+} is controlled by $Al(OH)_3$ amorphous for pH = 6-9 and by gibbsite when pH > 9. However, Geelhoed et al., (2002) and Mudd et al., (2004) indicated that at pH > 5.5, the activity of Al^{3+} could be controlled both by crystalline and amorphous forms of $Al(OH)_{3,}$, which is consistent with the results of the current study. Further, Roy and Griffin (1984) showed that amorphous and crystalline forms of Al hydroxides could control the solubility of Al under slightly acidic conditions. Mullite ($Al_2Si_2O_6$) could also be one of the main sources

of Al^{3+} cations in the aqueous solution that may be hydrolyzed to $Al(OH)_3$ and precipitates (Komonweeraket et al., 2010; Medina et al., 2010), and could possibly control another solid phase in this system. However, because of the lack of mineralogical data in the MINTEQA2, it was not possible to study the effect of mullite mineral on the solubility of Al^{3+} cations.

Table 5.1 Comparisons of Cr speciation laboratory test results to MINTEQA2 results

Specimens	pH	Color	Cr Oxidation Quick Test Results	MINTEQA2 Results
10 BS + 5 LKD	11.8	Pink	Cr(VI)	Cr(VI)
20 BS + 5 LKD	11.9	Pink	Cr(VI)	Cr(VI)
10 DP + 5 LKD	12	Pink	Cr(VI)	Cr(VI)
20 DP + 5 LKD	12.1	Pink	Cr(VI)	Cr(VI)
S – 10 MT	7.2	Yellow	Cr(III)	Cr(III)
S – 20 MT	8.7	Yellow	Cr(III)	Cr(III)
S – 40 MT	9.6	Pink	**Cr(VI)**	**Cr(III)**
100 MT	9.8	Pink	**Cr(VI)**	**Cr(III)**
S – 10 Co	11.8	Pink	**Cr(VI)**	**Cr(III)**
S – 20 Co	11.9	Pink	**Cr(VI)**	**Cr(III)**
S – 40 Co	12.1	Pink	**Cr(VI)**	**Cr(III)**
100 Co	12.15	Pink	**Cr(VI)**	**Cr(III)**
100 DP	8	Yellow	Cr(III)	Cr(III)
100 PSP	7.7	Yellow	Cr(III)	Cr(III)

Notes:BS: Brandonshores fly ash, DP: Dickerson Precipitator fly ash, MT: Morgantown fly ash, Co: Columbia fly ash, PSP: Paul Smith Precipitator fly ash. The Cr species has contradict results between speciation tests and MINTEQA2 are in **bold**.

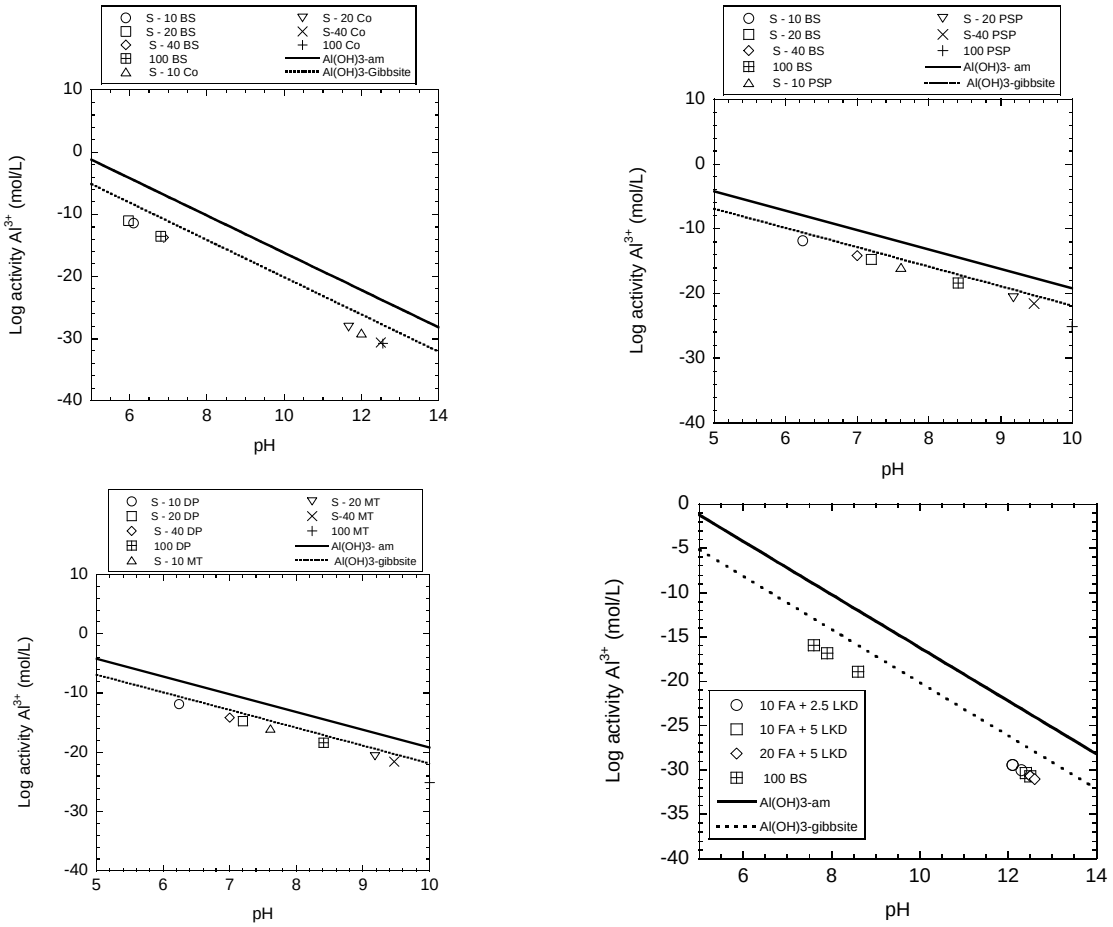

Figure 5.1 Log activity of Al^{3+} vs. pH in leachates (a) Brandon Shores and Columbia fly ashes, (b) Paul Smith Precipitator and Dickerson Precipitator, (c) Paul Smith Precipitator and Morgantown fly ashes, and (d) soil-fly ash-LKD mixtures

5.2.4 Speciation of As

As mentioned previously, As(V) is the predominant arsenic species in the aqueous solutions of fly ash, a finding consistent with Gitari et al., (2009), Pandey et al., (2011), Shah et al., (2007), and Su et al., (2011).

Figure 5.2 shows how As(V) as AsO_4^{3-} varies with the pH of effluent solutions of soil-fly ash mixtures. Even though there is a correlation between AsO_4^{3-} and pH of the aqueous solutions, it is certain that the leaching of As metals is not controlled by $As_2O_5(s)$ solid phase because As(V) concentrations are under-saturated with respect to $As_2O_5(s)$ line. These observations are consistent with those obtained by Kim et al., (2009).

As(V) can react with Al metals and form solid complexes with very low solubility products (Apul et al., 2005; Komonweeraket et al., 2010). Figure 5.3 shows that the activity of AsO_4^{3-} corresponds to activity of Al^{3+} and $AlAsO_4.2H_2O(s)$ solid phase, which was created by the MINTEQA2 database. Compared to As(v), the concentrations of Al^{3+} in aqueous solutions were generally 1 to 6 orders of magnitude lower. However, an increase in Al^{3+} concentrations moved species toward the solid line and made them closer to the $AlAsO_4.2H_2O$ solid phase. This increase indicates that with an adequate amount of Al^{3+} and AsO_4^{3-}, $AlAsO_4.2H_2O$ may form and control the solubility of As(V) species in the effluent solutions.

Based on the results obtained from MINTEQA2 about the speciation of As(V) and Mn^{2+}, these two species can form $Mn_3(AsO_4)_2.8H_2O$, a solid solution that appears to

be the main mechanism controlling the leaching of the solubility of As(V) in the aqueous solutions of all soil-fly ash mixtures used in the current study Figure 5.4 shows that the solubility of As(V) is generally controlled by the $Mn_3(AsO_4)_2.8H_2O$ compound, and in the presence of adequate As(V) concentrations, the complexation of AsO_4^{3-} with Mn^{2+} is likely to occur. An increase in the concentrations of AsO_4^{3-} and Mn^{2+} increases the possibility of the reaction between AsO_4^{3-} and Mn^{2+}, which would produce the $Mn_3(AsO_4)_2.8H_2O$, the solid phase that controls the leaching of AsO_4^{3-}. Cherry et al., (1979) and Turner (1981) said that the oxidation of As(III) to As(V) increases significantly in the presence of Fe^{3+} and Mn^{2+} and results in elevated concentrations of As(V) in the aqueous phase. The formation of soluble complexes with Fe and As(V) in neutral to slightly acidic pH levels was observed by Sadiq et al., (2002).

Arsenate can also form slightly soluble precipitates with metals such as Ba, Cd, Cu, Mn and Zn (Komonweerakter et al., 2010). Turner (1981) and Ettler et al., (2010) showed that $Ca_3(AsO_4)_2$, $Ba_3(AsO_4)_2$ are the main solid phases that may control the solubility of As(V). However, neither Ca nor Ba concentrations were measured in the effluent solutions collected from the soil-fly ash mixtures in the current study, thus, it is impossible to conclude that the leaching of As(V) was controlled by $Ca_3(AsO_4)_2$, $Ba_3(AsO_4)_2$.

Kim et al., (2009) said that iron oxides could be the oxide minerals that control the solubility of As metals. Ettler et al., (2010) and Pandey et al., (2011) also mentioned that the adsorption of As(V) by iron-oxides and aluminum-oxides is very likely to occur. The sorption of metals to minimize their contamination risks is generally achieved by

including hydrous ferric oxides and hydrous aluminum oxides (Ettler et al., 2010). Cornelis et al., (2008) said that the complexation of metals such as As(V) is possible with ettringite minerals, (e.g., $Ca_6Al_2(OH)_{12}(SO_4)_3.26H_2O$). In addition, the precipitation and dissolution of CO_3 minerals may affect the leaching of As(V) (Kim et al., 2009). Previous literature indicated that CO_3 carrier minerals such as $CaCO_3$, provide surfaces for As(V) metals to be adsorbed (Benedetto et al., 2006). An increase in CO_3 concentrations results in an increase of the sorption of As(V) metals. However, in the current study, CO_3^{2-} anion concentrations were not measured from the effluent solutions of the soil-fly ash mixtures, therefore it is not possible to conclude that leaching of As(V) was CO_3^{2-} sorption controlled.

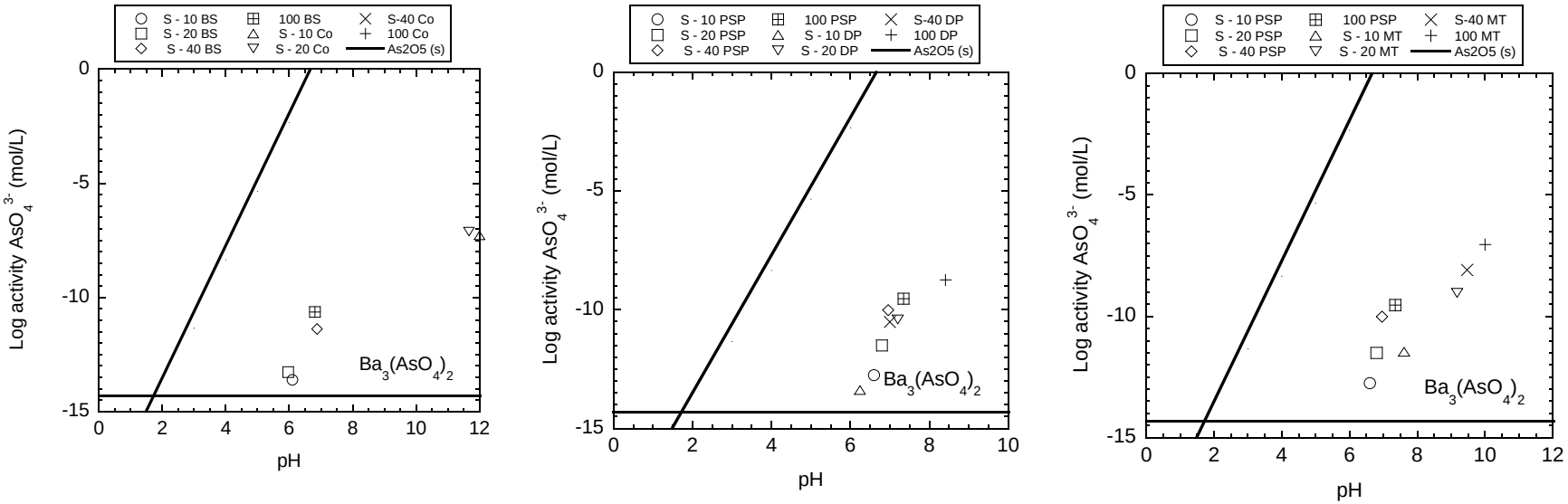

Figure 5.2 Log activity of AsO_4^{3-} vs. pH in leachates from fly ashes, soil-fly ash mixtures. (a) Brandon Shores and Columbia fly ashes, (b) Paul Smith Precipitator and Dickerson Precipitator, and (c) Paul Smith Precipitator and Morgantown fly ashes.

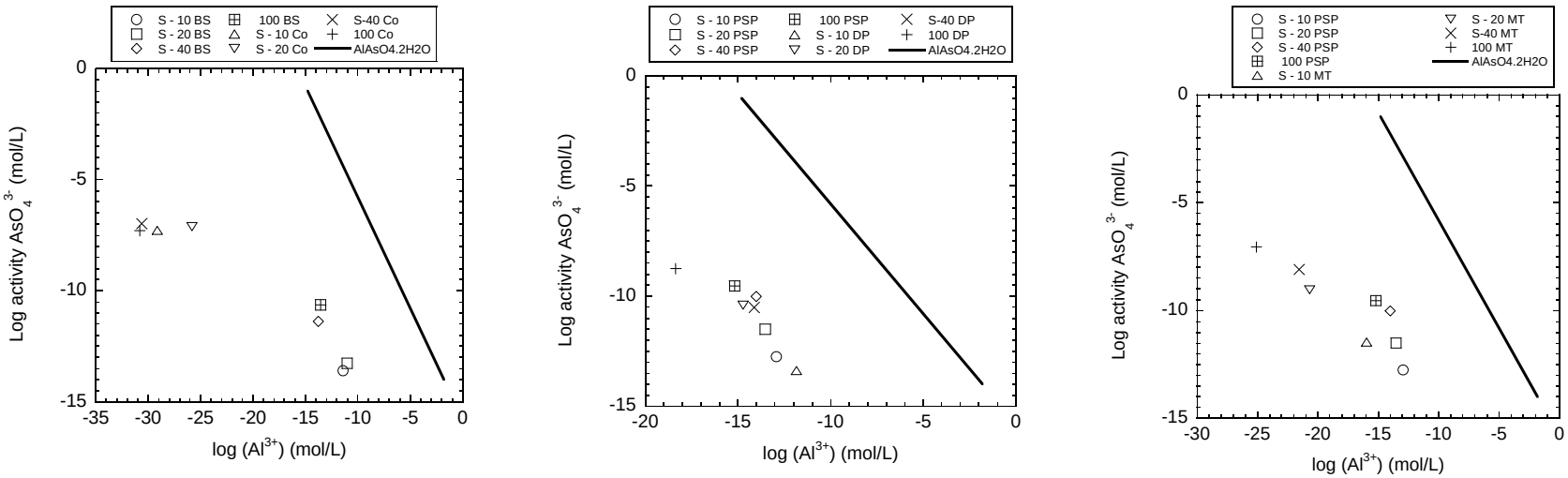

Figure 5.3 Log activity of AsO_4^{3-} vs. Al^{3+} in leachates from fly ashes and soil-fly ash mixtures: (a) Brandon Shores and Columbia fly ashes, (b) Paul Smith Precipitator and Dickerson Precipitator, and (c) Paul Smith Precipitator and Morgantown fly ashes.

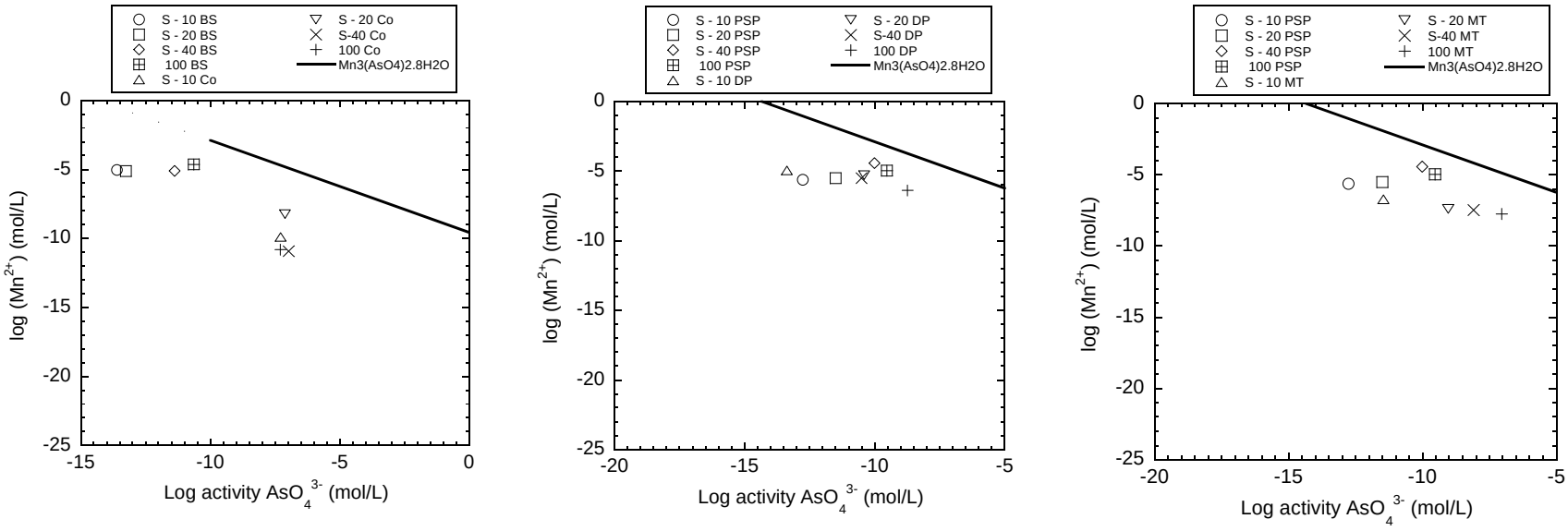

Figure 5.4 Log activity of AsO_4^{3-} vs. Mn^{2+} in leachates from fly ashes and soil-fly ash mixtures: (a) Brandon Shores and Columbia fly ashes, (b) Paul Smith Precipitator and Dickerson Precipitator, and (c) Paul Smith Precipitator and Morgantown fly ashes.

5.2.5 Speciation of Cr

The speciation analysis showed that Cr (III) as $Cr(OH)_2^+$ is the dominant oxidation state for the specimens prepared with fly ash-soil mixtures, whereas Cr(VI) as CrO_4^{2-} is the dominant oxidation state for the specimens prepared with fly ash-soil-LKD mixtures. These specimens will be discussed separately.

Figure 5.5 shows that the solubility of Cr is controlled by $Cr(OH)_3$ amorphous, $Cr(OH)_3$ and Cr_2O_3(s). However, it could also be argued that most of the controlling species was $Cr(OH)_3$ and Cr_2O_3(s) rather than amorphous $Cr(OH)_3$. Cr_2O_3 is a species present in all fly ashes at 2.5 % to 5% by weight in the fly ashes used in the current study. It is expected that solubility of Cr metals controlled by this chromium oxide mineral (Gitari et al., 2009). Mulugeta et al., (2010) indicated that the release of Cr(III) at neutral pH levels is because of the dissolution of mineral phases that Cr(III) bonds with. Cr_2O_3(s) and ferrihydrites are some of these minerals that Cr(III) could be complexed with ferrihydrites and released at neutral pH conditions (Engelsen et al., 2010). Geelhoed et al., (2002) and Karamadis and Voudrias (2008) also determined that Cr leaching from fly ashes is controlled by $Cr(OH)_3$(s). Fruchter et al., (1990) and Johnson et al., (1999) indicated that Cr^{3+} may form solid solutions with Fe hydroxides such as (Fe,Cr)(OH_3)(s). The solubility of this solid solution is very low at pH levels between 6 and 10 and the pH levels of the effluent solutions in the current study were at a range of 5.8 to 10 indicating that it is possible that Cr^{3+} solubility may have been dependent on the (Fe,Cr)(OH_3)(s) in addition to $Cr(OH)_3$ and Cr_2O_3.

Cr(VI) as chromate $(CrO_4)^{2-}$ was the predominant oxidation state of the Cr metal in the aqueous solutions of the specimens prepared with soil-fly ash-LKD materials. Figure 5.5d indicates that Cr(VI) leaching in these effluent solutions are not controlled by chromium (hydr)oxides. This behavior is expected because at very alkaline pH levels metal hydroxides begin dissolving and do not have significant impact on the leaching of Cr (VI) (Engelsen et al., 2010). $BaCrO_4$ could be the solid phase that may control the leaching of Cr(VI) at high pH levels such as pH>12 (Astrup et al., 2006). The solubility product of $BaCrO_4$ is very low and its precipitation could be very fast (Fruchter et al., 1990). As shown in Figure 5.6a, the comparison of Ba^{2+} and CrO_4^{2-} concentrations are very close to the solid $BaCrO_4$ line, indicating that the solubility of Cr(VI) could be controlled by this solid phase not by chromium (hydr)oxides. However, the Cr (VI) metals leached from specimens prepared with soil-fly ash-LKD mixtures, are slightly undersaturated with respect to the $BaCrO_4$(s) solid phase line. This also indicates that $BaCrO_4$(s) may not be the solid phase controlling the leaching of Cr(VI). In addition, $Ba(S,Cr)O_4$ could be one of the main solid phases that may control the leaching of Cr (VI) (Apul et al., 2005; Astrup et al., 2006). Because of a lack of measurements of the SO_4^{2-} anion concentrations in the effluent solutions, it was not possible to support this conclusion in the current study, despite the fact that leachates from nearly all types of fly ashes contain significant amount of SO_4^{2-} anions (Komonweeraket et al., 2010) and it could be suggested that the solubility of Cr (VI) may have been controlled by $Ba(S,Cr)O_4$ (s). In addition, Mn-(hydro)oxides may have an important effect on leaching of Cr(VI) species in basic conditions (pH>8). Further, MnO_2(s) and MnOOH(s) may create extra

adsorption sites for Cr(VI), thus affecting the control of Cr(VI) leaching. However, the sorption reaction was outside the scope of this study. Therefore, it was not determined whether the sorption of Cr(VI) was controlled by Mn(hydro)oxides or not. In future studies the measurements of SO_4^{2-} should be measured, as it plays a very important role in the solubility of Cr(VI) (Engelsen et al., 2010).

Johnson et al., (1999), Astrup et al., (2006), and Karamadis and Voudrias (2008) argued that $CaCrO_4$ and Cr(VI)-ettringite minerals may control Cr(VI) leaching at highly alkaline conditions (pH>10). Figure 12b shows the variation of log Ca values corresponding to log CrO_4^{2-} values. According to the solid line that represents the $CaCrO_{4(s)}$ is approximately 2 orders of magnitude above the log Ca and log CrO_4 values. This indicates that the solubility is CrO_4^{2-}, not $CaCrO_4$(s) controlled. In general, the solubility of Cr(VI) at high pH levels is controlled by Cr(VI)-ettringite minerals (Astrup et al., 2006; Engelsen et al., 2010; Karamadis & Voudrias, 2008). At pH levels greater than 10, Cr(VI) replaces SO_4^{2-} in ettringite minerals. This substitution is dependent on the amount of Cr(VI) concentrations in effluent solutions (Engelsen et al., 2010). Figure 5d shows that the leaching of Cr(VI) from the specimens prepared with soil-fly ash-LKD materials is not Cr(VI)-ettringite controlled. The CrO_4^{2-} concentrations are far above the Cr(VI)-ettringite solid phase line, indicating that this solid phase does not control the solubility of Cr(VI) in this study.

Fe-(hydro)oxides, Al-(hydro)oxides and Mn-(hydro)oxides are possible sorption sites that may adsorb the trace metals such as Cr(VI) (Geelhoed at al., 2002). However, Apul et al., (2005) said that leaching of Cr(VI) is not adsorption controlled, especially in

the presence of high amount of SO_4^{2-} anion in the effluent solutions. Adsorption of Cr(VI) on the iron and aluminum oxides is weak at high pH levels and in the presence of high amounts of SO_4^{2-} (Apul et al., 2005). Even though previous studies (Geelhoed et al. 2002, Fendorf 1995), said that the leaching of Cr(VI) is not adsorption controlled, it seems adsorption of Cr(VI) on the minerals or (hydro)oxides is the main leaching controlling mechanisms of this chromium species in this study. The scope of this study was focused on the leaching of solubility controlling mechanisms of the heavy metals. Therefore, no further geochemical analysis has been conducted to determine the adsorption properties of Cr(VI). However, future studies should take these possibilities into account.

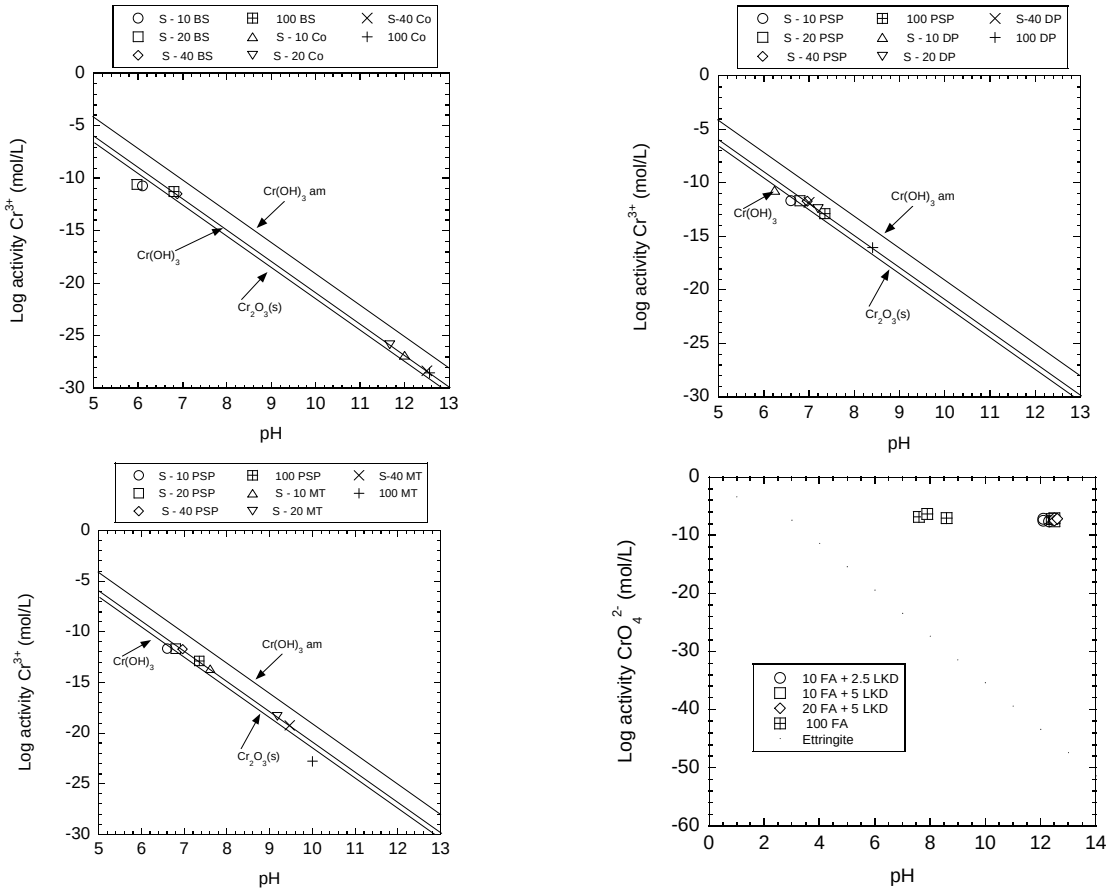

Figure 5.5 Log activity of Cr^{3+} and Cr^{6+} in leachates from fly ashes and soil-fly ash mixtures: (a) Brandon Shores and Columbia fly ashes, (b) Paul Smith Precipitator and Dickerson Precipitator, (c) Paul Smith Precipitator and Morgantown fly ashes, and (d) soil-fly ash-LKD mixtures

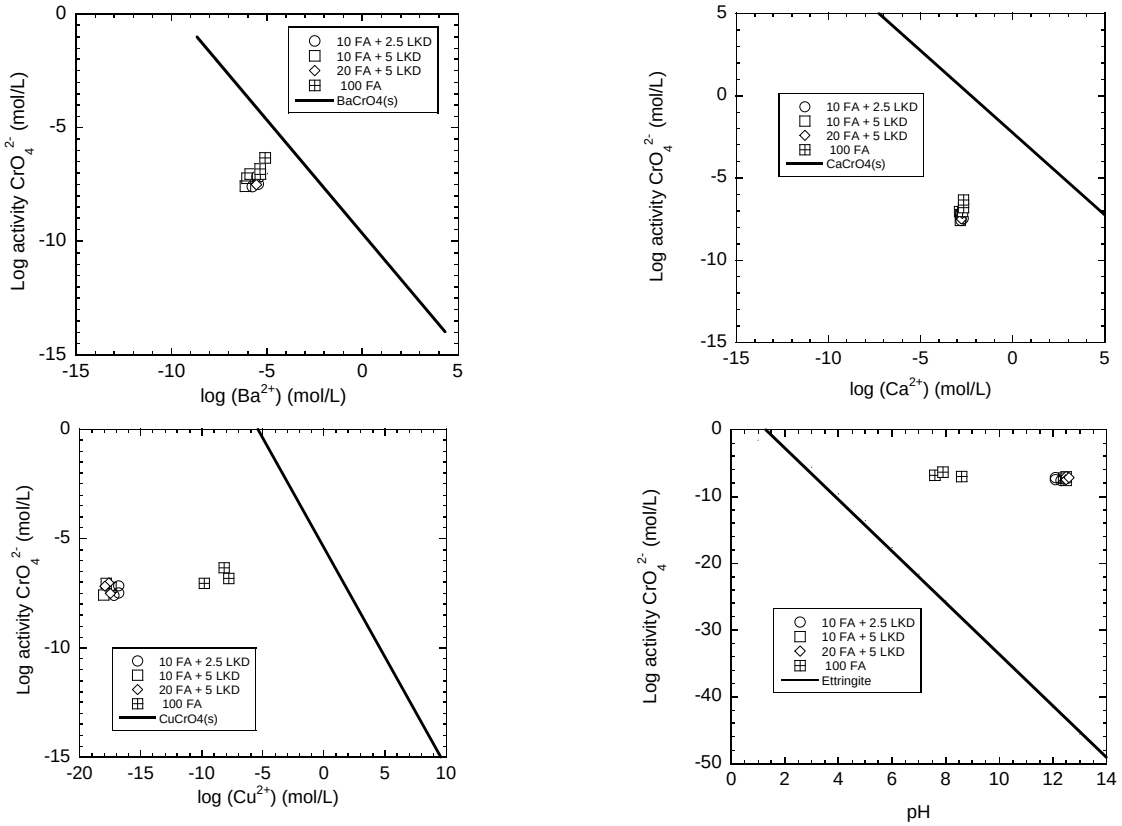

Figure 5.6 Log activity of (a) CrO_4^{2-} vs. Ba^{2+}, (b) CrO_4^{2-} vs Ca^{2+}(c) CrO_4^{2-} vs Cu^{2+} , and (d) CrO_4^{2-} vs ettringite leachates from fly ashes and soil-fly ash-LKD mixtures.

5.2.6 Speciation of Mn

The speciation analysis showed that Mn(II) as Mn^{2+} is the dominant oxidation state for both the specimens prepared with fly ash-soil mixtures and with fly ash-soil-LKD mixtures.

An increase in pH generally decreases the leaching concentrations of Mn because of the precipitation or dissolution of manganese (hydro)oxides (Su et al., (2011), Cetin et al.,(2012)). Figure 5.7 indicated that at a pH >10 the solubility of Mn(II) is controlled by pyrochroite ($Mn(OH)_2$). In neutral pH conditions ($5 < pH < 10$), Mn^{2+} cations are more freely available and increasingly precipitate as $Mn(OH)_2$ as the pH of the aqueous solutions increases (Gitari et al., 2009; Komonweeraket et al., 2010). This explains how the $Mn(OH)_2$(s) minerals control the solubility of Mn(II) metal species in the effluent solutions of the specimens prepared with soil-fly ash-LKD mixtures while $Mn(OH)_2$(s) minerals do not control the solubility of Mn(II) metal species in the effluent solutions of specimens prepared with soil-fly ash mixtures (Gitari et al., 2009). The pH values of the effluent solution of specimens prepared with soil-fly ash mixtures ranged from 6 to 10 (Table 4.5), while the pH values of the effluent solutions of specimens prepared with soil-fly ash-LKD mixtures are greater than 11 ($pH > 11$). This indicates the presences of two different leaching behavior of Mn(II).

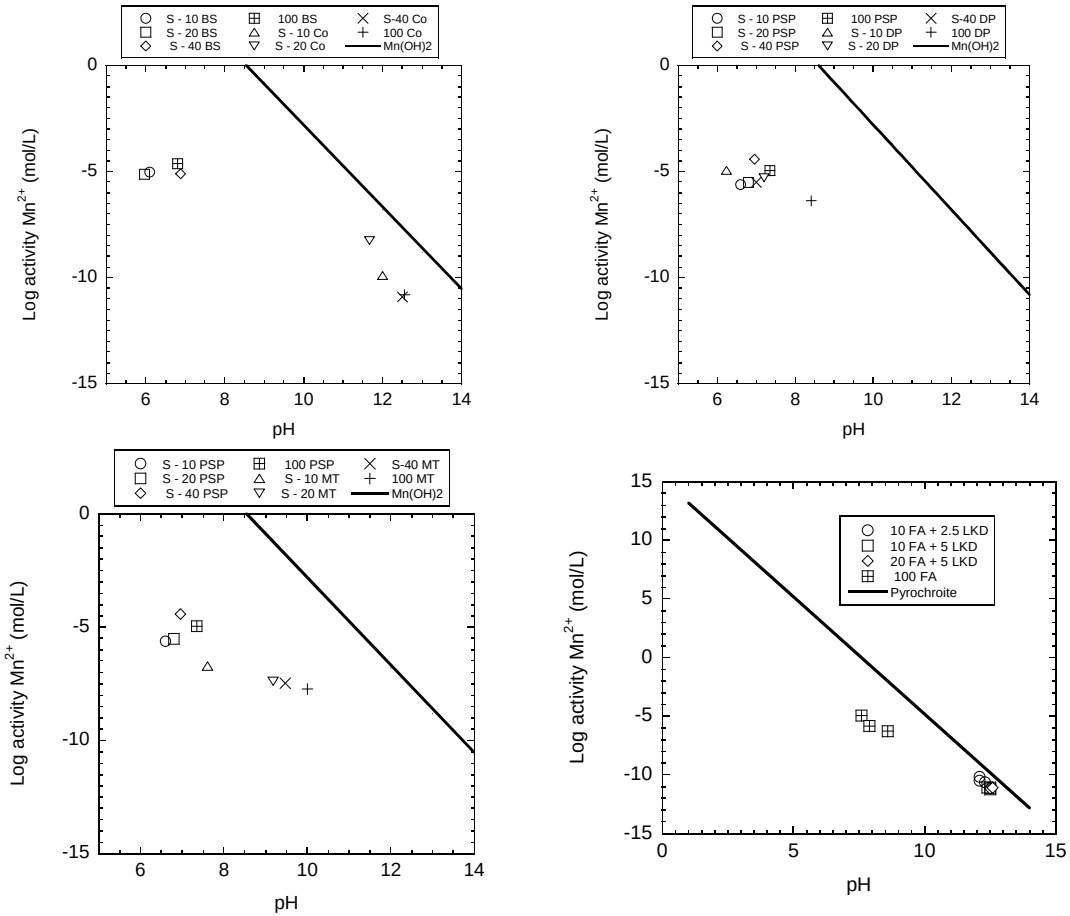

Figure 5.7 Log activity of Mn^{2+} vs. pH in leachates from fly ashes and soil-fly ash mixtures: (a) Brandon Shores and Columbia fly ashes, (b) Paul Smith Precipitator and Dickerson Precipitator, (c) Paul Smith Precipitator and Morgantown fly ashes, and (d) soil-fly ash-LKD mixtures

5.2.7 Speciation of Se

Dominant oxidation states of Se metals are Se(IV) as $HSeO_3^-$ in the soil-fly ash mixtures used in this study. This finding is consistent with the literature because it is expected that Se forms anionic species at neutral to alkaline pH levels (Medina et al., 2010; Su et al., 2011). Figure 5.8 shows that Se(IV) species are significantly undersaturated with respect to SeO_2(s), which indicates that the solubility of selenium, like arsenic, is not controlled by the dissolution/precipitation of (hydr)oxides. Baur and Johnson (2003) indicated that the solubility of Se(IV) may have been controlled by the $CaSeO_3.H_2O$ compound. In addition, $HSeO_3^-$ may complex with Ca^{2+} to produce $CaSeO_3$ solid solutions which controls the solubility of Se(IV), according to Essington (1988). Moreover, Izquierdo et al., (2011) indicated that solubility of Se(IV) is controlled by the gypsum ($CaSO_4.2H_2O$) in effluent solutions. SO_4^{2-} concentrations in the aqueous solutions may have significant impact on the leaching of Se(IV) like it has on leaching of Cr(VI) (Engelsen et al., (2010)). The gypsum effects were not shown herein since neither Ca^{2+} nor SO_4^{2-} concentrations were measured in the specimens prepared with soil and fly ash. Therefore, such a conclusion in this study is not warranted.

The formation of solid solution with ettringite mineral is very common at alkaline conditions, especially for anionic species such as CrO_4^{2-}, AsO_4^{3-}, $Sb(OH)_6^-$, and SeO_3^{2-} (Cornelis et al., 2008). Ettringite minerals present in the aqueous solutions may be the solid solutions responsible for the solubility of Se(IV). However, equilibrium was not obtained between Se(IV) and Ettringite in solid forms and minerals are available in the MINTEQA2 database.

Based on the MINTEQA2 results for Se(IV), it can be concluded that Se(IV) leaching from fly ashes and soil-fly ash mixtures are not solubility-controlled. In alkaline conditins, Se(IV) leaching is not solubility-controlled (Komonweeraket et al., 2010, Su et al., 2011). Moreover, in alkaline conditions the concentrations of oxyanionic species of Se may decrease significantly because of the adsorption and precipitation of oxyanions with minerals. Gibbsite and $Fe(OH)_3$ could provide an effective sorption site for Se(IV) species at pH levels between 8 and 9 (Langmuir, 1997).

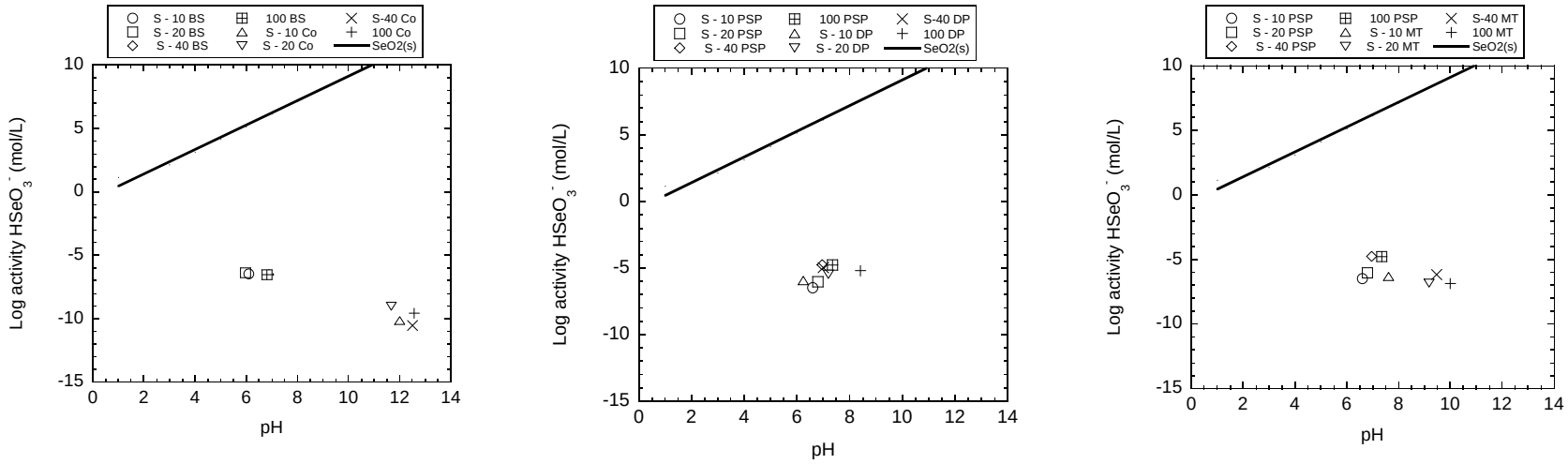

Figure 5.8 Log activity of $HSeO_3^-$ vs. pH in leachates from fly ashes and soil-fly ash mixtures: (a) Brandon Shores and Columbia fly ashes, (b) Paul Smith Precipitator and Dickerson Precipitator, and (c) Paul Smith Precipitator and Morgantown fly ashes.

5.2.8 Speciation of Cu

The dominant oxidations states of leached Cu metals from soil-fly ash-LKD mixtures were Cu (II). Based on Figure 9a, the crystalline phase of CuO mineral Tenorite(c) controls the solubility of Cu(II) metal species in the aqueous solutions collected from soil-fly ash-LKD mixtures. Engelsen at al. (2010) also said that at pH>9, tenorite or precipitation of $Cu(OH)_2(s)$ controls the leaching of Cu(II). $Cu(OH)_2(s)$ is also known as a solid phase that controls the leaching of Cu metals especially under alkaline conditions (Apul et al.,, 2005). Nevertheless, in the current study the leaching of Cu(II) cations are likely to be controlled by CuO(c) rather than $Cu(OH)_2(s)$.

At neutral pH levels, the Cu(II) cations tend to coprecipitate with Fe metals and are sorbed/adsorbed by hydrous oxides of Al and Fe minerals (Apul et al.,, 2005, Engelsen et al.,, 2010). In the current study the pH levels of the soil-fly ash-LKD mixtures were greater than11. In alkaline conditions it is not expected to observe the sorption of Cu by these minerals since the Fe oxides starts precipitating by themselves while Al oxides starts dissolving to their anion species in the aqueous solutions (Engelsen et al.,, 2010).

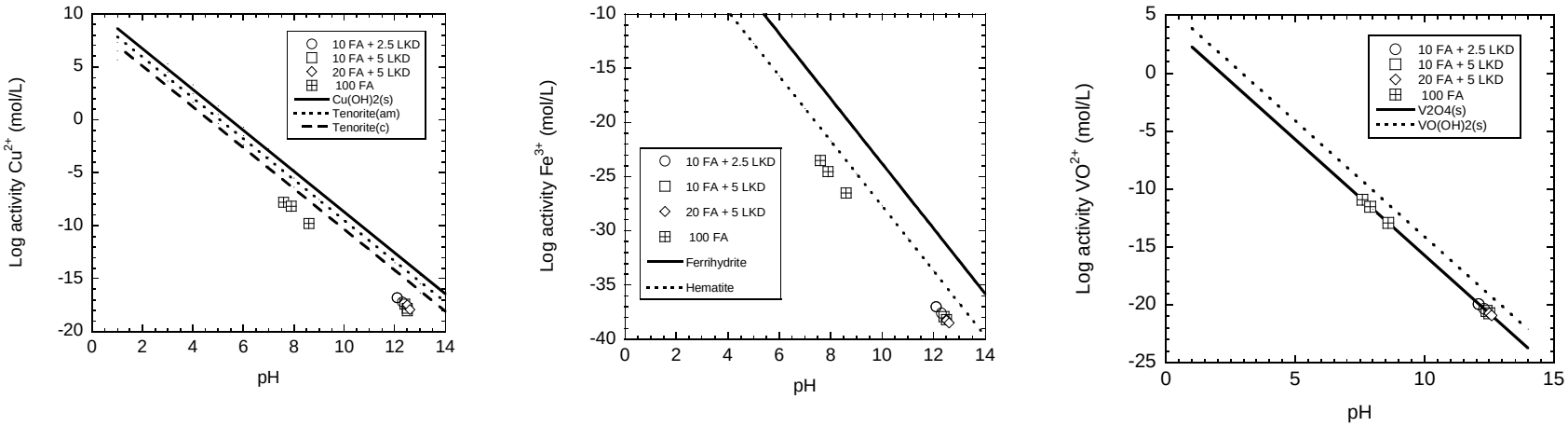

Figure 5.9 Log activity of (a) Cu^{2+} vs pH, (b) Fe^{3+} vs pH, and (c) V(IV) vs. pH in leachates from fly ashes and soil-fly ash-LKD mixtures.

5.2.9 Speciation of Fe

The speciation analysis found that Fe^{3+} is the dominant oxidation state of Fe metals in the aqueous solutions of the fly ash-based mixtures. Apul et al., (2005) and Komonweeraket et al., (2010) also said that the predominant Fe species in similar waste materials were Fe^{3+}. Fe solubility, like Al, is controlled by hydroxide minerals (Fruchter et al., 1990, Gitari et al., 2009). Figure 9b indicates that solubility of Fe is more likely controlled by hematite (Fe_2O_3) minerals rather than $Fe(OH)_3$-amorphous. These results are consistent with Black et al., (1992) which said that the solubility of Fe metals was controlled by Fe_2O_3 and Fe_3O_4. Fruchter et al., (1990) and Mudd et al., (2004) do not support the findings in this study about the solubility controlling phase of Fe. These previous studies, however, did not include highly basic conditions, i.e., pH>12 (Figure 9b). At such pH levels, it is possible for Fe^{3+} to be controlled by hematite instead of ferryhdrite ($Fe(OH)_3$). In addition, X-ray diffraction analysis indicated that hematite is the primary mineral phase of Fe in the fly ashes used in that study.

5.2.10 Speciation of V:

MINTEQA2 speciation analyses indicated that the dominant oxidation state of the leached V metals from soil-fly ash LKD mixtures was V(IV) as $V(OH)_3^+$ species. Even though previous literature suggested that V metals tend to be present in anionic form in alkaline conditions (Engelson et al., 2010; Izquierdo et al., 2011; Medina et al., 2010), these MINTEQA2 speciation analyses did not agree. Figure 9c suggests that V leaching

is solubility-controlled, a finding consistent with Apul et al., (2005). Furhtermore, the solubility of V(IV) metal species is controlled by V_2O_4(s) solid phase in all pH ranges. The V(IV) concentrations remained on the linear solid line that represent V_2O_4(s) (Figure 9c). It appears that $VO(OH)_2$(s) may also have some impact on leaching of V(IV) metals from the soil-fly ash-LKD mixtures used in this study. Izquierdo et al., (2011) said that at very high alkaline conditions the complexation of Ca and V metals helps remove V metals from leachates. This idea is consistent with the findings obtained in the current study because, as shown in Figure 9c, the concentrations of V(IV) decreased as pH increased. Ca-V precipitation could be one of the factors responsible for the leaching behavior of V(IV). Furthermore, precipitations of V metals with Pb metals will likely occur as $Pb_2V_2O_7$ and $Pb_3(VO_4)_2$ (Astrup et al., 2006). These $Pb_2V_2O_7$ and $Pb_3(VO_4)_2$ solid phases may also have significant effects on controlling the solubility of V metals. Nevertheless, the Pb concentrations leached from soil-fly ash-LKD specimens were below the detection limits, so it was not possible to observe a trend between V and Pb concentrations in the aqueous solutions. Figure 9c clearly shows that the dominant controlling mechanism of the leaching of V(IV) metals for the specimens used in this study is the V_2O_4(s) solid phase.

5.2.11 Speciation of Sb

Sb(V) as the $Sb(OH)_6^-$ was the dominant oxidation state of Sb metal species in the effluent solutions obtained from soil-fly ash-LKD mixtures. Narukawa et al., (2005) indicated that the dominant Sb species is Sb(III) leached from the fly ashes, but also that

Sb(III) is oxidized to Sb(V) very quickly under aerobic conditions, which indicates the presence of oxygen in the environment. In this study, leachates from the specimens were collected in a beaker exposed to atmosphere and, during the collection process, Sb(III) species may have been oxidized to Sb(V). This could explain Sb(V) as the dominant Sb species for the specimens used in the current study. Ettler et al., (2010) made similar observations during their testing of lead residues.

Figure 5.10a shows how $Sb(OH)_6^-$ varies with pH and indicates that the solubility of Sb(V) metal species are not Sb oxides controlled ($(Sb_2O_5)(s)$). Johnson et al., (2005) indicated that calcium antimonate ($Ca(Sb(OH)_6)_2(s)$) minerals may control the solubility of Sb metals. Figure 5.10b shows the variation of Sb(V) versus Ca(II) concentrations and indicates that the concentrations of Sb(V) metals leached from the soil-fly ash-LKD mixtures are 2-8 orders of magnitude lower than solid line that represents the $Ca(Sb(OH)_6)_2(s)$ solid phase ($-8 < SI < -2$). Figure 5.10b also shows that $Ca(Sb(OH)_6)_2(s)$ has some ability to control Sb(V) leaching.

The sorption of Sb metals onto hydrous ferric oxides and aluminum oxides are likely to occur and all these phases can act as possible carriers of Sb through processes of surface complexation and sorption (Ettler et al., 2010). Under very alkaline conditions ($pH > 10$), the presence of ettringite minerals in the aqueous solutions may also control the leaching of Sb(V) metals (Cornelis et al., 2008). However, neither sorption nor complexation reactions were included in the geochemical modeling analysis because they were outside the scope of this study. Therefore, it cannot be definitively decided that the

leaching of Sb(V) metals from soil-fly ash-LKD minerals are solubility- or sorption-controlled.

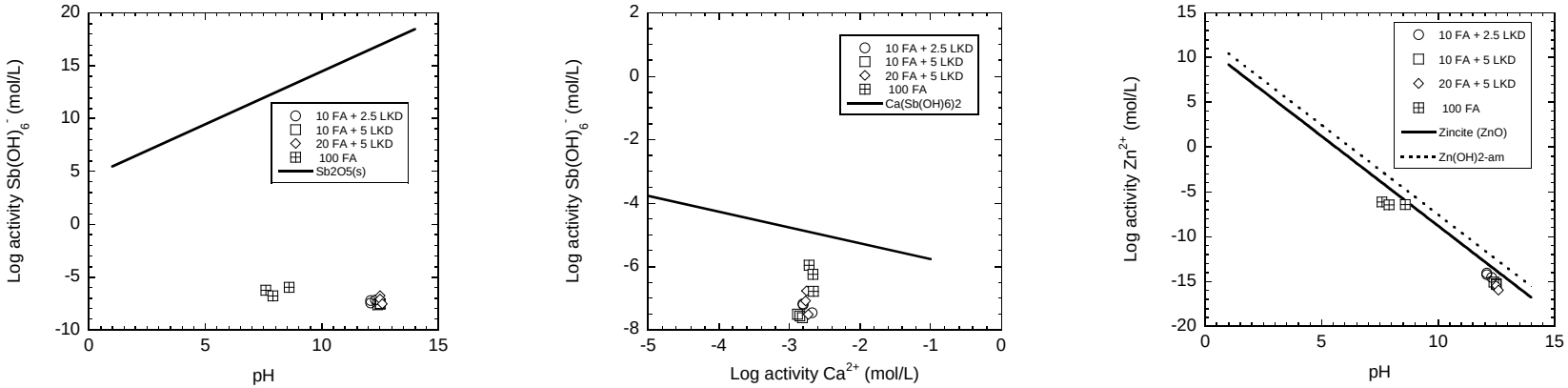

Figure 5.10 Log activity of (a) $Sb(OH)_6^-$ vs. pH, (b) vs Ca^{2+} , and (c) Zn^{2+} vs pH in leachates from fly ashes and soil-fly ash-LKD mixtures.

5.2.12 Speciation of Zn

Zn concentrations in the effluent solutions were only measured for specimens prepared with soil-fly ash-LKD materials. Speciation analyses indicated that the dominant oxidation state of the Zn metals leached from these specimens is Zn(II) as Zn^{2+}. Solubility of Zn metals are mainly controlled by precipitation and dissolution reactions in the soil matrix (Murarka et al., 1992). Figure 5.10c shows that the leaching of Zn(II) metal species is controlled by zincite (ZnO) minerals, especially for the specimens in very high alkaline aqueous solutions (pH > 9). The solid line representing the solubility of ZnO in Figure 5.10c covers all the Zn^{2+} cations leached from the specimens prepared with soil-fly ash-LKD mixtures. This confirms that ZnO is the main inorganic chemical compound that has a significant effect on the leaching of Zn^{2+} metals. Moreover, Astrup et al., (2006) and Karamalidis and Voudrias (2009) found that the solubility of Zn^{2+} is controlled by the ZnO minerals in aqueous solutions. $CaZn_2(OH)_6.2H_2O(s)$, often found in the soil matrix during cementititous reactions, could be another solid phase that may affect the solubility of Zn^{2+} under very alkaline conditions (Engelsen et al., 2010). The MINTEQA2 analysis, however, did not provide any information about the possibility of the occurrence of such mineral. Therefore, this mineral was not taken into account in the determination of the solid phases that may control the leaching of Zn^{2+} from the specimens used in this study.

Dijkstra et al., (2002) suggested that including surface precipitation of Zn on the soil particles in the speciation analyses would provide more detailed information about the leaching behavior of Zn. This, however, was outside the scope of this study, so it was not included in the MINTEQA2 analysis of Zn. The adsorption of Zn onto Fe and Al

(oxy)hydroxide minerals tends to occur at neutral pH levels (Dijkstra et al., 2004). The pH of the effluent solutions of the specimens prepared with soil-fly ash-LKD materials in this study are very high and the ZnO solid line closely matches the Zn^{2+} concentrations (Figure 5 10.c). The sorption of Zn onto Fe and Al (oxy)hydroxide minerals was not observed in the current study.

Apul et al., (2005) said that Zn may form $Zn(OH)_2$(am) at pH > 8. Even though the Zn^{2+} concentrations are undersaturated with respect to $Zn(OH)_2$(am) (the solid line phase in Figure 5.10c), it may have some controlling influences on leaching of Zn^{2+} cations into the aqueous solutions. This finding is also consistent with those reported by Apul et al., (2005).

Leached metals could be present as carbonates, oxides, or hydroxides. Zn could also be adsorbed on metal hydroxides, particularly Fe-oxide minerals. Hydrous ferric (HFO) is a very important mineral in the immobilization of heavy metals via sorption and sorption of Zn onto HFO is very likely to occur at pH~ 9.5 (Engelsen et al., 2010). Karamalidis and Voudrias (2009) indicated that dominant mechanisms controlling the leaching of Zn^{2+} is the combination of surface complexation and dissolution/precipitation of the minerals that includes Zn. However, Figure 5.10 suggests that the zincite (ZnO) minerals were controlling the solubility of the Zn^{2+} for the specimens used in this study.

5.2.13 Speciation of B

B(III) as H_3BO_3 was the dominant oxidation state of the boron metal that was leached from soil-fly ash mixtures. Engelsen et al., (2010) also determined that B(III) is

generally the dominant boron species in the environment. However, MINTEQA2 was not able to provide any solid phase that may control the solubility of B(III) in aqueous solutions. Therefore, no log graph was created to determine whether the leaching of B(III) metal species are solubility- or sorption-controlled. These findings are consistent with the previous studies on leaching controlling mechanisms of B. Fruchter et al., (1990) indicated that borate minerals such as pinnoite, inderite and nobleite do not control the solubility of B and so was unable to define any geochemical reactions to control the leaching of B. Furthermore, Mudd et al., (2004) said that borate minerals do not have any impact on controlling the B leaching. Additionally, Mudd et al., wrote that B leaching could be sorption-controlled instead of being solubility-controlled.

The pH levels of the effluent solutions of the all soil-fly ash mixtures ranged from 6 to10; at those levels, B leaching is minimal (Querol et al., 1995) The B(III) leaching controlling mechanisms in aqueous solutions could be the precipitation of B with $CaCO_3$ minerals (Hollis et al., 1988). Gitari et al., (2009) and Engelsen et al., (2010) reported that ettringite minerals at high pH (pH>8) may also have impact on controlling the leaching behavior of B(III). However, neither SO_4^{2-} nor CO_3^{2-} concentrations were measured in the current study, therefore such a conclusion cannot be warranted.

5.3 CONCLUSIONS

MINTEQA2 equilibrium geochemical code and laboratory column leaching tests results were used to determine the dominant oxidation states of the Al, As, B, Cr, Cu, Fe, Mn, Sb, Se, V, and Zn metals and to define the mechanisms that control leaching of the leached dominant metal species in the leachates. The geochemical modeling code was conducted

on the - soil-fly ash-LKD mixtures and soil-fly ash mixtures. The findings from the current study can be summarized as follows:

1) MINTEQA2 speciation analysis indicated that the As, Fe, Cu, Mn, Sb, and V were typically present in the oxidized forms As(V), Fe(III), Cu(II), Mn(II), Sb(V) and V(IV), respectively, with some exceptions that are discussed. The dominant oxidation states of Cr metals leached from soil-fly ash mixtures were in a reduced form as Cr(III) while the dominant oxidation states of Cr metals from soil-fly ash-LKD mixtures were in an oxidized form as Cr(VI). The speciation analysis indicated that, even though the Se(IV) was the dominant oxidation states of the leachates, there were still reasonable amounts of the oxidized form of Se as Se(VI) in the aqueous solutions. Even though Al is not a redox-sensitive metal element, speciation analysis indicated that Al(III) is the dominant oxidations state of the leached Al metals both for soil-fly ash mixtures and soil-fly ash-LKD mixtures.
2) Dissolution-precipitation reactions identified by the MINTEQA2 database were used to determine the leaching controlling mechanisms of all metals studied in the current study. Al(III), Cr(III), Mn(II), Cu(II), Fe(III), V(IV), and Zn(II) metals were able to be defined by these dissolution-precipitation reactions, indicating that leaching of these metals are solubility-controlled. However, no relationships were observed between the As(V), Sb(V), and Se(IV) metals indicating that leaching of these metals likely are sorption controlled. Confirming this was the outside the scope of this study, but should be the subject of future research. Therefore, it was

not possible, from the current research, to conclude which sorption reaction may control the leaching of As(V), Sb(V), and Se(IV) metal species.

3) $Al(OH)_3$(Gibbsite) was the dominant solid phase that controls the leaching of Al(III) in the aqueous solutions. B(III) as H_3BO_3 was the dominant oxidation state of the boron metal leached from soil-fly ash mixtures. However, MINTEQA2 was unable to provide a solid phase that may control the solubility of B(III) in the aqueous solutions. Therefore, no log graph was could be created to further characterize the leaching behavior of B(III) metal species.

4) Cr(III) was mainly controlled by $Cr(OH)_3$ and Cr_2O_3(s) rather than by $Cr(OH)_3$(am). Cr_2O_3, is original to all fly ashes, and varied in original concentrations from 2% to 5%. It is expected to see the solubility of Cr metals controlled by this chromium oxide mineral. In addition, the solubility of Mn(II), Cu(II), Zn(II), and V(IV) were controlled by $Mn(OH)_2$, $Cu(OH)_2$, ZnO, and V_2O_4(s) minerals respectively.

5) Based on MINTEQA2 results, As(V) was not controlled by As(hydro)oxides. The geochemical analysis indicated that the solubility of As(V) is generally controlled by the $Mn_3(AsO_4)_2.8H_2O$ compound. It is expected that in the presence of adequate As(V) concentrations; the complexation of AsO_4^{3-} with Mn^{2+} is likely to be observed.

6) None of the solid phases provided by MINTEQA2 analyses had control over the leaching of Se(IV) metal species. Previous studies agree that leaching of Se(IV) is not solubility-controlled in alkaline conditions. The concentrations of oxyanions

decrease significantly compared to metallate solubility because of the adsorption and solid solution formation of oxyanions with minerals at high pH levels. Gibbsite and $Fe(OH)_3$ could provide an effective sorption site for Se(IV) species at pH levels around 8 and 9. However, a separate study on the sorption mechanisms was not conducted.

7) The solubility of Sb(V) metal species were not controlled by Sb-oxide minerals such as $Sb_2O_5(s)$. Calcium antimonate ($Ca(Sb(OH)_6)_2(s)$) minerals may control the solubility of Sb metals. Based on the MINTEQA2 analyses, it can be concluded that $Ca(Sb(OH)_6)_2(s)$ have some ability to control the leaching of Sb(V) metals. The sorption of Sb metals onto hydrous ferric oxides and aluminum oxides is highly likely. All phases can act as possible carriers of Sb through processes of surface complexation and sorption. However, neither sorption nor complexation reactions were included in the geochemical modeling analysis.

8) Fe^{3+} was the dominant oxidation state of Fe metals in the aqueous solutions of fly ash-soil, fly ash-soil-LKD mixtures. The solubility of Fe was probably controlled by the hematite (Fe_2O_3) minerals rather than by $Fe(OH)_3(am)$, $Fe(OH)_3(s)$. X-ray diffraction analysis indicated that hematite is the primary mineral phase of Fe in the fly ashes used in that study, suggesting that leaching of Fe metals was controlled by Fe_2O_3 minerals.

9) The leaching of Cr(VI) in the effluent solutions are not controlled by chromium (hydr)oxides. The solubility of Cr(VI) could be controlled by $BaCrO_4$ solid phase. $Ba(S,Cr)O_4$ could be one of the main solid phases that may control the leaching of

Cr(VI); however, further SO_4^{2-} anion measurements are necessary to prove this phenomenon.

6 CONCLUSIONS AND RECOMMENDATIONS

6.1 CONCLUSIONS

Coal power plants generate approximately 50% of the electricity in the United States (Daniels & Das, 2006). As a result, large amounts of coal combustion byproducts especially fly ashes are produced annually. Only 40% of these fly ashes can be reused successfully in applications such as cement, concrete production and soil stabilization; most of these reused fly ashes are classified as C- and F-type fly ashes by ASTM C618. The rest of these waste materials are high-carbon fly ashes (HCFAs) and put into landfills each year. HCFAs contain significant amounts of unburned carbon (i.e., high loss on ignition) and cannot be used as a concrete additive (Cetin et al., 2010). Unless a beneficial reuse is identified, the only current alternative for this byproduct is to dispose of it in landfills.. The problem however, is that continuous disposal of these HCFAs are causing significant environmental and economical problems.

Several highway applications are potential options for the reuse of HCFAs (e.g., as a stabilizer in highway base layers, as a soil amendment in embankment constructions). Even though mechanical properties of the fly ash-amended highway base layers and embankments are deemed satisfactory, one key issue that precludes widespread use of HFCAs to stabilize highway base layers is the potential for negative effects on groundwater caused by metals in the fly ash (Bin-Shafique et al., 2006; Jankowski et al.,

2006; Wang et al., 2006). The main objective of this research study was to investigate the environmental suitability of high-carbon fly ash to stabilize highway base layers and amend embankments. This research study proceeded in two phases. The first experimentally evaluated the environmental suitability of HCFAs amended soils. The second was numerical evaluation of environmental suitability of HCFAs amended soils.

Experiments started with physical and chemical characterization of the fly ashes that were mainly collected from Maryland. Then, water leach tests (WLTs), toxicity characteristic leaching procedure tests (TCLPs), and column leach tests (CLTs) were conducted to determine the environmental suitability of utilization of high-carbon fly ashes to the geotechnical applications. These three leaching tests were specifically chosen because they were significantly different from each other. WLTs simulate metals' short-term leaching behavior, while CLTs simulate their long-term leaching behavior. TCLP tests were also conducted because those results are required by EPA whenever the environmental suitability of waste materials is being evaluated. Laboratory tests were performed on soil, fly ash alone, soil-fly ash-lime kiln dust, and soil-fly ash mixtures. This research study focused on the leaching behaviors of 12 different metals: arsenic (As), aluminum (Al), antimony (Sb), barium (Ba), boron (B), copper (Cu), chromium (Cr), iron (Fe), manganese (Mn), selenium (Se), vanadium (V), and zinc (Zn).

The results from the first phase of this study were used as input parameter in the groundwater contamination numerical computer model WiscLEACH in the second phase. WiscLEACH predicted the leached metal concentrations in the field. WiscLEACH simulations were conducted to study the locations of maximum metal concentrations in

the soil vadose zone and groundwater (e.g., at the centerline of the pavement structure, at the vicinity of point of compliance) and create contours of trace metals at different years as a function of depth physical and chemical properties of the fly ash-amended soils. In addition, the geochemical computer model MINTEQA2 conducted speciation analyses to determine the most dominant species of the leached metals that existed in the leachate and to estimate the mechanisms that controlled leaching. Total peak metal concentrations from CLTs, leachate pH, electrical conductivity (EC) and leachate Eh, were input into MINTEQA2. The results of these experimental and numerical tests were discussed in detail in the previous sections. This chapter offers only general conclusions:

1. As fly ash content increased, so did the pH of the effluent solutions of the soil-fly ash and - soil-fly ash-lime kiln dust mixtures regardless of the fly ash types. Even though most of the fly ashes did not have significant amounts of CaO and MgO, the release of these minerals still had an impact on effluent pH levels.
2. The addition of fly ash content generally caused an increase in the leached metal concentrations with few exceptions. Fly ashes were the main metal source in the soil mixtures. Therefore, it was expected that an increase in metal concentrations in the aqueous solutions would be seen with increases in the fly ash content in the soil mixtures.
3. The addition of lime kiln dust (LKD) significantly affects the pH of leachates in the soil-fly ash-LKD mixtures. The concentrations of the metals studied in this research were significantly influenced by the pH of effluent solutions. This finding suggests that the addition of LKD should be a critical consideration when

determining environmental suitability of using fly ashes as a stabilizing agent in highway base layers.

4. The concentrations of metals were generally below the EPA MCLs, WQLs, and Maryland ATLs. Al was only the exception, and only when combined with soil and LKD. Al is on the EPA list of secondary drinking water regulations, but there are no limits for Al specified in Maryland groundwater protection guidelines. On the other hand, the concentrations of the metals exceeded the EPA MCLs beyond the addition of 20% of the specimens prepared with only Mt and Co fly ashes.
5. WiscLEACH simulations for both fly ash-stabilized highway base layers and fly ash-amended embankments indicated that metal concentrations decreased over time and distance and that all the metals were sufficiently dispersed in the vadose zone. WiscLEACH results also indicated that the metal concentrations were much lower than metal concentrations obtained from the laboratory leaching tests. This discrepancy suggests that the results of laboratory tests are likely to provide a conservative estimate of field metal leaching.
6. MINTEQA2 indicated that the speciation of metals is highly dependent on the pH and Eh of effluent solutions. The most toxic form of some metal species of leached from soil-fly ash mixtures soil-fly ash-LKD mixtures. Extra care should, therefore, be taken when using some these soil mixtures geotechnical applications.
7. The reuse of high-carbon fly ash (HCFAs) as a stabilizing agent and for soil amendment in geotechnical applications is environmentally safe. However, designing the ratio of adding fly ash to soil in these geotechnical structures must

be done very carefully. The addition of large amounts of fly ash may yield an excessive amount of leached metals into the environment and groundwater which may cause significant health issues to aquatic life and humans.

6.2 RECOMMENDATIONS FOR FUTURE STUDIES

Although these results satisfactorily evaluated the environmental suitability of using fly ash in these applications, more static pH laboratory leaching tests should be conducted on the same mixtures to obtain more reliable information about these metals' leaching behaviors. Leaching of metals are highly dependent on the effluent pH levels and influent pH levels. Therefore, it is crucial to determine the leached metal concentrations from fly ash mixed soils at different stabilized pH levels. These studies would provide clearer information on defining the leaching patterns and would allow for more input data for MINTEQA2.

The boundary conditions of WiscLEACH computer model should be modified. Although the results obtained from WiscLEACH are conservative, some of the assumptions made in WiscLEACH should be modified to reflect chemical and biological reactions that occur in the field. These modifications would allow more accurate estimations of leached metal concentrations from fly ash-mixed soils. WiscLEACH does not account for surface runoff that may occur on the soil at the edge of the pavement and pavement surface, but does assume that the entirety of precipitated water infiltrates thorough the pavement structure and soil vadose zone. This is a very conservative assumption and may overestimate the leached metal concentrations in the groundwater.

Therefore, including the effects of the loss of precipitated water may yield more accurate prediction of the leached metal concentrations in the field.

Finally, performing large-scale field studies of the soil mixtures prepared for this study may help make the results of future lab tests more reliable. In addition, field studies would also help to validate the results obtained from numerical computer models and check their accuracy and efficiency.

6.3 IMPLEMENTATING RECOMMENDATIONS FROM THE STUDY

Based on the results obtained from this study, the application of fly ash amendments in soils used in highway base layers and embankments is feasible and environmentally safe. Additionally, such application of fly ashes poses few limitations. Ratios of fly ash in the soil mixtures must be carefully designed. As mentioned previously, adding fly ash greater than 20% by weight may cause environmental problems in specific conditions. The following steps should be followed in the construction of fly ash-amended highway structures:

1) The chemical and physical properties of the fly ashes and the soil should be determined.
2) The geomechanical stability of fly ash-amended highway structures should be evaluated.
3) Leachate samples should be collected from the construction site and should be analyzed for pH and leached metal concentrations.

4) The design of highway base layers and embankments with HCFA must be done carefully especially if the pH and leached metal concentrations of leachate exceed EPA Regulation limits. Extra care should be taken for the soil – fly ash mixtures prepared with Morgantown and Paul Smith Precipitator fly ashes. The contents of these fly ashes should not be higher than 20% by weight according to the laboratory tests and numerical analyses results.

7 ACKNOWLEDGEMENTS

This study was financially supported by the FHWA Recycled Materials Resource Center (RMRC), Maryland State Highway Administration (SHA), Maryland Water Resources Research Center (MWRRC), and Maryland Department of Natural Resources (MD DNR). Endorsement by RMRC, SHA, MWRRC, and MD DNR or the fly ash suppliers is not implied and should not be assumed.

APPENDIX A: LOCATIONS OF POWER PLANTS

APPENDIX B: ELUTION CURVES FOR METALS FOR HIGH-CARBON FLY ASH STABILIZED BASE LAYER

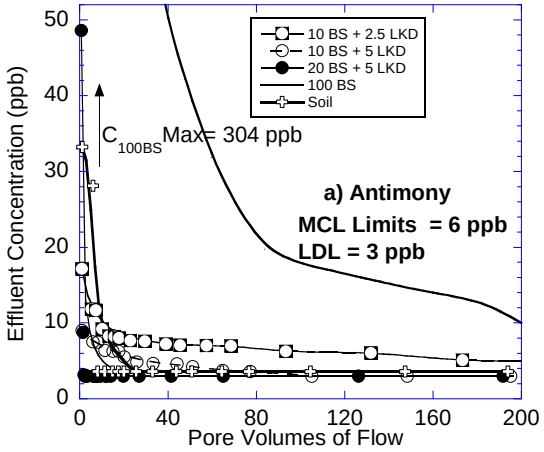
10 BS + 2.5 LKD
10 BS + 5 LKD
20 BS + 5 LKD
100 BS
Soil
C_{100BS} Max= 304 ppb
a) Antimony
MCL Limits = 6 ppb
LDL = 3 ppb
Effluent Concentration (ppb)
Pore Volumes of Flow

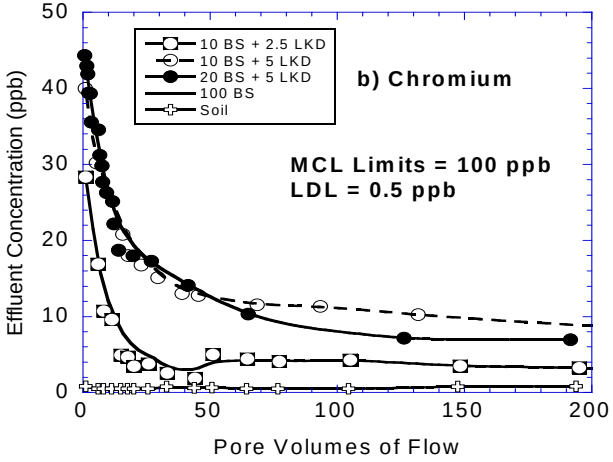
10 BS + 2.5 LKD
10 BS + 5 LKD
20 BS + 5 LKD
100 BS
Soil
b) Chromium
MCL Limits = 100 ppb
LDL = 0.5 ppb
Effluent Concentration (ppb)
Pore Volumes of Flow

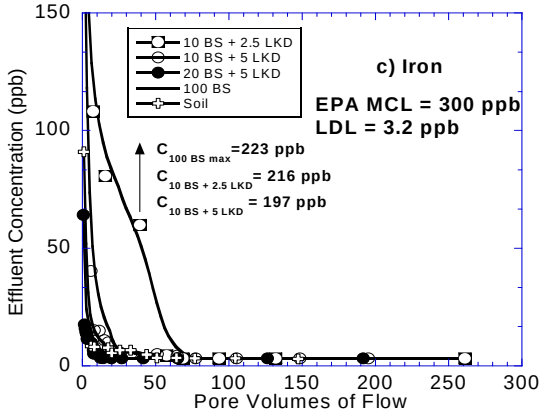
10 BS + 2.5 LKD
10 BS + 5 LKD
20 BS + 5 LKD
100 BS
Soil
c) Iron
EPA MCL = 300 ppb
LDL = 3.2 ppb
$C_{100\ BS\ max}$=223 ppb
$C_{10\ BS\ +\ 2.5\ LKD}$= 216 ppb
$C_{10\ BS\ +\ 5\ LKD}$ = 197 ppb
Effluent Concentration (ppb)
Pore Volumes of Flow

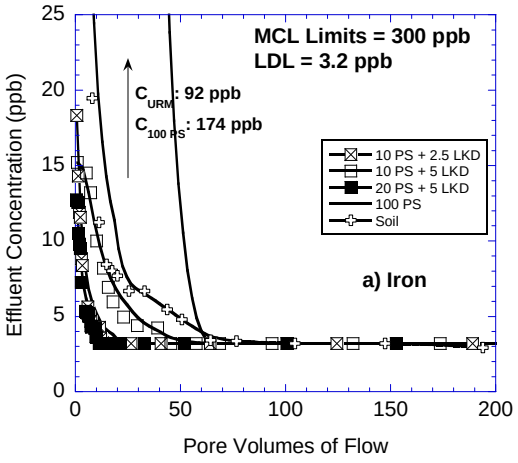
MCL Limits = 300 ppb
LDL = 3.2 ppb
C_URM: 92 ppb
C_100 PS: 174 ppb
10 PS + 2.5 LKD
10 PS + 5 LKD
20 PS + 5 LKD
100 PS
Soil
a) Iron
Effluent Concentration (ppb)
Pore Volumes of Flow

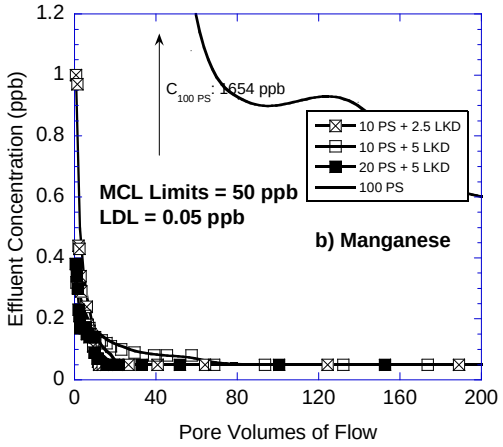
C_100 PS: 1654 ppb
10 PS + 2.5 LKD
10 PS + 5 LKD
20 PS + 5 LKD
100 PS
MCL Limits = 50 ppb
LDL = 0.05 ppb
b) Manganese
Effluent Concentration (ppb)
Pore Volumes of Flow

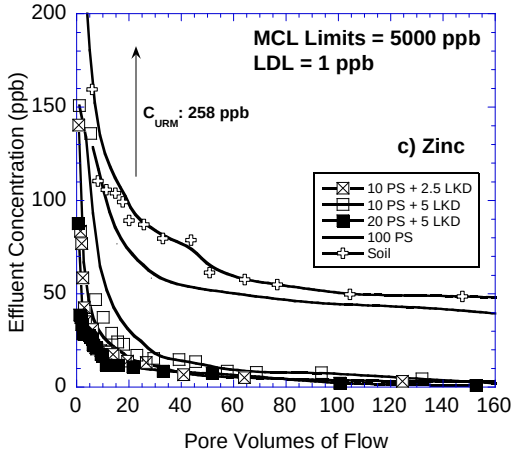
MCL Limits = 5000 ppb
LDL = 1 ppb
C_URM: 258 ppb
c) Zinc
10 PS + 2.5 LKD
10 PS + 5 LKD
20 PS + 5 LKD
100 PS
Soil
Effluent Concentration (ppb)
Pore Volumes of Flow

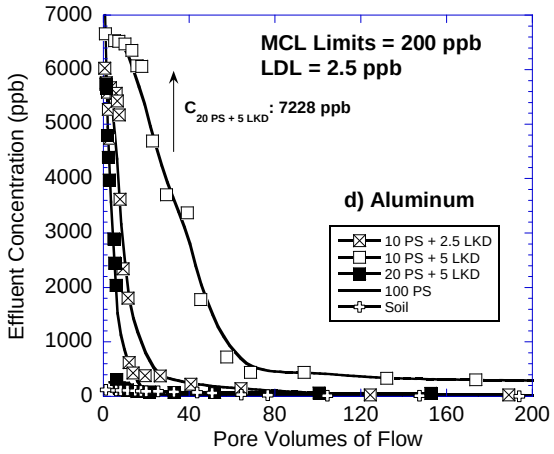
MCL Limits = 200 ppb
LDL = 2.5 ppb
C_20 PS + 5 LKD: 7228 ppb
d) Aluminum
10 PS + 2.5 LKD
10 PS + 5 LKD
20 PS + 5 LKD
100 PS
Soil
Effluent Concentration (ppb)
Pore Volumes of Flow

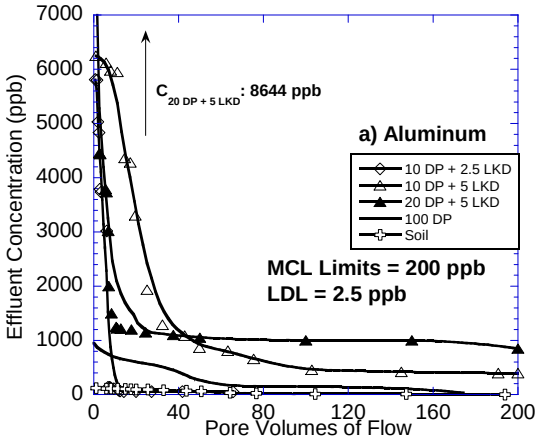
Effluent Concentration (ppb)
Pore Volumes of Flow
$C_{20\ DP + 5\ LKD}$: 8644 ppb
a) Aluminum
10 DP + 2.5 LKD
10 DP + 5 LKD
20 DP + 5 LKD
100 DP
Soil
MCL Limits = 200 ppb
LDL = 2.5 ppb

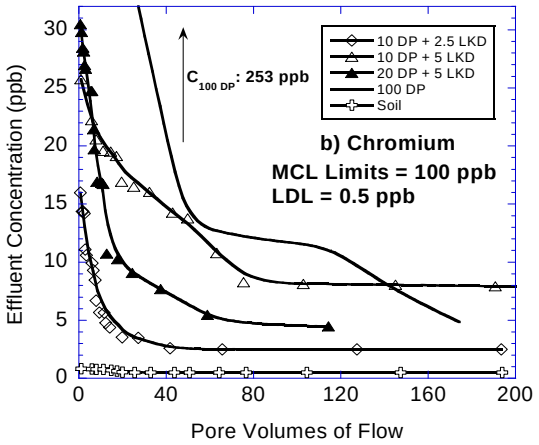
Effluent Concentration (ppb)
Pore Volumes of Flow
$C_{100\ DP}$: 253 ppb
10 DP + 2.5 LKD
10 DP + 5 LKD
20 DP + 5 LKD
100 DP
Soil
b) Chromium
MCL Limits = 100 ppb
LDL = 0.5 ppb

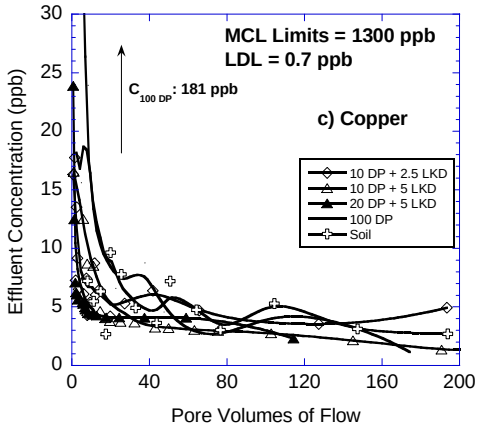
Effluent Concentration (ppb)
Pore Volumes of Flow
MCL Limits = 1300 ppb
LDL = 0.7 ppb
$C_{100\ DP}$: 181 ppb
c) Copper
10 DP + 2.5 LKD
10 DP + 5 LKD
20 DP + 5 LKD
100 DP
Soil

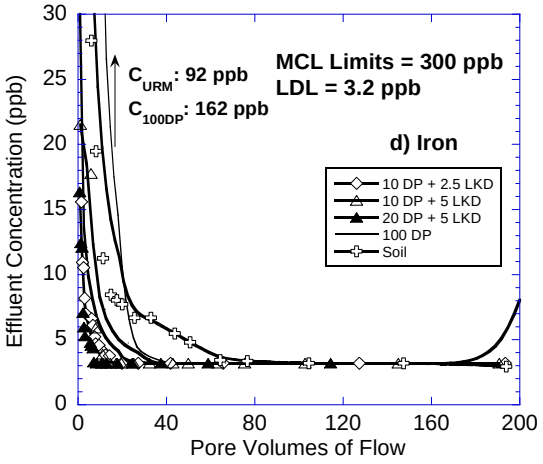
Effluent Concentration (ppb)
Pore Volumes of Flow
C_{URM}: 92 ppb
C_{100DP}: 162 ppb
MCL Limits = 300 ppb
LDL = 3.2 ppb
d) Iron
10 DP + 2.5 LKD
10 DP + 5 LKD
20 DP + 5 LKD
100 DP
Soil

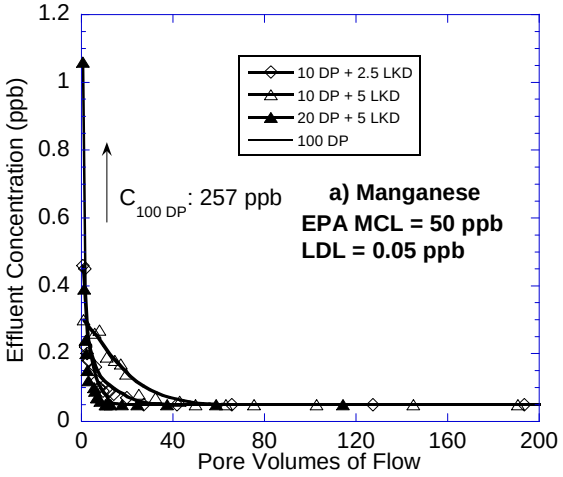
10 DP + 2.5 LKD
10 DP + 5 LKD
20 DP + 5 LKD
100 DP
C100 DP: 257 ppb
a) Manganese
EPA MCL = 50 ppb
LDL = 0.05 ppb
Effluent Concentration (ppb)
Pore Volumes of Flow

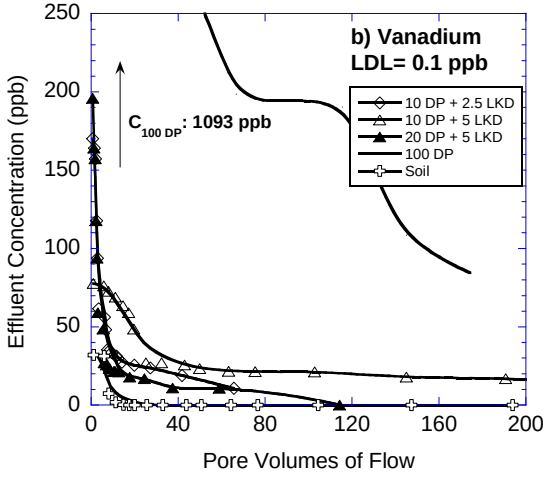
b) Vanadium
LDL= 0.1 ppb
C100 DP: 1093 ppb
10 DP + 2.5 LKD
10 DP + 5 LKD
20 DP + 5 LKD
100 DP
Soil
Effluent Concentration (ppb)
Pore Volumes of Flow

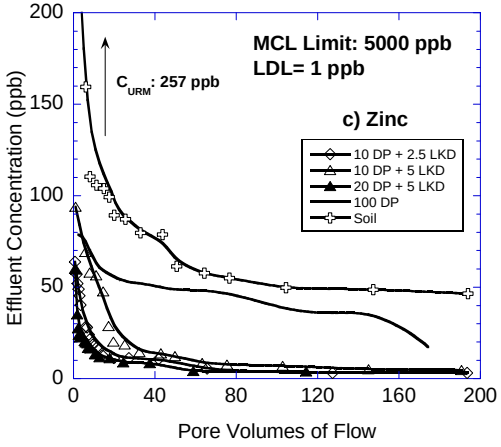
MCL Limit: 5000 ppb
LDL= 1 ppb
CURM: 257 ppb
c) Zinc
10 DP + 2.5 LKD
10 DP + 5 LKD
20 DP + 5 LKD
100 DP
Soil
Effluent Concentration (ppb)
Pore Volumes of Flow

APPENDIX C: PREDICTED METAL CONCENTRATIONS IN VADOSE ZONE AND GROUND WATER FOR HIGH-CARBON FLY ASH STABILIZED BASE LAYERS

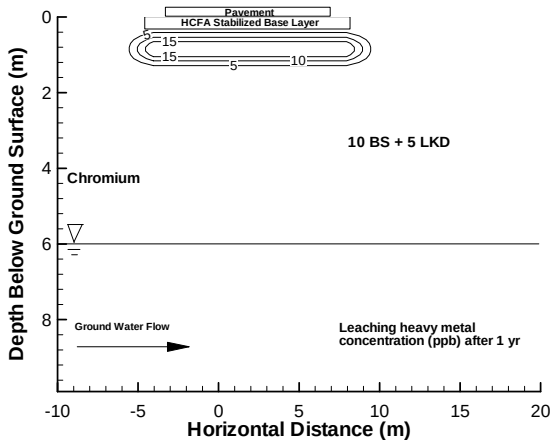
Pavement
HCFA Stabilized Base Layer
10 BS + 5 LKD
Chromium
Ground Water Flow
Leaching heavy metal
concentration (ppb) after 1 yr
Depth Below Ground Surface (m)
Horizontal Distance (m)

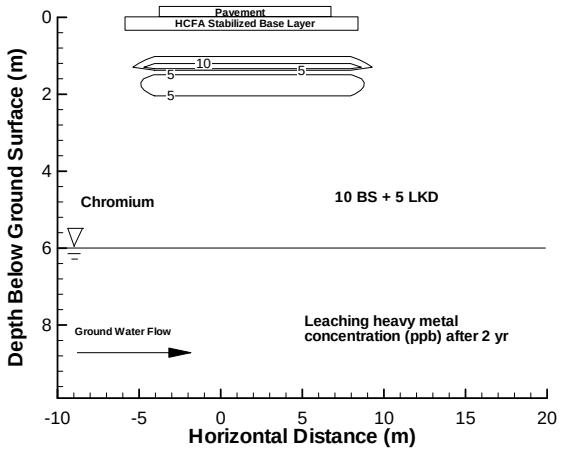
Pavement
HCFA Stabilized Base Layer
Chromium
10 BS + 5 LKD
Ground Water Flow
Leaching heavy metal
concentration (ppb) after 2 yr
Depth Below Ground Surface (m)
Horizontal Distance (m)

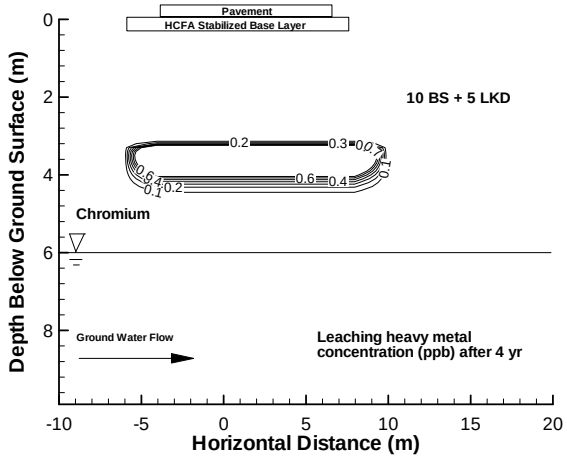
Pavement
HCFA Stabilized Base Layer
10 BS + 5 LKD
Chromium
Ground Water Flow
Leaching heavy metal
concentration (ppb) after 4 yr
Depth Below Ground Surface (m)
Horizontal Distance (m)

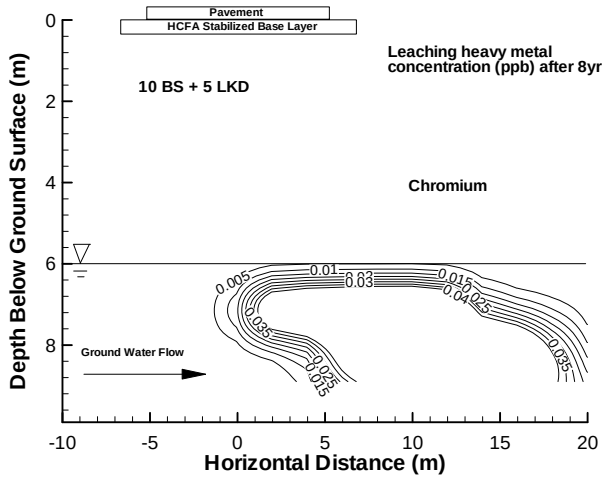
Pavement
HCFA Stabilized Base Layer
Leaching heavy metal
concentration (ppb) after 8yr
10 BS + 5 LKD
Chromium
Ground Water Flow
Depth Below Ground Surface (m)
Horizontal Distance (m)

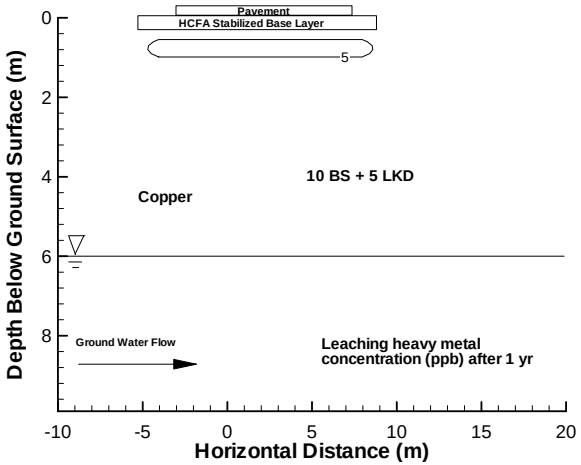
Pavement
HCFA Stabilized Base Layer
5
10 BS + 5 LKD
Copper
Ground Water Flow
Leaching heavy metal
concentration (ppb) after 1 yr
Depth Below Ground Surface (m)
Horizontal Distance (m)

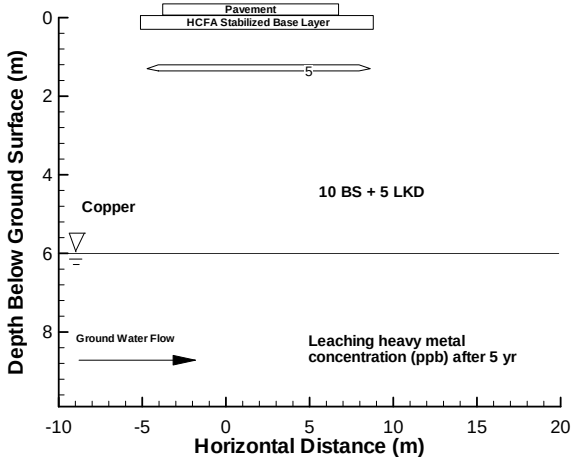
Pavement
HCFA Stabilized Base Layer
5
10 BS + 5 LKD
Copper
Ground Water Flow
Leaching heavy metal
concentration (ppb) after 5 yr
Depth Below Ground Surface (m)
Horizontal Distance (m)

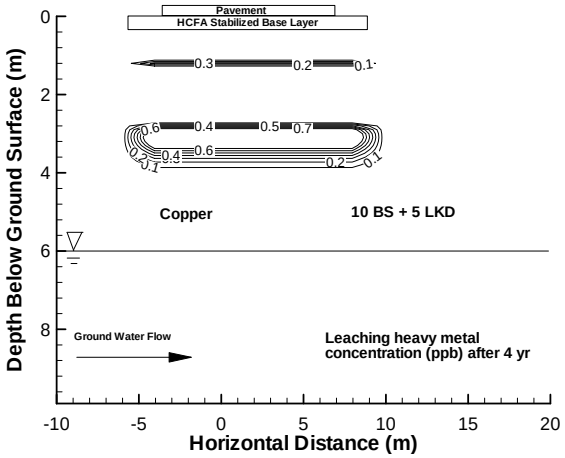
Pavement
HCFA Stabilized Base Layer
0.3
0.2
0.1
0.6
0.4
0.5
0.7
0.4
0.6
0.3
0.2
0.1
0.1
Copper
10 BS + 5 LKD
Ground Water Flow
Leaching heavy metal
concentration (ppb) after 4 yr
Depth Below Ground Surface (m)
Horizontal Distance (m)

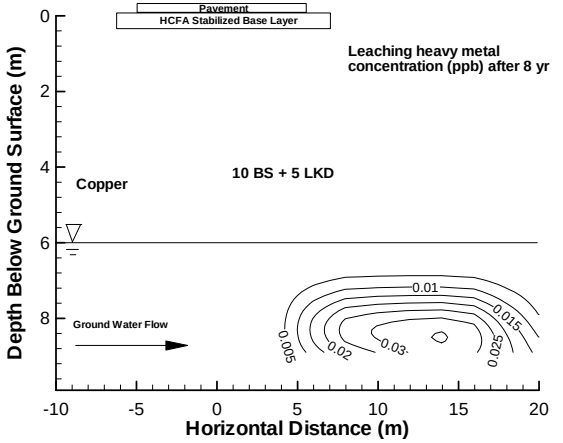
Pavement
HCFA Stabilized Base Layer
Leaching heavy metal
concentration (ppb) after 8 yr
Copper
10 BS + 5 LKD
Ground Water Flow
0.01
0.015
0.005
0.02
0.03
0.025
Depth Below Ground Surface (m)
Horizontal Distance (m)

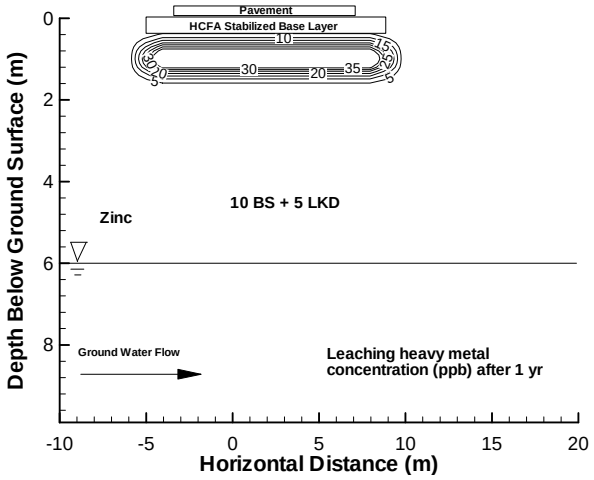
Pavement
HCFA Stabilized Base Layer
10 BS + 5 LKD
Zinc
Ground Water Flow
Leaching heavy metal
concentration (ppb) after 1 yr
Depth Below Ground Surface (m)
Horizontal Distance (m)

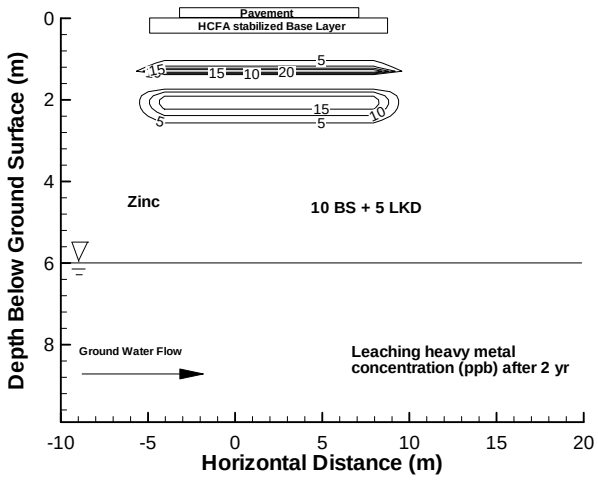
Pavement
HCFA stabilized Base Layer
Zinc
10 BS + 5 LKD
Ground Water Flow
Leaching heavy metal
concentration (ppb) after 2 yr
Depth Below Ground Surface (m)
Horizontal Distance (m)

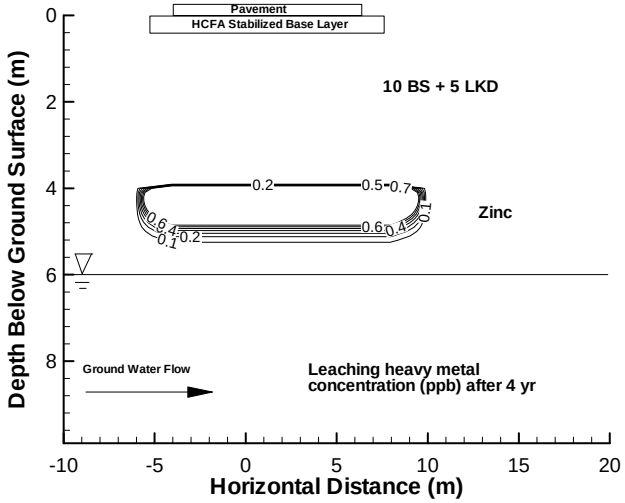
Pavement
HCFA Stabilized Base Layer
10 BS + 5 LKD
Zinc
Ground Water Flow
Leaching heavy metal
concentration (ppb) after 4 yr
Depth Below Ground Surface (m)
Horizontal Distance (m)

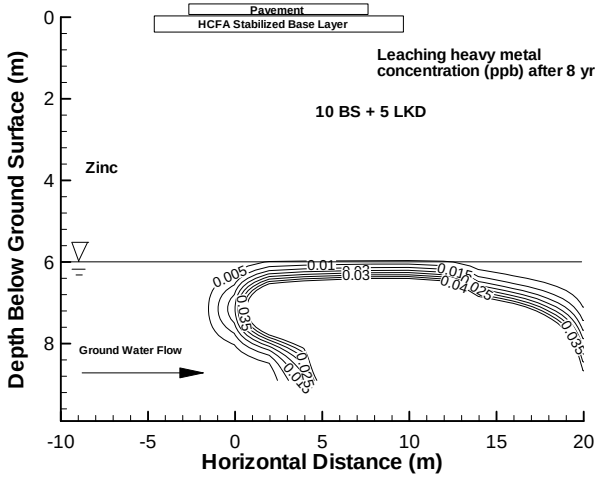
Pavement
HCFA Stabilized Base Layer
Leaching heavy metal
concentration (ppb) after 8 yr
10 BS + 5 LKD
Zinc
Ground Water Flow
Depth Below Ground Surface (m)
Horizontal Distance (m)

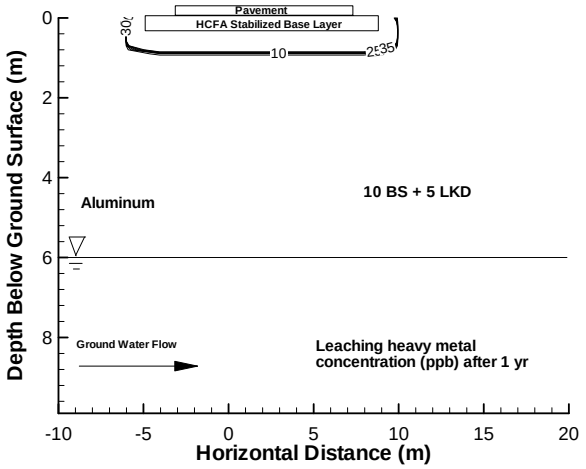
Pavement
HCFA Stabilized Base Layer
30
10
25
35
Aluminum
10 BS + 5 LKD
Ground Water Flow
Leaching heavy metal
concentration (ppb) after 1 yr
Depth Below Ground Surface (m)
Horizontal Distance (m)

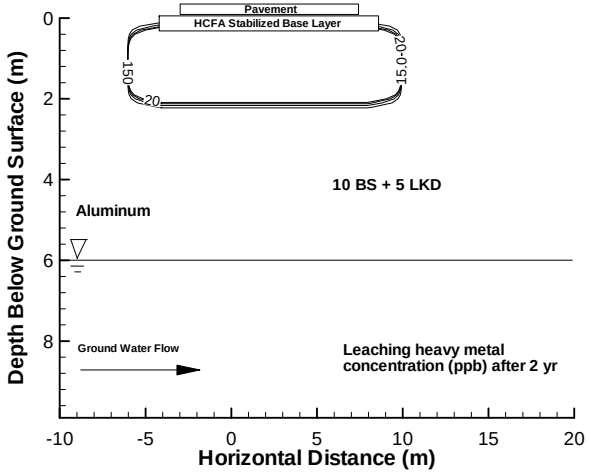
Pavement
HCFA Stabilized Base Layer
15
20
15
Aluminum
10 BS + 5 LKD
Ground Water Flow
Leaching heavy metal
concentration (ppb) after 2 yr
Depth Below Ground Surface (m)
Horizontal Distance (m)

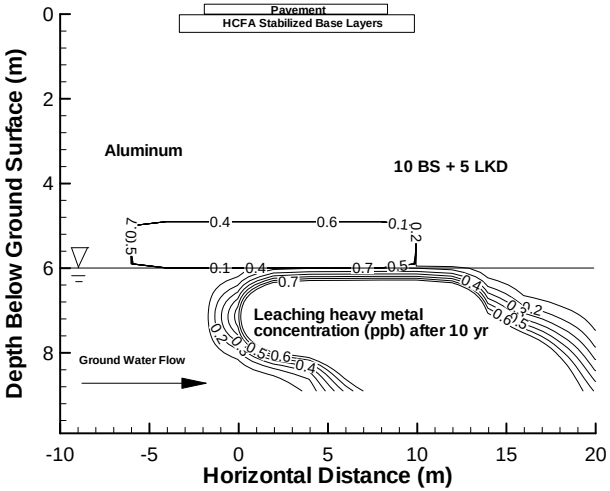
Pavement
HCFA Stabilized Base Layers
Aluminum
10 BS + 5 LKD
0.4
0.6
0.1
0.2
0.5
0.1
0.4
0.7
0.5
0.7
0.4
0.2
0.5
0.2
0.5
0.6
0.4
Leaching heavy metal
concentration (ppb) after 10 yr
Ground Water Flow
Depth Below Ground Surface (m)
Horizontal Distance (m)

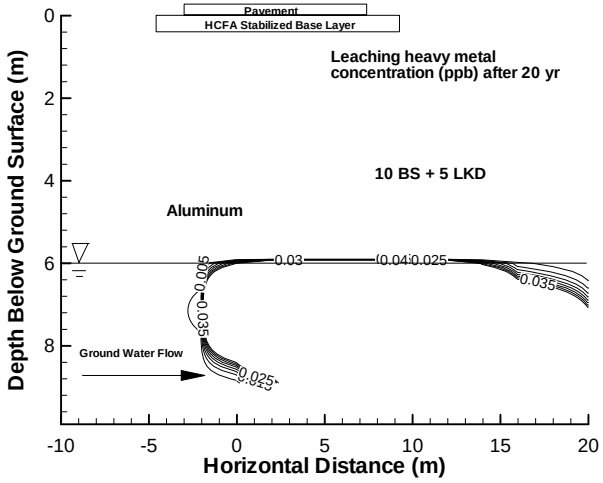
Pavement
HCFA Stabilized Base Layer
Leaching heavy metal
concentration (ppb) after 20 yr
10 BS + 5 LKD
Aluminum
0.03
0.04
0.025
0.035
0.035
0.025
Ground Water Flow
Depth Below Ground Surface (m)
Horizontal Distance (m)

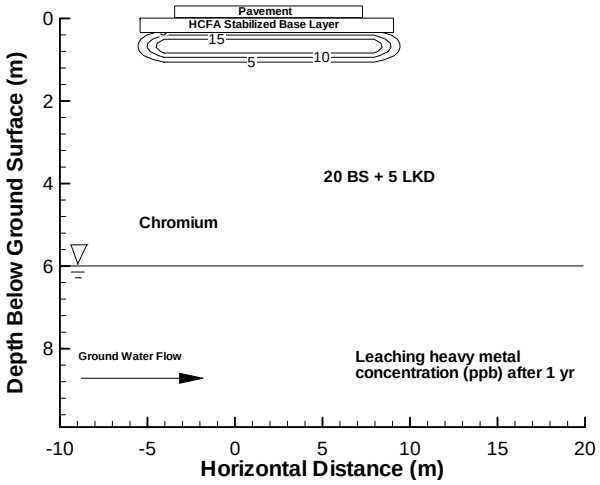
Pavement
HCFA Stabilized Base Layer
15
5
10
20 BS + 5 LKD
Chromium
Ground Water Flow
Leaching heavy metal
concentration (ppb) after 1 yr
Depth Below Ground Surface (m)
Horizontal Distance (m)

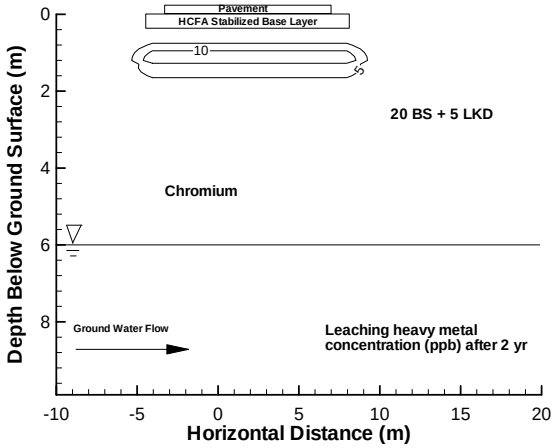
Pavement
HCFA Stabilized Base Layer
10
5
20 BS + 5 LKD
Chromium
Ground Water Flow
Leaching heavy metal
concentration (ppb) after 2 yr
Depth Below Ground Surface (m)
Horizontal Distance (m)

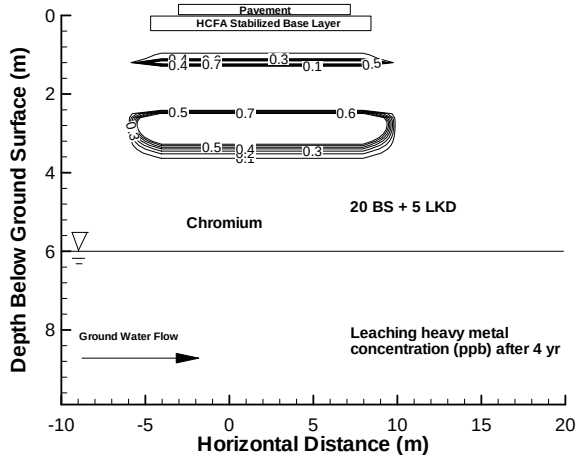
Pavement
HCFA Stabilized Base Layer
0.4
0.7
0.3
0.1
0.5
0.6
0.4
20 BS + 5 LKD
Chromium
Ground Water Flow
Leaching heavy metal
concentration (ppb) after 4 yr
Depth Below Ground Surface (m)
Horizontal Distance (m)

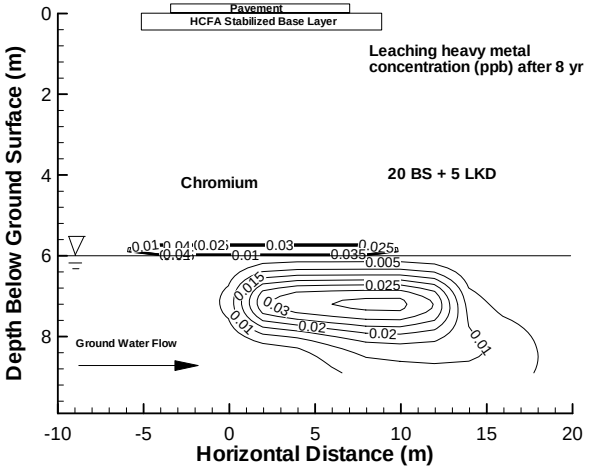
Pavement
HCFA Stabilized Base Layer
Leaching heavy metal
concentration (ppb) after 8 yr
Chromium
20 BS + 5 LKD
0.03
0.025
0.035
0.005
0.015
0.02
0.01
Ground Water Flow
Depth Below Ground Surface (m)
Horizontal Distance (m)

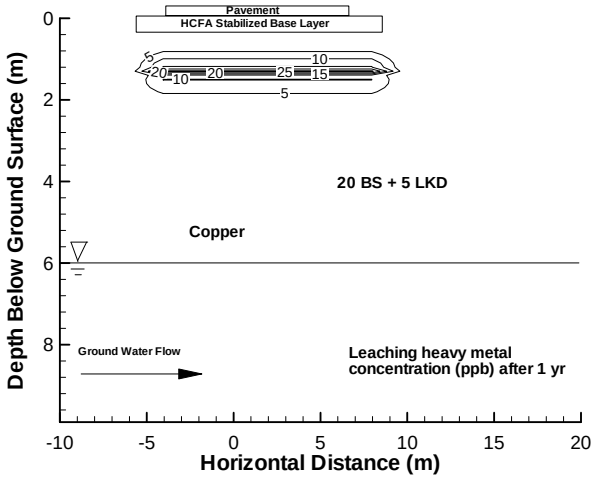
Pavement
HCFA Stabilized Base Layer
Depth Below Ground Surface (m)
Horizontal Distance (m)
20 BS + 5 LKD
Copper
Ground Water Flow
Leaching heavy metal
concentration (ppb) after 1 yr

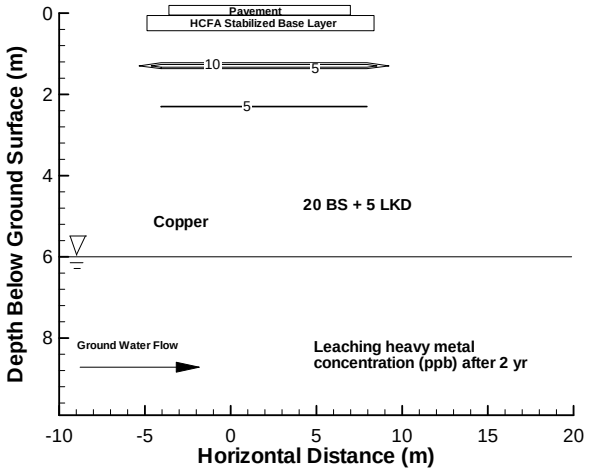
Pavement
HCFA Stabilized Base Layer
Depth Below Ground Surface (m)
Horizontal Distance (m)
20 BS + 5 LKD
Copper
Ground Water Flow
Leaching heavy metal
concentration (ppb) after 2 yr

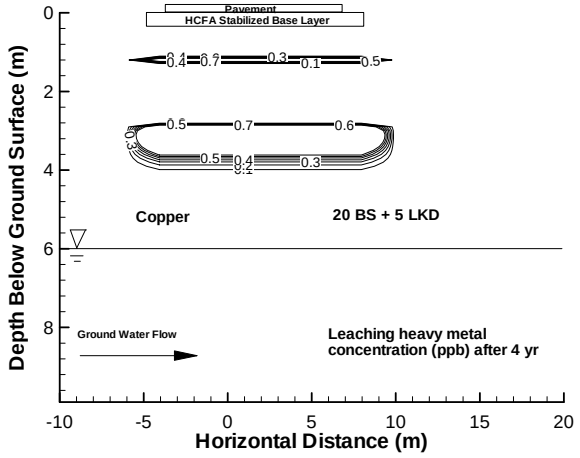
Pavement
HCFA Stabilized Base Layer
Depth Below Ground Surface (m)
Horizontal Distance (m)
20 BS + 5 LKD
Copper
Ground Water Flow
Leaching heavy metal
concentration (ppb) after 4 yr

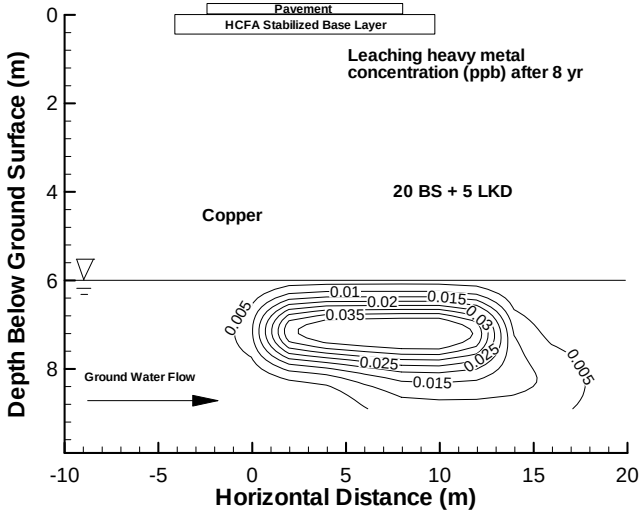
Pavement
HCFA Stabilized Base Layer
Depth Below Ground Surface (m)
Horizontal Distance (m)
Leaching heavy metal
concentration (ppb) after 8 yr
20 BS + 5 LKD
Copper
Ground Water Flow

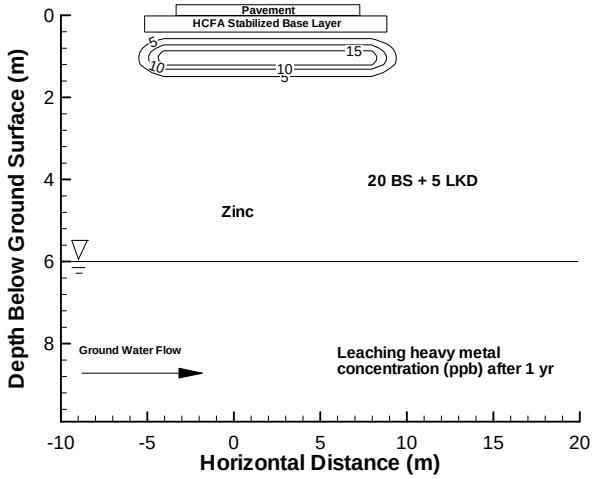
Pavement
HCFA Stabilized Base Layer
5
10
15
10
5
20 BS + 5 LKD
Zinc
Ground Water Flow
Leaching heavy metal
concentration (ppb) after 1 yr
Depth Below Ground Surface (m)
Horizontal Distance (m)

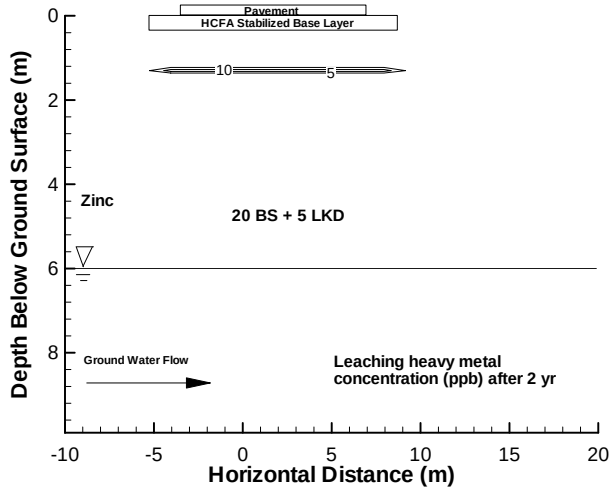
Pavement
HCFA Stabilized Base Layer
10
5
Zinc
20 BS + 5 LKD
Ground Water Flow
Leaching heavy metal
concentration (ppb) after 2 yr
Depth Below Ground Surface (m)
Horizontal Distance (m)

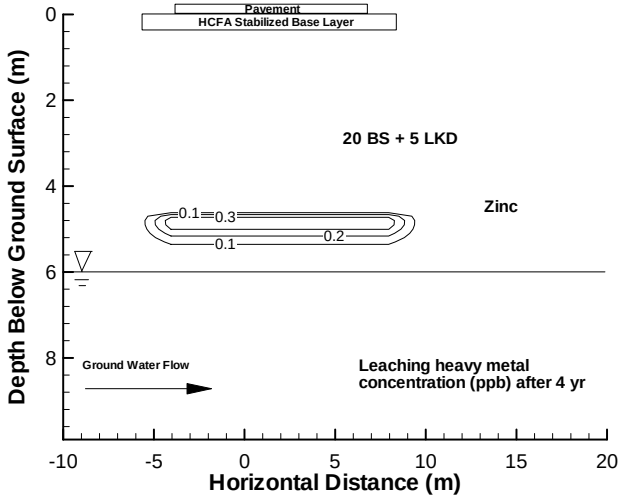
Pavement
HCFA Stabilized Base Layer
20 BS + 5 LKD
Zinc
0.1
0.3
0.2
0.1
Ground Water Flow
Leaching heavy metal
concentration (ppb) after 4 yr
Depth Below Ground Surface (m)
Horizontal Distance (m)

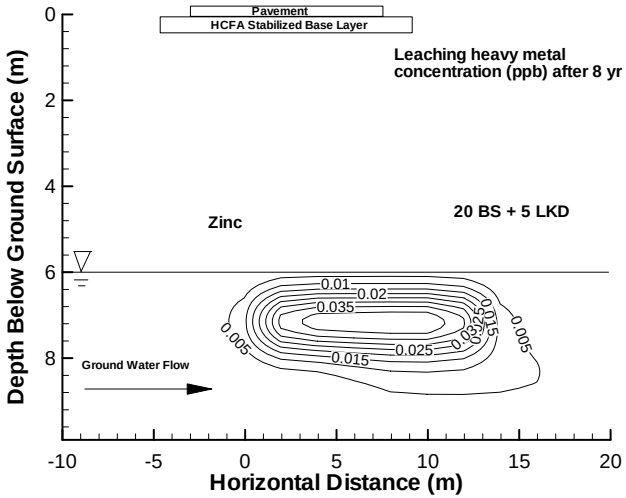
Pavement
HCFA Stabilized Base Layer
Leaching heavy metal
concentration (ppb) after 8 yr
Zinc
20 BS + 5 LKD
0.01
0.02
0.035
0.025
0.015
0.005
Ground Water Flow
Depth Below Ground Surface (m)
Horizontal Distance (m)

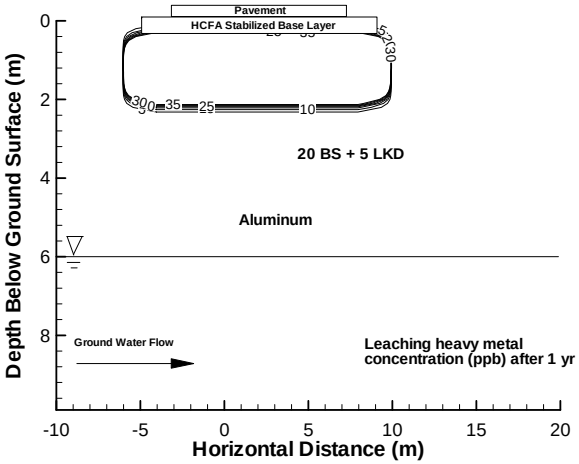
Pavement
HCFA Stabilized Base Layer
20 BS + 5 LKD
Aluminum
Ground Water Flow
Leaching heavy metal
concentration (ppb) after 1 yr
Depth Below Ground Surface (m)
Horizontal Distance (m)

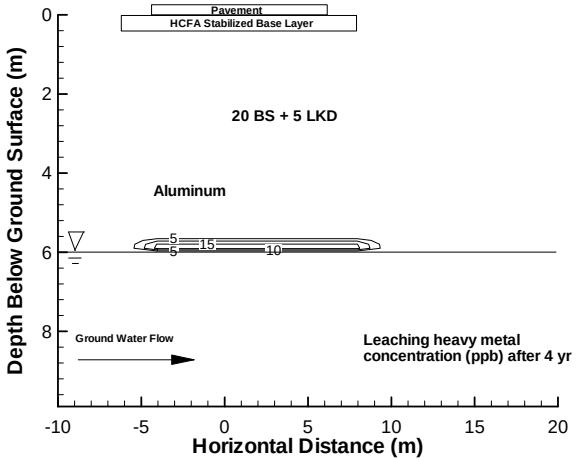
Pavement
HCFA Stabilized Base Layer
20 BS + 5 LKD
Aluminum
Ground Water Flow
Leaching heavy metal
concentration (ppb) after 4 yr
Depth Below Ground Surface (m)
Horizontal Distance (m)

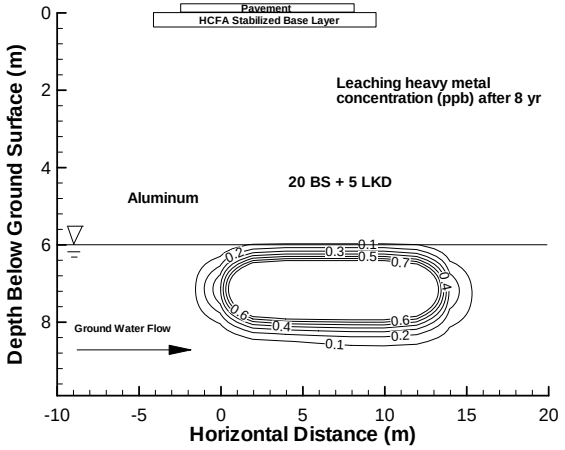
Pavement
HCFA Stabilized Base Layer
Leaching heavy metal
concentration (ppb) after 8 yr
20 BS + 5 LKD
Aluminum
Ground Water Flow
Depth Below Ground Surface (m)
Horizontal Distance (m)

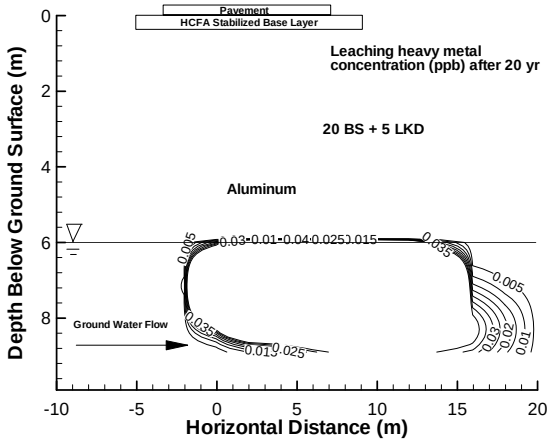
Pavement
HCFA Stabilized Base Layer
Leaching heavy metal
concentration (ppb) after 20 yr
20 BS + 5 LKD
Aluminum
Ground Water Flow
Depth Below Ground Surface (m)
Horizontal Distance (m)

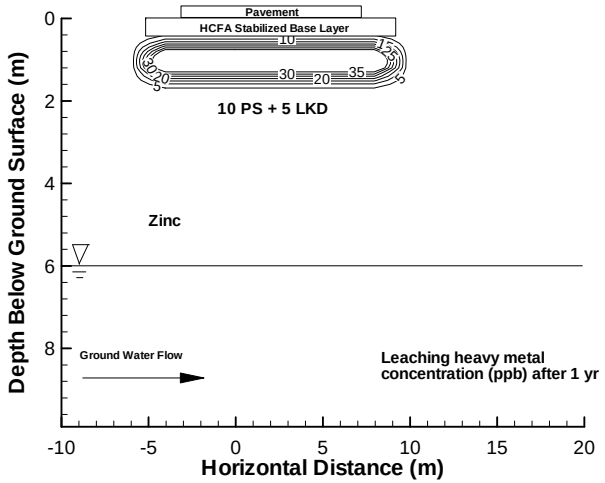
Pavement
HCFA Stabilized Base Layer
10
15
5
20
30
35
10 PS + 5 LKD
Zinc
Ground Water Flow
Leaching heavy metal
concentration (ppb) after 1 yr
Depth Below Ground Surface (m)
Horizontal Distance (m)

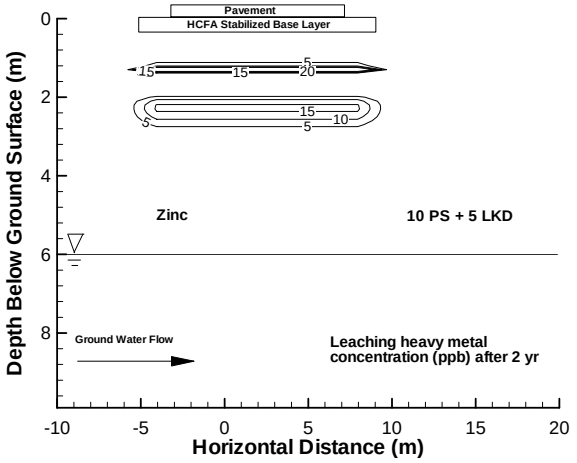
Pavement
HCFA Stabilized Base Layer
15
5
20
10
Zinc
10 PS + 5 LKD
Ground Water Flow
Leaching heavy metal
concentration (ppb) after 2 yr
Depth Below Ground Surface (m)
Horizontal Distance (m)

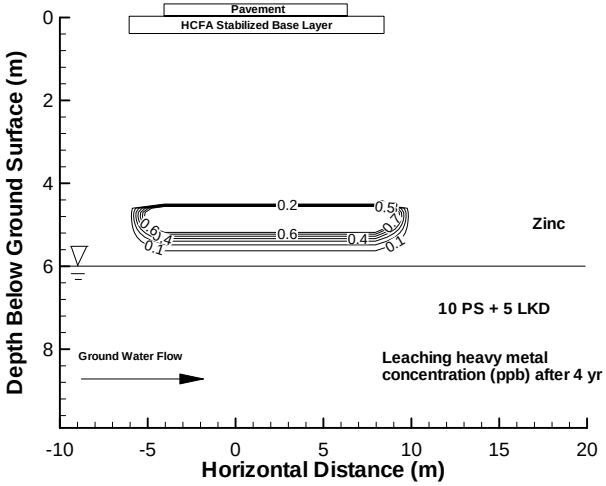
Pavement
HCFA Stabilized Base Layer
0.2
0.5
0.4
0.6
0.1
Zinc
10 PS + 5 LKD
Ground Water Flow
Leaching heavy metal
concentration (ppb) after 4 yr
Depth Below Ground Surface (m)
Horizontal Distance (m)

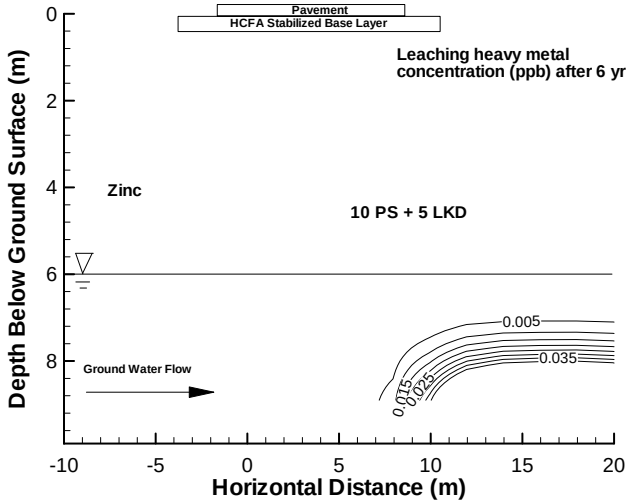
Pavement
HCFA Stabilized Base Layer
Leaching heavy metal
concentration (ppb) after 6 yr
Zinc
10 PS + 5 LKD
0.005
0.035
0.015
0.025
Ground Water Flow
Depth Below Ground Surface (m)
Horizontal Distance (m)

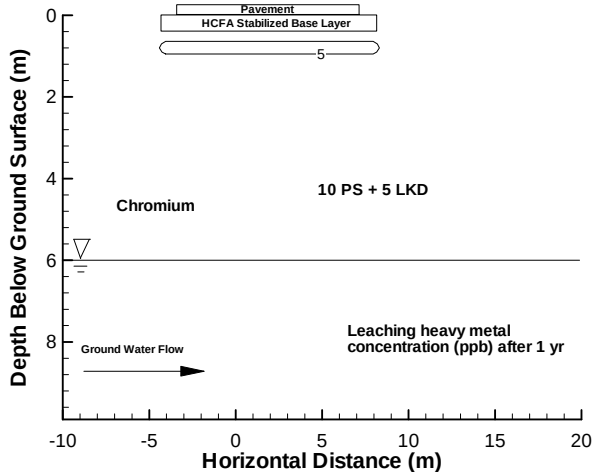
Pavement
HCFA Stabilized Base Layer
5
10 PS + 5 LKD
Chromium
Leaching heavy metal
concentration (ppb) after 1 yr
Ground Water Flow
Depth Below Ground Surface (m)
Horizontal Distance (m)

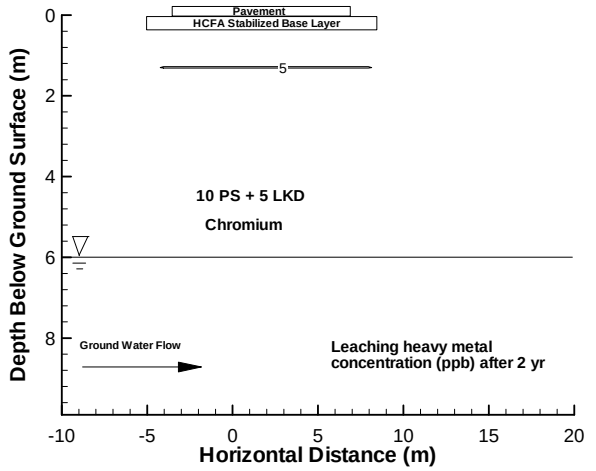
Pavement
HCFA Stabilized Base Layer
5
10 PS + 5 LKD
Chromium
Leaching heavy metal
concentration (ppb) after 2 yr
Ground Water Flow
Depth Below Ground Surface (m)
Horizontal Distance (m)

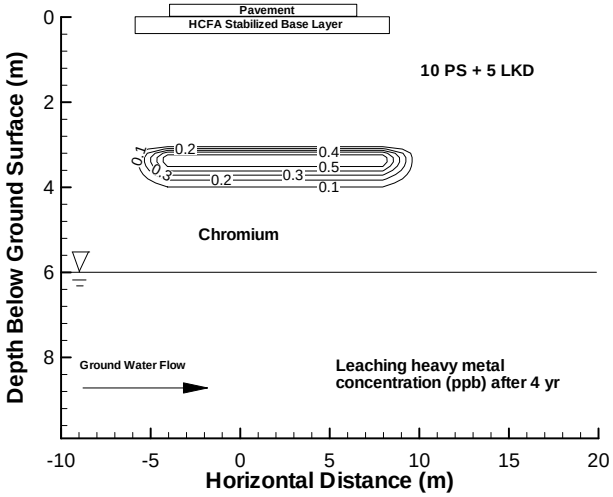
Pavement
HCFA Stabilized Base Layer
10 PS + 5 LKD
0.1
0.2
0.4
0.5
0.3
0.2
0.3
0.1
Chromium
Leaching heavy metal
concentration (ppb) after 4 yr
Ground Water Flow
Depth Below Ground Surface (m)
Horizontal Distance (m)

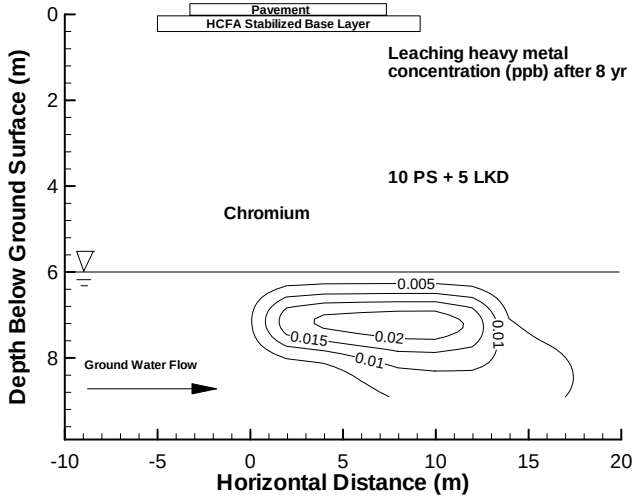
Pavement
HCFA Stabilized Base Layer
Leaching heavy metal
concentration (ppb) after 8 yr
10 PS + 5 LKD
Chromium
0.005
0.01
0.015
0.02
0.01
Ground Water Flow
Depth Below Ground Surface (m)
Horizontal Distance (m)

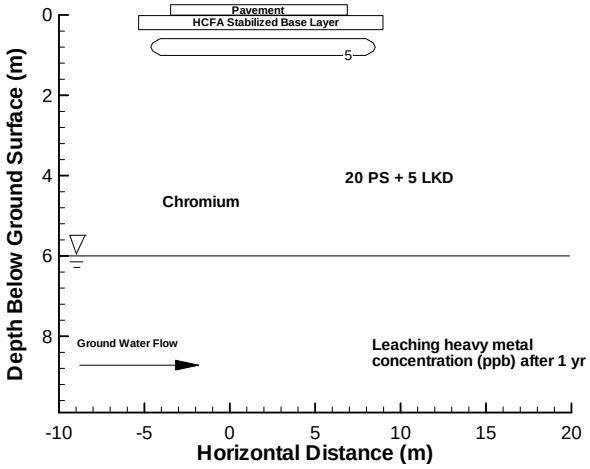
Pavement
HCFA Stabilized Base Layer
5
20 PS + 5 LKD
Chromium
Ground Water Flow
Leaching heavy metal
concentration (ppb) after 1 yr
Depth Below Ground Surface (m)
Horizontal Distance (m)

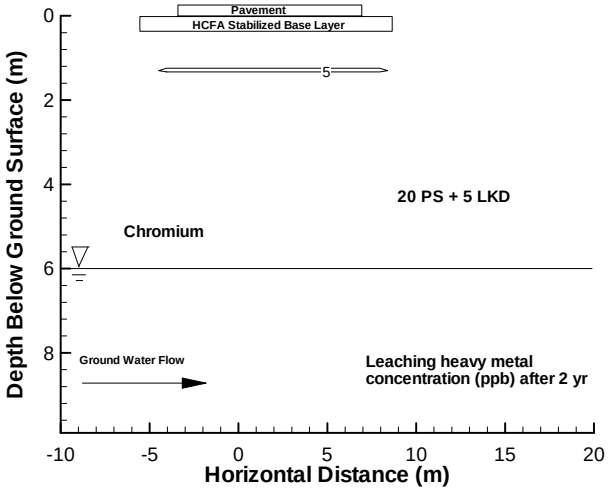
Pavement
HCFA Stabilized Base Layer
5
20 PS + 5 LKD
Chromium
Ground Water Flow
Leaching heavy metal
concentration (ppb) after 2 yr
Depth Below Ground Surface (m)
Horizontal Distance (m)

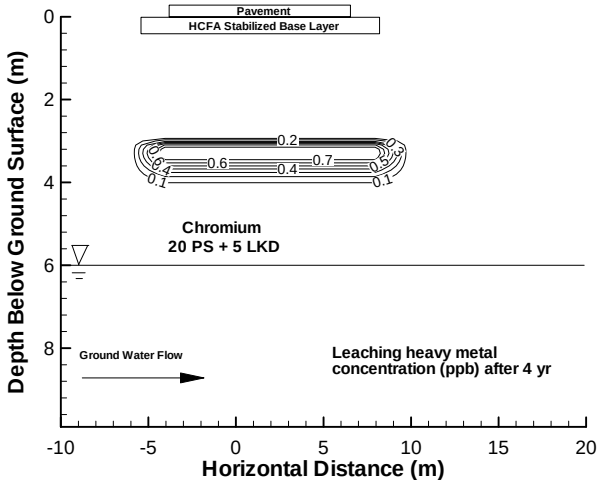
Pavement
HCFA Stabilized Base Layer
0.2
0.6
0.7
0.4
0.1
Chromium
20 PS + 5 LKD
Ground Water Flow
Leaching heavy metal
concentration (ppb) after 4 yr
Depth Below Ground Surface (m)
Horizontal Distance (m)

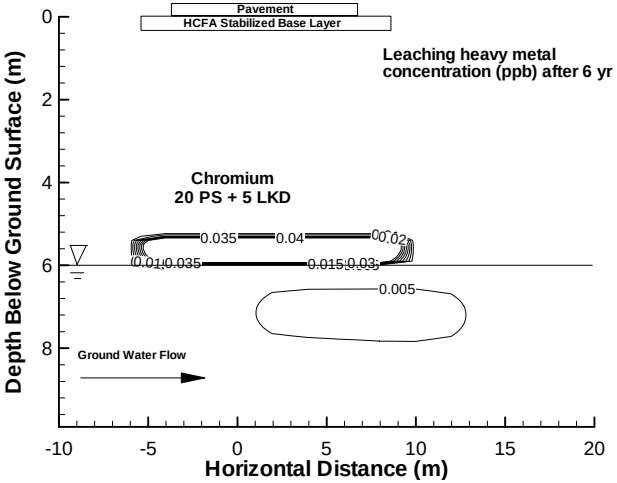
Pavement
HCFA Stabilized Base Layer
Leaching heavy metal
concentration (ppb) after 6 yr
Chromium
20 PS + 5 LKD
0.035
0.04
0.02
0.01
0.035
0.015
0.03
0.005
Ground Water Flow
Depth Below Ground Surface (m)
Horizontal Distance (m)

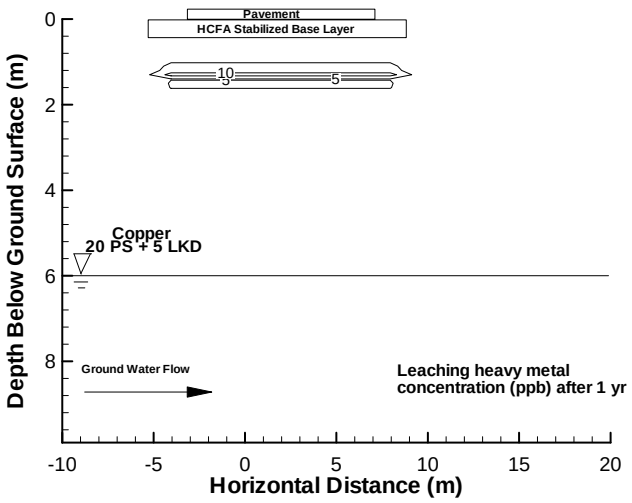
Pavement
HCFA Stabilized Base Layer
10
5
Copper
20 PS + 5 LKD
Ground Water Flow
Leaching heavy metal
concentration (ppb) after 1 yr
Depth Below Ground Surface (m)
Horizontal Distance (m)

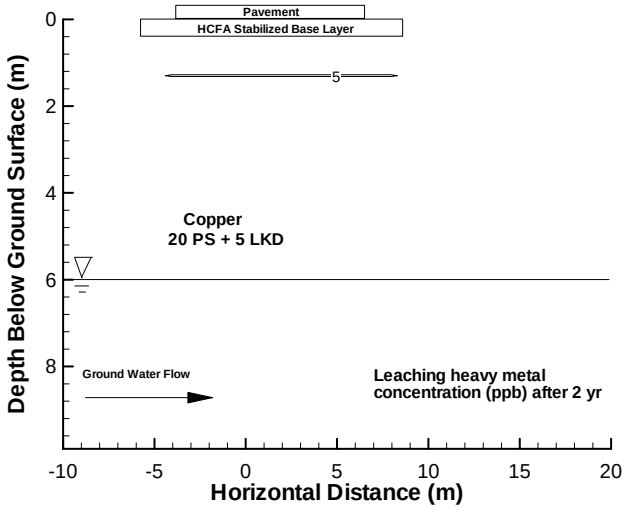
Pavement
HCFA Stabilized Base Layer
5
Copper
20 PS + 5 LKD
Ground Water Flow
Leaching heavy metal
concentration (ppb) after 2 yr
Depth Below Ground Surface (m)
Horizontal Distance (m)

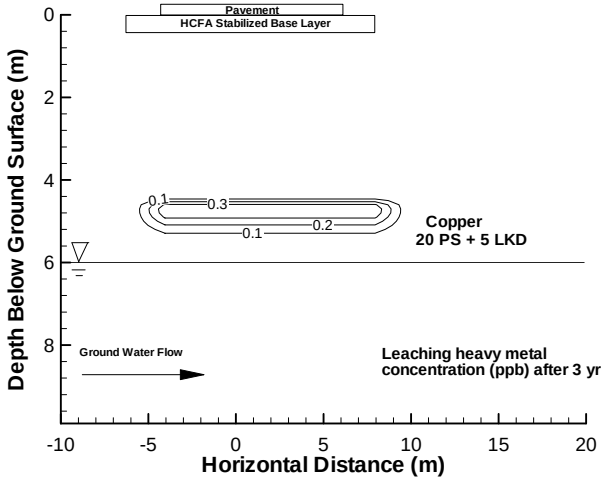
Pavement
HCFA Stabilized Base Layer
0.1
0.3
0.1
0.2
Copper
20 PS + 5 LKD
Ground Water Flow
Leaching heavy metal
concentration (ppb) after 3 yr
Depth Below Ground Surface (m)
Horizontal Distance (m)

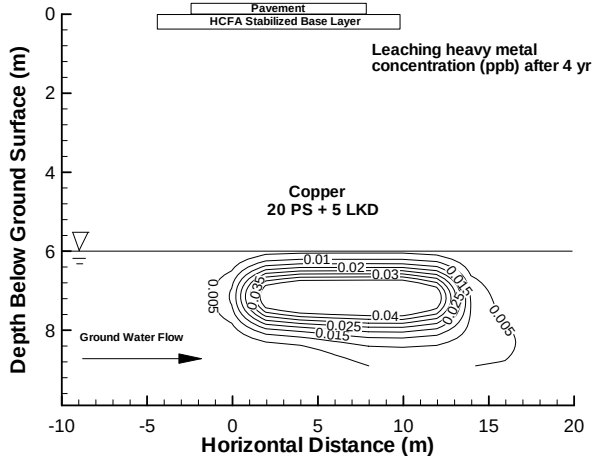
Pavement
HCFA Stabilized Base Layer
Leaching heavy metal
concentration (ppb) after 4 yr
Copper
20 PS + 5 LKD
0.01
0.02
0.03
0.04
0.025
0.015
0.005
Ground Water Flow
Depth Below Ground Surface (m)
Horizontal Distance (m)

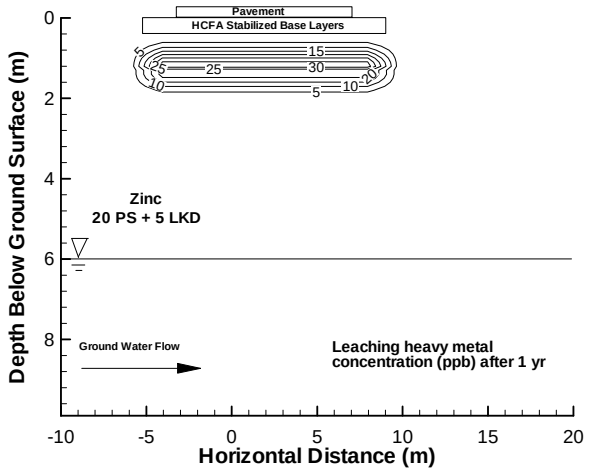
Pavement
HCFA Stabilized Base Layers
Zinc
20 PS + 5 LKD
Ground Water Flow
Leaching heavy metal
concentration (ppb) after 1 yr
Depth Below Ground Surface (m)
Horizontal Distance (m)

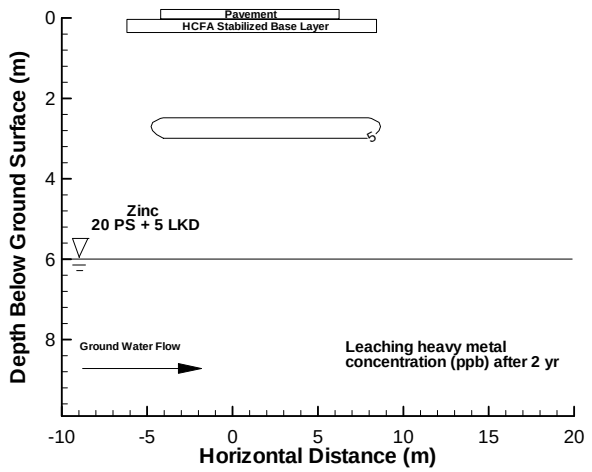
Pavement
HCFA Stabilized Base Layer
Zinc
20 PS + 5 LKD
Ground Water Flow
Leaching heavy metal
concentration (ppb) after 2 yr
Depth Below Ground Surface (m)
Horizontal Distance (m)

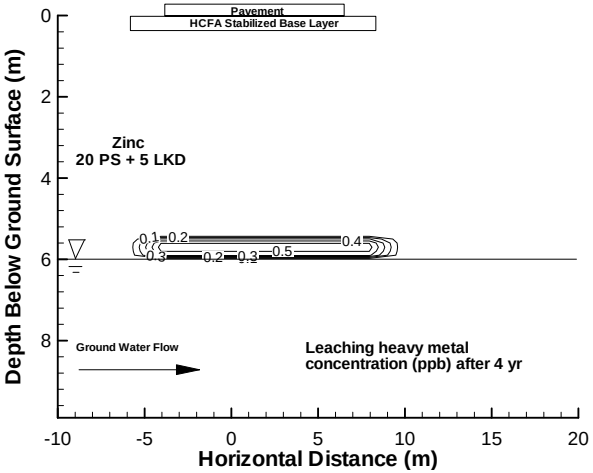
Pavement
HCFA Stabilized Base Layer
Zinc
20 PS + 5 LKD
Ground Water Flow
Leaching heavy metal
concentration (ppb) after 4 yr
Depth Below Ground Surface (m)
Horizontal Distance (m)

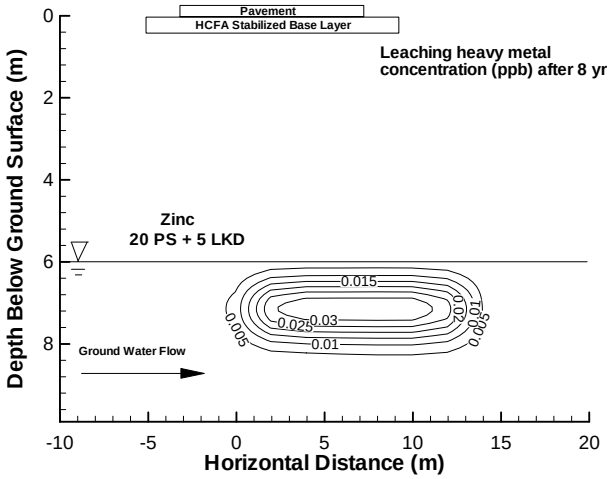
Pavement
HCFA Stabilized Base Layer
Leaching heavy metal
concentration (ppb) after 8 yr
Zinc
20 PS + 5 LKD
Ground Water Flow
Depth Below Ground Surface (m)
Horizontal Distance (m)

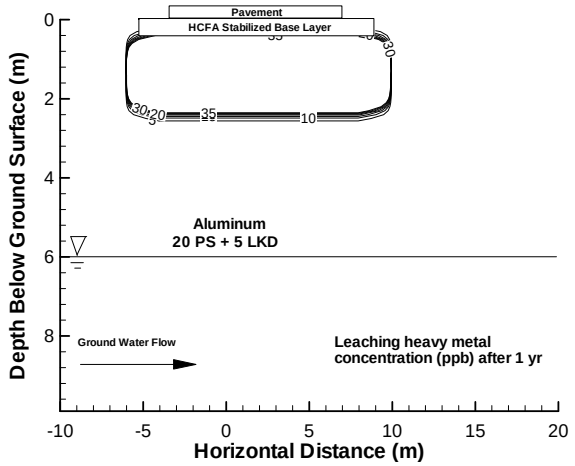
Pavement
HCFA Stabilized Base Layer
Aluminum
20 PS + 5 LKD
Ground Water Flow
Leaching heavy metal
concentration (ppb) after 1 yr
Depth Below Ground Surface (m)
Horizontal Distance (m)

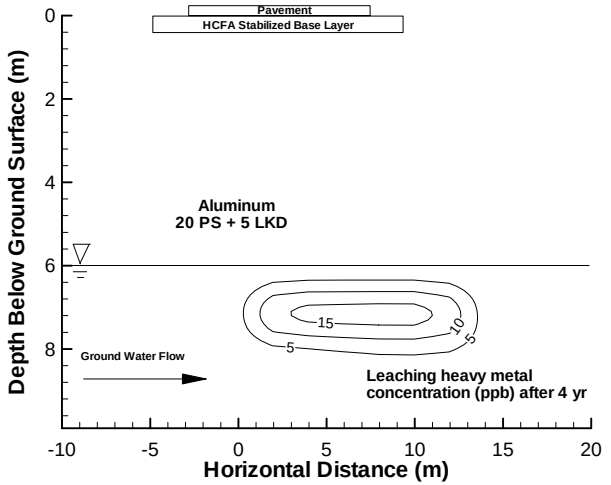
Pavement
HCFA Stabilized Base Layer
Aluminum
20 PS + 5 LKD
Ground Water Flow
Leaching heavy metal
concentration (ppb) after 4 yr
Depth Below Ground Surface (m)
Horizontal Distance (m)

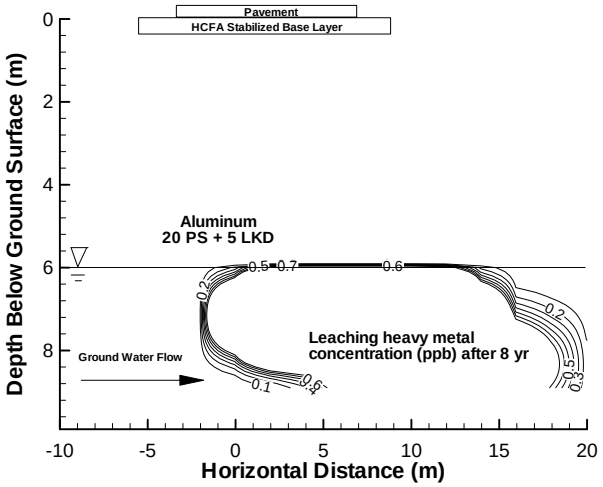
Pavement
HCFA Stabilized Base Layer
Aluminum
20 PS + 5 LKD
Ground Water Flow
Leaching heavy metal
concentration (ppb) after 8 yr
Depth Below Ground Surface (m)
Horizontal Distance (m)

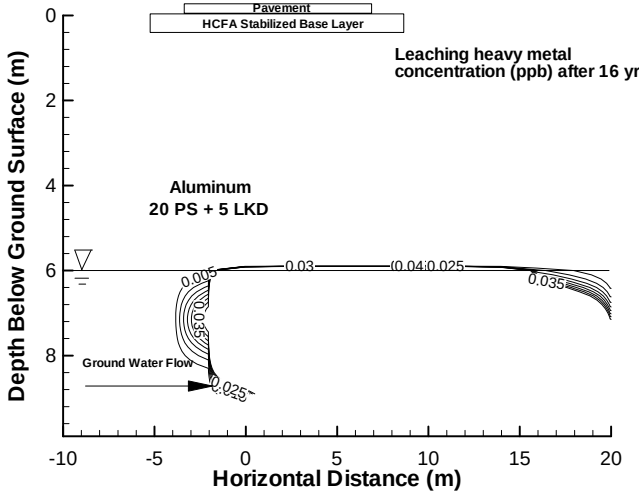
Pavement
HCFA Stabilized Base Layer
Leaching heavy metal
concentration (ppb) after 16 yr
Aluminum
20 PS + 5 LKD
Ground Water Flow
Depth Below Ground Surface (m)
Horizontal Distance (m)

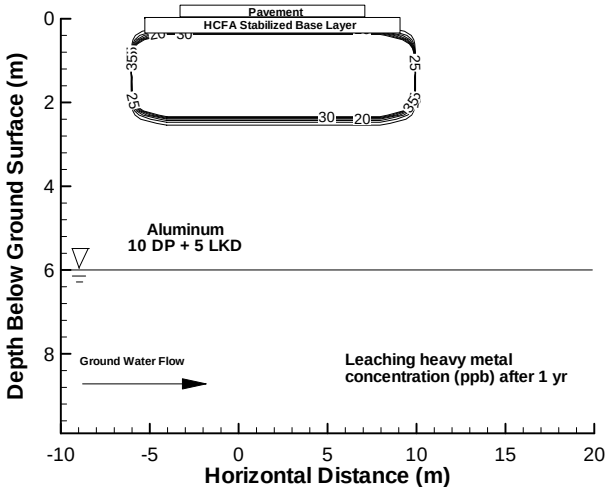
Pavement
HCFA Stabilized Base Layer
Aluminum
10 DP + 5 LKD
Ground Water Flow
Leaching heavy metal
concentration (ppb) after 1 yr
Depth Below Ground Surface (m)
Horizontal Distance (m)

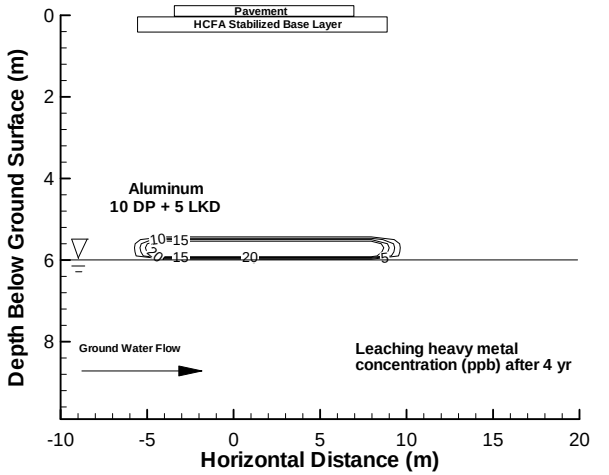
Pavement
HCFA Stabilized Base Layer
Aluminum
10 DP + 5 LKD
Ground Water Flow
Leaching heavy metal
concentration (ppb) after 4 yr
Depth Below Ground Surface (m)
Horizontal Distance (m)

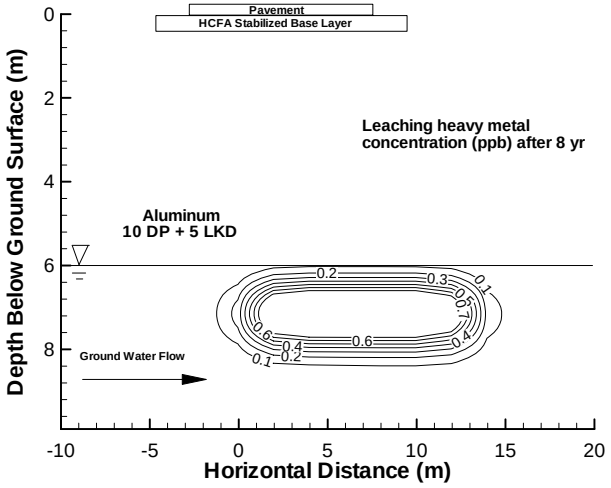
Pavement
HCFA Stabilized Base Layer
Leaching heavy metal
concentration (ppb) after 8 yr
Aluminum
10 DP + 5 LKD
Ground Water Flow
Depth Below Ground Surface (m)
Horizontal Distance (m)

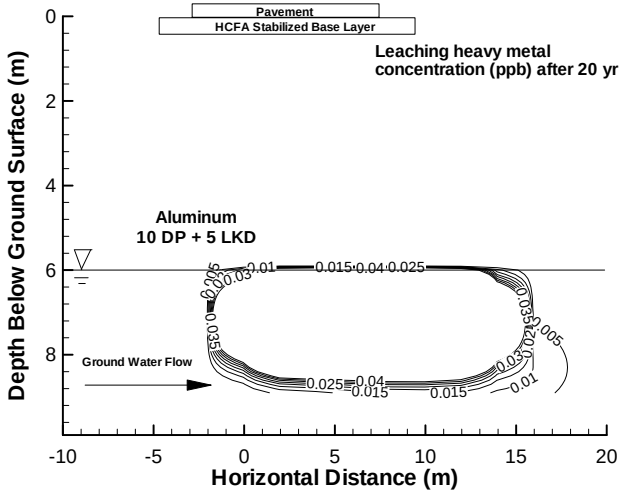
Pavement
HCFA Stabilized Base Layer
Leaching heavy metal
concentration (ppb) after 20 yr
Aluminum
10 DP + 5 LKD
Ground Water Flow
Depth Below Ground Surface (m)
Horizontal Distance (m)

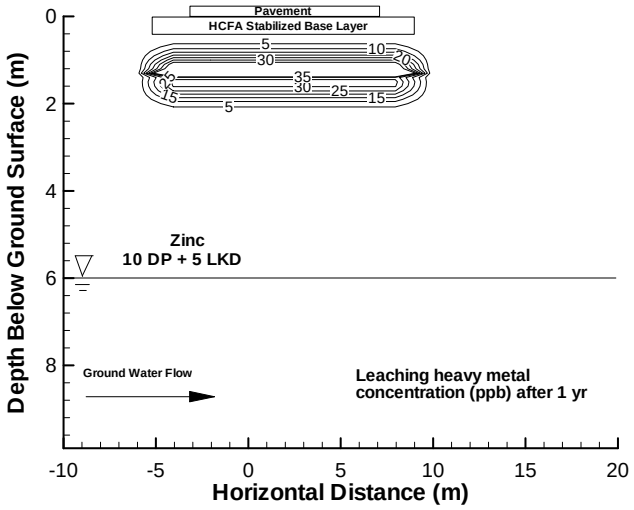
Pavement
HCFA Stabilized Base Layer
Zinc
10 DP + 5 LKD
Ground Water Flow
Leaching heavy metal
concentration (ppb) after 1 yr
Depth Below Ground Surface (m)
Horizontal Distance (m)

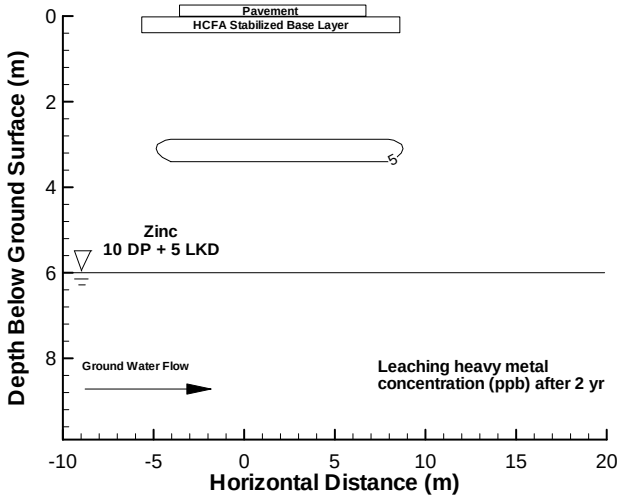
Pavement
HCFA Stabilized Base Layer
Zinc
10 DP + 5 LKD
Ground Water Flow
Leaching heavy metal
concentration (ppb) after 2 yr
Depth Below Ground Surface (m)
Horizontal Distance (m)

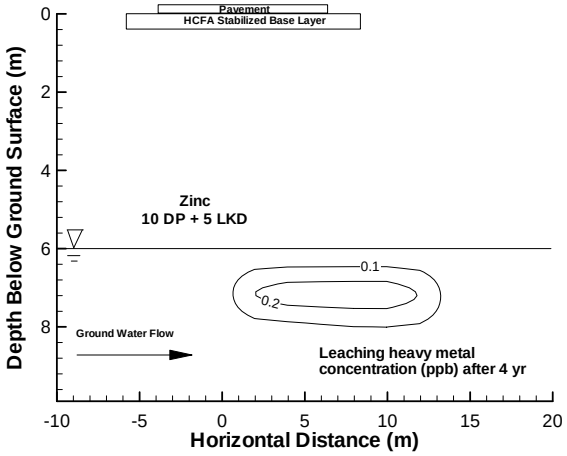
Pavement
HCFA Stabilized Base Layer
Zinc
10 DP + 5 LKD
Ground Water Flow
Leaching heavy metal
concentration (ppb) after 4 yr
Depth Below Ground Surface (m)
Horizontal Distance (m)

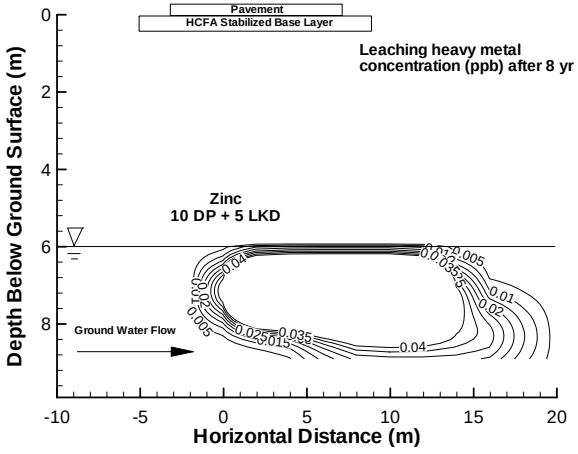
Pavement
HCFA Stabilized Base Layer
Zinc
10 DP + 5 LKD
Ground Water Flow
Leaching heavy metal
concentration (ppb) after 8 yr
Depth Below Ground Surface (m)
Horizontal Distance (m)

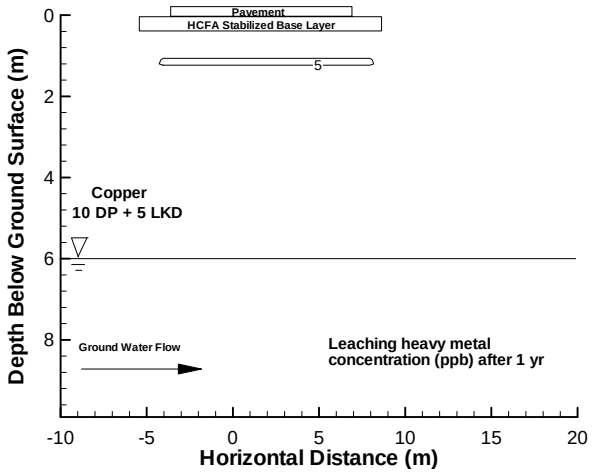
Pavement
HCFA Stabilized Base Layer
5
Copper
10 DP + 5 LKD
Ground Water Flow
Leaching heavy metal
concentration (ppb) after 1 yr
Depth Below Ground Surface (m)
Horizontal Distance (m)
0
2
4
6
8
-10
-5
0
5
10
15
20

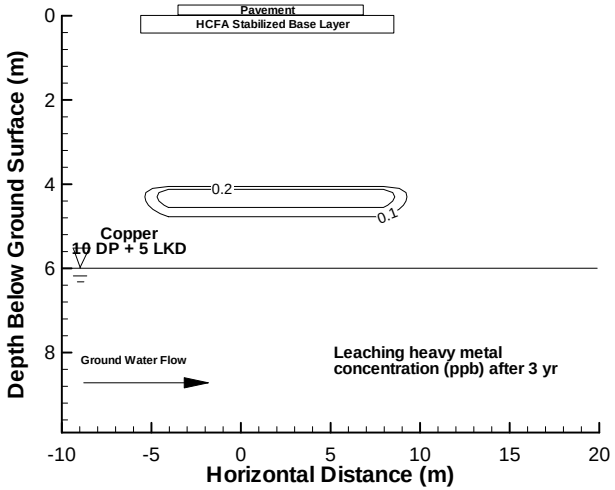
Pavement
HCFA Stabilized Base Layer
0.2
0.1
Copper
10 DP + 5 LKD
Ground Water Flow
Leaching heavy metal
concentration (ppb) after 3 yr
Depth Below Ground Surface (m)
Horizontal Distance (m)
0
2
4
6
8
-10
-5
0
5
10
15
20

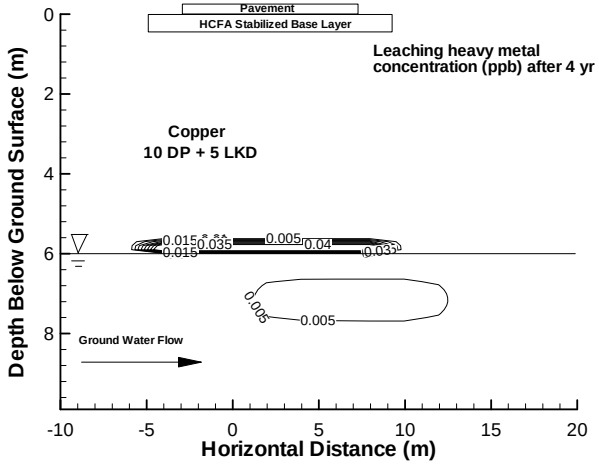
Pavement
HCFA Stabilized Base Layer
Leaching heavy metal
concentration (ppb) after 4 yr
Copper
10 DP + 5 LKD
0.015
0.035
0.005
0.04
0.03
0.015
0.005
0.005
Ground Water Flow
Depth Below Ground Surface (m)
Horizontal Distance (m)
0
2
4
6
8
-10
-5
0
5
10
15
20

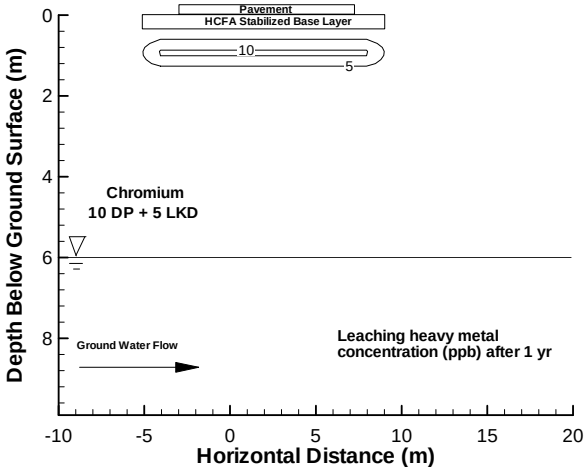
Pavement
HCFA Stabilized Base Layer
10
5
Chromium
10 DP + 5 LKD
Ground Water Flow
Leaching heavy metal
concentration (ppb) after 1 yr
Depth Below Ground Surface (m)
Horizontal Distance (m)

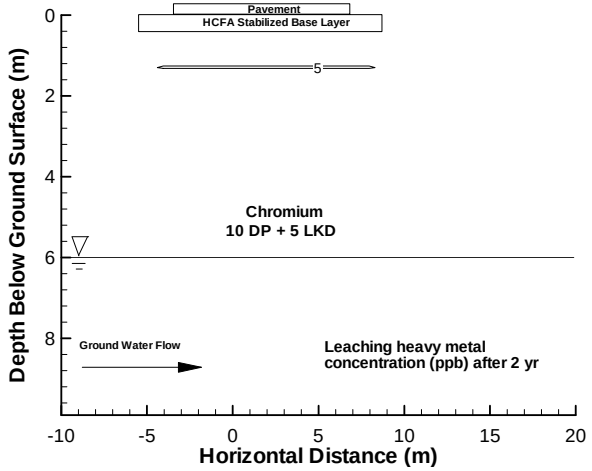
Pavement
HCFA Stabilized Base Layer
5
Chromium
10 DP + 5 LKD
Ground Water Flow
Leaching heavy metal
concentration (ppb) after 2 yr
Depth Below Ground Surface (m)
Horizontal Distance (m)

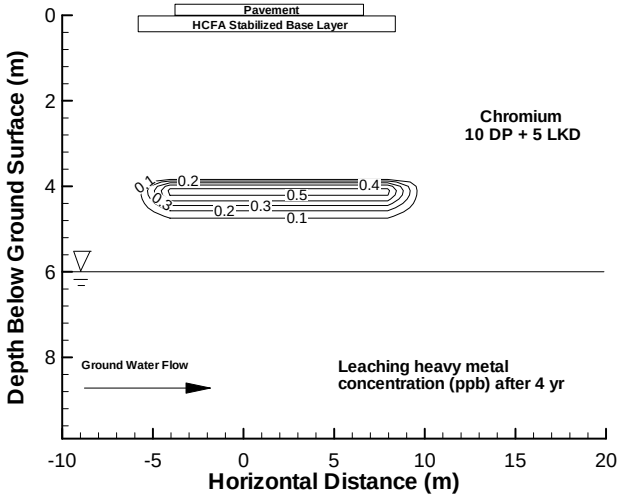
Pavement
HCFA Stabilized Base Layer
Chromium
10 DP + 5 LKD
0.4
0.5
0.2
0.3
0.1
Ground Water Flow
Leaching heavy metal
concentration (ppb) after 4 yr
Depth Below Ground Surface (m)
Horizontal Distance (m)

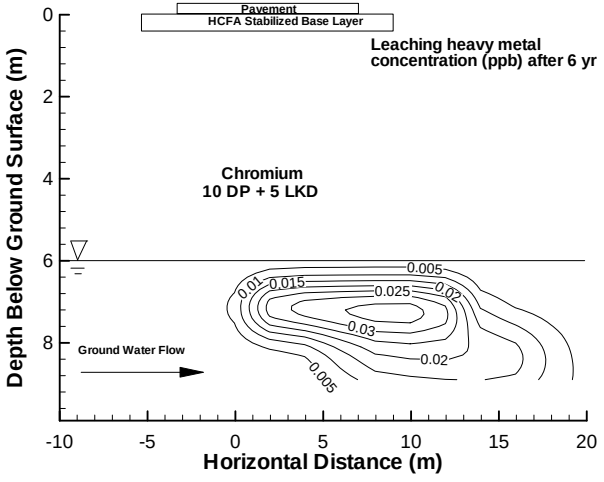
Pavement
HCFA Stabilized Base Layer
Leaching heavy metal
concentration (ppb) after 6 yr
Chromium
10 DP + 5 LKD
0.005
0.01
0.015
0.025
0.02
0.03
0.02
0.005
Ground Water Flow
Depth Below Ground Surface (m)
Horizontal Distance (m)

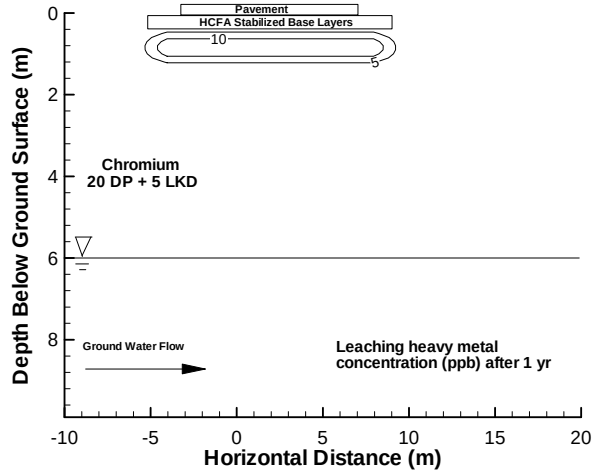
Pavement
HCFA Stabilized Base Layers
10
5
Chromium
20 DP + 5 LKD
Ground Water Flow
Leaching heavy metal
concentration (ppb) after 1 yr
Depth Below Ground Surface (m)
Horizontal Distance (m)

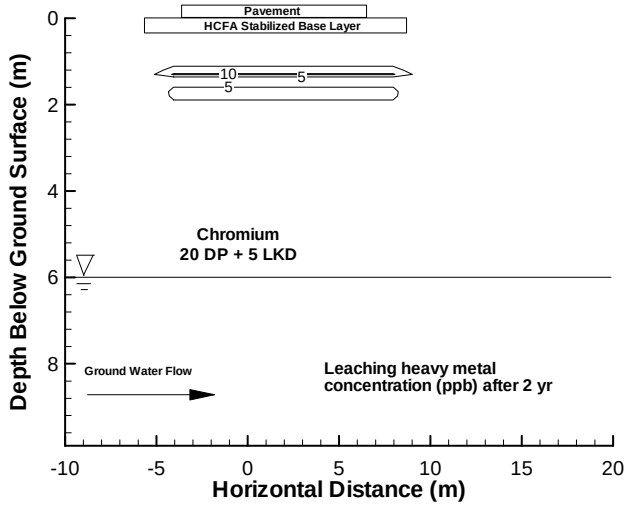
Pavement
HCFA Stabilized Base Layer
10
5
5
Chromium
20 DP + 5 LKD
Ground Water Flow
Leaching heavy metal
concentration (ppb) after 2 yr
Depth Below Ground Surface (m)
Horizontal Distance (m)

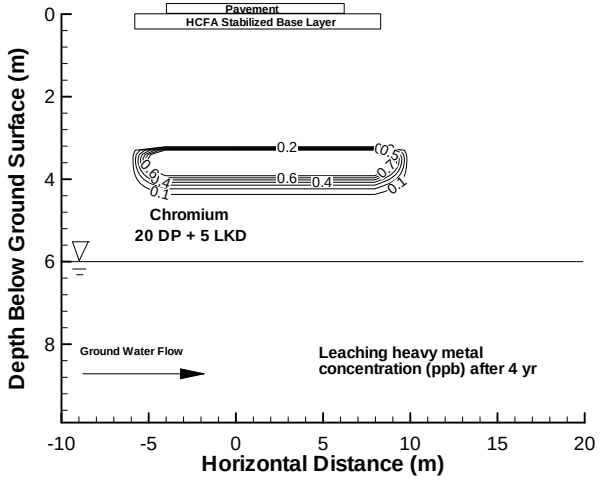
Pavement
HCFA Stabilized Base Layer
0.2
0.6
0.4
Chromium
20 DP + 5 LKD
Ground Water Flow
Leaching heavy metal
concentration (ppb) after 4 yr
Depth Below Ground Surface (m)
Horizontal Distance (m)

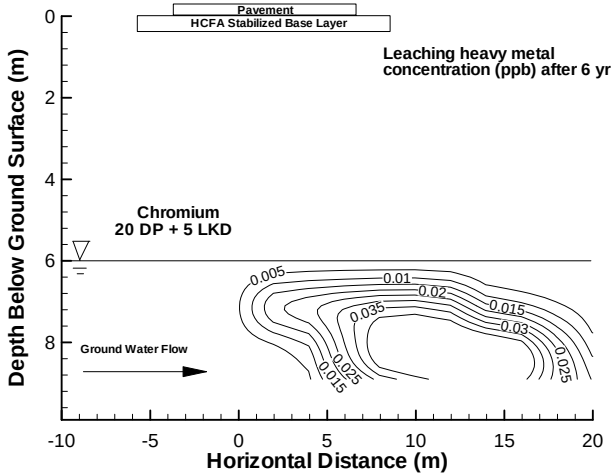
Pavement
HCFA Stabilized Base Layer
Leaching heavy metal
concentration (ppb) after 6 yr
Chromium
20 DP + 5 LKD
Ground Water Flow
0.005
0.01
0.02
0.035
0.015
0.03
0.025
Depth Below Ground Surface (m)
Horizontal Distance (m)

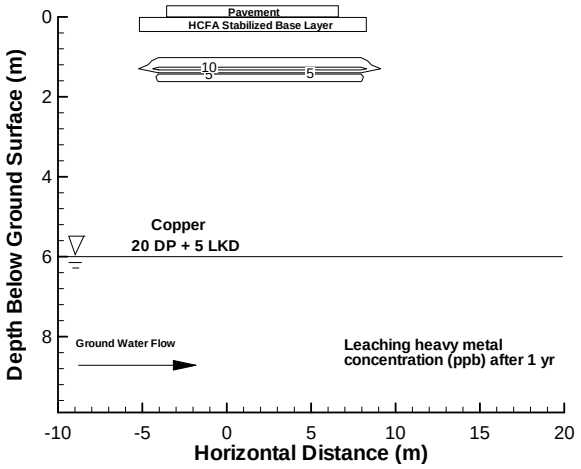
Pavement
HCFA Stabilized Base Layer
10
5
5
Copper
20 DP + 5 LKD
Ground Water Flow
Leaching heavy metal
concentration (ppb) after 1 yr
Depth Below Ground Surface (m)
Horizontal Distance (m)

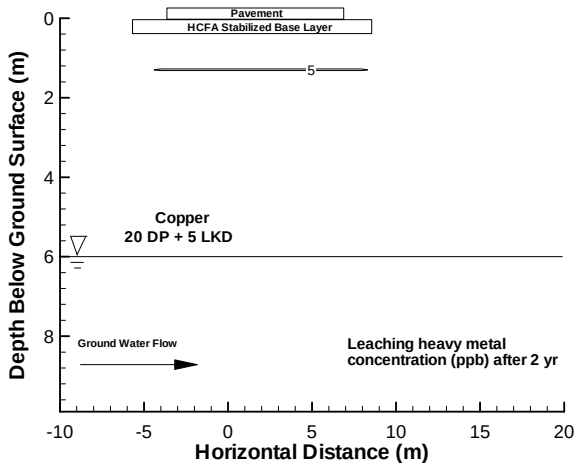
Pavement
HCFA Stabilized Base Layer
5
Copper
20 DP + 5 LKD
Ground Water Flow
Leaching heavy metal
concentration (ppb) after 2 yr
Depth Below Ground Surface (m)
Horizontal Distance (m)

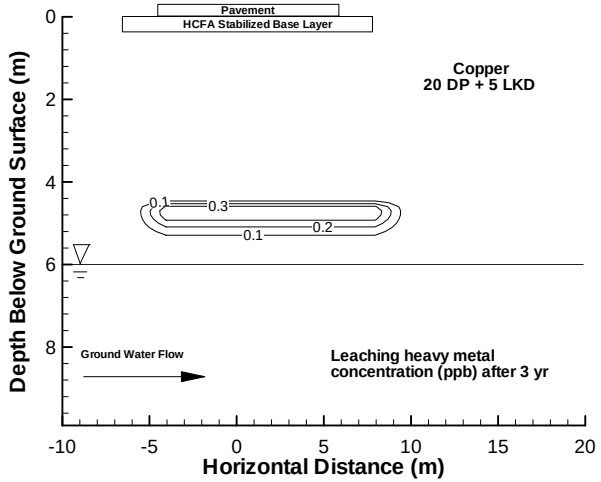
Pavement
HCFA Stabilized Base Layer
Copper
20 DP + 5 LKD
0.1
0.3
0.2
0.1
Ground Water Flow
Leaching heavy metal
concentration (ppb) after 3 yr
Depth Below Ground Surface (m)
Horizontal Distance (m)

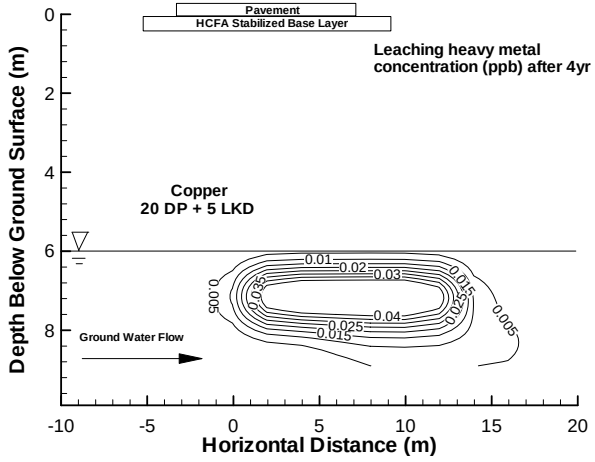
Pavement
HCFA Stabilized Base Layer
Leaching heavy metal
concentration (ppb) after 4yr
Copper
20 DP + 5 LKD
0.01
0.02
0.03
0.04
0.025
0.015
0.005
Ground Water Flow
Depth Below Ground Surface (m)
Horizontal Distance (m)

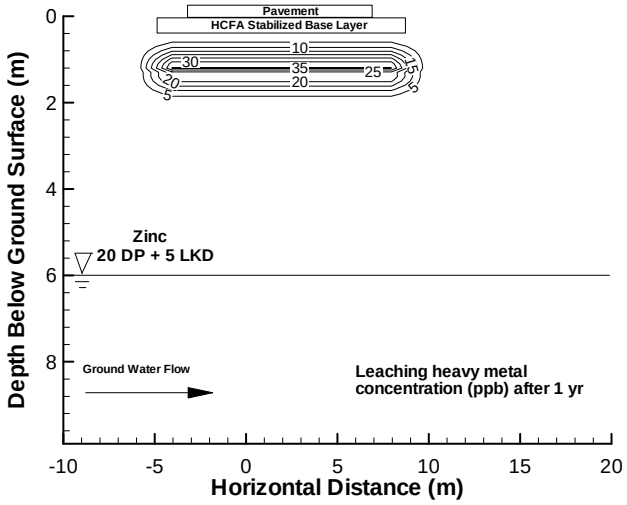
Pavement
HCFA Stabilized Base Layer
Zinc
20 DP + 5 LKD
Ground Water Flow
Leaching heavy metal
concentration (ppb) after 1 yr
Depth Below Ground Surface (m)
Horizontal Distance (m)

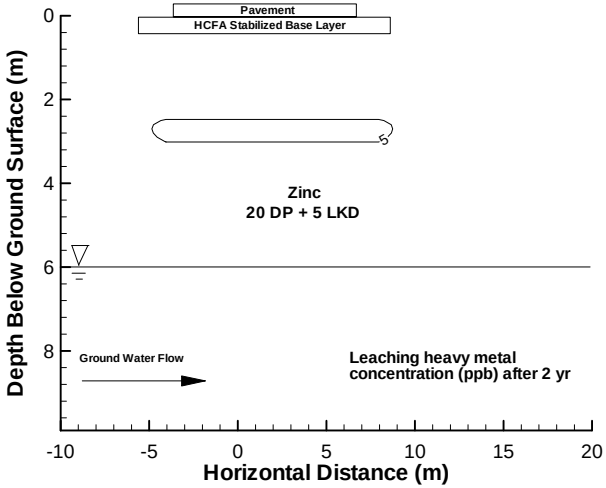
Pavement
HCFA Stabilized Base Layer
Zinc
20 DP + 5 LKD
Ground Water Flow
Leaching heavy metal
concentration (ppb) after 2 yr
Depth Below Ground Surface (m)
Horizontal Distance (m)

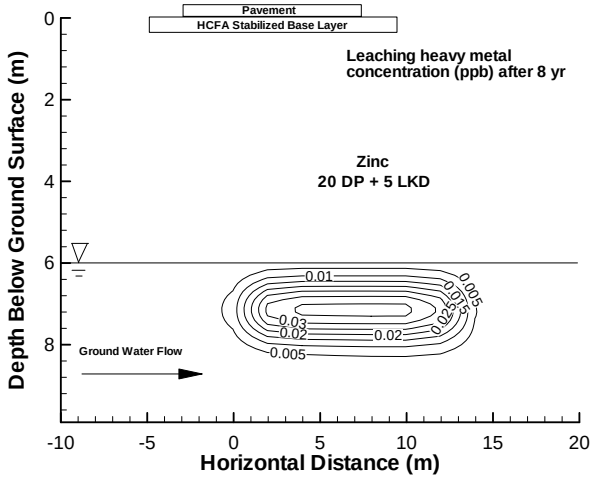
Pavement
HCFA Stabilized Base Layer
Leaching heavy metal
concentration (ppb) after 8 yr
Zinc
20 DP + 5 LKD
Ground Water Flow
Depth Below Ground Surface (m)
Horizontal Distance (m)

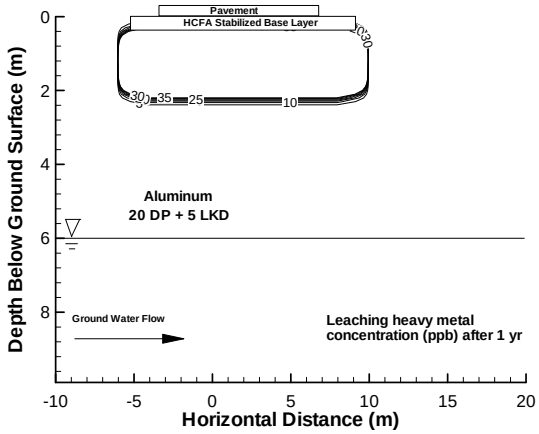
Pavement
HCFA Stabilized Base Layer
Aluminum
20 DP + 5 LKD
Ground Water Flow
Leaching heavy metal
concentration (ppb) after 1 yr
Depth Below Ground Surface (m)
Horizontal Distance (m)

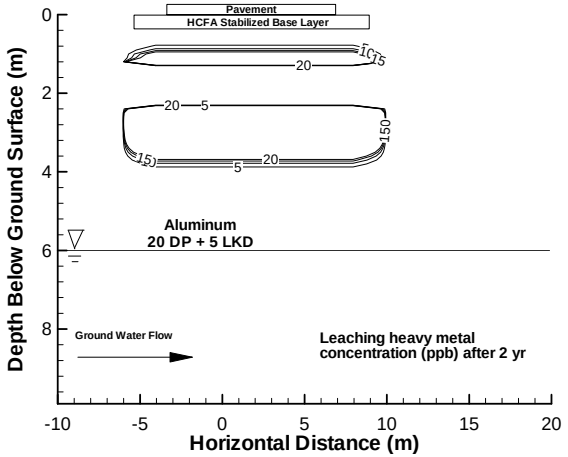
Pavement
HCFA Stabilized Base Layer
Aluminum
20 DP + 5 LKD
Ground Water Flow
Leaching heavy metal
concentration (ppb) after 2 yr
Depth Below Ground Surface (m)
Horizontal Distance (m)

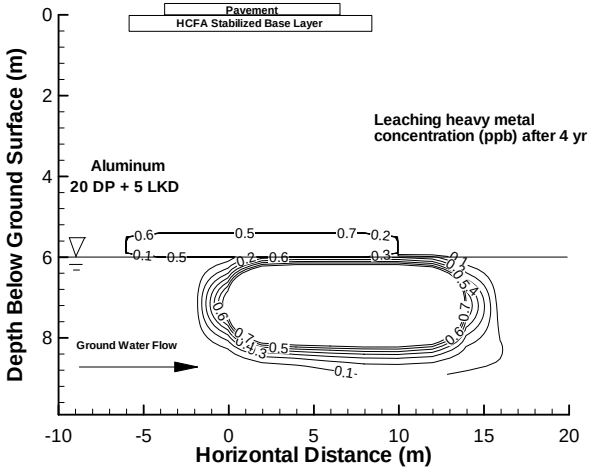
Pavement
HCFA Stabilized Base Layer
Aluminum
20 DP + 5 LKD
Ground Water Flow
Leaching heavy metal
concentration (ppb) after 4 yr
Depth Below Ground Surface (m)
Horizontal Distance (m)

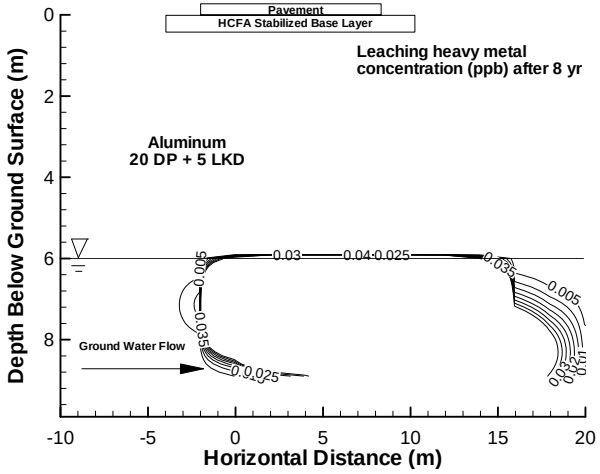
Pavement
HCFA Stabilized Base Layer
Aluminum
20 DP + 5 LKD
Ground Water Flow
Leaching heavy metal
concentration (ppb) after 8 yr
Depth Below Ground Surface (m)
Horizontal Distance (m)

APPENDIX D: MINTEQA2 GEOCHEMICAL ANALYSIS OF THE SPECIES OF THE LEACHED METALS

Table 1. Speciation of As, Cr, Mn, and Se calculated using MINTEQA2: Brandon Shores

Species	Concentration (mol/L)			
	S-10 BS	**S-20 BS**	**S-40 BS**	**100 BS**
AsO_4^{-3}	1.01E-13	2.95E-13	2.03E-11	1.89E-10
$Cr(OH)_2^{+1}$	5.38E-09	4.28E-09	3.38E-08	4.22E-08
$Cr(OH)_3$ (aq)	2.61E-09	1.49E-09	9.71E-08	9.62E-08
$Cr(OH)_4^{-}$	1.32E-14	5.77E-15	3.02E-12	2.72E-12
Cr^{+3}	7.33E-11	1.36E-10	1.46E-11	4.03E-11
$Cr_2(OH)_2^{+4}$	6.40E-14	1.14E-13	8.96E-14	4.37E-13
$Cr_2O_7^{-2}$	9.82E-34	3.31E-35	2.54E-24	8.86E-25
$Cr_3(OH)_4^{+5}$	1.32E-17	2.39E-17	1.34E-16	1.31E-15
CrO_4^{-2}	2.75E-18	3.99E-19	8.74E-13	4.94E-13
$CrOH^{+2}$	1.22E-08	1.43E-08	1.34E-08	2.35E-08
H^{+1}	9.16E-07	1.27E-06	1.55E-07	1.93E-07
$H_2AsO_3^{-}$	5.36E-22	4.02E-21	7.05E-23	7.83E-22
$H_2AsO_4^{-}$	1.26E-07	5.22E-07	6.04E-07	4.86E-06
H_2CrO_4 (aq)	2.00E-24	4.63E-25	1.62E-20	9.93E-21
H_2SeO_3 (aq)	1.29E-10	2.24E-10	1.92E-11	2.13E-11
H_3AsO_3	5.43E-19	5.32E-18	1.16E-20	1.42E-19
H_3AsO_4	1.73E-11	9.30E-11	1.35E-11	1.19E-10
$HAsO_3^{-2}$	8.21E-30	5.02E-29	6.87E-30	7.74E-29
$HAsO_4^{-2}$	2.50E-08	8.38E-08	7.58E-07	6.19E-06
$HCrO_4^{-}$	4.62E-18	8.22E-19	2.31E-13	1.28E-13
$HSeO_3^{-1}$	4.41E-07	5.88E-07	4.02E-07	4.08E-07
$HSeO_4^{-1}$	2.73E-15	2.00E-15	9.05E-14	6.64E-14
$Mn(OH)_4^{-2}$	4.25E-29	1.16E-29	5.09E-26	1.00E-25
Mn^{+2}	3.28E-05	2.97E-05	2.98E-05	1.12E-04
Mn^{+3}	3.76E-23	3.97E-23	3.74E-23	1.88E-22
$Mn_2(OH)_3^{+}$	1.02E-15	2.74E-16	1.63E-13	9.34E-13
Mn_2OH^{+3}	3.96E-14	2.48E-14	2.01E-13	2.54E-12

MnO_4^-	6.85E-49	5.15E-50	1.03E-42	8.87E-43
MnO_4^{-2}	1.97E-46	1.62E-47	3.11E-40	3.21E-40
$MnOH^+$	6.82E-10	4.17E-10	3.54E-09	9.46E-09
$MnSeO_4$ (aq)	2.96E-13	1.24E-13	4.91E-11	8.48E-11
OH^-	1.46E-08	1.12E-08	8.96E-08	8.09E-08
SeO_3^{-2}	3.38E-09	3.68E-09	1.96E-08	2.02E-08
SeO_4^{-2}	1.05E-10	6.27E-11	2.21E-08	1.65E-08

Table 2. Speciation of As, Cr, Mn, and Se calculated using MINTEQA2: Paul Smith Precipitator

	Concentration (mol/L)			
	S-10 PSP	S-20 PSP	S-40 PSP	100 PSP
AsO_4^{-3}	8.51E-13	8.70E-12	4.57E-10	3.3E-09
$Cr(OH)_2^{+1}$	6.2E-09	1.58E-08	2.81E-08	1.3E-08
$Cr(OH)_3$ (aq)	9.33E-09	3.72E-08	9.71E-08	9.5E-08
$Cr(OH)_4^-$	1.52E-13	9.73E-13	3.62E-12	9.8E-12
Cr^{+3}	9.83E-12	1.07E-11	8.27E-12	1.3E-12
$Cr_2(OH)_2^{+4}$	1.11E-14	3.27E-14	4.15E-14	5.3E-15
$Cr_2O_7^{-2}$	1.36E-28	8.94E-26	1.1E-23	2.1E-20
$Cr_3(OH)_4^{+5}$	3.08E-18	2.48E-17	5.08E-17	6.3E-18
CrO_4^{-2}	3.36E-15	1.39E-13	2.18E-12	2.9E-10
$CrOH^{+2}$	4.71E-09	7.77E-09	9.22E-09	2.2E-09
H^{+1}	2.95E-07	1.88E-07	1.28E-07	5.8E-08
$H_2AsO_3^-$	3.86E-23	5.80E-23	7.73E-22	7.1E-23
$H_2AsO_4^-$	9.12E-08	3.44E-07	9.57E-06	5.3E-06
H_2CrO_4 (aq)	2.26E-22	3.58E-21	2.82E-20	4.1E-19
H_2SeO_3 (aq)	4.02E-11	7.01E-11	9.11E-10	1.4E-10
H_3AsO_3	1.21E-20	1.14E-20	1.06E-19	3.5E-21
H_3AsO_4	3.86E-12	9.10E-12	1.78E-10	3.6E-11
$HAsO_3^{-2}$	1.98E-30	4.86E-30	9E-29	2.7E-29
$HAsO_4^{-2}$	6.02E-08	3.71E-07	1.43E-05	2.6E-05
$HCrO_4^-$	1.68E-15	4.28E-14	4.81E-13	1.9E-11
$HSeO_3^{-1}$	4.44E-07	1.24E-06	2.3E-05	1E-05
$HSeO_4^{-1}$	2.75E-14	1.93E-13	7.46E-12	2E-11
$Mn(OH)_4^{-2}$	1.19E-27	9.87E-27	5.03E-25	7.9E-24
Mn^{+2}	9.21E-06	1.21E-05	0.000141	6.1E-05
Mn^{+3}	1.16E-23	1.60E-23	1.75E-22	1.2E-22
$Mn_2(OH)_3^+$	2.23E-15	1.43E-14	6.43E-12	9.1E-12

Mn_2OH^{+3}	1E-14	2.76E-14	5.39E-12	2.7E-12
MnO_4^-	1.82E-45	9.22E-44	2.13E-41	9.1E-39
MnO_4^{-2}	5.52E-43	2.88E-41	6.42E-39	3.7E-36
$MnOH^+$	5.72E-10	1.16E-09	2.03E-08	1.6E-08
$MnSeO_4$ (aq)	2.4E-12	3.34E-11	2.33E-08	3.9E-08
OH^-	4.71E-08	7.54E-08	1.08E-07	2.9E-07
SeO_3^{-2}	1.14E-08	5.20E-08	1.34E-06	1.9E-06
SeO_4^{-2}	3.54E-09	4.05E-08	2.18E-06	1.9E-05

Table 3. Speciation of As, Cr, Mn, and Se calculated using MINTEQA2: Dickerson Precipitator

	Concentration (mol/L)			
	S-10 DP	S-20 DP	S-40 DP	100 DP
AsO_4^{-3}	2.4E-13	2.51E-10	2.2E-10	1.2E-08
$Cr(OH)_2^{+1}$	1.2E-08	1.67E-08	2.7E-08	1.4E-11
$Cr(OH)_3$ (aq)	7.5E-09	9.67E-08	9.6E-08	1.3E-09
$Cr(OH)_4^-$	5.4E-14	6.51E-12	4.2E-12	1.4E-12
Cr^{+3}	1.1E-10	2.14E-12	9.5E-12	6.9E-18
$Cr_2(OH)_2^{+4}$	2.6E-13	7.83E-15	6E-14	2.1E-23
$Cr_2O_7^{-2}$	1.2E-31	1.05E-21	2.8E-23	9.2E-16
$Cr_3(OH)_4^{+5}$	1.5E-16	7.48E-18	1E-16	1.7E-29
CrO_4^{-2}	4.6E-17	3.95E-11	4.2E-12	6E-07
$CrOH^{+2}$	2.1E-08	3.49E-09	9.2E-09	1.8E-13
H^{+1}	6.9E-07	7.64E-08	1.2E-07	4.7E-09
$H_2AsO_3^-$	2.6E-22	3.54E-23	1.8E-22	2.4E-26
$H_2AsO_4^-$	1.2E-07	1.33E-06	2.6E-06	2.4E-07
H_2CrO_4 (aq)	1.5E-23	1.48E-19	3.7E-20	8.5E-18
H_2SeO_3 (aq)	3.3E-10	7.23E-11	4.7E-10	1.5E-14
H_3AsO_3	1.8E-19	2.70E-21	2.1E-20	1.1E-25
H_3AsO_4	1.1E-11	1.36E-11	4.2E-11	1.5E-13
$HAsO_3^{-2}$	6.1E-30	7.93E-30	2.6E-29	8.8E-32
$HAsO_4^{-2}$	3.5E-08	3.82E-06	4.9E-06	1.1E-05
$HCrO_4^-$	5E-17	4.54E-12	7.3E-13	4.2E-09
$HSeO_3^{-1}$	1.6E-06	3.29E-06	1.4E-05	1.1E-08
$HSeO_4^{-1}$	1.9E-14	3.23E-12	5.3E-12	2.8E-12
$Mn(OH)_4^{-2}$	2.2E-28	7.10E-25	7.3E-26	2.4E-22
Mn^{+2}	4.7E-05	2.18E-05	1.4E-05	1.1E-07
Mn^{+3}	6.4E-23	3.20E-23	2.2E-23	1.6E-25
$Mn_2(OH)_3^+$	4.2E-15	6.37E-13	6.2E-14	6.6E-14

Mn_2OH^{+3}	1.1E-13	2.32E-13	6.3E-14	9.3E-17
MnO_4^-	1.2E-47	2.48E-40	3.9E-42	5.8E-33
MnO_4^{-2}	3.7E-45	8.26E-38	1.3E-39	2E-30
$MnOH^+$	1.2E-09	4.92E-09	1.9E-09	3.9E-10
$MnSeO_4$ (aq)	3.4E-12	2.27E-09	1.4E-09	1.6E-10
OH^-	2.1E-08	1.93E-07	1.2E-07	3.1E-06
SeO_3^{-2}	1.9E-08	3.69E-07	1E-06	2E-08
SeO_4^{-2}	1.1E-09	1.82E-06	2E-06	2.6E-05

Table 4. Speciation of As, Cr, Mn, and Se calculated using MINTEQA2: Morgantown

	Concentration (mol/L)			
	S-10 MT	S-20 MT	S-40 MT	100 MT
AsO_4^{-3}	2.3E-11	8.88E-09	7.8E-08	3.1E-07
$Cr(OH)_2^{+1}$	6.5E-09	1.56E-14	6.2E-16	3.5E-19
$Cr(OH)_3$ (aq)	9.7E-08	8.13E-12	6.3E-13	1.1E-15
$Cr(OH)_4^{-}$	1.7E-11	5.53E-14	8.4E-15	5.4E-17
Cr^{+3}	1.3E-13	3.17E-22	3.3E-24	2.1E-28
$Cr_2(OH)_2^{+4}$	1.9E-16	1.43E-30	6E-34	2.5E-41
$Cr_2O_7^{-2}$	2E-18	6.30E-14	8E-14	5.3E-15
$Cr_3(OH)_4^{+5}$	7.2E-20	1.84E-39	3.1E-44	9.3E-55
CrO_4^{-2}	4.5E-09	3.21E-05	7E-05	6.5E-05
$CrOH^{+2}$	5.4E-10	3.92E-17	8E-19	1.5E-22
H^{+1}	3E-08	8.39E-10	4.3E-10	1.3E-10
$H_2AsO_3^{-}$	7.2E-26	1.04E-29	6.3E-30	1.5E-31
$H_2AsO_4^{-}$	1.8E-08	3.55E-09	8.2E-09	2.2E-09
H_2CrO_4 (aq)	2.5E-18	1.08E-17	6.2E-18	4.4E-19
H_2SeO_3 (aq)	7.4E-13	1.18E-18	7E-19	1.6E-20
H_3AsO_3	2.1E-24	7.84E-30	2.5E-30	1.6E-32
H_3AsO_4	7.1E-14	3.61E-16	4.3E-16	3.3E-17
$HAsO_3^{-2}$	4.2E-32	2.56E-34	3E-34	2.7E-35
$HAsO_4^{-2}$	1.3E-07	1.12E-06	5.1E-06	5.1E-06
$HCrO_4^{-}$	2E-10	3.36E-08	3.8E-08	9.4E-09
$HSeO_3^{-1}$	8.7E-08	5.41E-12	6.3E-12	4.9E-13
$HSeO_4^{-1}$	5.6E-13	4.84E-14	2.1E-13	1.9E-13
$Mn(OH)_4^{-2}$	1.2E-24	1.71E-21	3.3E-21	1.3E-20
Mn^{+2}	8.4E-07	6.34E-10	8.5E-11	2.5E-12
Mn^{+3}	1.2E-24	1.17E-27	1.6E-28	5.4E-30
$Mn_2(OH)_3^{+}$	1.6E-14	3.38E-16	4.6E-17	1.2E-18
Mn_2OH^{+3}	8.8E-16	1.95E-20	6.9E-22	2.1E-24

MnO_4^-	1.8E-38	4.33E-29	1.2E-27	5.6E-25
MnO_4^{-2}	6E-36	1.66E-26	4.7E-25	2.4E-22
$MnOH^+$	4.8E-10	1.19E-11	3.1E-12	2.8E-13
$MnSeO_4$ (aq)	3.8E-11	7.42E-14	8.6E-14	6.5E-15
OH^-	5E-07	1.93E-05	3.8E-05	0.00013
SeO_3^{-2}	2.5E-08	6.67E-11	1.5E-10	4.4E-11
SeO_4^{-2}	8.2E-07	2.99E-06	2.6E-05	8.6E-05

Table 5. Speciation of As, Cr, Mn, and Se calculated using MINTEQA2: Columbia

	Concentration (mol/L)			
	S-10 Co	S-20 Co	S-40 Co	100 Co
AsO_4^{-3}	3.7E-07	7.52E-07	1.1E-06	7.3E-07
$Cr(OH)_2^{+1}$	2.2E-32	4.06E-30	1.4E-35	5.2E-35
$Cr(OH)_3$ (aq)	8E-27	6.55E-25	1.5E-29	6.1E-29
$Cr(OH)_4^-$	3.5E-26	1.38E-24	2.1E-28	1.1E-27
Cr^{+3}	7.8E-46	8.64E-43	7E-50	2.5E-49
$Cr_2(OH)_2^{+4}$	4.1E-72	1.01E-66	2.9E-79	4.8E-78
$Cr_2O_7^{-2}$	1.9E-21	3.40E-20	7.9E-23	4.7E-21
$Cr_3(OH)_4^{+5}$	6E-99	3.41E-91	4E-109	3E-107
CrO_4^{-2}	3.4E-06	7.29E-06	2.4E-06	2.3E-05
$CrOH^{+2}$	7.6E-38	3.30E-35	1.7E-41	6.1E-41
H^{+1}	1.2E-12	2.71E-12	4.1E-13	3.6E-13
$H_2AsO_3^-$	3E-39	9.66E-38	6.5E-41	1.9E-41
$H_2AsO_4^-$	4.5E-13	3.15E-12	9.6E-14	3.6E-14
H_2CrO_4 (aq)	3.1E-24	2.57E-23	1.8E-25	1.1E-24
H_2SeO_3 (aq)	1.8E-30	2.30E-28	2.3E-32	1.4E-31
H_3AsO_3	3.6E-42	2.36E-40	2.3E-44	5.5E-45
H_3AsO_4	7.2E-23	1.04E-21	4.6E-24	1.5E-24
$HAsO_3^{-2}$	4.4E-41	7.34E-40	3.4E-42	1.2E-42
$HAsO_4^{-2}$	8.5E-08	3.08E-07	6.6E-08	3.1E-08
$HCrO_4^-$	6.1E-12	2.47E-11	1.2E-12	8.8E-12
$HSeO_3^{-1}$	5.2E-21	3.27E-19	2.3E-22	1.6E-21
$HSeO_4^{-1}$	2E-17	2.79E-16	8.9E-18	8.3E-17
$Mn(OH)_4^{-2}$	5.2E-20	6.03E-20	2.1E-21	2.4E-21
Mn^{+2}	1E-19	2.45E-18	4.1E-23	2.7E-23
Mn^{+3}	1.6E-37	4.53E-36	8E-41	6E-41
$Mn_2(OH)_3^+$	3.2E-27	1.48E-25	1.2E-32	6.2E-33
Mn_2OH^{+3}	3.2E-37	8.98E-35	1.7E-43	8.6E-44

MnO_4^-	2.8E-16	1.39E-17	9.8E-16	1.8E-15
MnO_4^{-2}	9.6E-14	5.32E-15	3.9E-13	7.6E-13
$MnOH^+$	1.4E-18	1.42E-17	1.6E-21	1.1E-21
$MnSeO_4$ (aq)	3.9E-24	5.11E-22	1.7E-27	1E-26
OH^-	0.01233	5.98E-03	0.04085	0.04833
SeO_3^{-2}	3.8E-17	1.24E-15	6.1E-18	5.4E-17
SeO_4^{-2}	7.4E-07	5.33E-06	1.2E-06	1.4E-05

Table 6. Speciation of Cu, Cr, Fe, Mn, Sb and V calculated using MINTEQA2: BS+LKD

	Concentration (mol/L)			
	10 BS + 2.5 LKD	10 BS + 5 LKD	20 BS + 5 LKD	100 BS
$Cr(OH)_2^{+1}$	1.40E-29	1.35E-32	1.14E-24	4.93E-15
$Cr(OH)_3$ (aq)	6.17E-24	1.40E-26	1.22E-18	6.93E-13
$Cr(OH)_4^-$	3.43E-23	2.09E-25	1.77E-17	1.21E-15
Cr^{+3}	3.70E-43	8.23E-47	5.93E-39	1.25E-21
$Cr_2(OH)_2^{+4}$	1.39E-66	3.93E-73	2.12E-57	1.61E-30
$Cr_2O_7^{-2}$	2.99E-23	8.01E-24	1.05E-23	7.13E-16
$Cr_3(OH)_4^{+5}$	1.45E-90	5.75E-100	2.24E-76	5.68E-40
CrO_4^{-2}	5.67E-07	8.10E-07	8.91E-07	8.67E-07
$CrOH^{+2}$	4.07E-35	1.79E-38	1.43E-30	4.47E-17
$Cu(OH)_2$ (aq)	4.58E-10	1.45E-09	4.73E-12	2.38E-11
$Cu(OH)_3^-$	2.86E-08	2.42E-07	7.67E-10	4.67E-13
$Cu(OH)_4^{-2}$	5.76E-09	1.41E-07	4.20E-10	2.92E-17
Cu^{+1}	6.16E-21	1.91E-21	2.52E-21	1.94E-17
Cu^{+2}	1.23E-17	7.57E-18	2.25E-20	6.25E-12
$Cu_2(OH)_2^{+2}$	3.13E-21	6.19E-21	5.94E-26	8.23E-17
Cu_2OH^{+3}	4.66E-29	4.64E-29	4.03E-34	3.78E-21
$Cu_3(OH)_4^{+2}$	1.26E-24	8.01E-24	2.48E-31	1.72E-21
$CuOH^+$	2.51E-13	3.37E-13	1.07E-15	4.09E-11
$Fe(OH)_2$ (aq)	1.06E-26	2.41E-27	1.01E-24	2.05E-25
$Fe(OH)_2^+$	3.46E-19	1.44E-19	1.41E-19	1.09E-15
$Fe(OH)_3^-$	5.41E-25	3.29E-25	1.34E-22	3.28E-27
$Fe(OH)_3$ (aq)	1.92E-16	1.89E-16	1.91E-16	1.92E-16
$Fe(OH)_4^-$	6.15E-12	1.62E-11	1.59E-11	1.94E-15
Fe^{+2}	5.22E-30	2.30E-31	8.86E-29	9.87E-22
Fe^{+3}	7.45E-37	7.17E-38	5.96E-38	2.25E-26
$Fe_2(OH)_2^{+4}$	7.15E-52	3.80E-53	2.74E-53	6.59E-38
$Fe_3(OH)_4^{+5}$	3.41E-67	1.10E-68	6.61E-69	9.49E-50
$FeCrO_4^+$	1.26E-36	9.88E-38	1.16E-37	6.19E-26
$FeOH^+$	1.34E-27	1.29E-28	5.27E-26	8.14E-23

$FeOH^{+2}$	2.90E-27	5.55E-28	5.11E-28	2.84E-20
H^{+1}	9.95E-13	4.15E-13	4.07E-13	3.13E-09
H_2CrO_4 (aq)	2.91E-25	5.38E-26	6.48E-26	4.55E-18
$H_2V_2O_4^{+2}$	1.09E-22	2.08E-23	1.92E-23	1.07E-15
$HCrO_4^-$	7.41E-13	3.66E-13	4.28E-13	3.64E-09
$Mn(OH)_4^{-2}$	3.42E-17	1.49E-17	2.31E-14	6.48E-23
Mn^{+2}	2.65E-17	2.88E-19	4.49E-16	5.00E-09
Mn^{+3}	1.82E-36	4.31E-38	1.45E-37	5.48E-26
$Mn_2(OH)_3^+$	3.71E-22	5.03E-25	1.40E-18	4.34E-16
Mn_2OH^{+3}	2.79E-32	8.74E-36	2.07E-29	3.14E-19
MnO_4^-	4.15E-20	9.51E-18	1.25E-27	9.42E-29
MnO_4^{-2}	3.87E-16	5.92E-14	3.04E-21	5.28E-27
$MnOH^+$	4.28E-16	1.02E-17	1.69E-14	2.60E-11
OH^-	1.59E-02	4.18E-02	4.10E-02	5.00E-06
$Sb(OH)_2^+$	1.37E-41	6.14E-44	5.82E-38	9.15E-31
$Sb(OH)_3$	5.66E-31	5.97E-33	5.82E-27	1.20E-23
$Sb(OH)_4^{-1}$	1.37E-30	3.88E-32	3.67E-26	9.15E-27
$Sb(OH)_5$ (aq)	7.18E-17	1.42E-17	7.96E-17	4.09E-12
$Sb(OH)_6^{-1}$	1.74E-07	9.23E-08	5.03E-07	3.12E-06
$V(OH)_2^+$	1.52E-27	1.47E-28	6.00E-26	9.26E-23
$V(OH)_3^+$	3.72E-14	1.55E-14	1.52E-14	1.17E-10
V^{+3}	5.63E-44	1.25E-45	4.34E-43	3.28E-32
$V_2(OH)_2^{+4}$	5.14E-67	1.46E-69	1.83E-64	1.76E-50
VO^{+2}	2.89E-20	5.53E-21	5.10E-21	2.84E-13
VOH^{+2}	1.16E-34	5.11E-36	1.96E-33	2.19E-26

Table 7. Speciation of Cu, Cr, Fe, Mn, Sb and V calculated using MINTEQA2: PS+LKD

	Concentration (mol/L)			
	10 PS + 2.5 LKD	10 PS + 5 LKD	20 PS + 5 LKD	100 PS
$Cr(OH)_2^{+1}$	2.62E-27	3.09E-30	6.01E-27	1.27E-13
$Cr(OH)_3$ (aq)	1.78E-21	3.18E-24	6.18E-21	1.78E-12
$Cr(OH)_4^-$	1.61E-20	4.78E-23	9.31E-20	3.12E-16
Cr^{+3}	3.25E-41	1.98E-44	3.91E-41	3.29E-18
$Cr_2(OH)_2^{+4}$	2.57E-62	2.24E-68	8.72E-62	1.10E-25
$Cr_2O_7^{-2}$	1.69E-24	7.05E-25	1.09E-24	2.05E-13
$Cr_3(OH)_4^{+5}$	5.93E-84	7.87E-93	6.06E-83	1.02E-33
CrO_4^{-2}	2.23E-07	2.43E-07	3.04E-07	1.48E-06
$CrOH^{+2}$	5.11E-33	4.19E-36	8.20E-33	1.16E-14
$Cu(OH)_2$ (aq)	3.61E-11	2.12E-10	2.48E-09	9.59E-11
$Cu(OH)_3^-$	3.66E-09	3.57E-08	4.18E-07	1.89E-13
$Cu(OH)_4^{-2}$	1.24E-09	2.11E-08	2.49E-07	1.19E-18
Cu^{+1}	3.97E-21	2.59E-21	3.52E-19	1.94E-16
Cu^{+2}	4.21E-19	1.14E-18	1.34E-17	2.54E-09
$Cu_2(OH)_2^{+2}$	8.46E-24	1.36E-22	1.87E-20	1.35E-13
Cu_2OH^{+3}	8.81E-32	1.05E-30	1.46E-28	6.28E-17
$Cu_3(OH)_4^{+2}$	2.69E-28	2.57E-26	4.15E-23	1.14E-17
$CuOH^+$	1.28E-14	4.96E-14	5.82E-13	1.65E-09
$Fe(OH)_2$ (aq)	1.33E-25	2.21E-26	1.88E-27	5.07E-26
$Fe(OH)_2^+$	2.23E-19	1.45E-19	1.07E-21	1.09E-14
$Fe(OH)_3^-$	1.11E-23	3.04E-24	2.60E-25	8.15E-29
$Fe(OH)_3$ (aq)	1.91E-16	1.89E-16	1.39E-18	1.92E-16
$Fe(OH)_4^-$	9.95E-12	1.63E-11	1.20E-13	1.94E-16
Fe^{+2}	2.85E-29	2.17E-30	1.87E-31	2.47E-20
Fe^{+3}	2.25E-37	7.55E-38	5.66E-40	2.29E-23
$Fe_2(OH)_2^{+4}$	1.57E-52	4.18E-53	2.33E-57	6.82E-34
$Fe_3(OH)_4^{+5}$	5.68E-68	1.27E-68	5.33E-75	1.00E-44
$FeCrO_4^+$	1.17E-37	2.91E-38	2.66E-40	1.05E-22
$FeOH^+$	1.09E-26	1.19E-27	1.02E-28	2.02E-22

$FeOH^{+2}$	1.25E-27	5.68E-28	4.21E-30	2.87E-18
H^{+1}	6.41E-13	4.18E-13	4.18E-13	3.14E-08
H_2CrO_4 (aq)	4.18E-26	1.57E-26	1.95E-26	7.69E-16
$H_2V_2O_4^{+2}$	4.71E-23	2.13E-23	2.15E-23	1.08E-13
$HCrO_4^-$	1.73E-13	1.08E-13	1.34E-13	6.16E-08
$Mn(OH)_4^{-2}$	1.18E-15	5.66E-16	6.63E-15	1.62E-25
Mn^{+2}	1.44E-16	1.10E-17	1.29E-16	1.25E-07
Mn^{+3}	5.48E-37	1.84E-37	1.87E-37	5.59E-23
$Mn_2(OH)_3^+$	3.81E-20	7.01E-22	9.47E-20	2.67E-16
Mn_2OH^{+3}	1.35E-30	1.28E-32	1.75E-30	1.97E-17
MnO_4^-	2.63E-24	5.42E-21	2.98E-25	2.50E-27
MnO_4^{-2}	5.23E-19	3.15E-16	2.03E-19	3.50E-27
$MnOH^+$	3.49E-15	3.82E-16	4.44E-15	6.46E-11
OH^-	2.57E-02	4.21E-02	4.21E-02	5.01E-07
$Sb(OH)_2^+$	9.76E-40	4.62E-42	1.87E-39	2.88E-30
$Sb(OH)_3$	6.21E-29	4.44E-31	1.79E-28	3.77E-24
$Sb(OH)_4^{-1}$	2.45E-28	2.91E-30	1.18E-27	2.88E-28
$Sb(OH)_5$ (aq)	4.93E-17	1.25E-17	3.74E-17	2.09E-11
$Sb(OH)_6^{-1}$	1.95E-07	8.21E-08	2.46E-07	1.60E-06
$V(OH)_2^+$	1.24E-26	1.36E-27	1.58E-26	2.30E-22
$V(OH)_3^+$	2.40E-14	1.56E-14	1.57E-14	1.17E-09
V^{+3}	2.15E-43	1.21E-44	1.43E-43	8.28E-30
$V_2(OH)_2^{+4}$	1.80E-65	1.35E-67	1.88E-65	1.12E-47
VO^{+2}	1.25E-20	5.67E-21	5.71E-21	2.86E-11
VOH^{+2}	6.32E-34	4.81E-35	5.63E-34	5.47E-25

Table 8. Speciation of Cu, Cr, Fe, Mn, Sb and V calculated using MINTEQA2: PS+LKD

	Concentration (mol/L)			
	10 DP + 2.5 LKD	10 DP + 5 LKD	20 DP + 5 LKD	100 DP
$Cr(OH)_2^{+1}$	7.40E-25	1.77E-29	1.74E-26	1.54E-10
$Cr(OH)_3$ (aq)	3.09E-19	1.49E-23	2.35E-20	4.04E-09
$Cr(OH)_4^-$	1.82E-18	1.73E-22	4.27E-19	1.50E-12
Cr^{+3}	2.73E-38	1.54E-43	5.71E-41	1.44E-15
$Cr_2(OH)_2^{+4}$	6.91E-57	8.88E-67	3.12E-61	7.67E-20
$Cr_2O_7^{-2}$	8.28E-24	5.67E-24	3.29E-24	4.93E-13
$Cr_3(OH)_4^{+5}$	5.31E-76	1.53E-90	5.02E-82	1.24E-24
CrO_4^{-2}	3.24E-07	5.26E-07	6.28E-07	5.01E-06
$CrOH^{+2}$	2.44E-30	2.85E-35	1.73E-32	8.05E-12
$Cu(OH)_2$ (aq)	9.59E-12	1.98E-10	5.27E-10	6.38E-12
$Cu(OH)_3^-$	6.32E-10	2.58E-08	1.08E-07	2.66E-14
$Cu(OH)_4^{-2}$	1.44E-10	1.15E-08	7.42E-08	3.84E-19
Cu^{+1}	6.42E-21	3.19E-21	7.83E-20	1.02E-16
Cu^{+2}	3.08E-19	1.54E-18	1.59E-18	5.18E-11
$Cu_2(OH)_2^{+2}$	1.66E-24	1.72E-22	4.67E-22	1.86E-16
Cu_2OH^{+3}	3.03E-32	1.51E-30	2.51E-30	5.45E-20
$Cu_3(OH)_4^{+2}$	1.41E-29	3.02E-26	2.17E-25	1.06E-21
$CuOH^+$	5.55E-15	5.69E-14	9.44E-14	5.86E-11
$Fe(OH)_2$ (aq)	4.93E-25	2.40E-26	9.07E-27	7.40E-25
$Fe(OH)_2^+$	3.60E-19	1.79E-19	2.87E-21	5.72E-15
$Fe(OH)_3^-$	2.66E-23	2.55E-24	1.52E-24	2.52E-27
$Fe(OH)_3$ (aq)	1.90E-16	1.90E-16	4.88E-18	1.89E-16
$Fe(OH)_4^-$	6.41E-12	1.27E-11	5.11E-13	4.05E-16
Fe^{+2}	2.90E-28	3.43E-30	5.02E-31	1.10E-19
Fe^{+3}	1.08E-36	1.27E-37	7.66E-40	4.37E-24
$Fe_2(OH)_2^{+4}$	1.38E-51	7.68E-53	7.17E-57	8.98E-35
$Fe_3(OH)_4^{+5}$	9.52E-67	2.48E-68	3.52E-74	9.98E-46
$FeCrO_4^+$	6.37E-37	1.33E-37	1.04E-39	3.90E-23
$FeOH^+$	6.58E-26	1.59E-27	3.76E-28	1.57E-21

$FeOH^{+2}$	3.42E-27	8.33E-28	8.26E-30	8.66E-19
H^{+1}	1.04E-12	5.16E-13	3.23E-13	1.65E-08
H_2CrO_4 (aq)	1.39E-25	5.89E-26	2.88E-26	5.37E-16
$H_2V_2O_4^{+2}$	1.29E-22	3.13E-23	1.21E-23	3.25E-14
$HCrO_4^-$	3.74E-13	3.12E-13	2.39E-13	9.12E-08
$Mn(OH)_4^{-2}$	1.90E-15	3.56E-16	1.29E-14	1.15E-23
Mn^{+2}	1.47E-15	1.74E-17	9.94E-17	5.59E-07
Mn^{+3}	2.63E-36	3.08E-37	7.30E-38	1.06E-23
$Mn_2(OH)_3^+$	8.58E-19	1.00E-21	1.37E-19	3.08E-14
Mn_2OH^{+3}	8.99E-29	2.48E-32	1.28E-30	8.21E-16
MnO_4^-	8.75E-27	3.13E-21	1.04E-25	1.09E-31
MnO_4^{-2}	4.35E-21	1.47E-16	1.12E-19	5.15E-30
$MnOH^+$	2.10E-14	5.08E-16	4.70E-15	5.02E-10
OH^-	1.65E-02	3.28E-02	5.16E-02	1.05E-06
$Sb(OH)_2^+$	1.80E-38	7.43E-42	8.02E-40	4.89E-29
$Sb(OH)_3$	7.01E-28	5.85E-31	1.01E-28	1.20E-22
$Sb(OH)_4^{-1}$	1.80E-27	2.96E-30	8.02E-28	1.95E-26
$Sb(OH)_5$ (aq)	4.00E-17	1.42E-17	1.12E-17	3.04E-12
$Sb(OH)_6^{-1}$	1.03E-07	7.18E-08	8.92E-08	4.92E-07
$V(OH)_2^+$	7.49E-26	1.81E-27	1.67E-26	1.79E-21
$V(OH)_3^+$	3.88E-14	1.93E-14	1.21E-14	6.16E-10
V^{+3}	3.84E-42	2.19E-44	7.64E-44	2.34E-29
$V_2(OH)_2^{+4}$	2.21E-63	2.89E-67	8.99E-66	3.24E-46
VO^{+2}	3.41E-20	8.31E-21	3.22E-21	8.64E-12
VOH^{+2}	6.44E-33	7.60E-35	4.35E-34	2.45E-24

REFERENCES

ACAA, (2009). *2009 Coal combustion byproducts production and use*. American Coal Ash Association, Denver, Colorado

Allison JD, Brown DS, and Novo-Gradac KJ. *MINTEQA2/PRODEFA2 (1991), A Geochemical Assesment Model for Environmental Systems*, Version 3.11 Databases and Version 3.0 User`s Manual, US EPA, Athens.

Allison, J. D., Brown, D. S., and Novo-Gradac, K. J. (1991). *MINTEQA2/PRODEFA2 A geochemical Assessment model for environmental systems: Version 3.0 User's manual.* EPA/600/3-91/021, U.S. Environmental Protection Agency, Washington, D. C.

American Coal Ash Association (2009), *2009 Coal Combustion Product Production and Use*, Denver, Colorado.

Apul, D. S., Gardner, K. H., Eighmy, T. T., Fallman, A.-M., and Comans, R. N. J. (2005). Simultaneous application of dissolution/precipitation and surface complexation/surface precipitation modeling to contaminant leaching. *Environmental Science and Technology*, 39-15, 5736 - 5741.

Apul, D.S., Diaz, M., E., Gustafsson, J., P., and Hundal, L., S. (2010). Geochemical modeling of trace elements release from biosolids. *Environmental Engineering Science*, 27-9, 743 - 755.

Apul, D.S., Gardner, K.H., and Eighmy, T.T. (2007). Modeling hydrology and reactive transport in roads: The effect of cracks, the edge, and contaminant properties. *Waste Management* 27, 1465 - 1475.

Astrup, T., Dijkstra, J. J., Comans, R. N. J., Van der Sloot, H. A., and Christensen, T. H. (2006). "Geochemical modeling of leaching from MSWI air-pollution-control residues." *Environmental Science & Technology*, 40(11), 3551-3557.

Bankowski, P., Zou, L., and Hodges, R.H., (2004). Reduction of metal leaching in Brown coal fly ash using geopolymers. *Journal of Hazardous Materials* B14, 59 - 67.

Baur, I. and Johnson, C.A., 2003. The solubility of selenate Aft ($3CaO.Al_2O_3.3CaSeO_4.637H_2O$) and selenate-AFm ($3CaO.Al_2O_3.CaSeO_4.xH_2O$). Earth Planet. *Cement Concrete Research*, 33, 1741 - 1748.

Baykal, G., Edincliler, A., and Saygili, A.,(2004). Highway embankment construction using fly ash in cold regions. *Resources, Conversation and Recycling* 42 - 3, 209-222.

Becker JL, Aydilek AH, Davis AP, and Seagran EA (2011). *Evaluation of leaching protocols for the testing of coal combustion byproducts*. Environmental-Geotechnical Report, 11-01; University of Maryland – College Park, College Park, MD.

Benedetto, F.D., Costaglia, P., Benvenuti, M., Lattanzi, P., Romanelli, M., and Tanelli, G., (2009). Arsenic incorporation in natural calcite lattice. Evidence from electron spin echo spectroscopy. Earth Planet. *Science Letter*, 246, 458 - 465.

Benson, C., Edil, T., Lee, J., and Bradshaw, S., (2010). *Quantifying the benefits of using coal combustion products in sustainable construction*. Report No. 1020552. Electric Power Research Institute, Palo Alto, California.

Bin-Shafique, S., Benson, C., Edil, T. and Hwang, K., (2006). Leachate concentrations from water leach and column leach tests on fly – ash stabilized soil. *Environmental Engineering Science* 23(1), 51-65.

Black,C.J. , Brockway, D., Hodges, S., and Milner A. (1992). "Utilisation of Latrobe Valley brown coal fly ash ",C.M. Barton et al., eds, *Proc. Energy, Economics & Environment-Gipssland Basin Symp.,*, AusIMM, Melbourne, Australia. 149-155.

Brookins DG (1988). *Eh-pH Diagrams for Geochemistry*. 1st edition. United States: Springer-Verlag Berlin Heidelberg.

Brown, S., Christensen, B. Lombi, E., McLaughin, M., McGrath, S., Colpaert, J., and Vangronsveld, J., (2005). An inter-laboratory study to test the ability of amendments to reduce the availability of Cd, Pb, and Zn in situ.. *Environmental Pollution* 138, 34-45.

Camargo F.F (2008), *Strength and stiffness of recycled base materials blended with fly ash*, M.S. Thesis; 123, University of Wisconsin-Madison.

Cetin, B., Aydilek, A.H., and Guney, Y., (2010). Stabilization of recycled base material using high-carbon fly ash, *Resources, Conservation and Recycling* 54, 879-892.

Chand SK, and Subbarao C (2007), In – place stabilization of pond ash deposits by hydrated lime columns, Resources, *Journal of Geotechnical and Geoenvironmental Engineering*, 133:1609 - 1616.

Chavez, M.L., dePablo, L., and Garcia, T.A., (2010) Adsorption of Ba^{2+} by Ca- exchange clinoplite tuff and montmorollinite clay. *Journal of Hazardous Materials* 175, 216 - 223.

Cherry, J. A., Shaikh, A. U., Tallman, D. E., and Nicholson, R. V. (1979). Arsenic species As an indicator of redox conditions in groundwater. *Journal of Hydrology*, 43, 1-4, 373-392.

Chichester, D.L. and Landsberger, S.,(1996). Determination of the leaching dynamics of metals from municipal solid waste incinerator fly ash using a column test. *Journal of Air and Waste Management Association* 46, 643-649.

Cornelis, G., Johnson, C.H., Van Gerven, T., and Vandecasteele, C (2008). "Leaching Mechanisms of Oxyanionic Metalloid and Metal Species in Alkaline Solid Wastes", *Applied Geochemistry*, Vol. 23, 955-976.

Cornell RM, Schwertmann U. (2003), *The Iron Oxides : Structure, Properties, Reactions, Occurences and Uses,* 2nd edition., Weinheim: Wiley – VCH.

Cotton, A.F, and Wilkinson, G., (1999). *Advanced Inorganic Chemistry*, 5th ed. John Wiley & Sons, Inc., New York.

Coz, A., Andres, A., Soriano, S., and Irabien, A. (2004) "Environmental behavior of cement-based stabilized foundry sludge", *Journal of Hazardous Materials*, 109(1-3), 95-104.

Daniels JL, and Das GP (2006), Leaching behavior of lime – fly ash mixtures, *Environmental Engineering Science*, 23-1:42-52.

Dijkstra, J. J., Meeussen, J. C. L., and Comans, R. N. J. (2004). Leaching of heavy metals from contaminated soils: An experimental and modeling study. *Environmental Science and Technology*, 38-16, 4390-4395.

Dixit S., and Herring JG. (2003). Comparison of arsenic (V) and arsenic (III) sorption onto iron oxide minerals; implications for arsenic mobility. *Environmental Science and Technology*, 37:4182-4189.

Dutta, B.K., Khanra and S., and Mallick, D. (2009). "Leaching of elements from coal fly ash: Assesment of its potential for use in filling abandoned coal mines", *Fuel*, Vol. 88, pp. 1314-1323.

Dzombak DA, and Morrel FMM (1990). *Surface Complexation Modeling: Hydrous Ferric Oxide*. 1st edition, New York:John Wiley and Sons.

Edil TB, Sandstorm LK, and Berthouex PM. (1992), Interaction of inorganic leachate with compacted pozzolanic fly ash. *Journal of Geotechnical Engineering*, 118-9:1410-1430.

Edil, T.B., Acosta, H., and Benson, C.H., (2006). Stabilizing soft fine-grained soils with fly ash. *Journal of Materials in Civil Engineering* 18 - 2 ASCE, 283 – 294.

Elsayed-Ali, O.H., Abdel-Fattah, T., and Elsayed-Ali, H.E. (2011). Copper cation removal in an electrokinetic cell containing zeolite, *Journal of Hazardous Materials*, 185, 1550-1557.

Elseewi, A.A., Page, A.L., and Grimm, S.R., (1980). Chemical characterization of fly ash aqueous systems. *Journal of Environmental Quality* 9, 424 - 428.

Elseewi, A.A., Page, A.L., and Grimm, S.R., (1980). Chemical characterization of fly ash aqueous systems. *Journal of Environmental Quality* 9, 424 - 428.

Engelsen, C.J., van der sloot, H.A., Wibetoe, G., Justnes, H., Lund, W., and Hansson, E.S. (2010). Leaching characterization and geochemical modeling of minor and trace elements released from recycled concrete aggregates. *Cement and Concrete Research*, 40, 1639-1649.

Espana JS, Pamo EL, Santofimia E, Aduvire O, Reyes J, and Barettino D. (2005). Acid mine drainage in the Iberian Pyrite Belt (Odiel River Water Shed, Huelva, Spain):Geochemistry, mineralogy and environmental implication. *Applied Geochemistry,* 20:1320-56.

Essington, M.E. (1988). Estimation of the standard free energy of formation of metal arsenates, selenates and selenites. *Soil Science Society of America Journal*, 52, 1474 - 1579.

Ettler, V., Mihaljevic, M., and Sebek, O. (2010). Antimony and arsenic leaching from secondary lead smelter air-pollution-control residues. *Waste Management & Research* 28, 587-595.

Fendorf, SE (1995), Surface reactions of chromium in soils and waters, *Geoderma*, 67:55 – 71.

Frankenberger, W. T., Jr. (2002). *Environmental Chemistry of Arsenic,* Marcel Dekker, New York.

Fruchter, J. S., Ral, D., and Zachara, J. M. (1990). Identification of solubility-controlling solid phases in a large fly ash field lysimeter. *Environmental Science and Technology*, 24-8, 1173 - 1179.

Geelhoed, J.S., Meeussen, J.C.L., Hillier, S., Lumsdon, D.G., Thomas, R.P., Farmer, J.G., and Paterson, E. (2002). Identification and geochemical modeling processes controlling leaching of Cr(VI) and other major elements from chromite ore processing residue. *Geochimica et Cosmochimica Acta*, 66 - 22, 3927-3942.

Gelhar LW, Welty C., and Rehfeldt KR (1992), A critical review of data on field-scale dispersion in aquifers, *Water Resources Research*, 28-7:1955–1974.

Ghosh, A. and Subbarao, C., (1998). Hydraulic conductivity and leachate characteristics of stabilized fly ash. *Journal of Environmental Engineering* 124 - 9, 812-820.

Gitari, W.M., Fatoba, O.O., Petrik, L.F., and Vadapalli, W.R.K (2009). Leaching characteristics of selected South African fly ashes: Effect of pH on the release of major and trace species. *Journal of Environmental Science and Health Part A*, 44, 206-220.

Goh, A. T. C., and Tay, J. H.,(1993). Municipal solid waste incinerator fly ash for geotechnical applications. *J. of Geotech. Engrg*., ASCE, New York,

Goswami RK, and Mahanta C. (2007), Leaching characteristics of residual lateric soils stabilized with fly ash and lime for geotechnical applications, *Waste Management*, 27:466 – 481.

Goswami, R.K. and Mahanta, C., (2007). Leaching characteristics of residual lateric soils stabilized with fly ash and lime for geotechnical applications, *Waste Management* 27, 466 – 481.

Hatipoglu B, Edil TB, and Benson CH. (2008), Evaluation of base prepared from road surface gravel stabilized with fly ash, *ASCE Geotechnical Special Publication*, 177:288-295.

Heimann, R.B., Conrad, D., Florence, L.Z., Neuwirth, M., Ivey, D.G., Mikula, R.J., and Lam, W.W. (1992) . Leaching of simulated heavy-metal waste stabilized solidified in different cement matrices. *Journal of Hazardous Materials*, 31-1, 39 - 57.

Hollis, J.F., Keren, R., and Gal, M., (1988). Boron release and sorption by fly ash as affected by pH and particle sizes. *Journal Environmental Quality* 17, 181 – 185.

Ischii, Y., Fujizuka, N., and Takahashi, T. (1993). A fatal case of acute boric acid poisoning. *Clin. Toxicol.*, 31-2, 345-352.

Iwashita, A., Sajaguchi, Y., Nakajima, T., Takanashi, H., Ohki, A., and Kambara, S., (2006). Leaching characteristics of boron and selenium for various coal fly ashes. *Fuel*, 84, 479 - 485.

Izquierdo, M., Koukouzas, N., Touliou, S., Panopoulos, K., Querol, X., and Itskos, G., (2011). Geochemical controls on leaching of lignite-fired combustion by-products from Greece, *Applied Geochemistry*, 26, 1599-1606.

Jackson BP, Miller WP, Schumann AW, and Sumner ME. (1999). Trace element solubility from land application of fly ash / organic waste mixtures, *Journal of Environmental Quality*, 28-2:639.

Jankowski J., Colin, R.W., French, D., Groves, S., and (2006). Mobility of trace elements from selected Australian fly ashes and its potential impact on aquatic ecosystems. *Fuel* 85, 243 – 256.

Jegadeesan G, Al-Abed SR, and Pinto P (2008). Influence of trace metal distribution on its leachability from coal fly ash. *Fuel*, 87:1887-1893.

Jing C, Liu S, Korfiatis P, and Meng X. (2006). Leaching behavior of Cr (III) in stabilized / solidified soil, *Chemosphere*, 64:379-385.

Johnson, C.A., Kaeppeli, M., Brandenberger, S., Ulrich, A., and Bauman, W., (1999). Hydrological and geochemical factors affecting leachate composition in municipal solid waste incinerator bottom ash Part II. The geochemistry of leachate from Landfill Lostorf, Switzerland. *Journal of Contaminant Hydrology* 40, 239-259.

Johnson, C.A., Moench, H., wersin, P., Kugler, P., and Wenger, C. (2005). Solubility of antimony and other elements in samples taken from shooting ranges. *Journal of Environmental Quality*, 34, 248 - 254.

Karamalidis, A. K., and Vouidrias, E. A., (2009). Leaching and immobilization behavior of Zn and Cr from cement-based stabilization/solidification of ash produced from incineration of refinery oily sludge. *Environmental Engineering Science*, 26 - 1, 81 - 96.

Karamalidis, A., K., and Vouidrias, E., A., (2008). Anion leaching from refinery oily sludge and ash from incineration of oily sludge stabilized/solidified with cement. Part II. Modeling. *Environmental Science and Technology*, 42, 6124 - 6130.

Karuppiah, M. and Gupta, G., (1997). Toxicity of and metals in coal combustion ash leachate. *Journal of Hazardous Materials* 56, 53 – 58.

Kenkel J., (2003). *Analytical Chemistry for Technicians*. 3rd Edition, , Boca Raton - Florida: Lewis Publishers.

Kim, A.G., (2006). The effect of alkalinity of class F PC fly ash on metal release. *Fuel* 85, 1403 – 1413.

Kim, K., Park, S., M., Kim, J., Kim, S., H., Kim, Y., Moon, J., T., Hwang, G., S., and Cha, W., S., (2009). Arsenic concentration in porewater of an alkaline coal ash disposal site: Roles of siderite precipitation/dissolution and soil cover. *Chemosphere,* 77, 222 - 227.

Komonweeraket K, Benson CH, Edil TB, and Bleam WF (2010), *Mechanisms controlling leaching of heavy metals from soil stabilized with fly ash*, Geo Engineering Report No. 02-14, 2, Geo Engineering Program, University of Wisconsin-Madison, Madison, WI.

Kumar, A., Walia, B.S., and Bajaj, A., (2007). Influence of fly ash, lime, and polyster fibers on compaction and strength properties of expansive soils. *Journal of Materials in Civil Engineering* 19-3, 242-248.

Kumpiene, J., Lagerkvist, A., and Maurice, C., (2007). Stabilization of Pb and Cu contaminated soil using coal fly ash and peat. *Environmental Pollution* 145, 365 – 373.

Langmuir D. (1997). *Aqueous Environmental Geochemistry*. 1st edition, New Jersey: Prentice – Hall, Inc..

Leuz AK, Monch H, and Johnson AC. (2006). Sorption of Sb(III) and Sb(V) to geothite: Influence on Sb(III) oxidation and mobilization, *Environmental Science and Technology*; 40:7277 - 7282.

Li, L, Benson, C.H., Edil, T.B., and Hatipoglu, B., (2007). Groundwater impacts from coal ash in highways. *Waste and Resource Management* 159, 151 – 163.

Li, L., B. Peng, F. Santos, Y. Li, and F. Amini, (2011). Groundwater Impacts from Leaching of Coal Combustion Products in Roadways Embankment Constructions, *Journal of ASTM International*, 8(8): 1-12.

Lim TT, Tay JH, Tan LC, and Choa V. (2004). The, Changes in mobility and speciation of heavy metals in clay-amended incinerator fly ash, *Environmental Geology*, 47: 1-10.

Liu, Y., Li, Y., Li, X., and Jiang, Y., (2008). Leaching behavior of heavy metals and PAHs from MSWI bottom ash in long – term static immersing experiment. *Waste Management* 28, 1126 - 1136.

McBride, M. B. (1994). *Environmental Chemistry of Soils*, Oxford University Press, New York.

McKinley JD, Thomas HR, Williams KP, and Reid JM. (2001), Chemical analysis of contaminated soil strengthened by the addition of lime, *Engineering Geology*, 60: 181-192.

MD-SHA, (2004). *Roadway design manual*. Maryland State Highway Administration.

Medina, A., Gamero, P., Querol, X., Moreno, N., De Leon, B., Almanza, M., Vargas, G., Izquierdo, M., and Font, O. (2010). Flay ash from a Mexican mineral coal I:Mineralogical and chemical characterization. *Journal of Hazardous Materials*, 181, 82 - 90.

Morar DL. (2008), *Leaching of metals from fly ash – amended permeable reactive barriers*, M.S. Thesis, University of Maryland – College Park.

Morar, D., Aydilek, A.H., Seagren, E.A., and Demirkan, M.M. (2012). Metal Leaching from Fly Ash- Sand Reactive Barriers, *Journal of Environmental Engineering*, in press, doi:10.1061/(ASCE)E.E. 1943-7870.0000531.

Morar, D.L., (2008). *Leaching of metals from fly ash – amended permeable reactive barriers*. M.S. Thesis, University of Maryland – College Park.

Mudd, G.M., Weaver, T.R., and Kodikara, J. (2004). Environmental Geochemistry of Leachate from Leached Brown Coal Ash. *Journal of Environmental Engineering* 130-12, 1514-1526.

Mulugeta, M., Wibetoe, G., Engelsen, C.J., and Lund, W. (2010). Overcoming matrix interferences in ion-exchange solid phase extraction of As, Cr, Mo, Sb, Se and V species from leachates of cement-based materials using multiple extractions. *Talanta*, 82, 158 -163.

Murarka, I. P., Rai, D., and Ainsworth, C. C. (1992). "Geochemical basis for predicting leaching of inorganic constituents from coal-combustion residues." *Waste Testing and Quality Assurance Symposium*, Washington, DC, USA, 279-288.

Narukawa, T., Takatsu, A., Chiba, K., Riley, K. W., and French, D. H. (2005). Investigation on chemical species of arsenic, selenium and antimony in fly ash from coal fuel thermal power stations. *Journal of Environmental Monitoring*, 7(12), 1342-1348.

O'Donnell JB (2009), *Leaching of trace elements from roadway materials stabilized with fly ash*, M.S. Thesis, University of Wisconsin – Madison.

Ogunro VO, and Inyang HI (2003). Relating batch and column diffusion coefficients for leachable contaminants in particulate waste materials. *Journal of Environmental Engineering, ASCE*, 129-10:930-942.

Pagenkopf, G.K., and Connolly, J.M., (1982). Retention of boron by coal ash. *Environmental Science & Technology* 16 – 9, 609 - 613.

Pandey, V.C., Singh, J.S., Singh, R.P., Singh, N., and Yunus, M. (2011). Arsenic hazard in coal fly ash and its fate in Indian scenario. *Resource, Conservation and Recycling*. 55, 819-835.

Pandian NS, and Balasubramonian S. (2000). Leaching behavior of fly ashes by jar method, *Indian Geotechnical Journal*, 30-4: 367-374.

Papini MP, Kahie YD, Troia B, and Majone M. (1999), Adsorption of lead at variable pH onto a natural porous medium: Modeling of batch and column experiments, *Environ. Sci. and Technol.*, 33:4457-4464.

Pavageau M, Morin H., Seby F, Guiman C, Krupp E, and Pecheyran C, et al., (2004), Partioning of metal species during an enriched fuel combustion experiment: Speciation in the gaseous and particulates phases, *Environmental Science and Technology*, 38:2252-2263.

Peacock CL, and Sherman DM (2004). Vanadium (V) adsorption onto geothite (α – FeOOH) at pH 1.5 to pH 12: A surface complexation model based on an initio molecular geometries and EXAFS spectroscopy, *Geochim. Cosmochim*., 68:1723 - 1733.

Perry, H.M, Jr., Kopp, S.J., and Perry, E.F., (1989). Hypertension and associated cardiovascular abnormalities induced by chronic Barium feeding. *J. Toxicol Environ. Health*. 28-3, 373-388.

Piantone P, Bodenan F, and Chatelet – Sniduro L. (2004). Minerological study of secondary mineral phases from weathered MSWI bottom ash: Implications for the modelling and trapping of heavy metals, *Applied Geochemistry*; 19:1981-2004.

Praharaj, T., Powell, M.A., Hart, B.R., and Tripathy, S., (2002). Leachability of elements from sub-bituminous coal fly ash from India. *Environment International* 27, 609 - 615.

Querol X, Fernandez – Turiel, J.L., and Lopez-Soler, A, (1995). Trace elements in coals and their behavior during combustion in a large power station. *Fuel*, 74-3, 331 - 343.

Querol X, Fernandez – Turiel, J.L., and Lopez-Soler, A, (1995). Trace elements in coals and their behavior during combustion in a large power station. *Fuel*, 74-3, 331 - 343.

Querol X, Umana, J.C., Alastuey, A., Ayora, C. Lopez-Soler, A., and Plana F. (2001). The extraction of soluble major and trace elements from fly ash in open and closed leaching systems. *Fuel* 80, 801 - 813.

Quina MJ, Bordado JCM, and Quinta-Ferreira RM (2009), The influence of pH on the leaching behavior of inorganic components from municipal solid waste APC residues. *Waste Management*, 29:2483-2493.

Ricou, P., Lecuyer, I., and Le Cloirec, P., (1999). Removal of Cu^{2+}, Zn^{2+} and Pb^{2+} by adsorption onto fly ash and fly ash/lime mixing. *Wat. Sci. Tech*. 39, 239 – 247.

Sadiq, M., Locke, A., Spiers, G., and Pearson, D., A., B., (2002). Geochemical behavior of arsenic in Kelly Lake Ontario. *Water, Air, and Soil Pollution*, 141, 299-312.

Samaras P, Papadimitriou CA, Haritou I, and Zouboluis AI (2008). Investigation of sewage sludge stabilization potential by the addition of fly ash and lime. *Journal of Hazardous Materials*, 154:1052-1059.

Sauer JJ, Benson CH, and Edil TB (2005), *Leaching of heavy metals from organic soils stabilized with high-carbon fly ash,* Geo Engineering Report No. 05-01, Geo Engineering Program, University of Wisconsin – Madison, Madison, WI.

Sparks DL (2003), *Environmental Soil Chemistry*, second edition, Academic Press, California.

Stumm, W. and Morgan, J.J. (1996). *Aquatic Chemistry, Chemical Equilibria and Rates in Natural Waters*, 3rd ed. John Wiley & Sons, Inc., New York, 1022 p.

Su, T., Shi, H., and Wang, J., (2011), Impact of trona-based SO_2 control on the elemental leaching behavior of fly ash. *Energy & Fuels*, 25, 3514-3521.

Svilovic, S. Rusic, D., and Stipisic, R. (2009). Modeling batch kinetics of copper ions sorption using synthetic zeolite NaX, *Journal of Hazardous Materials* 170, 941-947.

van der Hoek EE, van Elteren JT, and Comans RNJ (1996), Determination of As, Sb, and Se speciation in fly ash leachates. *Internat. Environ.,* 63:67-79.

van der Hoek, E. E., Bonouvrie, P. A., and Comans, R. N. J. (1994). Sequential extraction procedure for the speciation of particulate trace metals. *Anal. Ch*em. 51, 844-851.

Vitkova, M., Ettler, V., Sebek, O.,and Mihaljevic, M. (2008). "Metal – ContamiNAnt Leaching from Lead Smelter Fly Ash Using pH – Stat Experiments", *Mineralogical Magazine*, Vol. 72, pp. 521 – 524.

Wang, J., Wang, T., Burken, J.G., Ban, H., and Ladwig, K., (2007). The leaching characteristics of selenium from coal fly ashes. *Journal of Environmental Quality*, 36, 1784-1792.

Wang, J.,Teng, X., Wang, H.,and Ladwig, K., (2006). Impacts of pH and ammonia on the leaching of Cu(II) and Cd(II) from coal fly ash. *Chemosphere* 64, 1892 – 1898.

Wegman, D.H., Eise, E.A., and Hu, X., (1994). Acute and chronic respiratory effects of sodium borate particulate exposures. *Environ. Health Perspect*. 100-7, 119-128.

Wehrer, M. and Totsche, K.U., (2008). Effective rates of heavy metal release from alkaline wastes – quantified by column outflow experiments and inverse simulations. *Journal of Contaminant Hydrology* 101, 53 – 66.

Whalley C, Hursthouse A., Rowlat S., Iqbal-Zahid P, Vaughan H, and Durant R. (1999). Chromium speciation in natural waters draining contaminated land, Glasgow, U.K.. *Water Air Soil Pollution*, 112:389 – 395.

Wones, R.G., Stadler, B.L., and Frohman, L.A. (1990). Lack of effect of drinking water barium on cardiovascular risk factor. *Environ. Health Perspect*. 85, 355-359.

Yan, R., Gauthier, D., and Flamant, G., (2001). Volatility and chemistry of trace elements in a coal combustor. *Fuel* 80, 2217 – 2226.

Yoon, S., Balunaini, U., Yildirim, Z.I., Prezzi, M.,and Siddiki, N., (2009). Construction of embankment with fly and bottom ash mixture, Field performance study. J.*Mat. in Civ. Engrg*. 21 – 6, 271 – 278.